AGARD-CP-195

AGARD

ADVISORY GROUP FOR AEROSPACE RESEARCH & DEVELOPMENT

7 RUE ANCELLE 92200 NEUILLY SUR SEINE FRANCE

AGARD CONFERENCE PROCEEDINGS No. 195

on

Through-flow Calculations in Axial Turbomachinery

NORTH ATLANTIC TREATY ORGANIZATION

AGARD-CP-195

NORTH ATLANTIC TREATY ORGANIZATION

ADVISORY GROUP FOR AEROSPACE RESEARCH AND DEVELOPMENT

(ORGANISATION DU TRAITE DE L'ATLANTIQUE NORD)

AGARD Conference Proceedings No.195

THROUGH-FLOW CALCULATIONS IN AXIAL TURBOMACHINERY

Papers presented at the 47th Meeting of the AGARD Propulsion and Energetics Panel held at the DFVLR Research Center, Porz-Wahn, Köln, Germany, on 20 and 21 May 1976.

THE MISSION OF AGARD

The mission of AGARD is to bring together the leading personalities of the NATO nations in the fields of science and technology relating to aerospace for the following purposes:

- Exchanging of scientific and technical information;
- Continuously stimulating advances in the aerospace sciences relevant to strengthening the common defence posture;
- Improving the co-operation among member nations in aerospace research and development;
- Providing scientific and technical advice and assistance to the North Atlantic Military Committee in the field of aerospace research and development;
- Rendering scientific and technical assistance, as requested, to other NATO bodies and to member nations in connection with research and development problems in the aerospace field;
- Providing assistance to member nations for the purpose of increasing their scientific and technical potential;
- Recommending effective ways for the member nations to use their research and development capabilities for the common benefit of the NATO community.

The highest authority within AGARD is the National Delegates Board consisting of officially appointed senior representatives from each member nation. The mission of AGARD is carried out through the Panels which are composed of experts appointed by the National Delegates, the Consultant and Exchange Program and the Aerospace Applications Studies Program. The results of AGARD work are reported to the member nations and the NATO Authorities through the AGARD series of publications of which this is one.

Participation in AGARD activities is by invitation only and is normally limited to citizens of the NATO nations.

A large part of the content of this publication has been
reproduced directly from material supplied by AGARD or the authors;
the remainder has been set by Technical Editing and Reproduction Ltd.

Published October 1976

ISBN 92-835-0179-9

Printed by Technical Editing and Reproduction Ltd
Harford House, 7–9 Charlotte St. London, W1P 1HD

AGARD PROPULSION AND ENERGETICS PANEL OFFICERS

Chairman: M.l'Ing. en Chef M.Pianko, ONERA, Châtillon-sous-Bagneux, France
Deputy Chairman: Dr Ing. G.Winterfeld, DFVLR, Porz-Wahn, Germany

PROGRAM COMMITTEE 47th(B) SPECIALISTS' MEETING

Professor J.Chauvin VKI, Rhode-St-Genèse, Belgium (Chairman)
Professor C.Casci, Politecnico di Milano, Instituto di Macchine, Milano, Italy
M. J.F.Chevalier, SNECMA, Centre d'Essais de Villaroche, Moissy-Cramayel, France
Dr J.Dunham, NGTE, Pyestock, Farnborough, Hants, England
Professor A.E.Fuhs, Mechanical Engineering, Naval Postgraduate School, Monterey, California, USA
Dr R.B.Whyte, Division of Mechanical Engineering, National Research Council, Ottawa, Canada
Dr Ing. G.Winterfeld, DFVLR, Institut für Luftstrahlantriebe, Porz-Wahn, Germany

HOST COORDINATOR FOR THE 47th MEETING

Dr Ing. G.Winterfeld, DFVLR, Germany

PANEL EXECUTIVE

Lt. Colonel J.B.Catiller, USAF – Meeting Organisation
Dipl. Ing. J.H.Krengel, D.I.G. – Conference Proceedings

The Propulsion and Energetics Panel wishes to express its thanks to the German National Delegates to AGARD for the invitation to hold its 47th Meeting at DFVLR, Germany, and for the facilities and personnel made available for this meeting.

PREFACE

The purpose of this meeting is to review the current knowledge, methods and techniques available to evaluate the flow pattern at design and off-design conditions, in single and multi-stage turbomachines, inside and outside the bladings, along the meridional surfaces, concentrating on the axisymmetric approach.

Papers will cover the methods of calculation of transonic through flow and their numerical problems, as well as spanwise and end loss distribution; there will also be a detailed review of a few particular methods regarding accuracy, time, cost and comparison with experimental data.

The meeting will be concluded by a round table discussion concerning the advantages and disadvantages of the various approaches, from both technical and practical aspects.

AVANT PROPOS

Cette réunion a pour but de passer en revue les connaissances, méthodes et techniques dont on dispose à l'heure actuelle pour évaluer le schéma d'écoulement, dans des conditions nominales ou non, des turbomachines à un seul ou plusieurs étages, tant à l'intérieur qu'à l'extérieur des aubages et le long des surfaces méridiennes; l'accent sera mis en particulier sur les méthodes symétrie axiale.

Les conférences présentées traiteront des méthodes de calcul utilisées pour l'analyse globale des écoulements transsoniques et la résolution de problèmes numériques qu'ils posent, ainsi que de la répartition des pertes dans le sens de l'envergure et aux extrémités. Il ser également procédé à un examen détaillé de quelques méthodes particulières relatives à la précision, à la durée et au prix de revient. Des comparaisons seront établies avec les données expérimentales.

La réunion sera clôturée par une "table ronde" sur les avantages et les inconvénients des diverses méthodes d'approche utilisées, du point de vue technique aussi bien que pratique.

CONTENTS

TURBOMACHINERY THROUGH-FLOW CALCULATION METHODS

Technical Evaluation Report

by

J.Chauvin
Von Kármán Institute
Rhode-St-Genèse, Belgium

and

H.Weyer
DFVLR Research Center,
Porz-Wahn, Koln, Cermany

1. INTRODUCTION

This meeting was certainly timely and stimulating. It was very well attended. The papers provided a well documented state of the art, including a rather clear and unanimous evaluation of the main shortcomings of the methods at hand, and of the most urgent points for improvement. For some of those, the availability of a useful, but not fully experted tool, e.g., numerical methods, was pointed out The practice in industry and its requirements were clearly defined.

The practical exercise of comparison between measured and calculated data, if not perfect, provided useful information on the practical difficulties in both obtaining sufficiently good experimental data and using rather sophisticated, but relatively poorly flexible computer programs.

The exercise could have been more profitable if it had provided separate checks on the characteristics of the computer programs and on the validity of the correlations used.

A part of its post-meeting usefulness, i e , that providing reference to well documented cases for calibrating the computing method, was diminished as permission for publication at large of the geometric data was refused in 3 cases out of 5 by the authorities who sponsored the research programs in the organisations which provided the test cases.

The meeting was very lively and the discussions were enlightening.

In what follows, we will try to express the conclusions that can be drawn from the meeting, and to suggest future course of action.

I. DUCT AND THROUGH-FLOW METHODS. SOLUTION OF THE INVISCID MERIDIONAL FLOW EQUATIONS

The use of degenerated S-2 surfaces of Wu assuming either an axisymmetric or a pitch-averaged flow, and neglecting the viscous terms, but introducing enthalpy and entropy variations produced by the bladings, either as axial discontinuities (duct flow calculation) or at one or several stations inside the blading (through-flow calculation) has led, in the past two years, to the design of quite successful turbines and compressors. Although this model does not represent entirely the physics of the flow (e.g., row interaction or inter streamline energy migration, for instance) when the inviscid flow calculations are coupled with sets of coherent correlation for losses and turning, design and analysis of compressors and turbines can be performed relatively successfully, at least on a comparative basis.

The test cases presented during this meeting have shown that, especially for compressors, the performance map could not be reproduced accurately, nor certain local flow characteristics. The differences are imputed, for a part to the limitation of the correlations, and for an other, to the simplification introduced in specifying the model.

However, the model will remain as a very useful tool in the future, as the calculation times required are of the right order for systematic industrial and research use, when using contemporary digital computers.

I.1 Calculations Schemes

The calculations schemes available, i.e., the streamline curvature methods and the matrix inversion schemes using either finite difference or finite elements seem to have reached their maturity and to need only minor improvements.

None of these seems to have an overwhelming advantage over the others. The streamline curvature approach might be somewhat easier to incorporate the manufacturer's practical experience, while the matrix inversion offers much better possibilities of extension to three-dimensional and quasi-three-dimensional calculations.

This is especially true for the finite element approach, which allows a good description of complicated geometries, and gives less convergence problems, at the expense of a larger requirement on memory size, but which is well within the realm of current computers.

Most of the computer programs in existence, except the most recent ones, seem specialized (i.e. turbine or compressor, analysis or design) which is not bad in itself. However, the current need for detailed off-design analysis seems to require an effort in improving the flexibility of data input. Data preparation is in many cases the most tedious and sometimes expensive part in the use of the computer program, as witnessed in the present exercise.

I.2 Duct Flow Versus Through-Flow

The test cases have shown no significant advantages of through-flow method versus the duct flow ones, in the accuracy of prediction.

However, as pointed out by several of the authors, the duct flow approach is absolutely necessary for the cases where large change of radius of the streamline occurs, i.e., for machines using big bladings, or when non radial blades are selected.

This is true for design, where a knowledge of the flow path, even approximate, allows for a better blading optimization, or at off-design where the effective geometry of the blading, as seen by the flow changes considerably with the flow rate (from convergent to convergent-divergent in large steam turbines, for instance), affecting the blade performance

II. DUCT AND THROUGH-FLOW METHODS: BLADE AND END WALL EFFECTS

The blade effects, i.e., change of entropy, of energy and flow direction are taken into account by correlations on losses and turning In the design cases, the blades are also selected mostly on the basis of correlation.

Usually, each company has its own brand of correlation. None of those, except in one turbine calculation case, were described during the meeting.

For the published computation method, in the compressor field, the basis is the NACA-correlation, which is essentially made for design purposes, complemented by elementary corrections, for compressibility effects, including shock losses, axial velocity ratio, and secondary losses. No correction is made for the effect of secondary flows on deviation A separate correction is usually made for hub and casing boundary layer blockage.

For turbine, classical correlations, like Ainley, Dunham-Came, Soderberg or Traupel are used, usually on a mean radius basis Mosts of those experimental correlations include implicitly or explicitly secondary flow effects

The results obtained by the calculation methods are heavily conditioned by the quality of the blade correlation methods, and their coherence with the flow model selected for the computation.

It is the general experience that the correlations existing are valid for a limited number of machine geometries. For instance, the performance prediction method of one manufacturer is quite satisfactory for its own machine, but not so when applied to machines built by another one.

Correlations for blade and end wall are thus still rather unsatisfactory, and the largest improvement to be expected for the meridional flow model will come from improvement on those correlations, whose form should be more or less maintained, but with a much broader range of validity.

II.1 Improvement of Blade Section Performance Prediction

As expressed by members of the round table panel, it seems that in view of the number of variables, the difficulty of controlling all the variables in the compressible flow range, the specialisation of the blading in that range, and the relatively qualitative nature of the information obtained, the improvement cannot be obtained only by systematic rectilinear or annular cascade tests programs.

A combination of carefully carried out tests and of the systematic use of the numerical techniques of computation available (compressible singularity methods, finite difference and fast time marching method, plus boundary layer correction possible and achieved even with shock interaction) could provide the type of information requested for the unseparated or moderately separated flow cases. Notwithstanding their imperfections, the computing methods allow the control of the conditions, incorporate the two-dimensional axial velocity ratio effects, as well as those of change of radius in fixed and rotating bladings, and allow for at least a relative prediction of the overall and local characteristics, the latter needed for the application of the through-flow scheme.

By this, it is not suggested that those numerical computation methods be incorporated as subroutines in the meridional flow programs, but that they be used in conjunction with carefully selected cascade and machine tests which remain indispensable, to provide relatively simple correlations, to be used in the duct and through-flow calculations.

This type of program could be initiated on classical families of blading, to conform the validity of the approach. This would require a cooperative effort that a number of the participants to the meeting are ready to undertake, preferably under AGARD auspices. Detailed proposals are being prepared for submission to the PEP.

Efforts of development of the methods for the separated cases have of course to be undertaken, and the existing one can only fill in part of the gap.

II.2 End Wall Leakage and Secondary Flow Corrections

The end wall leakage and secondary flow corrections are, for a large number of cases, as important as the blade section performance (need for blockage and additional loss correction, for instance). The available correlations are not satisfactory again, and the angle corrections are practically neglected up to now, although they can be important and affect an important part of the flow, beyond that influenced at the loss point of view.

The physics of the related phenomenon are not entirely understood, for the machine case and even for the simpler straight or annular cascade.

This was realised a few years ago, and an array of experiments aimed at identifying the flow mechanisms are being carried out in the USA., and in Europe, making use of classical instrumentation (pressure directional probes and hot wire) laser velocimetry and flow visualisation, and scrutinizing the flow throughout the whole blade passage. The PEP is organizing a technical meeting on the subject in the Spring of 1977.

This meeting should provide useful guidance for future efforts.

As mentioned during the meeting, there are now broadly two approaches, one of correction of the basic flow (loss correction, and non-viscid clearance and secondary flow effects on angle) and the pseudo-boundary layer approach based on the work of Mellor. In our view, both are valid, and should be pursued.

At this point in time, it would seem possible to attempt an angle correction based on the inviscid calculation existing, as described by Marsh, for instance, but which must be extended to twisted bladings. This is in progress in various research groups, and a concerted effort seems possible, as suggested by several participants to the meeting.

III. THREE-DIMENSIONAL FLOW APPROACH

A limited, but very important effort is being invested in the investigation of the three-dimensional time average flow occurring in turbomachinery, with another, maybe too small one, on some aspects of the unsteady flows, like the wake transmission.

On the experimental side, the laser valocimeter provides the first really workable tool for a deeper understanding of what happens, as typified by the results obtained in the US., and at the DFVLR, the latter having been presented at this meeting.

On the calculation side, two approaches are being followed, one based on the iterative coupling of Wu's S1 and S2 surface, the other on a direct solution of the three-dimensional equation. Inviscid flows only are considered. As mentioned during the meeting, work is in progress mainly in the US., and Great Britain, and to our knowledge, to a lesser extent on the continent. The presentation of Thompkins indicates what can be achieved, and the cost of calculation although very large, is still much lower in money and time than the cost of the equivalent experiment.

It is clear however, that both the experiments which should be extended to multistage machines and the three-dimensional calculations, will not become part of the industrial and analysis system in the foreseeable future

Both the experimental and numerical approaches must be considered as laboratory tools leading to a better qualitative and order of magnitude understanding of the flow, which should lead to the definition of more correct flow models whose complexity should not exceed much those in present use, if they have to be of practical value

MODELES DE CALCUL DE L'ECOULEMENT DANS LES TURBOMACHINES AXIALES

par
Jean-Marie THIAVILLE
SNECMA
Centre de Villaroche
77550 Moissy-Cramayel
FRANCE

RESUME

Le problème du calcul de l'écoulement dans les turbomachines axiales est abordé à partir du modèle des surfaces de courant S 1 et S 2 de C. H. WU, combiné avec l'introduction des effets visqueux sous forme de pertes et d'effets de déplacement. L'hypothèse d'un écoulement stationnaire de révolution y est généralement admise et les phénomènes visqueux sont limités aux parois de la veine et des aubages. Dans ce cadre simplifié, les problèmes suivants sont successivement analysés du point de vue de l'utilisateur : - Couplage des calculs sur les surfaces S 1 et S 2.
- Traitement des écoulements transsoniques.
- Schémas de pertes et d'angles hors adaptation.
- Blocage et écoulements secondaires.

On examine ensuite, dans une deuxième partie, des exemples d'application où le modèle simplifié peut être mis en défaut : nageoires, double-flux, réintroductions sur les parois ou sur les aubes, distorsion, veines fortement convergentes ou divergentes sur turbomachines chargées, pompage et décollement tournant, machines haute pression où les effets visqueux peuvent s'étendre sur toute la hauteur de veine.

NOMENCLATURE

δ^*	Epaisseur de déplacement
m	Direction méridienne
r,θ,z	Coordonnées cylindriques
F	Fonction aérodynamique (équation (1))
S_1, S_2	Surfaces de courant (figure 2)
V	Vitesse dans le système absolu
W	Vitesse dans le système relatif
$\Theta(r,z)$	Surface S 2 particulière
n	Fonction égale à $\mathrm{tg}\,\beta$
β	Angle de la vitesse relative avec le plan méridien
K	Obstruction des aubages définie par l'équation A1 (8)
t	Temps
ω	Vitesse angulaire de rotation
S	Entropie
H	Enthalpie totale
h	Enthalpie statique
T	Température
$I = H - \omega r V_\theta$	Rothalpie
x	Déplacement curvilingue sur une ligne de courant
q	Quantité de chaleur par unité de masse
D	Opérateur de dérivation en suivant une particule
Φ	Terme de frottement (équation (8))
K_D	Facteur de blocage
N	Normale à la surface Θ
Z	Nombre d'aubes
e	Epaisseur des aubes dans le sens périphérique
ψ	Fonction de courant.

Indices

I	Intrados
E	Extrados
i	Intérieur (moyeu)
e	Extérieur (carter)
r,θ,z	Projections sur les directions r,θ,z
m	Projection méridienne.

MODELES DE CALCUL DE L'ECOULEMENT DANS LES TURBOMACHINES AXIALES

par J.M. THIAVILLE (SNECMA-FRANCE)

INTRODUCTION

La conception des aubages de turbomachines axiales reste encore basée, pour de nombreux projets, sur la théorie des éléments d'aubes. Chaque aubage est constitué d'un empilage sur la hauteur d'un certain nombre de coupes, soit prises dans des catalogues de grilles, soit définies analytiquement par des méthodes de type "inverse-aube à aube" telles que celles portées références [1] et [2] . La liaison entre les caractéristiques aérodynamiques des différentes coupes est faite par un calcul "d'équilibre radial". Celui-ci peut être simplifié en un nombre limité de plans hors aubages perpendiculaires à l'axe de la machine avec introduction ou non des effets de courbure des lignes de courant (références [3] , [4] , [5]).

Mais les performances de plus en plus poussées des turbomachines modernes ont incité les constructeurs a faire appel à des méthodes de calcul pénétrant jusqu'à l'intérieur des aubages dont une première approximation de la géométrie est alors nécessaire. Ces méthodes sont généralement présentées sous l'appellation anglaise : "Through-Flow". Elles font l'objet du présent colloque.

Dans le cas projet, le calcul complet n'a pour but que la détermination, pour chaque tube de courant, des triangles de vitesses en amont et en aval de chaque grille, agrémentés de l'évolution dans l'aube de la hauteur du tube de courant considéré. Des essais de grilles faisant varier ce paramètre ont, en effet, mis son importance en évidence ([6] , [7]). Le calcul est en général effectue en un seul point de fonctionnement où le débit, le taux de compression (ou le travail réduit), le coefficient de blocage aux parois de la veine sont des données. Un bouclage est quelquefois réalisé sur les pertes après que les aubes aient été définies.

Un problème plus ardu est posé au spécialiste par le calcul d'analyse dont le but est la détermination des performances et du champ de vitesses dans tout le domaine de fonctionnement d'une turbomachine dont la géométrie est seule fixée. Dans ce cas il est naturel que les utilisateurs se soient tournés vers des modèles d'écoulement sensiblement basés sur les mêmes hypothèses que celles du calcul projet. Ce sont ces modèles d'écoulement que nous tenterons d'examiner dans l'étude qui suit.

I.MODELE DE BASE

Le problème d'ensemble de l'écoulement dans une turbomachine, essentiellement tridimensionnel, visqueux, instationnaire et limité à un volume de formes complexes présentant des échanges avec l'extérieur est divisé artificiellement en un certain nombre de problèmes plus simples, le couplage entre ceux-ci étant effectué sous forme directe ou itérative. Ce partage cartésien des difficultés a été résumé dans le tableau I.

1. Hypothèse "couches limites" :

La richesse de l'hypothèse couches limites, démontrée sur les profils d'aile ou de grilles, a conduit naturellement les spécialistes turbomachines à simplifier les équations de Navier-Stokes en supposant que les effets de viscosité et de conductivité thermique sont limités à une couche mince le long des parois de la veine et des profils. Ce modèle simplifie énormément le calcul en dehors des aubages où l'écoulement peut être considéré sans frottement jusqu'aux parois de la veine, l'effet de couche limite pariétale étant pris en compte dans la continuité du débit par le classique coefficient de blocage K_D. Cette méthode peut d'ailleurs être modifiée facilement en remplaçant K_D par un calcul qui s'arrête à une distance de la paroi égale à l'épaisseur de déplacement de la couche limite (figure 1).

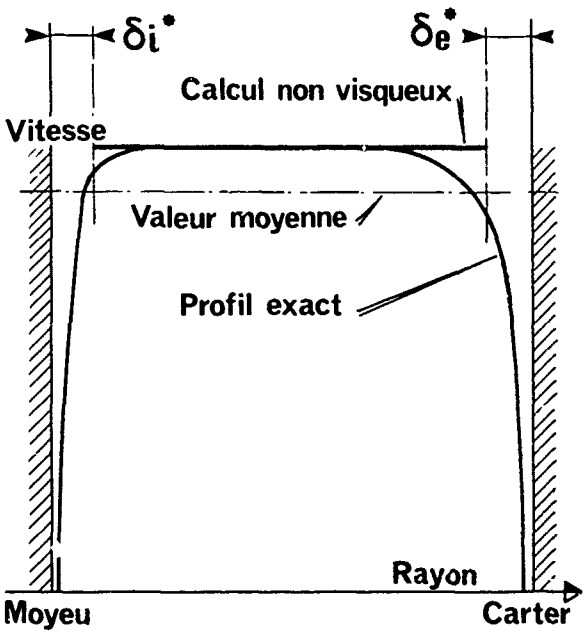

Fig.1 - Effets de déplacement à la paroi

Cette dernière solution permet une meilleure prise en compte de l'effet de lissage des accidents de parois par la couche limite (changements de pente ou de courbure). Elle peut cependant poser des difficultés de convergence hors adaptation, lorsqu'il y a décollement par exemple.

A l'intérieur des aubages, l'introduction dans l'écoulement principal de l'effet de couche limite sur les profils dépend naturellement de la manière dont on modélise l'écoulement tridimensionnel non visqueux. Dans tous les cas il est nécessaire d'introduire des pertes dans le calcul non visqueux de manière à respecter le bilan d'énergie.

TABLEAU I_ Modèle de calculs d'écoulements dans les turbomachines_

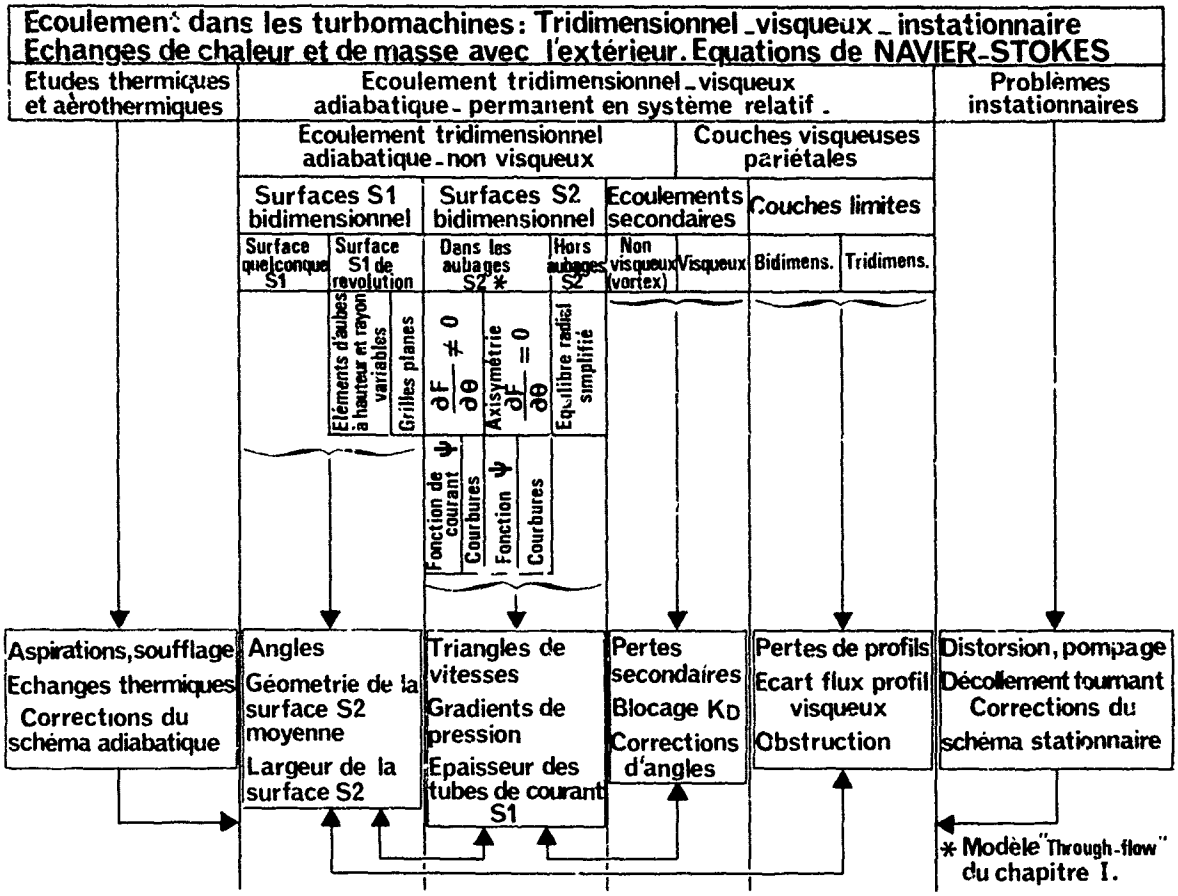

Ce point particulier est examiné dans le chapitre II (paragraphes 1-3 et 2-2). On peut cependant noter dès à présent que l'écoulement principal (hors couches limites) est considéré comme laminaire, sans forces de viscosité ni conduction de chaleur

2. Hypothèse « C. H. WU » [8]

L'écoulement tridimensionnel sans frottement est lui-même partagé en deux problèmes tridimensionnels .

a - L'un consiste à considérer les surfaces de courant générées par des particules situées sur des cercles centrés sur l'axe. Ces surfaces S1 dites du premier ordre sont généralement supposées de révolution. Cette hypothèse peut être très restrictive mais il semble difficile de la lever sans compliquer les calculs. L'intersection de chacune de ces surfaces avec les aubages (figure 2) définit une "grille" autour de laquelle l'écoulement non visqueux puis les couches limites peuvent être calculés.

Les résultats de ces calculs : angle de sortie, pertes de profil effets,d'obstruction (épaisseur de déplacement) dans le sens périphérique sont, en fait, souvent générés par un schéma empirique beaucoup plus souple d'emploi dans le calcul complet que les méthodes analytiques.

En effet le calcul de grilles fait appel à des méthodes très variables selon les conditions de l'écoulement et elles ne sont pas toutes compatibles : - Différences finies centrées ([9]), courbures des lignes de courant, méthodes de singularités ([10] , [11]) en subsonique.

- Méthodes pseudo-instationnaires ([12] , [13] , [14]) ou différences finies excentrées ([15] , [16]) en transsonique.

- Méthode des caractéristiques en supersonique.

De plus, les calculs de couche limite qui doivent lui être associés sont quelquefois insuffisants pour une définition correcte des pertes hors adaptation, surtout en compresseur, au décollement ou en présence d'effets intenses de compressibilité. Même en turbine ces calculs, bien que plus efficaces, nécessitent souvent des ajouts empiriques pour tenir compte, par exemple, des effets de culot (bord de fuite épais) et des interactions choc-couche limite.

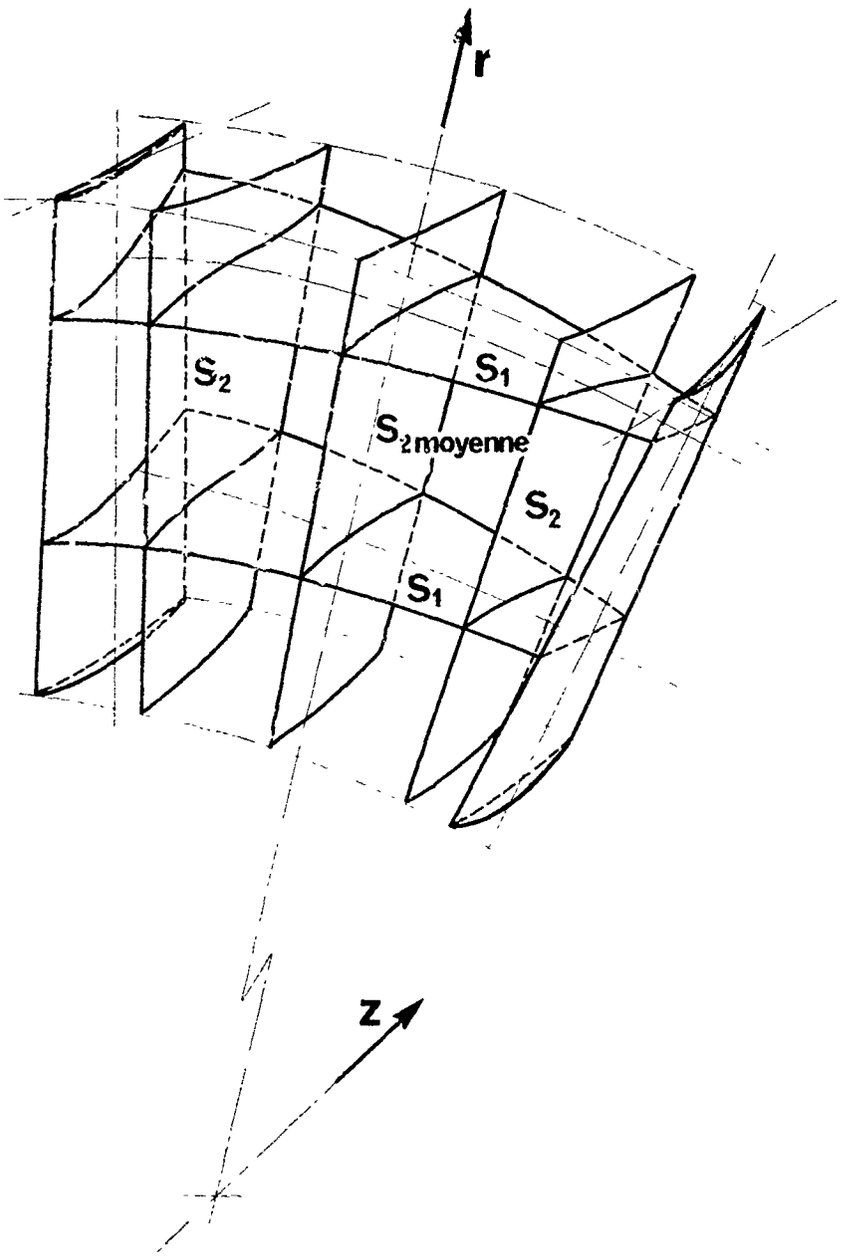

Fig.2 - Exemples de surfaces S_1 et S_2 .

b - L'autre problème bidimensionnel qui est justement à la base des travaux de ce congrès consiste à effectuer les calculs sur des surfaces de courant, dites du deuxième genre, générées par des particules situées sur un rayon en un plan perpendiculaire à l'axe en amont ou dans la roue. Deux surfaces particulières de ce type sont les surfaces extrados et intrados des aubes (déplacées de l'épaisseur de déplacement déterminée sur le profil par le calcul dans l'autre sens).

Leur définition apparait clairement figure 2. L'hypothèse (a) précédente de surfaces S1 de révolution implique que l'on peut passer d'une surface S2 à une autre par simple rotation autour de l'axe de la machine et que l'on peut donc se contenter d'effectuer le calcul sur une seule surface S2 moyenne. Les fonctions aérodynamiques sont alors considérées sur cette surface comme moyennées périphériquement en θ. Des exemples de méthodes de ce type peuvent être trouvés en [17], [18], [19] et [20].

Une simplification est souvent utilisée qui consiste à considérer l'écoulement comme entièrement "axisymétrique" c'est-à-dire que les variations en θ des mêmes fonctions sont prises nulles : $\frac{\partial F}{\partial \theta} = 0$ pour tout F. Cette hypothèse, plus restrictive que de prendre simplement les surfaces S1 de révolution, suppose, pour le calcul à l'intérieur des aubages, l'introduction de forces volumiques dans les équations de quantité de mouvement et d'un coefficient d'obstruction des aubages dans l'équation de continuité. Cette simplification n'est possible que si l'on ne cherche pas, dans un calcul général de l'écoulement, à déterminer les caractéristiques aérodynamiques locales sur les aubes mais si l'on cherche simplement les performances globales (débit, pression, rendement) et les triangles de vitesses en amont et en aval des roues. L'hypothèse axisymétrique est cohérente avec un schéma de pertes empirique global mais elle ne l'est plus si le schéma de pertes est complexe au point de tenir compte des répartitions de vitesse locale sur les aubes ou s'il est remplacé par une méthode complète analytique (calcul aube-à-aube et couches limites).

En fait, les fonctions considérées (pression, vitesses etc...) ont une allure en "dents de scie" en θ avec discontinuité au passage des aubes. Les turbomachinistes ont l'habitude de dire que le fait de considérer leur moyenne en θ avec $\left(\frac{\partial ()}{\partial \theta} = 0\right)$ suppose un nombre infini d'aubes, les termes négligés ne devenant importants que pour un faible nombre de pales. En fait, dès 1965, L. H. SMITH Jr. a montré que ces termes (fonctions "G" référence [17]) dépendent plus précisément de la charge.

On peut démontrer par exemple qu'à charge donnée la différence de vitesse entre l'extrados et l'intrados tend vers zéro quand le nombre d'aubes tend vers l'infini alors que la dérivée $\frac{\partial V}{\partial \theta}$ sur la surface S2 tend vers une valeur non nulle. Un cas d'application assez fréquent en aéronautique nécessite la prise en compte soit des composantes de la force volumique F dans les aubages soit d'une valeur non nulle des dérivées $\frac{\partial}{\partial \theta}$ des différentes fonctions calculées sur la surface S2 :

Il s'agit du cas des aubes penchées schématisées figure 3 surtout si elles sont très vrillées (référence 21). Une méthode simple de prise en compte de ces dérivées est suggérée en [22] dans le cas d'une méthode de courbures.

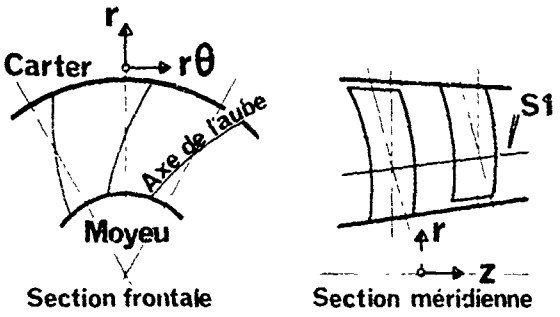

Fig.3_ Aubes penchées et aubes en flèche.

Elle consiste à linéariser les variations en θ entre intrados et extrados sous la forme :

$$(1) \qquad \frac{\partial F}{\partial \theta} = \frac{F_I - F_E}{\theta_I - \theta_E}$$

Par exemple, pour la fonction $n = \operatorname{tg} \beta$, on obtient facilement (voir Annexe 1):

$$(2) \qquad \frac{1}{r}\frac{\partial n}{\partial \theta} = \frac{1}{K}\frac{\partial K}{\partial m}$$

K et $\frac{\partial K}{\partial m}$ étant des données liées à la géométrie des aubes (ou au calcul dans l'autre sens, sur les surfaces S1).

3. Hypothèse stationnaire

Une autre hypothèse simplificatrice consiste à considérer l'écoulement comme permanent dans le mouvement relatif. Cette simplification n'est pas aussi restrictive que celle d'un écoulement complètement stationnaire. Elle conduit à négliger les termes $\frac{\partial}{\partial t}$ dans les équations du mouvement écrites dans un système de référence lié au rotor. Mais un observateur fixe voit tout de même l'écoulement sous forme instationnaire, au moins dans la roue mobile, les variations en fonction du temps dans le système absolu étant liées aux gradients tangentiels dans le système relatif par :

$$(3) \qquad \left[\frac{\partial ()}{\partial t}\right]_{\substack{\text{système} \\ \text{fixe}}} = -\omega \left[\frac{\partial ()}{\partial \theta}\right]_{\substack{\text{système} \\ \text{mobile}}}$$

ω étant la vitesse angulaire de rotation du rotor qui est prise constante.

Physiquement, l'hypothèse suppose que les sillages des grilles fixes sont amortis lorsqu'on entre dans la roue mobile et que les sillages des grilles mobiles sont amortis lorsqu'on entre à l'intérieur de la roue fixe.

En résumé, le modèle retenu représente un fluide adiabatique, non visqueux, permanent en espace mobile, calculé sur une surface de courant "moyenne" de type S2 de CH. WU. L'écoulement peut être rotationnel ; l'enthalpie totale et l'entropie peuvent varier d'un point à un autre. Les frottements et les écoulements secondaires y sont introduits sous forme de pertes et d'effets de déplacements déterminés par un schéma empirique (voir tableau 1).

II. FORMULATION ET RESOLUTION

Le modèle d'écoulement étant choisi, les deux questions qui se posent ensuite au spécialiste désireux de programmer sur ordinateur et d'appliquer la méthode de calcul à des cas concrets sont la formulation et la méthode de résolution.

1. Formulation

1.1. Calcul Projet et Calcul d'Analyse

Certains termes des équations peuvent être négligeables au point d'adaptation et ne plus l'être dans l'ensemble du champ de caractéristiques. On pouvait se demander si des simplifications supplémentaires n'étaient pas souhaitables dans la formulation du calcul projet. De telles simplifications étaient utilisées avec succès dans les années 50 alors que la puissance des ordinateurs ne permettait pas encore un traitement efficace du modèle exposé ci-dessus. La prévision du champ de performances était alors plus ou moins confiée à un empirisme d'ailleurs souvent très efficace.

Mais les recherches récentes sur la prévision analytique des performances nous incitent à souhaiter une formulation uniforme de manière à ce que les deux calculs puissent intervenir l'un sur l'autre de façon cohérente : correction du projet en fonction des résultats hors-adaptation ou amélioration de la prévision hors-adaptation par "cadrage" des valeurs projet.

Dans le calcul d'écoulement des turbomachines, sur une surface de type S2, on peut définir, à la manière des calculs de grilles, deux types de méthodes :

- l'une, dite méthode inverse, part de l'évolution des vitesses, ou plus précisément du moment cinétique rV_θ donné le long de la surface, considérée pour calculer les angles donc la géométrie de cette surface.

- l'autre, dite méthode directe, consiste à calculer les vitesses sur la surface de courant en partant des angles comme donnée. Pour éviter toute confusion entre calcul projet - calcul d'analyse d'une part et méthode inverse - méthode directe d'autre part nous pensons qu'il est utile d'insister ici sur le point qu'un calcul projet peut être effectué indifféremment avec une méthode inverse ou une méthode directe, de même qu'un calcul de performances peut être mené à bien par une méthode inverse comme par une méthode directe. Le tableau II (suivant) résume cette analyse.

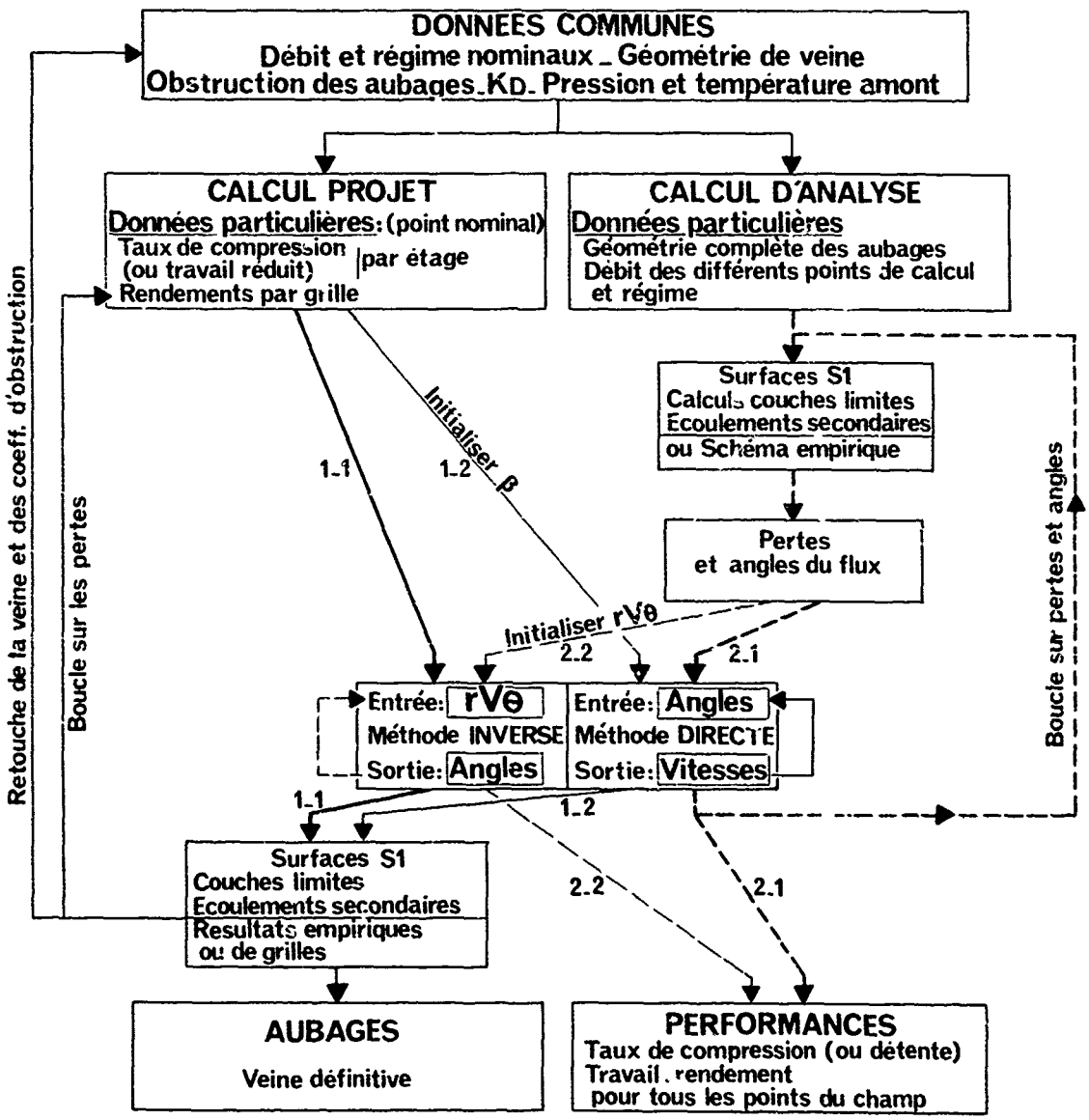

Le chemin naturel pour le calcul projet est l'utilisation de la méthode inverse, trajet (1-1) mais la méthode directe est possible, trajet (1-2) avec une boucle itérative sur rV_θ . Le chemin naturel pour le calcul d'analyse est la méthode directe, trajet (2-1) mais on peut aussi utiliser la méthode inverse avec une boucle itérative sur les angles.

1.2. Problèmes transsoniques

Les écoulements transsoniques, pris au sens général, c'est-à-dire où cohabitent des zones subsoniques et des zones supersoniques, posent surtout des problèmes au niveau de la résolution des équations (elliptiques ou hyperboliques selon les zones). Cependant nous pensons qu'une grande partie des cas rencontrés par l'industriel, surtout en aéronautique, peut être résolue au niveau de la formulation même, du moins en ce qui concerne l'écoulement non visqueux. En effet, on peut montrer ([8] , [22] , [23]) que l'utilisation d'une formulation de type "méthode inverse" où rV_θ est pris comme donnée ne conduit à une indétermination que si la composante méridienne du nombre de Mach atteint l'unité. D'où l'intérêt de ce type de méthode pour les turbomachines axiales aéronautiques où ce terme est généralement subsonique. Ceci ne veut d'ailleurs pas dire que le problème du passage d'une zone supersonique à une zone subsonique (chocs, blocage) se trouve "escamoté" à l'intérieur des aubages mais qu'il est plus simplement reporté sur la loi de rV_θ d'une part, le schéma de pertes et d'angles d'autre part.

1.3 Introduction des pertes

Dans le calcul à l'intérieur des aubages, J. H. HORLOCK 24 a soulevé le problème, dès 1971, de la cohérence entre les équations de quantité de mouvement d'une part et l'introduction de pertes donc de variations d'entropie d'autre part. En effet si l'on écrit l'équation du mouvement sans frottements (second principe de Newton) et que l'on suppose le mouvement permanent en système relatif, la projection de cette équation sur la vitesse conduit à l'équation d'énergie : (4) $\frac{DI}{Dt} = T\frac{DS}{Dt}$

($\frac{D()}{Dt}$, dérivation par rapport au temps en suivant une particule dans son mouvement.

I = Rothalpie définie par $I = h + \frac{W^2}{2} - \omega(rV_\theta)$ égale à l'enthalpie totale si $\omega = 0$).

Or l'hypothèse du modèle - écoulement adiabatique - permet d'écrire par application du premier principe de la thermodynamique : (5) $DH = DW + Dq = D(\omega rV_\theta)$

DW est le travail par unité de masse échangé par une particule avec l'extérieur lorsqu'elle se déplace d'une quantité Dx sur sa ligne de courant. Dq est la quantité de chaleur par unité de masse échangée dans les mêmes conditions (ici $Dq = 0$). Les équations (4) et (5) indiquent donc que ni la rothalpie I ni l'entropie S ne peuvent varier le long d'une ligne de courant.

Comme l'introduction de pertes de profil sur la surface S2 moyenne suppose que l'entropie varie sur une ligne de courant, une force de frottement doit bien être introduite au niveau de l'équation de quantité de mouvement. Il est prouvé que ce terme demeure faible en valeur numérique lorsqu'on reste aux alentours de l'adaptation où les pertes sont par définition minimales. Il semble cependant que certains déboires trouvés quelquefois dans l'introduction des pertes hors-adaptation et mis généralement sur le compte d'un mauvais calibrage du schéma de pertes empirique, puissent être dus à une sous-estimation de cet effet lorsque l'augmentation d'entropie est élevée. Des cas de ce type sont inévitables si l'on désire décrire analytiquement l'ensemble du champ de performances avec une méthode suffisamment générale pour supporter des phénomènes tels que décollement, ondes de choc, etc...

Nous avons vérifié qu'une force de frottement opposée à la vitesse peut remplir ce rôle sans trop compliquer les équations. On écrit ([8] , [22]) l'équation de quantité de mouvement sous la forme :

(6) $W \wedge (\mathrm{rot}\, V) = \mathrm{grad}\, I - T\,\mathrm{grad}\, S + \Phi W$

où $-\Phi W$ est la force de frottement assimilée à un terme dissipatif. En projetant (6) sur la vitesse relative W on obtient :

(7) $W.\mathrm{grad}\, I - W.T\,\mathrm{grad}\, S = -\Phi W^2$

et $\frac{DI}{Dt} = 0$ par (5) entraine :

(8) $\boxed{\Phi = \frac{T}{W^2}\frac{DS}{Dt}}$

1.4. Echanges de chaleur

Dans le cas particulier où les échanges de chaleur avec l'extérieur ne sont plus négligeables (turbines fortement refroidies par exemple) il n'y a pas lieu d'ajouter de termes à l'équation fondamentale de la dynamique mais il faut alors remarquer que la rotalpie I varie sur une ligne de courant car l'équation (5) n'est plus vérifiée ($\Delta q \neq 0$) ce qui modifie l'équation (8) sous la forme :

(8)' $$\Phi = \frac{T}{W^2}\frac{DS}{Dt} - \frac{1}{W^2}\frac{DI}{Dt}$$

et donc toute la formulation.

Cependant on peut, dans la plupart des cas, considérer les echanges de chaleur dus au refroidissement des aubes et des parois dans une turbine comme réduits aux couches limites et donc conserver le modèle de base non visqueux sans conduction et introduire dans ce modèle les effets thermiques sur l'entropie comme on le faisait pour les pertes.

2. RESOLUTION

2.1. Fonction de courant ou courbures :

On sait que les méthodes de résolution du système de 4 équations déduit de (6) et de l'équation de continuité consistent en général à réduire le problème à l'intégration d'une équation différentielle unique. Elles se partagent en deux familles selon que l'intégration est effectuée

- en somme double sur une surface : méthodes utilisant les dérivées de la fonction de courant ou
- en intégrale curviligne sur une ligne quelconque, la géométrie des lignes de courant étant fixée : méthodes de courbures. La première famille compor e les méthodes d'éléments unis et les méthodes matricielles, dans la seconde l'intégration peut être effectuée sur des rayons (équilibre radial) ou sur des quasi-orthogonales ou encore sur l'intersection de la surface S2 par des plans perpendiculaires à l'axe (aubes penchées : figure 3).

Dans les deux cas, le maillage reste fixe et se sont soit la fonction de courant soit la géométrie de la ligne de courant qui sont retouchées au cours des itérations jusqu'à convergence du calcul. Il est naturellement possible de projeter les équations sur les lignes de courant elles-mêmes et leurs normales, les équations obtenues sont alors plus simples mais on doit utiliser un maillage variable au cours des itérations et la correction est plus compliquée.

Du point de vue de l'utilisateur (précision, rapidité, facilité de mise en oeuvre) des analyses et des comparaisons entre méthodes de "courbure" et méthodes "fonction de courant" ont déjà été effectuées ([22] , [23] , [25]). Aucun des deux systèmes ne semble avoir définitivement pris le pas sur l'autre et il est souvent difficile de comparer deux types de résolution au même stade de sophistication, en particulier en ce qui concerne la pondération des corrections itératives et l'introduction du schéma de perte et d'angles. Cette concurrence peut être elle même génératrice de progrès car les spécialistes vont encore certainement apporter des améliorations dans l'une et l'autre famille de résolution. Deux remarques peuvent être faites ici :

- La première est que l'historique des méthodes de projet chez les constructeurs les conduit souvent à développer de préférence une méthode de type "courbures" qui leur permet de faire plus facilement la liaison entre les méthodes modernes analytiques et leur expérience propre des performances d'éléments d'aubes corrigées par les effets d'interaction entre grilles (référence [26]).
- La seconde est que les méthodes faisant appel à la fonction de courant sont peut être un point de départ plus riche de possibilités pour une extension vers des modèles plus compliqués (méthodes d'éléments finis en instationnaire, méthodes tridimensionnelles, etc...).

2.2. Schémas de pertes

Il n'entre pas non plus dans le cadre de ce papier d'étudier dans le détail les schémas de pertes les mieux adaptés. Chaque spécialiste et chaque constructeur a d'ailleurs le sien propre dérivé de son expérience et appliqué à ses propres exemples. La plupart des auteurs s'accordent d'ailleurs à dire que le schéma de pertes et d'angles revêt une grande importance dans la qualité des résultats et que même un bon schéma peut quelquefois éviter une trop grande complication de la formulation de base.

Cependant les progrès réalisés dans les calculs de couches limites et surtout dans la détermination analytique des pertes, des angles et des épaisseurs de déplacement dus aux écoulements secondaires - [27] , [28] , [29] , [30] et [31] - laissent entrevoir la possibilité de remplacer les schémas empiriques généralement utilisés par un calcul entièrement analytique sur surfaces S1, couches limites et écoulements secondaires.

2.3. Blocage

Le cas du blocage pose un problème particulier. En effet il suppose que dans certains plans de calcul une relation supplémentaire (continuité du débit bloqué) relie pertes et angles et les deux paramètres ne peuvent plus être introduits séparément. Dans le cas des turbines supercritiques cet effet a lieu à la sortie des aubages alors que la plupart des pertes ont déjà été prises en compte. On peut donc souvent simplifier le phénomène par modification de l'angle à pertes constantes pour satisfaire la continuité ("angle de sortie unique").

Dans le cas des compresseurs, le blocage intervient à l'intérieur du canal inter-aubages et provoque lui-même des pertes supplémentaires par apparition d'ondes de choc. Il est alors nécessaire de corriger ensemble les angles et les pertes. Les compresseurs supersoniques, quant à eux, sont à rapprocher des turbines supercritiques et leur problème peut également être simplifié par modification de l'angle à l'entrée ("incidence unique") à pertes constantes.

III. DIFFICULTES D'APPLICATION

Un certain nombre de cas de turbomachines aéronautiques peuvent éventuellement remettre en cause le modèle de base adopté et faire appel soit à des corrections empiriques soit à un modèle plus compliqué.

1. Soufflante de moteur double-flux

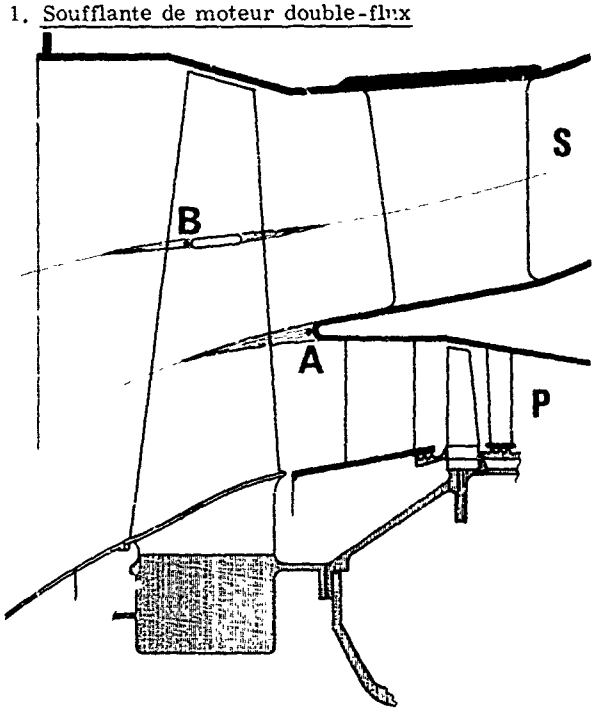

Fig.4_Soufflante de moteur double-flux_

La présence d'un bec de séparation des flux (A) en aval de la roue mobile et éventuellement d'une "nageoire" (B) pour amortir les vibrations provoque des discontinuités et des conditions aux limites complexes dans le calcul méridien (figure 4). Cette configuration ne remet pas en cause l'hypothèse de surfaces S1 de révolution. Mais le calcul sur surface S2 peut être fondamentalement perturbé, en particulier hors adaptation. Les contre-pressions en P et en S peuvent différer fortement et il faut théoriquement calculer autant de champs de la partie secondaire qu'il y a de vannages sur la partie primaire et vice-versa. Heureusement, les contre-pressions en P et en S ne sont pas indépendantes sur moteur complet ; elles sont reliées par le cycle thermodynamique et la configuration de moteur choisie.

Avec une méthode du type courbures des lignes de courant, une adaptation du programme peut être organisée autour de trois calculs : partie secondaire seule, partie primaire seule, veine complète sans séparation. Le passage d'un calcul à l'autre peut s'effectuer par coefficients d'obstruction ou facteurs K_D judicieusement répartis sur les tubes de courants considérés. Le schéma de pertes est également à reconsidérer du fait des couches limites sur les nageoires et le bec et les nouveaux écoulements secondaires créés par ce type de géométrie. Mais un calcul type "éléments finis" dans le plan méridien devrait pouvoir répondre élégamment au problème posé par cette configuration.

2. Turbomachines chargées avec veine fortement évolutive

L'évolution toujours croissante des charges par étage dans les turbomachines modernes conduit à considérer deux cas où les effets tridimensionnels importants risquent de rendre insuffisant le modèle des surfaces S1 de révolution ; ils sont présentés figures 5 et 6 respectivement.

Le premier (fig. 5) concerne les coupes de pied de compresseur à forte déviation et Mach amont subsonique élevé, la convergence étant importante pour éviter le décollement par ralentissement trop sévère ; l'exemple présenté figure 5 réalise 55 degrés de déviation à Mach 0,85 avec un taux de convergence du tube de courant de 0,8.

Le second (fig. 6) concerne des coupes de distributeurs de turbine basse pression "compacts" où la forte divergence est nécessaire pour éviter des nombres de Mach de sortie trop élevés ; l'exemple présenté figure 6 réalise une déviation de 80 degrés avec un nombre de Mach aval de 0,8 (amont 0,4) et un rapport de section du tube de courant de 1,6.

Calculés sur une surface S2 moyenne (écoulement de révolution) ils donnent lieu à des corrections "tridimensionnelles" du type de celles portées figures 5 et 6. On voit alors que les gradients Intrados-Extrados sont tels qu'on peut se demander si l'hypothèse de surfaces S1 de révolution est encore raisonnable. Du simple point de vue de la continuité du débit, surtout lorsque la vitesse extrados est transsonique, il parait clair que le tube de courant ne peut pas présenter la même hauteur côté extrados et côté intrados.

Il parait alors important de considérer avec intérêt toutes les tentatives modernes d'un calcul vraiment tridimensionnel et si possible transsonique.

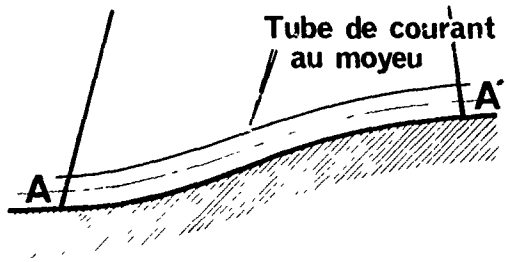

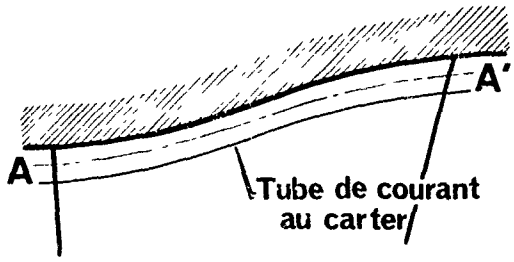

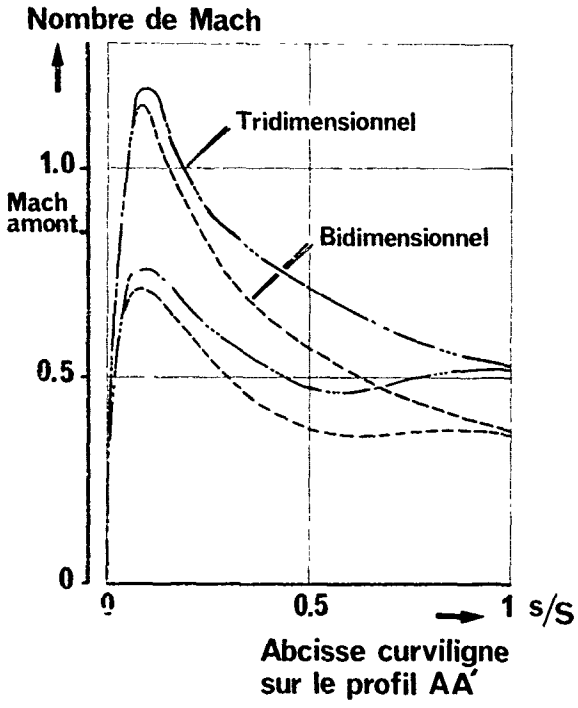

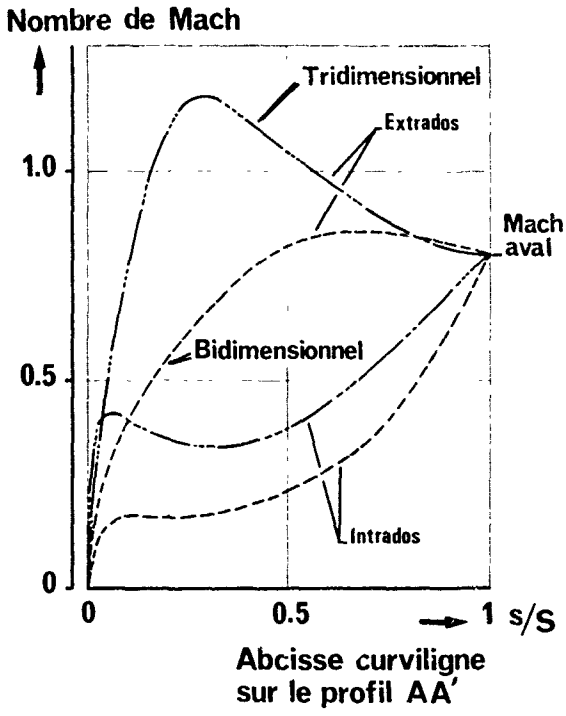

Fig.5_ Coupe de pied d'un compresseur chargé_ (redresseur)

Fig.6_ Coupe de tête d'une turbine basse pression_ (distributeur)

3. Réintroductions ou aspirations aux parois ou sur les profils

Ce cas d'application est très fréquent dans les turbomachines aéronautiques : prélèvements d'air dans les compresseurs, décharges, circulations internes, refroidissement des turbines, circulations parasites autour de viroles fixes ou de talons tournants. Une mention a déjà été faite ci-dessus (chapitre II - 1.4) de ce problème du point de vue de la formulation des échanges thermiques. Il concerne en fait deux parties du calcul de l'écoulement : la première, au niveau des parois, affecte essentiellement les écoulements secondaires. Des travaux récents tels que ceux des références [30] , [31] montrent qu'il est possible de prendre en compte de tels phénomènes dans une méthode intégrale où les écoulements sont moyennés périphériquement.

La seconde concerne surtout les émissions sur les profils qui conduisent, à l'intérieur des aubages, à une cohabitation tridimensionnelle d'écoulements à niveaux d'énergie différents. Seules, à notre connaissance, des corrections empiriques sont apportées pour tenir compte de ce phénomène.

4. Distorsion, décollement tournant, pompage :

Si l'on observe la figure 7 tirée de la référence [32] où se trouvent portés les phénomènes rencontrés dans le champ de caractéristiques d'un compresseur haute pression multi-étages très chargé, on peut se demander si le modèle choisi peut permettre de décrire de telles caractéristiques, en particulier les changements apportés par des modifications de de géométrie (versions 1, 2 et 3).

Le problème se pose alors de savoir si les calculs d'écoulements instationnaires actuellement à notre disposition peuvent être introduits dans la méthode pour prévoir le décollement tournant et le pompage (compresseurs) ou tenir compte d'effets instationnaires de distorsion, par exemple pertes de charges d'entrées d'air ou dissymétries thermiques de chambre de combustion.

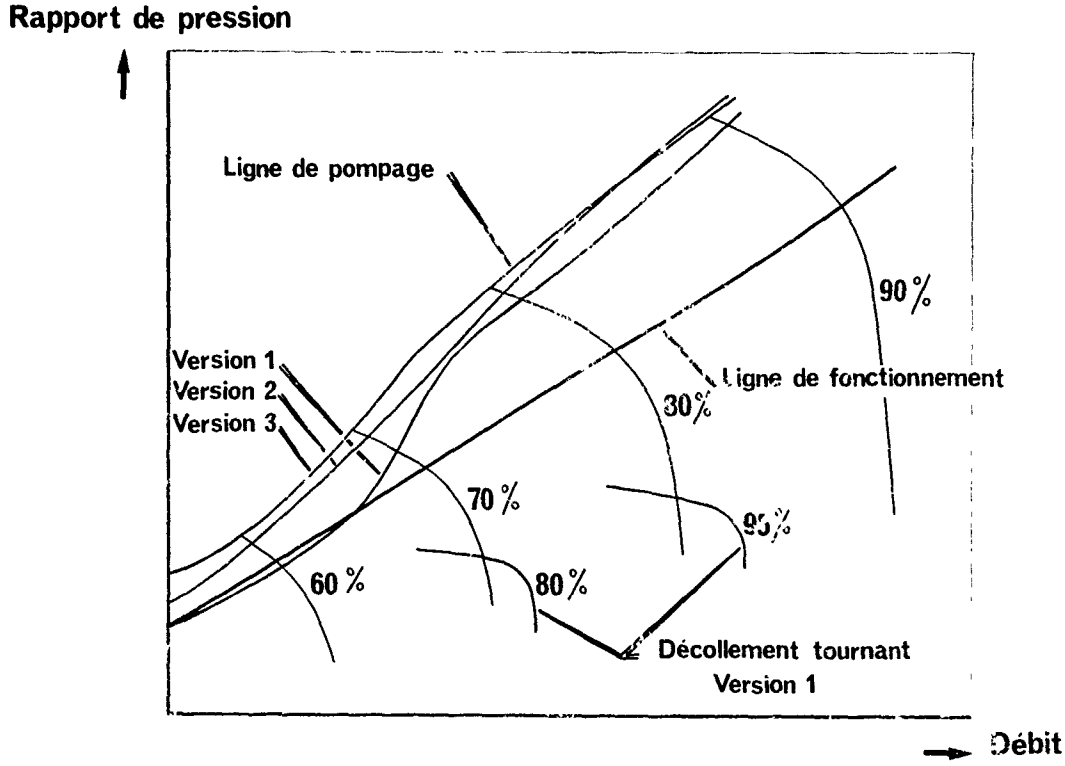

Fig.7_ Compresseur HP à 5 étages_ Doubles caractéristiques_

Deux approches sont possibles : l'une consiste à étudier la réponse du système à des perturbations instationnaires ([33] , [34]), l'autre à refondre complètement le modèle de base ([35] , [36]) en y introduisant naturellement les termes instationnaires. Les progrès récents réalisés dans ces techniques permettent d'espérer la prise en compte à moyen terme de tels phénomènes. Ce sujet déborde d'ailleurs du cadre du présent colloque.

5. Effets visqueux généralisés

Dans les moteurs aéronautiques à taux de compression très élevé (par exemple 30 : 1) il est connu des turbomachinistes que l'écoulement, dans les derniers étages de compression où le rapport de moyeu dépasse 0,9, supporte des phénomènes secondaires et en particulier des effets visqueux qui finissent par envahir toute la veine, au point d'aboutir à un écoulement de type "tuyau". Il nous parait alors difficile, du point de vue théorique, de conserver l'hypothèse des couches limites.

L'introduction de forces de viscosité et de la conductivité complique alors beaucoup la formulation et la résolution. Il semble heureusement que dans de nombreux cas pratiques l'apport d'énergie au fluide par les rotors, réitéré à chaque étage, conduise l'écoulement dans le compresseur à un état asymptotique dont au moins les performances globales se rapprochent des résultats obtenus par un calcul simplifié du type de celui présenté tableau I. La recherche d'aubages sophistiqués capables de s'adapter à des variations radiales importantes sur une faible hauteur pose du reste des problèmes de fabrication et de fiabilité aux constructeurs.

Une fois encore, la solution le plus souvent utilisée réside, pour le calcul des performances, dans un calibrage habile du schéma de pertes et d'angles introduit dans le calcul.

CONCLUSION

Après la présentation du modèle de base généralement utilisé par les turbomachinistes dans le calcul de l'écoulement, un bilan des difficultés rencontrées dans la formulation et la résolution a été effectué. L'examen d'un certain nombre de cas d'application difficiles montre ensuite que des solutions simples sont souvent possibles par modification du schéma empirique de pertes et d'angles.

Mais l'augmentation constante des performances demandées aux turbomachines modernes et le besoin d'une méthode de prévision plus précise capable d'éviter aux constructeurs de coûteuses heures d'essais, incitent le spécialiste à créer des méthodes entièrement analytiques programmées sur ordinateur puissant. Des recherches récentes, en particulier sur les écoulements secondaires et les phénomènes instationnaires permettent d'envisager de telles solutions dans un avenir proche.

On ne saurait cependant trop recommander aux chercheurs de travailler à des modèles de plus en plus représentatifs des phénomènes physiques, s'approchant ainsi de la solution générale des équations de Navier-Stokes. Leur résolution avec des conditions aux limites compliquées et des nombres de Reynolds élevés reste un problème extrêmement difficile. Mais il n'est pas d'exemple où une nouvelle méthode analytique, même à précision égale avec les méthodes empiriques, n'ait pas fait progresser la technique des turbomachines.

REFERENCES

[1] G. KARADIMAS "Définition des profils d'aubes des turbines transsoniques par une méthode d'hodographe" 2nd International Symposium on Air Breathing Engines. Sheffield - March 1974

[2] J.D. STANITZ, "Design of two-dimensional channels with prescribed velocity distributions along the channel walls" NACA TN 2593/2595 - 1952

[3] J. CALMON "L'Ecoulement d'un fluide compressible dans un étage de Turbomachine". Entropie N° 27, 28, 29 - 1969

[4] R. SIESTRUNCK et J. FABRI - "Ecoulements tourbillonnaires dans les machines axiales" ONERA N° 45 - 1950

[5] C.H. WU et L. WOLFENSTEIN "Application of radial equilibrium condition to axial flow compressor and turbine design" NACA Report 955 - 1950

[6] W. HEILMANN, H. STARKEN and H. WEYER "Cascade Wind Tunnel tests on blades designed for transonic compressors" AGARD - PEP 32nd Meeting Toulouse - Sept 1968

[7] G. MEAUZE et J.J. THIBERT "Méthode d'Etude expérimentale de grilles d'aubes transsoniques à Forte déviation" ATMA Paris 1972

[8] Chung-Hua WU "A general theory of three-dimensional flow in subsonic and supersonic turbomachines of axial, radial and mixed Flow types" NACA TN 2604 - 1952

[9] T. KATSANIS "Computer Program for calculating velocities and streamlines on a blade-to-blade streamlines on a blade-to-blade stream surface of a turbomachine" NASA TN D-4525 April 1968

[10] M. RIBAUT "Three-Dimensional calculation of flow in turbomachines with the Aid of singularities" ASME Paper N° 68-GT-20 - March 17-21 1968

[11] E. MARTENSEN "Die Berechnung der Druckverteilung on dicken Gitterprofilen mit Hilfe von Fredholmschen Integralgleichung en zweiter art" Max Planck Institut Für Strömungsforschung - Mitteilung Nr 23 - 1968

[12] S. GOPALARSNAN and R. BOZZOLA "Computation of Shoked Flows in compressor Cascades"- ASME Paper n° 72-GT-31 1972

[13] J.P. VEUILLOT "Calculs d'Ecoulements stationnaires transsoniques de Fluide Parfait dans des Grilles d'aubes données" - Rapport ONERA N° 15/7077 AY - Janvier 1974

[14] P.W. MAC DONALD " The computation of Transonic Flow through two dimensional gas turbine cascades" - ASME Paper N° 71-GT-89 - 1971

[15] T.S. LUU et G. WORMS "Calcul des grilles d'aubes transsoniques avec choc. Confrontation avec les essais en soufferie" 12e colloque d'Aérodynamique appliquée AAAF 5-7/11/75 - 1975

[16] E.M. MURMAN and J.D COLE "Calculation of Plane steady transonic flow"- AIAA Journal, vol 9, N° 1, 1971

[17] L. H. SMITH Jr. "The Radial Equilibrium Equation of Turbomachinery" - ASME Paper N° 65 WA/GTP-1

[18] R.A. NOVAK "Streamline Curvature computing procedures" - Journal of Engineering for Power, Transactions of the ASME Series A. Vol. 89 N° 4 - Oct. 1967.

[19] H. MARSH "Through-flow analysis of axial flow compressors" AGARD Lecture Series N° 39 - 1970

[20] T. KATSANIS "Use of arbitrary quasi-orthogonals for calculating flow distribution in a meridional plane of a turbomachine" - NASA TN-D-2546 - 1964

[21] L.H. SMITH Jr. And HSUAN YEH "Sweep and dihedral effects in axial-flow turbomachinery" ASME Paper 62 WA - 102 - 1962
Transactions of the ASME p. 401-416 (Sept. 1963)

[22] J.M. THIAVILLE and J. PAULON "Design of an Annular Channel for testing highly loaded compressor blades" ASME Paper 76 New Orleans Gaz Turbine Meeting 22-26 March 1976

[23] W.R. DAVIS and D.A.J. MILLER "A comparison of the matrix and streamline Curvature Methods of axial flow turbomachinery analysis. from a User's point of view" ASME Paper 74 WA/GT4 - 1974.

[24] J.G. HORLOCK "On Entropy Production in Adiabatic Flow in Turbomachines" ASME Paper N° 71-FE-3 - 1971

[25] D.H. WILKINSON "Stability, convergence and accuracy of two-dimensional streamline Curvature methods using quasi-orthogonals" Institution of mechanical engineers - Thermodynamics and Fluid Mechanics Convention, Paper 35 - 1970

[26] J.M. THIAVILLE "Tassement des compresseurs axiaux" l'Aéronautique et l'Astronautique 1974-1/44 Congrès DGLR - Baden-Baden 1971

[27] W.A. HAWTHORNE "Rotational flow through cascades, Part 1 : The components of vorticity" Quarterly Journal of Mechanics and Apply Mathematics Vol 8 pages 266-279- 1955

[28] J.G. HORLOCK "Cross flows in bounded 3D Turbulent Boundary Layers" Cambridge University CUED/A - Turbo/TR28 - 1971

[29] K.D. PAPAILLIOU "Secondary Flows in axial compressor" VKI Lecture Series 72 - Jan 13-17 - 1975

[30] G.L. MELLOR and G.M. WOOD "An axial Compressor end-wall boundary layer theory" ASME Paper 70-GT-80 Brussels May 24-28 - 1970

[31] K.D. PAPAILIOU, R. FLOT and J. MATHIEU "Secondary Flows in compressor bladings" ASME Paper 76 New Orleans Gaz Turbine Division Meeting March 22-26 1976.

[32] J.F. CHEVALIER "L'Importance des phénomènes instationnaires dans la conception et le developpement des Turbomachines" AGARD P.E.P. 46th Meeting Monterey 22-26 Sept 1975

[33] C.J. DANIELE, J. BLAHA and K SELDNER "Prediction of axial-flow instabilities in a turbojet engine by use of a multistage compressor simulation on the digital computer" NASA TM x 3134 1975

[34] J. FABRI (ONERA, France) "Rotating stall in axial flow compressors" ROYAL SOCIETY, 5th session paper N° 9 on Unsteady Flow Effets 19-21/7/1967

[35] H. TAKATA and S. NAGANO "Non linear Analysis of Rotating Stall" ASME Paper N° 72GT3 - 1972

[36] N. ORNER, D. ADLER and J. ISENBERG "The Prediction of the behaviour of axial compressors near surge" P.E.P. AGARD 46th Meeting - Monterey 22-26 Sept 1975.

ANNEXE 1

Variations périphériques de la fonction n

Une des fonctions aparaissant dans l'équation différentielle du calcul sur surfaces S2 et dont les variations en θ peuvent ne pas être négligeables a forte charge, même si le nombre d'aubes est élevé, est la fonction n définie par :

$$(1) \qquad n = \operatorname{tg}\beta = \frac{W_\theta}{Vm}$$

β étant l'angle de la vitesse relative avec le plan méridien. Dans le cas d'un nombre d'aubes suffisant on peut écrire pour une fonction F dans un canal inter-aubages :

avec I = Intrados
E = Extrados

$$(2) \qquad \frac{\partial F}{\partial \theta} = \left[\frac{F_I - F_E}{\theta_I - \theta_E}\right]_{r,z \text{ fixés}}$$

en négligeant les termes du second ordre en $(\theta_I - \theta_E)$. Cette linéarisation est même exacte si l'évolution de F à (r, z) fixés est parabolique en θ ce qui est souvent. Toute surface S2 peut être définie par

$$(3) \qquad \theta = \Theta(r,z)$$

Le vecteur normal à cette surface $\vec{N}$ a pour coordonnées dans le système cylindrique (r, θ , z) :

$$\vec{N} \left| \begin{array}{c} \dfrac{\partial \Theta}{\partial r} \\ -\dfrac{1}{r} \\ \dfrac{\partial \Theta}{\partial z} \end{array} \right.$$

La condition de glissement $\vec{N} \cdot \vec{W} = 0$ du vecteur vitesse sur cette surface s'écrit donc :

$$(4) \qquad Vr \frac{\partial \Theta}{\partial r} + Vz \frac{\partial \Theta}{\partial z} - \frac{1}{r} W_\theta = 0$$

ou encore :

$$(5) \qquad Vm \frac{\partial \Theta}{\partial m} = \frac{W_\theta}{r}$$

si $\Theta_I(r,z)$ et $\Theta_E(r,z)$ sont respectivement les fonctions (données) définissant les surfaces intrados et extrados de l'aubage, l'application de (5) à ces deux surfaces particulières conduit à l'expression :

$$(6) \qquad \frac{\partial \Theta_I}{\partial m} - \frac{\partial \Theta_E}{\partial m} = \frac{1}{r}\left(\frac{W_{\theta I}}{Vm_I} - \frac{W_{\theta E}}{Vm_E}\right)$$

En prenant n comme fonction F dans (2) et en utilisant (6) il vient :

$$(7) \qquad \frac{1}{r}\frac{\partial n}{\partial \theta} = \left(\frac{1}{r}\right)\frac{n_I - n_E}{\Theta_I - \Theta_E} = \frac{\partial (\Theta_I - \Theta_E)}{\partial m} \Big/ (\Theta_I - \Theta_E)$$

Par définition le coefficient K d'obstruction des aubages s'écrit :

$$(8) \qquad 2\pi K = \frac{2\pi r - Ze}{r} = 2\pi\left(1 - \frac{Ze}{2\pi r}\right) = \Theta_I - \Theta_E$$

donc (6) devient :

$$(9) \qquad \boxed{\frac{1}{r}\frac{\partial n}{\partial \theta} = \frac{1}{K}\frac{\partial K}{\partial m}}$$

qui détermine les variations en θ de la fonction n à partir des données K et $\frac{\partial K}{\partial m}$

COMMENTS

Comment by R.I.Lewis, Newcastle University, UK

Does the author believe in the validity of superimposing either empirical cascade data obtained between rigid side walls, or solutions obtained upon S1 surfaces, to complete blade flows? Here I am questioning the validity of stacking two-dimensional solutions to form a quasi-three-dimensional flow when the S1 solutions vary from subsonic, through transonic, to supersonic involving strong compressibility effects, three-dimensional shocks and radial flows due to locally chocked flows. It seems to me that research into these real fluid conditions should be next on the agenda.

Authors' response:

I think the process is essentially iterative between S1 and S2 solutions. If S1 surfaces are computed, it is possible to go from S2 solutions to S1 solutions using the streamtube thickness distribution as an iterative parameter. If S1 solutions are experimental cascades data, we can, at least, use a contoured wall cascade with bleeding systems and correct the loss scheme as a function of AVR distribution. I agree the so called quasi-three-dimensional calculation can be inaccurate inside the blade rows in the transonic cases but the accuracy seems to be sufficient regarding other unknowns like three-dimensional secondary flows and three dimensional shock-boundary layers interaction.

Comment by J.Chauvin, von Kármán Institute, Belgium

Quel est le temps de calcul acceptable pour une méthode à utiliser industriellement?

Authors' response:

Les programmes utilisés quotidiennement doivent être relativement rapides (moins de deux minutes sur IBM 370-145, par exemple) pour une question de débit du système d'exploitation et de temps de réponse pour l'ingénieur. D'autres programmes très puissants (problèmes transsoniques, calculs instationnaires) utilisés plus rarement peuvent être acceptables même si le temps de calcul atteint deux ou trois heures. La limite semble être le prix de fabrication de la machine elle-même (calculs tri-dimensionnels).

Comment by D.Millar, Carleton University, Canada

With reference to the figure on page 6, could you clarify the statement that the use of (rV_θ) + iteration in the off-design or analysis case is successful in avoiding the limitation imposed by relative or absolute Mach number > 1.0, even though the angle is effectively constrained by the blade angles of the machine being analyzed. In setting up our own calculations, Davis and I concluded that the fact that the angle is constrained will cause the calculations to diverge if the absolute, rather than the meridional Mach number exceeded unity.

Authors' response:

We could succeed in avoiding the sonic relative Mach number limitation because we tried only to converge on the flow angles outside the blade row. I am not sure the process is converging if the angles are imposed inside.

Comment by R.Parker, University College of Swansea, UK

Could the author please explain the double characteristics shown in Figure 7? Could these be predicted by the calculations, and, if so, how was this achieved? What physical situation exists in the machine when operating on the lower characteristics?

Authors' response:

The beginning of rotating stall phenomena could be predicted regarding the stability of the compressor's operating equations but the rotating stall phenomena like hysteresis were not predicted. The double characteristics were experimentally analyzed. They appear when rotating stall is stabilized in the first stage and when we increase the r.p.m, cells are appearing in the second stage too, and then in the third.

Comment by J.Denton, C.E.C.B., UK

For the results shown in Figures 5 and 6, how many calculating points did you have inside the blade passage to define the streamtube thickness?

Authors' response:

Only 3 or 4. The so called three-dimensional correction is significant only at the outlet in compressor. It seems necessary to have different correction on pressure and suction side, in the supersonic bubble region in particular. For the turbine case, the correction is not made downstream, but upstream, because the outlet Mach number is fixed.

Comment by H.Cox, G.E.C., UK

Coming back to the problem of computing more complicated through-flow solutions, this will lead you into situation where solutions are derived for precise flow conditions, very accurately. However, for industrial machines, blades have to be designed not for one specific condition but for a range of conditions. For a same blading geometry, you will have varying streamline geometries to match. In fact, to go to a highly complicated design system to take into account precise shapes under one condition may mislead you in terms of other conditions, where the streamline pattern may be different. The precise value of complicated computing techniques could be in doubt, to some extent, as far as design is concerned.

Authors' response:

The operation implies mixed subsonic supersonic conditions in the turbine; one needs time marching method mixed with another through-flow calculation, or else have to take into account heat and mass transfer for cooled blades; it is necessary to use methods which need a lot of time on the computer, and should be applied for the whole range of flow conditions.

Comment by J.Railly, University of Birmingham, UK

Concerning the correction for the anulus wall boundary layer development, this leads you to bring your effective end walls closer to the centre. Is this the best way to do it? You might have spent a considerable amount of time preparing the input data (blade angles, etc...) at a number of points, and the matrix coefficients have been set up. Applying the end wall correction, they have to be changed and the process repeated. Is there no better way of doing it?

Authors' response:

We do not use a matrix inversion method, and we do not have to redefine the coefficient, as we are using a streamline curvature method, which, to my mind, is better adapted in this case.

THROUGH-FLOW CALCULATIONS IN AXIAL TURBOMACHINERY: A TECHNICAL POINT OF VIEW

by
H. Marsh
Department of Engineering Science
University of Durham
Durham
England

SUMMARY

The paper outlines the through-flow theory for turbomachines and includes a detailed discussion on the methods of streamline curvature and matrix through-flow. These two methods of solution are shown to be two different techniques for calculating the flow on a mean stream surface. The Mach number limitations are outlined and the lack of a rigorous definition for the mean stream surface is discussed. The use of a consistent loss model leads to an improved form of the matrix method. Recent advances in the calculation of wall boundary layers and secondary flows are reported. Work on time-marching techniques is reviewed and it appears likely that a three-dimensional flow calculation for a cascade will soon be possible.

NOTATION

a	local velocity of sound,
B	surface thickness parameter,
c	chord,
D_{eq}	equivalent diffusion factor,
$\bar{F}$	force vector,
h	static enthalpy,
H	stagnation enthalpy,
I	rothalpy ($H - \omega r V_\theta$),
m	meridional direction,
M_m	meridional Mach number,
M_{rel}	relative Mach number,
$\bar{n}$	vector normal to the mean stream surface,
$\bar{N}$	vector normal to $\bar{n}$ and $\bar{S}$,
p	pressure,
q	velocity (secondary flow theory),
r	radius,
R	gas constant,
R_m	radius of curvature of meridional streamlines,
s	pitch,
s	entropy,
S	mean stream surface,
$\bar{S}$	vector lying in the direction of flow,
T	temperature,
v_n	secondary velocity across the blade passage,
$\bar{V}$	velocity vector,
w	secondary velocity along the span,
$\bar{W}$	relative velocity vector,
z	axial direction for through-flow analysis,
z	spanwise direction for secondary flow theory,

α air angle,

δ^* displacement thickness,

θ momentum thickness,

λ, μ angles defining the mean stream surface,

ρ density,

σ solidity (chord/pitch),

τ_w wall shear stress,

ϕ slope of meridional streamlines,

ψ stream function,

$\bar{\omega}$ angular velocity,

ω total pressure loss coefficient.

SUBSCRIPTS

1 inlet

2 outlet

r radial

z axial

θ circumferential

INTRODUCTION

The overall objective of through-flow analysis is to provide the design engineer with a method for predicting the performance of a turbomachine. By combining mathematical analysis with experimental data on the behaviour of cascades, it has been possible to develop computer programs which allow the designer to calculate the flow pattern within a turbomachine. The design engineer can now use these programs to determine the effect of changes in the blade or casing geometry. With the increasing use of these techniques, it is hoped that a more efficient aeroengine can be designed with fewer stages, less weight, better specific fuel consumption and with a reduced time for development.

Over the past fifty years, methods of flow analysis have progressed from the mean line analysis to the method of simple radial equilibrium, now part of many undergraduate courses, then to actuator disc theory, which included the effect of blade row interaction, and finally to the numerical methods of streamline curvature, matrix through-flow and time marching. The calculation of the flow in a turbomachine is a very complex mathematical problem and a major step in this field was Wu's (1) general theory in 1952. From 1952 until the early 1960s, the mathematical model for the flow in turbomachines was more advanced than the methods of computation and numerical solutions to Wu's equations could not be obtained. By 1965, the speed and storage capacity of digital computers had developed to a level where it became possible to solve the turbomachinery flow problem, first for the through-flow on a mean stream surface and later for the blade-to-blade flow. The techniques now exist for calculating the flow in turbomachines on the basis of a flow model which includes the effects of compressibility, losses, blade row interaction, secondary flows and the development of the wall boundary layers. This model is based on our understanding of the flow through linear cascades, isolated blade rows and single stage machines. As we learn more about the flow in these simple situations, then the flow model can be revised and improved to give a more accurate prediction for the performance of a multi-stage machine.

WU'S THROUGH-FLOW THEORY

In Wu's general theory for the flow in turbomachines, ref. (1), the equations of fluid flow are satisfied on two intersecting families of stream surfaces, the complete three-dimensional flow being obtained by an iterative process between the solutions for the flow on the two sets of surfaces. The two sets of stream surfaces are the S1 blade-to-blade surfaces and the S2 surfaces which pass through the blade row. The general theory assumes that the flow relative to a blade row is steady. However, at exit from a blade row, the flow and gas state vary circumferentially and if the following blade row has a motion relative to the first, then it receives a time varying inlet flow. It is only for an isolated blade row that the relative flow is steady and the general theory is therefore restricted to the annular cascade or isolated rotor row.

Wu's through-flow theory is similar to the general theory, but the equations of flow are only solved for the mean S2 stream surface. The definition of this surface will be discussed later and for the present, it will be assumed that the flow and fluid state on the surface may be regarded as average values for the flow within the blade passage. For a multi-stage turbomachine, the time dependence of the flow is removed by treating the through-flow solution as an axially symmetric flow for the duct region between each pair of blade rows.

In the r, θ, z coordinate system, the equations of continuity, motion, energy and state are

CONTINUITY

$$\frac{1}{r}\frac{\partial}{\partial r}(r\rho W_r) + \frac{1}{r}\frac{\partial}{\partial \theta}(\rho W_\theta) + \frac{\partial}{\partial z}(\rho W_z) = 0 \tag{1}$$

MOTION

$$-\frac{W_\theta}{r}\left[\frac{\partial}{\partial r}(rV_\theta) - \frac{\partial W_r}{\partial \theta}\right] + W_z\left[\frac{\partial W_r}{\partial z} - \frac{\partial W_z}{\partial r}\right] = T\frac{\partial s}{\partial r} - \frac{\partial I}{\partial r} \tag{2}$$

$$\frac{W_r}{r}\left[\frac{\partial}{\partial r}(rV_\theta) - \frac{\partial W_r}{\partial \theta}\right] - W_z\left[\frac{1}{r}\frac{\partial W_z}{\partial \theta} - \frac{\partial W_\theta}{\partial z}\right] = \frac{T}{r}\frac{\partial s}{\partial \theta} - \frac{1}{r}\frac{\partial I}{\partial \theta} \tag{3}$$

$$-W_r\left[\frac{\partial W_r}{\partial z} - \frac{\partial W_z}{\partial r}\right] + W_\theta\left[\frac{1}{r}\frac{\partial W_z}{\partial \theta} - \frac{\partial W_\theta}{\partial z}\right] = T\frac{\partial s}{\partial z} - \frac{\partial I}{\partial z} \tag{4}$$

ENERGY (ADIABATIC FLOW)

$$W_r\frac{\partial I}{\partial r} + \frac{W_\theta}{r}\frac{\partial I}{\partial \theta} + W_z\frac{\partial I}{\partial z} = 0 \tag{5}$$

STATE (PERFECT GAS)

$$\rho = f(h, s) = A\, h^{\frac{1}{\gamma-1}}\, e^{-s/R} \tag{6}$$

These equations, together with their boundary conditions, define the steady flow through any duct or blade row.

In the through-flow analysis, the flow pattern is only calculated for the mean S2 stream surface which is defined as

$$\theta = \theta(r, z) \tag{7}$$

and it is assumed that the surface is single valued in θ.

If $\overline{\partial q/\partial r}$ and $\overline{\partial q/\partial z}$ are partial derivatives taken along the stream surface, then

$$\left.\begin{aligned}\overline{\frac{\partial q}{\partial r}} &= \frac{\partial q}{\partial r} - \frac{n_r}{n_\theta r}\frac{\partial q}{\partial \theta}\\ \overline{\frac{\partial q}{\partial z}} &= \frac{\partial q}{\partial z} - \frac{n_z}{n_\theta r}\frac{\partial q}{\partial \theta}\end{aligned}\right\} \tag{8}$$

where n_r, n_θ and n_z are the components of the unit vector $\bar{n}$ normal to the mean stream surface. These special derivatives must be distinguished from simple partial derivatives. The special derivative $\overline{\partial q}/\partial r$ is the rate of change of q with r on the stream surface at a given value of z, whereas $\partial q/\partial r$ is the rate of change of q with r at given values of z and θ.

The equations governing the flow may now be written in terms of these special derivatives.

CONTINUITY

$$\frac{1}{r}\overline{\frac{\partial}{\partial r}}(r\rho W_r) + \overline{\frac{\partial}{\partial z}}(\rho W_z) = -\frac{\rho}{r n_\theta}\left[n_r\frac{\partial W_r}{\partial \theta} + n_\theta\frac{\partial W_\theta}{\partial \theta} + n_z\frac{\partial W_z}{\partial \theta}\right] = \rho\, C(r, z) \tag{9}$$

MOTION

$$-\frac{W_\theta}{r}\overline{\frac{\partial}{\partial r}}(rV_\theta) + W_z\left[\overline{\frac{\partial W_r}{\partial z}} - \overline{\frac{\partial W_z}{\partial r}}\right] = T\overline{\frac{\partial s}{\partial r}} - \overline{\frac{\partial I}{\partial r}} + F_r \tag{10}$$

$$\frac{W_r}{r}\overline{\frac{\partial}{\partial r}}(rV_\theta) + \frac{W_z}{r}\overline{\frac{\partial}{\partial z}}(rV_\theta) = F_\theta \tag{11}$$

$$-W_r\left[\frac{\overline{\partial W_r}}{\partial z}-\frac{\overline{\partial W_z}}{\partial r}\right]-\frac{W_\theta}{r}\frac{\overline{\partial}}{\partial z}(rV_\theta)=T\frac{\overline{\partial s}}{\partial z}-\frac{\overline{\partial I}}{\partial z}+F_z \tag{12}$$

where $\bar{F}=-\frac{1}{\rho n_\theta}\cdot\frac{\partial p}{\partial\theta}\cdot\bar{n}$

ENERGY

$$W_r\frac{\overline{\partial I}}{\partial r}+W_z\frac{\overline{\partial I}}{\partial z}=0 \tag{13}$$

For an inviscid flow, the force vector $\bar{F}$ is normal to the stream surface and is therefore normal to the velocity vector,

$$W_r F_r+W_\theta F_\theta+W_z F_z=0 \tag{14}$$

It is convenient to define the local shape of the stream surface by two angles λ and μ where

$$\left.\begin{aligned}\operatorname{Tan}\lambda&=\frac{n_r}{n_\theta}=\frac{F_r}{F_\theta}\\ \operatorname{Tan}\mu&=\frac{n_z}{n_\theta}=\frac{F_z}{F_\theta}\end{aligned}\right\} \tag{15}$$

The three velocity components are then related by

$$W_\theta=-W_r\operatorname{Tan}\lambda-W_z\operatorname{Tan}\mu$$

which is the geometrical condition that the flow should follow the stream surface.

Wu introduced an integrating factor B such that the equation of continuity became

$$\frac{\overline{\partial}}{\partial r}(B r\rho W_r)+\frac{\overline{\partial}}{\partial z}(B r\rho W_z)=0 \tag{16}$$

where

$$\frac{W_r}{B}\cdot\frac{\overline{\partial B}}{\partial r}+\frac{W_z}{B}\frac{\overline{\partial B}}{\partial z}=-C(r,z)$$

Equation (16) indicates that the factor B is proportional to the local angular thickness of the stream surface and as a first approximation, the thickness of the stream surface is taken as being proportional to the width of the blade passage

$$B=\frac{\text{circumferential width of blade passage}}{\text{blade pitch}}$$

For flow in a region where there are no blades, the factor B is taken as unity.

The through-flow analysis has been presented here in detail so as to provide a basis for discussing more recent developments in flow calculation methods.

STREAMLINE CURVATURE

The method of streamline curvature can be regarded as one approach to solving the through-flow equations, starting from the radial equation of motion,

$$T\frac{\overline{\partial s}}{\partial r}-\frac{\overline{\partial I}}{\partial r}+F_r=-\frac{W_\theta}{r}\frac{\overline{\partial}}{\partial r}(rV_\theta)-W_z\frac{\overline{\partial W_z}}{\partial r}+W_z\frac{\overline{\partial W_r}}{\partial z} \tag{17}$$

The last term can be expressed in terms of the meridional velocity W_m,

$$W_z\frac{\overline{\partial W_r}}{\partial z}=W_m\frac{\overline{\partial W_r}}{\partial m}-W_r\frac{\overline{\partial W_r}}{\partial r} \tag{18}$$

and introducing the steamline slope ϕ and radius of curvature R_m, the radial equation of motion becomes

$$T\frac{\overline{\partial s}}{\partial r}-\frac{\overline{\partial I}}{\partial r}+F_r=-\frac{W_\theta}{r}\frac{\overline{\partial}}{\partial r}(rV_\theta)-W_m\frac{\overline{\partial W_m}}{\partial r}-\frac{W_m^2\cos\phi}{R_m}+W_r\frac{\overline{\partial W_m}}{\partial m} \tag{19}$$

The last term in this equation can be evaluated from the equations of continuity, energy and state,

CONTINUITY

$$\frac{W_m}{\rho}\frac{\overline{\partial \rho}}{\partial m} = -\frac{W_z}{r}\frac{\overline{\partial}}{\partial r}(r\,\mathrm{Tan}\,\phi) - \frac{W_m W_r}{W_z R_m} - \frac{\overline{\partial W_m}}{\partial m} - \frac{W_m}{B}\frac{\overline{\partial B}}{\partial m} \tag{20}$$

ENERGY

$$W_m \frac{\overline{\partial h}}{\partial m} = -W_m^2 \frac{\overline{\partial W_m}}{\partial m} - W_\theta F_\theta + \frac{W_r V_\theta^2}{r} \tag{21}$$

STATE

$$\frac{1}{\rho}\frac{\overline{\partial \rho}}{\partial m} = \frac{1}{a^2}\frac{\overline{\partial h}}{\partial m} - \frac{1}{R}\frac{\overline{\partial s}}{\partial m} \tag{22}$$

where a is the local velocity of sound. Substitution of equations (20) and (21) into (22) gives

$$\frac{\overline{\partial W_m}}{\partial m}\left[1-M_m^2\right] = \frac{W_m}{R}\frac{\overline{\partial s}}{\partial m} - \frac{W_z}{r}\frac{\overline{\partial}}{\partial r}(r\,\mathrm{Tan}\,\phi) - \frac{W_m W_r}{W_z R_m} - \frac{W_m}{B}\frac{\overline{\partial B}}{\partial m} + \frac{W_\theta F_\theta}{a^2} - \frac{W_r W_\theta^2}{r a^2} \tag{23}$$

and the radial equation of motion is then

$$\begin{aligned} T\frac{\overline{\partial s}}{\partial r} - \frac{\overline{\partial I}}{\partial r} + F_r = {} & -\frac{W_\theta}{r}\frac{\overline{\partial}}{\partial r}(rV_\theta) - W_m\frac{\overline{\partial W_m}}{\partial r} - \left[\frac{1-M_z^2}{1-M_m^2}\right]\frac{W_m^2}{R_m \cos\phi} \\ & - \left[\frac{M_r^2}{1-M_m^2}\right]\frac{V_\theta^2}{r} + \left[\frac{M_r M_\theta}{1-M_m^2}\right]F_\theta \\ & + \left[\frac{W_r}{1-M_m^2}\right]\left[\frac{W_m}{R}\frac{\overline{\partial s}}{\partial m} - \frac{W_z}{r}\frac{\overline{\partial}}{\partial r}(r\,\mathrm{Tan}\,\phi) - \frac{W_m}{B}\frac{\overline{\partial B}}{\partial m}\right] \end{aligned} \tag{24}$$

This equation is often written in the form

$$W_m \frac{\overline{\partial W_m}}{\partial r} + W_m^2 K(r) + L(r) = 0 \tag{25}$$

Although the method of streamline curvature was developed independently by Smith (2), Novak (3), and Silvester and Hetherington (4), it is interesting to note that the governing equation can be derived from Wu's through-flow analysis. It follows that streamline curvature is merely one method for solving the equations for the flow on the mean stream surface.

In the streamline curvature method, it is assumed that an estimate of the flow pattern is known, so that the functions K(r) and L(r) are known functions of the radius. At any axial position, a value for the meridional velocity W_m is chosen at some radial position, such as the mid-annulus, and equation (25) is integrated radially to obtain the velocity profile. The mass flow rate at this position is calculated and compared with the specified mass flow rate. If necessary, a new value for W_m at the mid-annulus is chosen and the calculation repeated until the required mass flow rate is obtained. When the velocity profiles are known throughout the machine, then a new streamline pattern can be calculated and new values obtained for K(r) and L(r). The complete cycle of calculations is repeated until a convergence criterion is satisfied. This is one approach to the streamline curvature method, but there are several variations used by other authors.

A major difficulty in applying the streamline curvature method is that it is necessary to calculate the streamline pattern and then obtain the slope and curvature of the streamlines. The shape of the streamlines is often approximated by a spline fit through points of equal stream function on neighbouring calculation planes. The spline curve may be differentiated once to obtain the slope and twice to obtain the curvature, a procedure which can lead to a loss of accuracy.

Shaalan and Daneshyar (5) have suggested that a more accurate estimate of the curvature is obtained by fitting a second spline curve to the variation of slope and then differentiating to obtain the curvature. They refer to this as a double-spline fit. The most important conclusions reached by Shaalan and Daneshyar are that a single spline fit requires about 10 points per wavelength in order to obtain a good estimate for the curvature and that a double spline fit requires only four or five points. In a turbomachine, the basic wavelength is the length of a stage and it follows that a good estimate for the curvature of the streamlines can only be obtained by taking calculation planes within the blade rows. This is relatively simple for subsonic flows, but in a transonic flow with shocks, the mathematical model may not be adequate. Many streamline curvature programs analyse the flow in transonic compressors by placing the calculation planes outside the blade rows and treating the blade rows as devices having a specified behaviour, even though this may reduce the accuracy of the overall calculation. The level of agreement which has been obtained between experiments and the predictions based on calculation planes placed outside the blade rows suggests that the solution for the flow pattern may not be too sensitive to errors in the calculation of the curvature of the streamlines.

MATRIX THROUGH-FLOW ANALYSIS

An alternative method for solving the equations governing the flow on the mean stream surface is to define a stream function ψ where

$$\left.\begin{aligned} \frac{\partial \psi}{\partial r} &= B r \rho W_z \\ \frac{\partial \psi}{\partial z} &= -B r \rho W_r \end{aligned}\right\} \tag{26}$$

The radial equation of motion can then be expressed as

$$\frac{\partial^2 \psi}{\partial r^2} + \frac{\partial^2 \psi}{\partial z^2} = \frac{\partial \psi}{\partial r}\frac{\partial}{\partial r}\left[\ln (B r \rho)\right] + \frac{\partial \psi}{\partial z}\frac{\partial}{\partial z}\left[\ln (B r \rho)\right] + \frac{B r \rho}{W_z}\left[\frac{\partial I}{\partial r} - T\frac{\partial s}{\partial r} - F_r - \frac{W_\theta}{r}\frac{\partial}{\partial r}(r V_\theta)\right] \tag{27}$$

or

$$\frac{\partial^2 \psi}{\partial r^2} + \frac{\partial^2 \psi}{\partial z^2} = q(r,z) \tag{28}$$

This is often referred to as Wu's principal equation; it is a non-linear equation, but it can be solved by the repeated solution and correction of the quasi-linear equation (28). For a given distribution q(r, z), a solution is obtained for the stream function ψ, the function q(r, z) is then corrected using the new values for ψ and the process is repeated until a convergence criterion is satisfied. The basic method of solution was outlined by Wu (1) in 1952, but it was not until 1965 that the storage capacity and speed of computers were sufficient to allow numerical solutions of equation (28), ref. (6).

Mathematically, Wu's analysis is extremely simple, the difficulty lies in obtaining numerical solutions for the stream function. Many finite difference approximations use a rectangular grid of points, since this leads to simple expressions for the derivatives. However, for calculating the flow through a turbomachine, a more suitable form of grid is a distorted or non-rectangular grid. Figure 1a shows the grid used in ref. (6) which has radial lines with equally spaced points between the inner and outer casings. The machine casings form curved grid lines and there are no additional difficulties for grid points which lie close to or on the boundaries. There is an automatic refining of the grid as the annulus height is reduced. The use of radial lines in ref. (6) was dictated by the limited storage capacity of the computer. The leading and trailing edges of a blade row may not be radial and if sufficient computer storage is available, then it is more convenient to define a grid in which the straight lines may be inclined to the radial direction, Figure 1b.

In the grid shown in Figure 1a, there is no difficulty in forming finite difference approximations for the radial derivatives, but there is no simple expression for derivatives with respect to z. The textbooks available in 1965 offered very little guidance since they were largely concerned with square and rectangular meshes, meshes for which the finite difference approximations could be derived by hand calculation. It was realised that the derivation of finite difference approximations was a very systematic procedure and that a computer program could be written to obtain a finite difference in terms of the function values at neighbouring points, points which need not be regularly spaced. Ref. (6) describes a general procedure for obtaining the finite difference approximations in the distorted mesh of Figure 1a. It was found that as the distorted mesh became locally square or rectangular, then more than one finite difference approximation was possible and the procedure broke down. This singularity was removed by re-phrasing equation (28) as

$$\frac{\partial^2 \psi}{\partial r^2} + \frac{\partial^2 \psi}{\partial z^2} + E\frac{\partial \psi}{\partial z} = q(r,z) + E\frac{\partial \psi}{\partial z} = Q(r,z) \tag{29}$$

where

$$E = 2\left[\frac{1}{z_{i+1} - z_i} - \frac{1}{z_i - z_{i-1}}\right]$$

With the problem in this form, the procedure for determining the finite difference approximation cannot become singular. The principal equation (29) and its boundary conditions can be written in the matrix form

$$[M][\psi] = [Q] \tag{30}$$

where $[\psi]$ and $[Q]$ are column vectors and $[M]$ is a band matrix which remains unchanged throughout the calculation. Only the band of non-zero elements is formed and stored in the computer. Equation (30) is solved by calculating the band triangular factors $[L]$ and $[U]$ where

$$[L][M] = [U]$$

and then re-phrasing equation (30) as

$$[U][\psi] = [L][Q] \tag{31}$$

The matrices $[U]$ and $[L]$ remain unchanged throughout the calculation. The method of solution for the

stream function ψ is to solve for a given vector $[Q]$, to correct $[Q]$ using the new flow pattern and then repeat the cycle of calculation until convergence is obtained. Although many workers in this field have followed ref. (6) and used the matrix method, a few have solved equation (30) using a Gauss-Seidel technique. The main advantage of the matrix method is that it avoids the possibility of numerical instability on the inner loop of the calculation.

A UNIFIED APPROACH TO THROUGH-FLOW ANALYSIS

For several years, the matrix through-flow and streamline curvature methods were regarded as two separate methods for calculating turbomachinery flows. It was not until 1970, ref. (7), that it was shown that these two mathematical techniques were based on the same model and that they could be regarded as two different methods for solving the governing equations for flow on the mean stream surface. The analysis of ref. (7) has been repeated here to draw attention to the common basis for these two mathematical techniques.

MACH NUMBER LIMITATIONS

It is a fundamental assumption of the matrix through-flow and streamline curvature methods that there exists a unique solution for the flow in a turbomachine. It is clear that in the matrix method, the solution for the flow pattern on each cycle of the iterative process is itself unique, this being the solution of a single matrix equation for the stream function. However, at each grid point there are two solutions for the density, one corresponding to subsonic flow and the other to supersonic flow. In ref. (6), the ambiguity was avoided by restricting the analysis to flows in which the Mach number limitations at all grid points are:

(a) duct flows, $M_m < 1$,
(b) flow within or behind a blade row, $M_{rel} < 1$

Later, Gelder (8) suggested that these Mach number limitations might be relaxed if the velocity components were calculated using a value for the density which is taken from the previous iteration. The calculation of density then lags behind that of velocity, but if the process converges, then this is not important. Smith (9) has used Gelder's modification and has found that it improves the stability of the matrix method at high Mach numbers. According to Gelder, this technique allows the matrix method to continue operating at Mach numbers of up to 1.2, but the solution cannot include any shocks.

The uniqueness of the streamline curvature solutions is discussed in ref. (10) and it is shown that if the density is calculated on the basis of the current iteration, then a sufficient condition for uniqueness is

(a) for duct flows, $M_m < 1$,
(b) for the flow within or behind a blade row, $M_{rel} < 1$ at all radii, or $M_{rel} > 1$ at all radii

These conditions are the same as those which are applied to the matrix method in ref. (6). Uniqueness can be assured by evaluating the mass integral for continuity using the values of density from the previous iteration. It should be noted that the conditions given here are sufficient to ensure uniqueness; the method may converge to a true solution at higher Mach numbers, but the uniqueness cannot be shown by the analysis of ref. (10).

More recently Davis and Millar (11) have compared the two methods of solution and they have arrived at similar conclusions concerning the Mach number limitations. They suggest that to some extent, the problem might be overcome by choosing a coarse grid to avoid areas of difficulty. This approach is similar to that which is frequently used with the streamline curvature method, namely to place all of the calculation planes in the duct regions.

DEFINITION OF THE MEAN STREAM SURFACE

The use of the matrix through-flow or the streamline curvature method within the blade rows requires the definition of the mean stream surface. This may be loosely defined as the average for all of the S2 stream surfaces. This is not a rigorous definition and there is a need to arrive at a method for specifying the mean stream surface for an arbitrary cascade. Horlock and Marsh (29) have considered several simple flow models for cascades, including flow on a mean stream surface. Their conclusion is that it is not possible to define a surface such that the flow and gas state at all points on that surface are the same as the passage averaged values for the actual flow. It is therefore not possible to give a definition of the mean stream surface for either incompressible or compressible flow. The analysis of ref. (29) shows that the mean stream surface flow model can predict the correct overall change of the flow across the blade row, but the calculated flow variations may not provide a good local representation of the averaged actual flow within the blade passage. This is a disappointing conclusion in that it suggests that placing calculation planes within the blade row and thereby refining the grid, will not necessarily give a numerical solution for the flow pattern which approaches the actual flow. As the grid is refined, the solution approaches the exact mathematical solution for the flow model, but it is known that the flow model cannot fully represent the local passage averagod flow. Horlock and Marsh did not estimate the difference between the flow calculated for the mean stream surface and the averaged actual flow; it is possible that the difference is small and that the failure to obtain an exact local representation has little effect on the overall accuracy of flow calculations for turbomachines. A mean stream surface which has the correct inlet and exit flow angles will give the correct overall changes of flow across the blade row and the shape within the blade passage should be chosen to be representative of the S2 stream surfaces.

A COMPARISON OF THE MATRIX AND STREAMLINE CURVATURE METHODS

The most comprehensive comparison of the two methods of solution is that of Davis and Millar (11) who have compared solutions for

(a) a duct flow,
(b) a transonic fan, and
(c) a three stage axial flow compressor.

They found little difference in the difficulty, or ease, of programming, but the matrix method required about 50% more high speed storage in the computer. The matrix method converged within a few iterations whereas the streamline curvature program required 40 to 60 iterations, probably due to difficulty in calculating the curvature of the streamlines. The net result was that the matrix method required less computer time. Their conclusion was that there was a marginal advantage for the matrix method on the grounds of greater stability and accuracy. It was surprising that their paper attracted very little discussion from other users.

A CONSISTENT LOSS MODEL FOR THE MATRIX METHOD

The through-flow analysis has been based on the following six equations, continuity (1), motion (3), energy (1), and state (1). These are the equations for a reversible adiabatic flow and from the equations of motion and energy, it can be shown that entropy remains constant along a streamline. This is contrary to the use of a loss model since a loss of stagnation pressure on passing through a cascade requires an increase in entropy.

Bosman and Marsh (12) have examined this problem and have suggested the use of a loss model in which a dissipative force $\bar{D}$ opposes the velocity vector. For the flow on a prescribed stream surface, they define an S-n-N coordinate system as shown in Figure 2. The body force $\bar{F}$ acts in the n direction, the dissipative force D opposes the velocity vector and the equation of motion for the N direction does not contain a component of either $\bar{F}$ or D. For flow on the mean stream surface, there are six governing equations,

1. continuity,
2. motion (in the N direction),
3. entropy (the loss model),
4. geometrical condition for the flow to follow the surface,
5. energy,
6. state.

Bosman and Marsh show that the equation of motion for the N direction can be written in terms of the r, θ, z coordinate system. The analysis leads to a modified form of Wu's principal equation,

$$\frac{\partial^2\bar{\psi}}{\partial r^2} + \frac{\partial^2\bar{\psi}}{\partial z^2} = \frac{\partial\bar{\psi}}{\partial r}\frac{\partial}{\partial r}\left[\ln(B r\rho)\right] + \frac{\partial\bar{\psi}}{\partial z}\frac{\partial}{\partial z}\left[\ln(B r\rho)\right] + (B r\rho)^2 \frac{dI}{d\psi}$$
$$- \frac{B r\rho T}{W^2}\left[\frac{\partial s}{\partial r}(V_z - W_\theta \tan\mu) - \frac{\partial s}{\partial z}(V_r - W_\theta \tan\lambda)\right]$$
$$+ B\rho\left[\frac{\partial}{\partial r}(rV_\theta)\tan\mu - \frac{\partial}{\partial z}(rV_\theta)\tan\lambda\right] \qquad (32)$$

This equation can be solved by the matrix method described earlier. By formulating the principal equation in the r, θ, z coordinate system, the existing matrix through-flow programs can easily be modified to include this consistent loss model.

TIME MARCHING

For the flow in a duct or nozzle, the governing equations are elliptic for subsonic flow, $M_m < 1$, and hyperbolic for supersonic flow, $M_m > 1$. This means that both the matrix through-flow and the streamline curvature methods can be used for calculating subsonic axially symmetric duct flows, including swirl.

If the flow in a duct or nozzle is supersonic, then the governing equations become hyperbolic and the method of solution differs from that for elliptic equations. For a convergent-divergent nozzle operating at a high pressure ratio, the upstream flow may be subsonic, the sonic velocity occurs at the throat, there is a region of supersonic flow followed by a shock and a downstream region of subsonic flow to reach the required exit pressure. The boundaries for the region of supersonic flow are not known in advance, but form part of the solution. A method of solution is required which can deal with subsonic and supersonic flows and locate the correct position and strength of any shock.

Although the equations for steady flow are elliptic for subsonic flow and hyperbolic for supersonic flow, the equations for unsteady flow are always hyperbolic. This suggests that if the time dependent equations of continuity, motion and energy are used, then the same method of solution may be applicable to both subsonic and supersonic flows. The steady state flow, with regions of supersonic and subsonic flow, is then regarded as the ultimate steady state for the time dependent flow. The basic technique is to start with an approximate solution and then to integrate, or march, the time dependent equations forward in time until the steady state solution is reached with sufficient accuracy. A major problem is stability and this is often achieved by taking very small time steps, or by introducing artificial viscosity.

In 1971, Marsh and Merryweather (13) described a stable time marching technique which was based on finite differences and did not rely on the use of artificial viscosity to achieve stability. It was found that several stable procedures could be developed for flow in convergent-divergent nozzles. The characteristic feature of the stable schemes was that the derivatives of all quantities other than pressure were approximated by backward differences, while the derivative of pressure contained a forward element. Figure 3 shows the contours of constant Mach number for flow in a two dimensional divergent nozzle, ref. (13). There is seen to be a clearly defined shock.

The computer program developed by Marsh and Merryweather (13) was relatively slow, some 2700 iterations being required to obtain the solution shown in Figure 3 to an accuracy of 0.01 per cent. Further work by Daneshyar and Glynn (14) has been based on the method of characteristics and this has led to a much faster method of calculation. This method has been extended by Glynn to deal with cascade flows.

In 1972, McDonald (15) used a time marching method to calculate the pressure distribution around aerofoils in cascade. The problem was formulated in terms of a finite area approach which led to the conservation equations in an integral form. The flow was assumed to be isentropic on the grounds that only weak shocks are normally encountered in cascades. McDonald obtained very good agreement between his calculated pressure distribution and that measured in the experimental cascade. The use of the isentropic flow assumption is interesting in that Marsh and Merryweather had tried this same assumption for purely subsonic flows and had experienced a severe numerical instability, which was removed by allowing the program to calculate for itself that the flow was isentropic.

In 1974, Denton (16) proposed a time marching scheme for cascade flows using a simpler grid than that of McDonald. Denton's grid consists of quasi-streamlines and straight lines across the blade passage. The conservation equations for mass, momentum and energy are derived for a control volume. Instead of assuming isentropic flow, Denton assumes constant stagnation enthalpy, an assumption which becomes exact when the solution converges to the steady state flow. In Denton's scheme, the pressure at the central point of an element is assumed to act on the upstream face of the element, whereas the velocity at the centre controls the flow through the downstream face. The maximum time step for this scheme is far greater than for the method of Marsh and Merryweather (13).

Denton has applied his time marching method to calculating the blade to blade flow in several cascades and has obtained encouraging results. He has also extended the method to three-dimensional flows, although this does require a large amount of high speed store in the computer. The predictions obtained with this program have been compared with experiments performed with a rectangular duct having 60° of turning. Good agreement was obtained between the calculated and experimental pressure variations for the four corners of the duct. This time marching scheme should be capable of extension to deal with three-dimensional flow in cascades.

THE LOSS MODEL

When calculating the flow in a turbomachine, it is necessary to estimate the loss of relative stagnation pressure, or the entropy change, on passing through each blade row. This problem is perhaps best phrased in terms of entropy in that it is then clear that the effect of loss in a multi-stage machine is cumulative. It is the radial gradient of entropy which enters directly in the governing equations for the matrix method. As the flow passes through each blade row, then for adiabatic flow, the entropy steadily increases along the streamlines. For flow through an isolated blade row, the change in entropy and the entropy gradient are small and have little effect on the flow. However, in a multi-stage machine, the flow passes through many blade rows, there is a large change of entropy and the entropy gradient term becomes more important. For the multi-stage machine, the accurate prediction of performance is dependent on forming a good loss model for each blade row.

The early through-flow programs used a polytropic efficiency as a simple method for including losses in the calculation. This was quickly superseded by incorporating Lieblein's (17) loss correlation as a subroutine which could be replaced as better data became available. Lieblein studied the flow in two dimensional cascades and found that the ratio of the wake momentum thickness, θ, to the blade chord, c, could be correlated with the loss coefficient ω,

$$\frac{\theta}{c} \simeq \frac{\omega \cos\alpha_2}{2\sigma}\left[\frac{\cos\alpha_2}{\cos\alpha_1}\right]^2$$

The losses in this model are caused by fluid friction, flow separation and wake mixing. In the discussion of Lieblein's paper, Klapproth suggested the use of a modified equivalent diffusion factor which included the effect of a change of axial velocity across the blade row and a radial movement of the streamlines.

Later Swan (18) showed that a similar correlation to that of Lieblein could be obtained for compressor data. Swan's correlation is in two parts, the first relating θ/c to the equivalent diffusion factor D_{eq} at the minimum loss condition,

$$\left(\frac{\theta}{c}\right)^* \quad \text{vs} \quad D_{eq}^*$$

the asterisk denoting minimum loss. The second part was a correlation for operation away from minimum loss,

$$\left[\left(\frac{\theta}{c}\right) - \left(\frac{\theta}{c}\right)^*\right] \quad \text{vs} \quad \left[D_{eq} - D_{eq}^*\right]$$

which gave curves which were independent of radial position, but very dependent on Mach number.

Swan also suggested that the loss model could be extended to transonic blade rows by adding a shock loss coefficient, ω_s, directly to the profile loss coefficient, ω_p, predicted from D_{eq},

$$\omega_{total} = \omega_s + \omega_p$$

The Swan-Lieblein loss model has been found to give satisfactory agreement between the predicted and observed performance of compressors. However, these correlations are best regarded as a temporary approximation for the loss model, a starting point which must be revised as more data becomes available.

ANNULUS WALL BOUNDARY LAYERS

As the flow passes through a turbomachine, boundary layers develop on the hub and tip casings. These wall boundary layers cause a reduction in flow area and as shear layers, they give rise to secondary flow when the flow is turned. Separation may also occur causing an end wall stall. In 1967, Stratford (19) put forward a simple method for calculating the development of the wall boundary layer, this being based on the momentum integral equation for the axial direction. Stratford assumed that the pressure distribution around the blade was transmitted unchanged through the boundary layer and he did not consider the cross flow. There was considerable debate about the validity of Stratford's assumptions, but the method did lead to reasonable predictions for the growth of the wall boundary layer.

In 1972, Marsh and Horlock (20) reviewed the work on wall boundary layers, including that of Stratford and the theory of Mellor and Wood (21). After examining the earlier work, it was suggested that instead of assuming that the pressure was transmitted through the boundary layer, the analysis might be based on the passage averaged mean pressure $\bar{p}$ being constant through the boundary layer. With this new approach, the change in the mean pressure across the cascade is the same for the mainstream flow and for the boundary layer. It is shown in ref. (20) that this assumption leads to a variation of the blade force within the boundary layer and when this force defect term is included in the analysis, then the axial and tangential momentum integral equations both reduce to

$$\frac{d}{dz}\left(V_z^2\theta_{zz}\right) + \delta_z^x V_z \frac{dV_z}{dz} + V_z^2 \tan\alpha\left(\theta_{zz} + \delta_z^x\right)\frac{d\alpha}{dz} = \frac{\tau_{wz}}{\rho} \qquad (33)$$

This equation is the same as that which is obtained from the analysis of Mellor and Wood with the assumption that the effective blade force is normal to the mainstream flow. Marsh and Horlock compared their predictions from equation (33) and those of Stratford with the experimental results obtained by Gregory-Smith (22) for a row of inlet guide vanes, Figure 4. For these highly loaded blades, a turning of about 54° at the tip, Stratford's method is seen to give better agreement with the experimental results.

Horlock and Perkins (23) re-examined the assumptions of $\bar{p}$, or $\partial\bar{p}/\partial z$, being constant through the boundary layer and suggested that this might be replaced by $\partial p/\partial x$ being constant. With this modification, the axial force deficit is zero and the axial momentum integral equation is

$$\frac{d}{dz}\left(V_z^2\theta_{zz}\right) + \delta_z^x V_z \frac{dV_z}{dz} = \frac{\tau_{wz}}{\rho} \qquad (34)$$

which is the equation derived by Stratford (19) in 1967. The work of Horlock and Perkins provides a more rigorous basis for Stratford's method of calculating the blockage due to the wall boundary layers. In Part II of ref. (23), the authors discuss the application of wall boundary layer calculations in through-flow methods. They suggest that for the matrix method, the values for the stream function on the hub and tip casings can be modified to allow for the presence of the wall boundary layer. The calculation of the wall boundary layer can then become an integral part of the through-flow calculation.

SECONDARY FLOW

When a shear flow, such as a wall boundary layer, is turned in a cascade, then at exit from the cascade there is a streamwise vorticity. This problem was analysed by Hawthorne (24) who identified three streamwise components of vorticity at exit from a blade row,

1. the distributed secondary vorticity in the blade passage

$$\xi_{sec} = \xi_x \frac{\cos\alpha_1}{\cos\alpha_2} + \frac{\xi_n}{\cos\alpha_1\cos\alpha_2}\left[\frac{(\sin 2\alpha_2 - \sin 2\alpha_1)}{2} + \alpha_2 - \alpha_1\right] \qquad (35)$$

2. the trailing filament vorticity

$$\frac{1}{s}\cdot\xi_{fil} = -\frac{\xi_n(\alpha_2 - \alpha_1)}{\cos\alpha_1} \qquad (36)$$

3. the trailing shed vorticity

$$\frac{1}{s}\xi_{shed} = -\xi_n\cos\alpha_1\left[\tan\alpha_2 - \tan\alpha_1\right] \qquad (37)$$

At exit from the cascade, a secondary flow stream function can be defined

$$v_n = -\frac{\partial \psi}{\partial z}$$

$$w = \frac{\partial \psi}{\partial y_n}$$

where v_n is the velocity across the blade passage in the y_n direction and w is the velocity along the span of the blades in the z direction. The secondary flow stream function is given by

$$\frac{\partial^2 \psi}{\partial y_n^2} + \frac{\partial^2 \psi}{\partial z^2} = \xi_{sec} \tag{38}$$

and the variation of exit flow angle is

$$\Delta \alpha_2 = \frac{v_n}{q}$$

where q is the velocity in the direction of the mainstream flow. Experiments with linear cascades have shown good agreement between Hawthorne's theory and the measured variation of exit flow angle.

An alternative approach to secondary flow theory has been given by Came and Marsh (25). By using Kelvin's circulation theorem, expressions were derived for the distributed secondary and trailing filament vorticities which agreed with Hawthorne's analysis. However, a new expression was obtained for the trailing shed vorticity,

$$\frac{1}{s}\xi_{shed} = \frac{-\xi_n}{2\cos\alpha_1}\left[\sin 2\alpha_2 - \sin 2\alpha_1\right] - \xi_s \cos\alpha_1 - q_2 \cos\alpha_2 \frac{d\alpha_2}{dz} \tag{39}$$

Came and Marsh showed that with this new expression for ξ_{shed}, the strength of the trailing vortex sheet was entirely consistent with the calculated value for the secondary velocity, w, along the span of the blades. The new theory also removed certain anomalies from secondary flow theory.

Figure 5 shows the variation of exit angle for a cascade at N.G.T.E. tested by Dr. S.L. Dixon. The cascade date is $\alpha_1 = 0^\circ$, $\alpha_2 = -62.4^\circ$ and $\delta/s^* = 0.60$. The inlet boundary layer was 25 mm in thickness with a 1/7th power law profile. In order to avoid a discontinuity in the normal component of vorticity at the edge of the boundary layer, the calculations have been based on a smoothed profile with the same displacement thickness and zero slope at the edge of the boundary layer. The theoretical variation in the exit flow angle is seen to be in good agreement with the measured values.

Using Dixon's data, Dunham (26) has calculated the pitch averaged streamwise vorticity $\bar{\xi}$ for the downstream flow and this can be compared with the theoretical values:

(a) Hawthorne

$$\bar{\xi} = \xi_n \tan\alpha_2 \left[\frac{\cos\alpha_2}{\cos\alpha_1} - \frac{\cos\alpha_1}{\cos\alpha_2}\right] \tag{40}$$

(b) Came and Marsh

$$\bar{\xi} = -q_2 \frac{d\alpha_2}{dz} \tag{41}$$

In Figure 6 the experimental results are seen to lie close to the curve predicted by equation (41). The experiments suggest that the new expression for the trailing shed vorticity, equation (39), gives better results for the vorticity which passes downstream to the next blade row.

The theory of secondary flow has been extended to compressible flow in cascades, ref. (27). The analysis is based on applying Kelvin's circulation theorem for compressible flow to the flow through a cascade. It has been shown that for a compressor cascade, a decelerating flow, the effect of a high inlet Mach number is to increase the distributed secondary vorticity. For a turbine nozzle, the theory indicates that compressibility has little effect of the distributed secondary vorticity. These results are in agreement with the early work of Loos (28) on compressible secondary flow.

CONCLUSIONS

Although the method of through-flow analysis was published by Wu (1) some 24 years ago, it is only within the past eleven years that digital computers have become sufficiently large and fast to allow the method to be applied. This paper has reviewed the progress which has been made since 1965 with the streamline curvature and matrix through-flow methods. It has been shown that although these two methods were developed independently, they can be regarded as two different methods for solving the same governing equations for flow on the same mean stream surface. The continued use of both methods over a period of eleven years indicates that neither has shown sufficient superiority to become the accepted method of solution for turbomachinery flows.

With the two methods of through-flow analysis, it is now possible to estimate the performance of a

turbomachine operating on-design or off-design. However, the accuracy of the predictions is dependent on the mathematical model. There remains a need for more accurate methods for estimating the losses, for calculating the development of the wall boundary layer and for predicting the secondary flows. These are all areas of current research and we may expect further improvements in through-flow analysis during the next few years.

The development of time marching methods has been discussed in this paper. This technique is now being applied to transonic cascade flows and also to flow in three-dimensional ducts. It is likely that within the next year, solutions will be obtained for three-dimensional flow in linear and annular cascades. However, this does not imply that a numerical solution can be obtained for three-dimensional flow in a multi-stage turbomachine. For a multi-stage machine, the relative flow in each blade row is time dependent and the numerical solution would require a very large computer and a time marching program capable of calculating the unsteady flow. This may become technically feasible within the next few years, but it is doubtful whether our understanding of the physical flow will be sufficient to support this advance in computation techniques.

REFERENCES

1. Wu, C.H. A general theory of three-dimensional flow in subsonic and supersonic turbomchines of axial, radial and mixed flow types, N.A.C.A. TN2604, 1952

2. Smith, L.H. The radial equilibrium equation of turbomachinery, Trans. A.S.M.E., Series A, vol 88, 1966

3. Novak, R.A. Streamline curvature computing procedures for fluid flow problems, A.S.M.E. paper 66-WA/GT-3, 1966

4. Silvester, M.E. and Hetherington, R. Three-dimensional compressible flow through axial flow turbomachines, published in Numerical Analysis - An Introduction, Academic Press, 1966

5. Shaalan, M.R.A. and Daneshyar, H. Methods of calculating slope and curvature of streamlines in fluid flow problems, Proc. I.Mech.E., vol 186, 1972

6. Marsh, H. A digital computer program for the through-flow fluid mechanics in an arbitrary turbomachine using a matrix method, N.G.T.E. Report R282, 1966, also Aero. Res. Counc. R & M 3509, 1968

7. Marsh, H. The through-flow analysis of axial flow compressors, AGARD Lecture Series 39, Advanced Compressors, 1970

8. Gelder, D. private communication, 1969

9. Smith, D.J.L. Computer solutions of Wu's equations for the compressible flow through turbomachines, Int. Symp. Fluid Mech. Turbomach., Penn. State Univ., 1970

10. Marsh, H. The uniqueness of turbomachinery flow calculations using the streamline curvature and matrix through-flow methods, I.Mech.E., Jnl. Mech. Eng. Sci., vol 13, no 6, 1971

11. Davis, W.R. and Millar, D.A.J. A comparison of the matrix and streamline curvature methods of axial flow turbomachinery analysis, from a user's point of view, Trans. A.S.M.E., Series A, vol 97, no 4, 1975

12. Bosman, C. and Marsh H. An improved method for calculating the flow in turbomachines, including a consistent loss model, I.Mech.E., Jnl. Mech. Eng. Sci., vol 16, no 1, 1974

13. Marsh, H. and Merryweather, H. The calculation of subsonic and supersonic flow in nozzles, Symp. on Internal Flows, I.Mech.E., paper 22, 1971

14. Daneshyar, H. and Glynn, D.R. The calculation of flow in nozzles using a time marching technique based on the method of characteristics, Int. Jnl. Mech. Sci., 1973, p 921

15. McDonald, P.W. The computation of transonic flow through two-dimensional gas turbine cascades, A.S.M.E., paper 71-GT-89, 1971

16. Denton, J.D. A time marching method for two and three dimensional blade to blade flows, A.R.C. 35567, 1974

17. Lieblein, S. Loss and stall analysis of compressor cascades, Trans. A.S.M.E. Series D, vol 81, 1959

18. Swan, W.C. A practical method of predicting transonic compressor performance, Trans. A.S.M.E., Series A, vol 83, 1961

19. Stratford, B.S. The use of boundary layer techniques to calculate the blockage from the annulus boundary layers in a compressor, A.S.M.E. paper 67-WA/GT-7, 1967

20. Marsh, H. and Horlock, J.H. Wall boundary layers in turbomachines, I.Mech.E., Jnl. Mech. Eng. Sci., vol 14, no 6, 1972

21. Mellor, G.L. and Wood, G.M. An axial compressor end-wall boundary layer theory, Trans. A.S.M.E., Series D, vol 93, 1971

22. Gregory-Smith, D.G. An investigation of annulus wall boundary layers in axial flow turbomachines, A.S.M.E. paper 70-GT-92, 1970

23. Horlock, J.H. and Perkins, H.J. Annulus wall boundary layers in turbomachines, AGARD, Agardograph 185, 1974

24. Hawthorne, W.R. Rotational flow through cascades, Part I: The components of vorticity, Q. Jnl. Mech. appl. Math., vol 8, pt 3, 1955

25. Came, P. and Marsh, H. Secondary flow in cascades: two simple derivations for the components of vorticity, I.Mech.E., Jnl. Mech. Eng. Sci., vol 16, no 6, 1974

26. Dunham, J. private communication

27. Marsh, H. Secondary flow in cascades: The effect of compressibility, ARC 35835, 1975 to be published as R & M 3778

28. Loos, H.G. Compressibility effects in secondary flows, J. Aero. Sci., vol 23, pp 76-80, 1956

29. Horlock, J.H. and Marsh, H. Flow models for turbomachines, I.Mech.E., Jnl. Mech. Eng Sci., vol 13, no 5, 1971

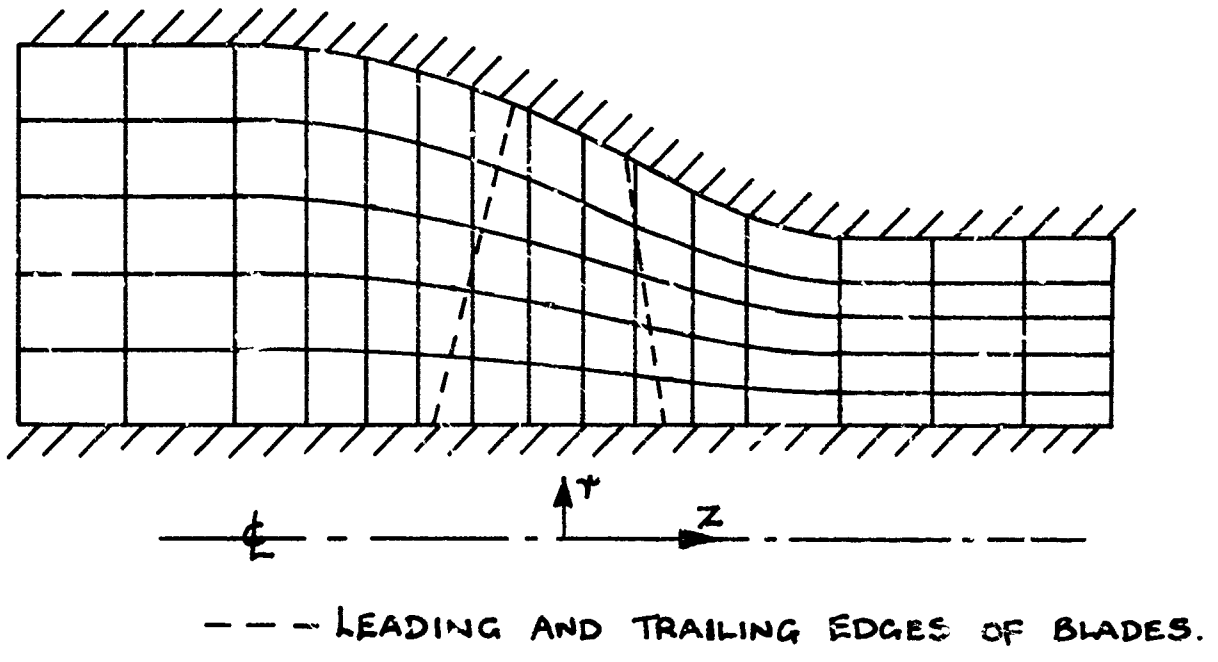

Fig. 1(a) Distorted grid. (6)

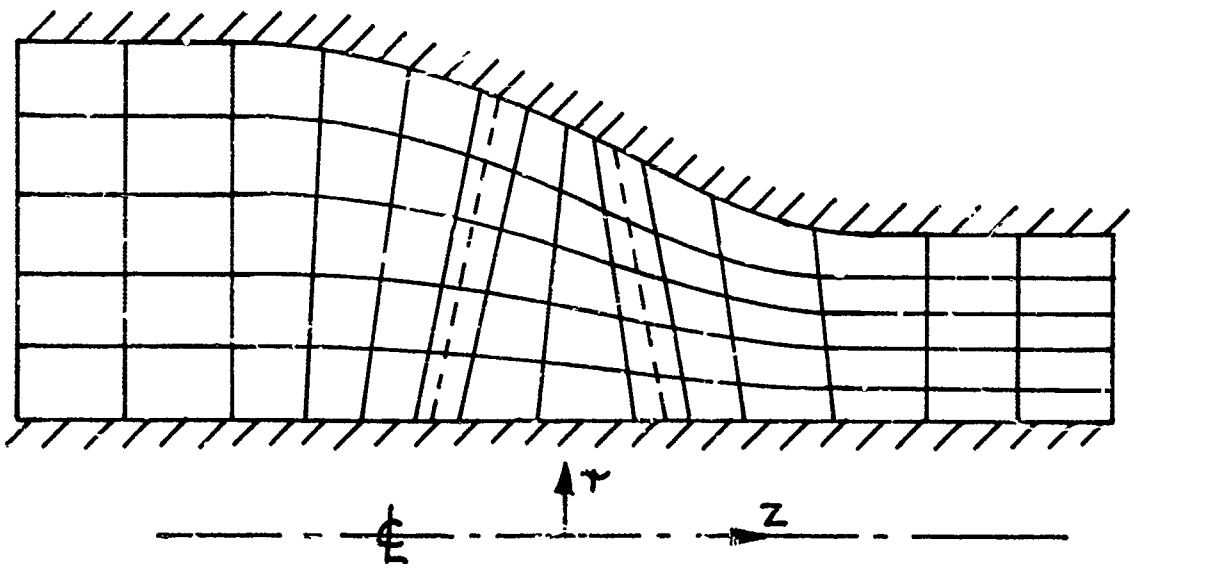

Fig. 1(b) Improved grid

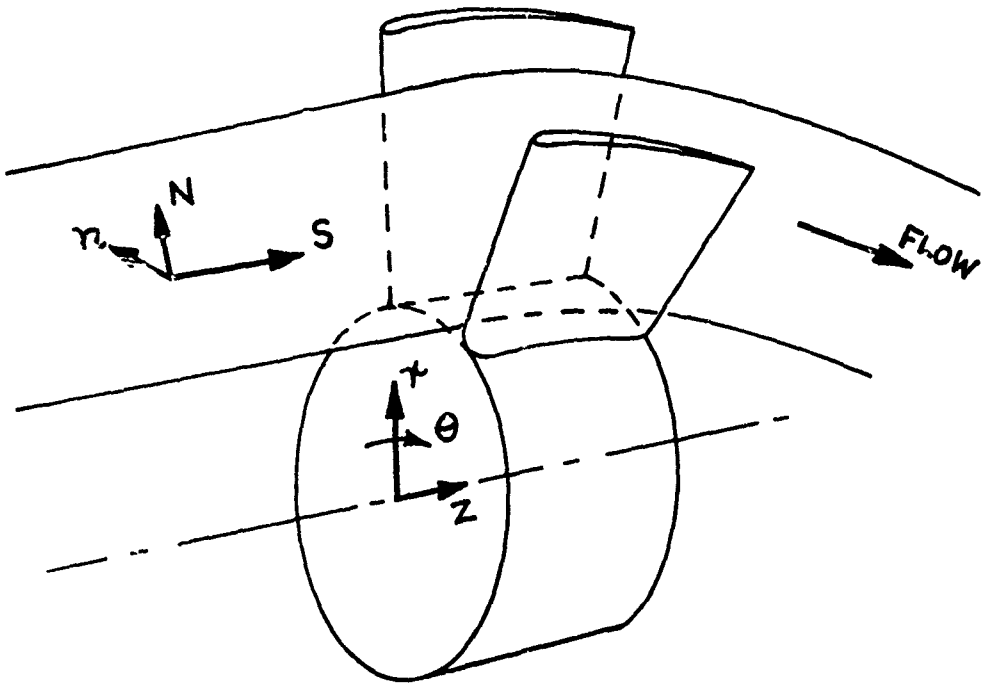

Fig.2 Stream surface and coordinate systems (12)

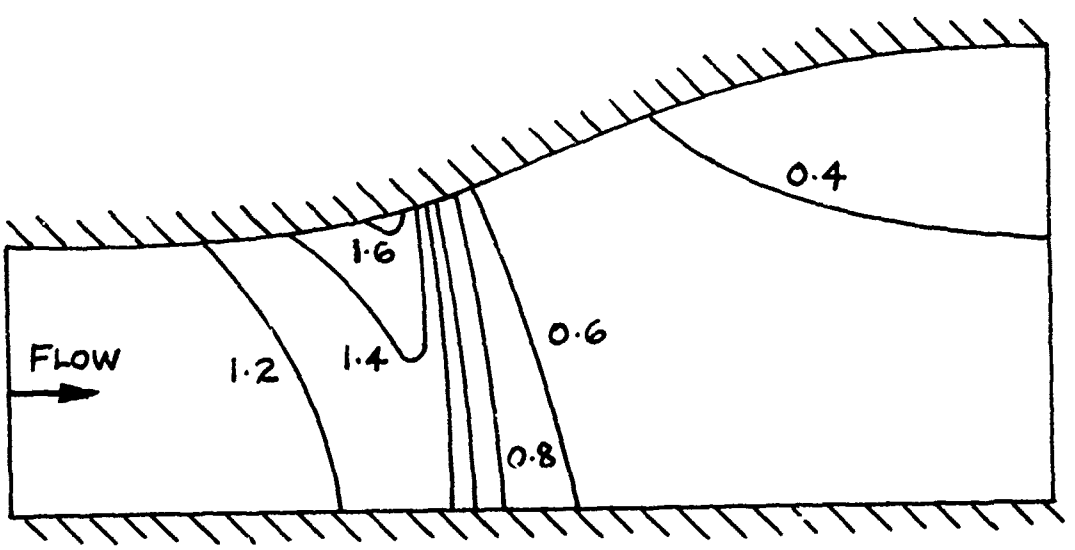

Fig.3 Mach No. contours (13)

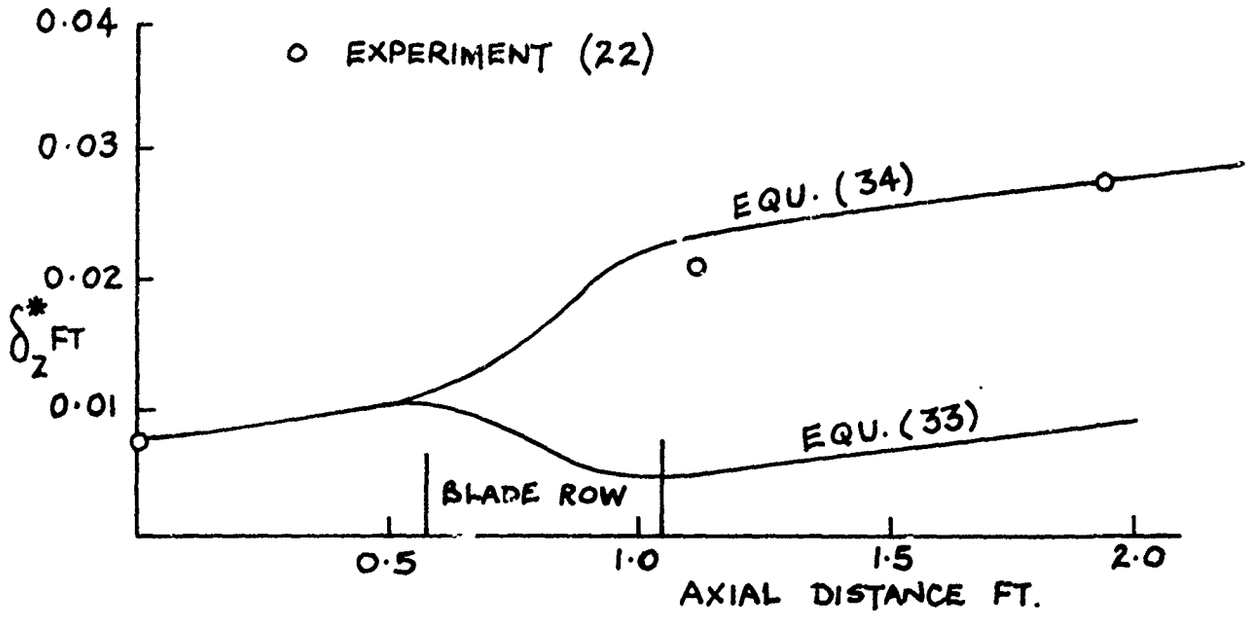

Fig.4 Flow through inlet guide vanes (22)

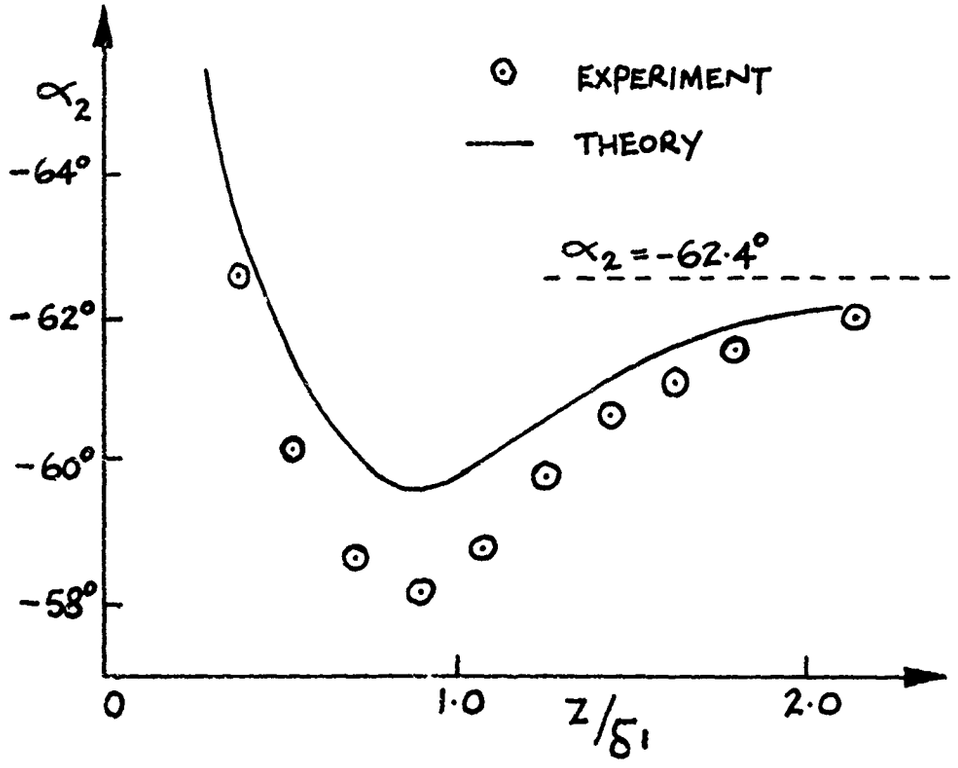

Fig.5 Variation of exit air angle

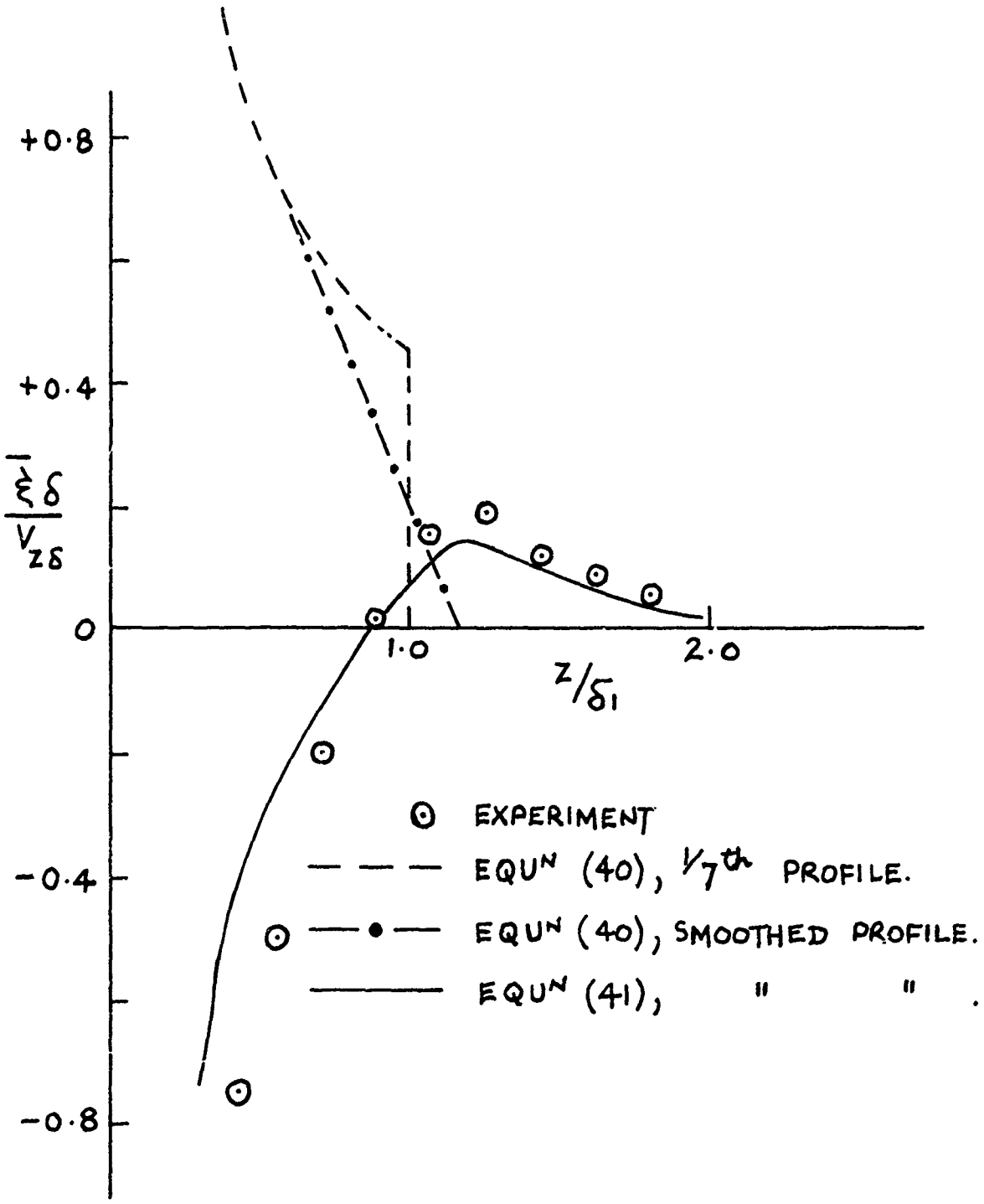

Fig.6 Pitch averaged streamwise vorticity

COMMENTS

Comment by H.J.Cox, C.E.G.B., UK

I have a few comments on Dr Marsh's paper. First, the effect of curvature. We would agree that under normal conditions, the curvature term is fairly small. This is largely due to the fact that the pressure gradient is dominated by the tangential velocity and slope terms. If you extend the streamline solution into duct regions, where the swirl velocities are low and slopes not so high, you can run into convergence problems because curvature effects provide the dominant term. Secondly, the question of uniqueness of solution. The streamline curvature program always solves this uniqueness problem because it has a given position of streamline at inlet and outlet, and from those two positions it makes an assumption as to where the throat is. If one defines another way of joining the two points (at inlet and outlet) one finds another solution. If one could leave the position of the throat free relative to the two end points, then the streamline curvature program would have exactly the same non-uniqueness problem as the matrix through flow programs.

Another point that I want to mention is the secondary flow problem. In this context, when talking about large diameter ratio turbines at high Mach numbers, we believe that concentrated secondary flows do not exist at root and tip but appear to be merged into the overall losses almost just downstream of the blade. We find in a lot of traverses, and Dr Denton has published similar data, that it is very difficult to distinguish the existence of concentrated loss cores, and it is also difficult on downstream traverses to see the overturning. This effect possibly arises from the fact that the static pressure gradient in the main flow is very large, while the corresponding static pressure gradient in the wake is negligible, and there are enormous static pressure differences acting in the system which can produce strong radial flows in the wake. Unless in time marching methods, or in any other method of calculating secondary flows, one does not introduce the effect of this radial motion, one will not calculate correctly the secondary flows in high Mach number situations. Concerning Gelder's approach, I think that your remark is rather optimistic. We use a method based on Gelder's approach and we always appear to get a breakdown at Mach number one, and consequently we restrict our Gelder technique to Mach numbers lower than one.

Finally, I have mentioned in my own paper at off designs one cannot use streamline curvature. The flows in an off design situation have broken away from the walls. Russian data has demonstrated that immense curvatures and slopes are produced and that one cannot rely on any method of computing performance.

Authors' response:

First of all, I am rather pleased by what you said about curvature, because I feel that curvature is important. In my paper, I was merely trying to argue from implication that the level of agreement which has been obtained by the manufacturers who have only computing stations between the blade rows is so good that it might not be important to go further. With regard to uniqueness, I agree entirely with you. For the secondary flows. the NGTE cascade was turning the flow through 62°, and we still managed to obtain good agreement with our calculation. What is then the difference between this experiment and the tests which have been conducted by Dr Denton and have shown a large transfer in the whole region?

Finally, my remarks on Gelder's work were based on calculations made by Gelder himself. One or two other people have managed to get the calculation through Mach numbers greater than unity, but how much greater, I do not know. Gelder went to a Mach number of about 1.2.

Comment by J.W.Railly, University of Birmingham, UK

There are two small points that I want to take on. The first one concerns the legitimacy of equation 14 which states the normality of the blade force with the relative velocity vector. I suggest that this is only permissible when the prior assumption is made of very closely pitched blades. In the general case of a large pitch of a blade, it can be shown that the arithmetic mean velocity direction is different from the inclination of this blade surface. The implication of equation 14 is that it is because of the influence of secondary flows which the computation show to extend far in the free stream, as in the experiment.

The second point is that, in regard to the anulus wall boundary layer solution, we must recognize that the non zero axial blade force deficit is necessary to account for the steady flow in a multistage machine of identical blades as shown by Leroy Smith.

Authors' response:

For the first point, one has to distinguish very clearly between the blade surface and the mean stream surface. I pointed out that there is a problem in trying to define that surface. If we just assume for the moment that we can do it, I will accept that this surface may differ significantly from the shape of the blade. What equation 14 is expressing is that the force vector must be normal to the stream surface and that it is required to make the flow follow the surface. The mean surface will certainly differ from the blade surface for wide pitched blades. For closed spaced blade, it will look just like the blade. Referring to the secondary flows, you have pointed out one of the anomalies. If you calculate the secondary velocity component using conventional secondary flow theories, you will find that the secondary velocities extend out into the main stream. If one looks at the conventional expressions derived for the trailing filament and trailing shed vorticity, they are both proportional to ξ_n, the normal component of vorticity and these only exist within the shear layer. There is thus a basic inconsistency in the conventional theory. It is only when you go to this new theory using Kelvin's theorem that you resolve that difficulty. Finally, I agree that the non zero axial force deficit should be taken into account. It is just that the simplified Stratford approach gives good agreement between experiment and theories. The other methods which consider this deficit have all done badly.

Comment by H.H.Frühauf, TH Stuttgart, Germany

Regarding the definition of the mean stream surface, it can be shown that when one integrates the three-dimensional equation for the compressible flow, with the assumptions that the local flow quantities deviation are small with respect to the averaged ones, and use infinitely thin three-dimensional blades, the mean blade surface having the same geometry leads to the same axisymmetric flow as defined by Lorenz, by integration.

Authors' response:

This would be true for lightly loaded blades only.

Comment by U.Stark, TH Braunschweig, Germany

You gave three expressions for the distributed, static and filament vorticity, assuming constant AVR. What can be the improvement on the outlet angle prediction that can be obtained, using the formulae that you have defined for the AVR?

Authors' response:

For the NGTE case that we treated, we got about 75% of the underturning. Using the AVR correction (as streamtube area) one gets a slight improvement, but not very much.

THROUGH FLOW CALCULATIONS BASED ON MATRIX INVERSION: LOSS PREDICTION

W. Roland Davis
Davis & Associates
1755 Woodward Drive
Ottawa, Ontario
K2C 0P9

Prof. D.A.J. Millar
Faculty of Engineering
Carleton University
Ottawa, Ontario
K1S 5B6

SUMMARY

The inviscid flow field in the meridional (hub-to-shroud) plane of an axial compressor is solved by a finite-difference technique which employs matrix inversion. The viscous flow effects are accounted for by using empirical data, and the performance of the compressor is determined by an interactive solution.

This paper describes the loss and deflection system which is used to model the effects of blade passage and end wall losses, and of blade passage deflection of the working fluid. The manner in which this system interacts with the matrix inviscid solution is described. The results of the test cases which were supplied for the meeting are discussed.

LIST OF SYMBOLS

A	area
a	speed of sound
a	constant in diffusion factor relation
b	exponent in deviation-angle relation
c	chord length
C_p	specific heat at constant pressure
D	diffusion factor
D_{eq}	equivalent diffusion factor
f	function
g_o	dimensional constant
i	incidence angle, angle between inlet air direction and tangent to blade mean camber line at leading edge, $\beta_1 - \kappa_1$
i_o	incidence angle of uncambered blade section
i_{ss}	incidence angle relative to the tangent to the suction surface at the leading edge
K_1	constant in diffusion factor relation
K_{sh}	blade profile shape correction factor
K_t	blade profile thickness correction factor
M	Mach number
$\dot{m}$	mass flow rate (kg/sec)
m	factor in deviation angle relation
P_o	stagnation pressure
p	static pressure
$\bar{R}$	percent blade height
r	leading edge radius
R	radius (from axis of rotation)
R_g	gas constant
R_u	suction surface radius of curvature
s	blade spacing
S	entropy
T	temperature
t_m	blade maximum thickness
V	air absolute velocity
V_{max}	maximum suction surface velocity
W	velocity relative to rotating coordinate system
z	coordinate along axis
α	angle of attack, angle between inlet air direction and blade chord, $\beta_1 - \gamma$
β	air angle, angle between air velocity and axial direction
$\Delta\beta$	air turning angle, $\beta_1 - \beta_2$
γ	blade chord angle, angle between the blade chord and axial direction
γ	ratio of the specific heats (C_p/C_v)
δ	deviation angle, angle between outlet air direction and tangent to blade mean camber line at the trailing edge, $\beta_2 - \kappa_2$
δ^*	boundary layer displacement thickness
δ_o	deviation angle of uncambered blade section
θ	wake momentum defect thickness
θ	strength of Prandtl-Meyer expansion wave
κ	blade angle, angle between tangent to blade mean camber line and the axial direction
ν	Prandtl-Meyer angle
ξ	dimensionless radius, R/R_{tip}
ρ	density
σ	solidity (c/s)
ϕ	blade camber angle, difference between the blade angles at the leading and trailing edges, $\kappa_1 - \kappa_2$
ψ	stream function
$\bar{\omega}$	total pressure loss coefficient, $\frac{P_{o_2} - P_{o_1}}{P_{o_1} - P_1}$
ω	rotational speed

1. INTRODUCTION

The techniques for design or analysis of the flow in axial flow turbomachinery have been highly developed over the past ten years. With large high speed computers it is possible to calculate in some detail the flow and performance of a mathematical model of an axial flow compressor which has speed lines and velocity profiles quite similar to an actual compressor. This is done by using an inviscid flow calculation technique, together with an empirical stagnation pressure loss and flow deflection model. In particular, if the loss and deflection model is made "adjustable", it can be individually tuned for each compressor so as to reproduce that compressor's performance with considerable fidelity. Whether or not a general model can be produced which will deal with a variety of compressor types effectively over a wide range of off-design conditions, will perhaps be discovered as a result of the test cases being run for this symposium. The authors of this paper attempted unsuccessfully for some years to find such a general loss and deviation model, and reluctantly concluded that the search was probably a vain one. We hope that we were wrong to so conclude.

2. INVISCID FLOW FIELD COMPUTATION

The matrix through-flow method, which is used for the inviscid flow calculation in this model, has been described in detail elsewhere (1, 2), so only an outline is given here.

FIGURE 1. MATRIX GRID AND COORDINATE SYSTEM

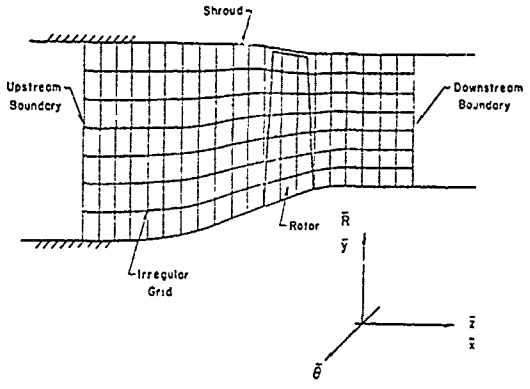

The matrix technique involves covering the region of interest with a fixed irregular grid as shown in Figure (1), and writing a finite difference approximation to the principal equation (equation (1)) at every interior grid point.

$$\frac{\partial^2\psi}{\partial x^2} + \frac{\partial^2\psi}{\partial y^2} = q\left(x,y,\frac{\partial\psi}{\partial x},\frac{\partial\psi}{\partial y}\right) \qquad (1)$$

This will result in one algebraic equation for every interior grid point in terms of the stream function at that and neighboring points. This system of equations can be expressed in matrix form as:

$$[A]\ [\psi] = [Q] \qquad (2)$$

where [A] is the coefficient matrix derived from replacing the differential operator $\nabla^2(q)$, $[\psi]$ is the vector of unknown stream function values, and [Q] is the vector of the quantities a(x,y) from equation (1) and the boundary values.

Since the right hand side of equation (2) is a function of ψ and its derivatives, the system of equations is nonlinear and must be solved iteratively, that is, by first estimating $[\psi]$, computing [Q], and then repeatedly solving equation (2) for $[\psi]$. The value for [Q] is improved each iteration using the previous value of $[\psi]$.

Since [A] is a function of the grid shape only, it need be computed and inverted only once. This is done by factoring [A], which is a square banded matrix, into triangular matrices [L] and [U] and saving these matrices on tape or disc. They can then be used for successive iterations and different boundary conditions. This feature saves computer time when successive calculations with different flow rates or conditions must be made with a fixed machine geometry, such as in the calculation of a compressor map.

This method offers fast convergence, second or third order accuracy, and stability at high flow rates and machine speeds.

The advantages and disadvantages of this technique compared to the streamline curvature method are discussed in (3), but the authors have felt for some time that is is the cascade model, which is described in the next section, which deserves the most attention. In fact, as will be pointed out later, the same cascade model is used in conjunction with both inviscid-flow computation techniques.

3. THE CASCADE MODEL

The cascade model must meet two requirements. When the main program is operating in the "design"mode, the model must determine the cascade blade inlet and outlet angles which will produce the minimum loss, and will provide the desired outlet angle, and it must determine this minimum loss. That is, it must find the minimum-loss incidence, i^*, and the corresponding deviation, δ^*, for the velocity diagrams, type of blading, and spanwise location of the blade section concerned. When the main program is operating in the "analysis" or "off-design" mode, the cascade model must determine the incidence onto the blading, as already specified, and the corresponding loss and deviation. Cascade terminology is shown in Figure 2.

Various loss-and-deviation correlations were previously examined and tested, and the most complete and well-proven at that time (1972) were chosen to build into the cascade model. In selecting these correlations, we felt that it was important that the model have the following capabilities and characteristics.

Figure 2
Cascade Terminology

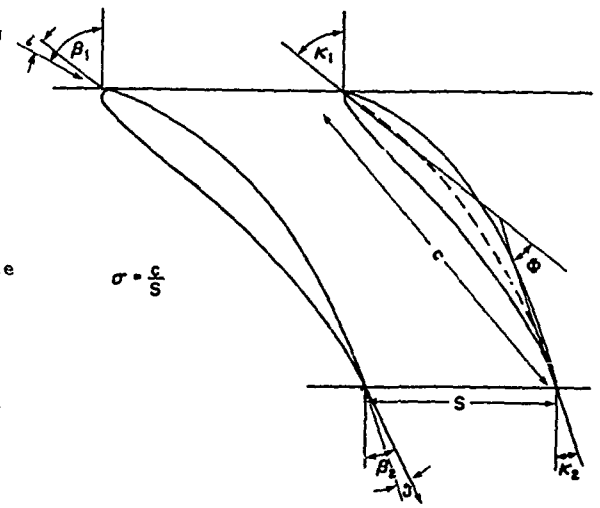

(a) It must be able to give data for the standard blade sections, 65-series, C-series, and D.C.A. (double circular arc), for which reasonably extensive low-speed data existed.

(b) It should be compatible with the inviscid-flow model, using as input the velocities, etc., which that model generated, and providing as output the appropriate pressure loss and flow deflection or outlet angle.

(c) It should, if possible, compensate for Reynolds number and Mach number variation, including shock losses at supersonic inlet speeds.

(d) It should allow for non-uniform axial velocity through the cascade (AVR - axial velocity ratio).

(e) It should include secondary losses, and effects of tip clearance or tip leakage on losses, at least.

In searching for correlations which would meet these criteria, it soon became apparent that the bulk of available information was based on low Mach number, two-dimensional cascade tests, and that limited data was available on the effects of Mach and Reynolds number, and practically none on the effect of axial velocity ratio, except in its implicit effect on measurements made in full scale compressors. Consequently, the cascade model described here is still relatively crude, and reflects the need for more experimental data, especially at high Mach numbers.

The cascade model is described briefly in the following section. Further details can be found in reference (4).

3.1 The Design Point Correlations

The input required for the design point correlations are the cascade solidity, blade section and thickness, and the flow angles determined by the inviscid-flow analysis.

3.1.1 Minimum Loss Incidence

The correlation given in NASA SP36(5) is used to find the minimum-loss incidence, i^*, for subsonic entry flows. This gives the incidence for low speed 2-D cascades as:

$$i^* = K_{sh}K_t i_o - n\phi \qquad (3)$$

where: $i_o = i_o(\beta_1^*, \sigma)$,

$n = n(\beta_1^*, \sigma)$,

K_{sh}, K_t are shape and thickness factors

β^* and σ are flow inlet angle & solidity

For sonic or supersonic entry, the minimum-loss incidence is assumed to correspond to the inlet velocity being tangent to the suction surface at the blade inlet (assuming a sharp leading edge blade).

$$i^*_{ss} = \tan^{-1}\left(\frac{4}{\phi}\cdot\frac{t_m}{c}\sin\frac{\phi}{2}\right) = \tan^{-1}\left(2\frac{t_m}{c}\right).$$

For inlet Mach numbers between 0.5 and 1, a sine function is used to interpolate between i^* and i^*_{ss}.

3.1.2 Deviation at Minimum-Loss Incidence

Similar to design incidence, NASA SP36(5), presents correlations for low speed, two-dimensional deviation angle:

$$\delta^* = K_{sh}K_t\delta_o + \frac{m\phi}{\sigma b}, \qquad (4)$$

where: $\delta_o = \delta_o(\beta_1^*, \sigma)$

and m and b are $f(\beta_1^*)$

A correction, suggested by Moffatt (6), is applied for inlet Mach numbers higher than the critical Mach number.

$$\delta_M^* - \delta^* = 8(M_1' - M_{1_c})$$

When the inlet flow is supersonic, the value of the exit Mach number from the leading edge shock is used for M_1'.

3.1.3 Total Pressure Loss Coefficient at Design

The profile loss is determined from Monsarrat's curves (7) of wake momentum thickness as a function of diffusion factor. He gives different functions for rotors and stators as shown in Figure (3)

Figure 3a

Monsarrat Design Loss for Rotors

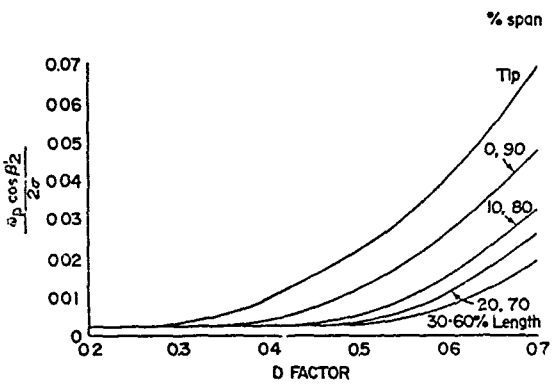

Figure 3b

Monsarrat Design Loss for Stators

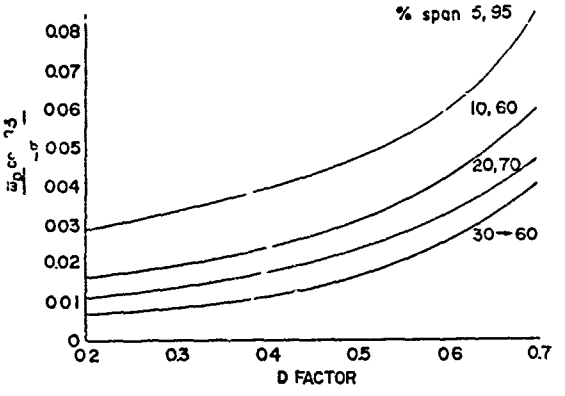

This correlation is used for two reasons; first, he shows a variation in loss with blade height where the minimum loss occurs at mid-span and increases towards the root and tip of the blade, which seems more realistic than that of Reference (5). Second, he gives a different set of curves for the stators which yield larger values of $(\frac{\theta}{c})$. Experience has shown that using the same loss curves for rotors and stators gives stator losses which are too small.

The loss is given by curves of the type,

$$\frac{\bar{\omega}^* \cos\beta_2^*}{2\sigma} = f_1(D^*, R) \quad \text{for rotors,} \qquad (5)$$

$$= f_2(D^*, R) \quad \text{for stators,}$$

where: $\bar{\omega}^* = (P_{o_1}' - P_{o_2}') \div (P_{o_1}' - p_1)$,

and: $$D^* = 1 - \frac{V_{m_2}\cos\beta_1^*}{V_{m_1}\cos\beta_2^*} + \frac{R_1\cos\beta_1^*}{\sigma(R_1+R_2)}\left[\tan\beta_1^* - \frac{R_2}{R_1}\frac{V_{m_2}}{V_{m_1}}\tan\beta_1^*\right].$$

The design loss is corrected for Mach number effects using the relation given in Reference (6),

$$\bar{\omega}_c^* = \bar{\omega}^*[2(M_1' - M_{1_c}) + 1.0] \qquad (6)$$

where M_{1_c} is the critical Mach number for the blade section and may be calculated from the value of $\frac{V_{max}}{V_1}$ as described in Reference (6).

3.2 Off-Design Correlations

For the off-design calculation the input quantities are the cascade geometry and the flow conditions at inlet to the cascade. The cascade model provides the outlet flow angle and the outlet stagnation pressure.

3.2.1 Off-Design Deviation

A correlation given by Swan (8) was chosen for the variation of deviation angle with off-design incidence angle. This relates the change in deviation to the change in the equivalent diffusion factor. The equivalent diffusion factor, D_{eq}, developed by Lieblein (9), is similar to the D^* given in 3.1.3.

$$D_{eq} = \frac{V_{m_1}}{V_{m_2}} \cdot \frac{\cos\beta_2}{\cos\beta_1} \left[.12 + K_b (i-i^*)^{1.43} + 0.61\ K \right] ,$$

$$\text{Where: } K = \frac{\cos^2\beta_1}{\sigma} \left[\tan\beta_1 - \frac{R_2}{R_1} \frac{V_{m_2}}{V_{m_1}} \tan\beta_2 \right] ,$$

and K_b is a constant which depends on the blade type.

Swan's equation for off-design deviation, shown in Figure (4) is given by:

$$\delta = \delta^* + \{6.4 - 9.45(M_1 - 0.6)\} (D_{eq} - D_{eq}^*) . \qquad (7)$$

Figure 4

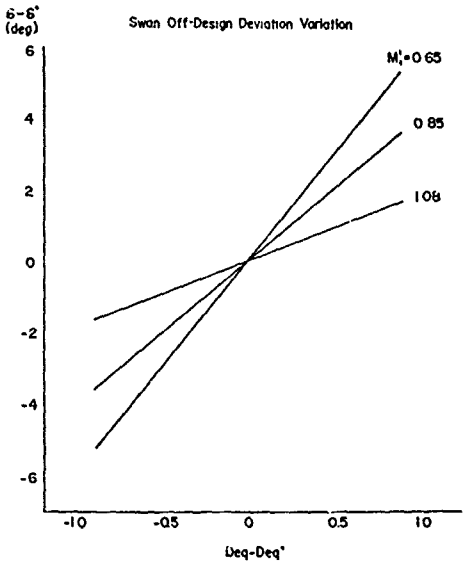

Figure 5

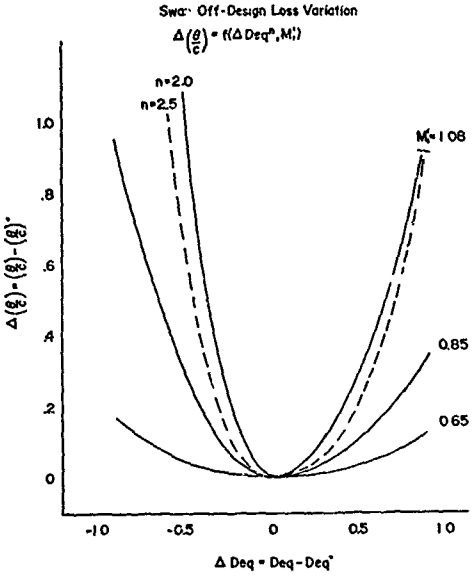

3.2.2 Off-Design Loss

The off-design loss is the sum of profile and shock loss. The profile loss is assumed to vary with equivalent diffusion factor in a manner suggested by Swan (8), but modified to reduce the sensitivity of the loss to variations in D_{eq}. The correlation shown in Figure (5), is given by:

$$\left(\frac{\theta}{c}\right) - \left(\frac{\theta}{c}\right)^* = f\{(D_{eq} - D_{eq}^*)^n,\ M_1'\} , \qquad (8)$$

$$\text{where: } \left(\frac{\theta}{c}\right) \text{ is related to } \bar{\omega} \text{ by, } \quad \bar{\omega} = \frac{2\sigma}{\cos\beta_2} \left(\frac{\cos\beta_1}{\cos\beta_2}\right)^2 \left(\frac{\theta}{c}\right) .$$

The exponent n was originally 2 in Swan's work. We have found n>2 to be a better value for most compressors, but even this value does not represent all compressors well. The effect of changing the exponent n is shown in Figure (5) for $M_1' = 1.08$.

The shock loss is calculated as the loss through a normal shock standing across the throat of the blade, similar to the technique of Reference (10). The inlet Mach number to the shock is taken as the average of the upstream Mach number, and the Mach number following a Prandtl-Meyer expansion over the suction surface. This expansion is based on the turning over that surface, and for the frequently used J-blade sections of supersonic compressors, the radius of curvature of that surface must be specified. For a double circular-arc blade, the radius can be calculated from the blade geometry.

The Prandtl-Meyer expansion is calculated from the inlet Prandtl-Meyer angle γ, based on M_1', and the turning angle θ, calculated as shown in the sketch on the next page.

3.3 Reynolds Number Effects

It is essential to account for the increased loss which occurs with small Reynolds numbers. Reference (5), Figures (151) and (152) were used to guide this formulation. It is apparent from these curves that it is currently impossible to establish any one value of limiting Reynolds number which will hold for all blade shapes. (The term limiting Reynolds number refers to the value at which a large rise in loss is obtained.) However, the results of tests of blade element performance and overall performance indicate that there is no significant variation in loss for Reynolds numbers greater than 2.5×10^5. Since the loss correlations are based on data at Reynold numbers greater than this value, no Reynolds number effects are believed to exist for the data.

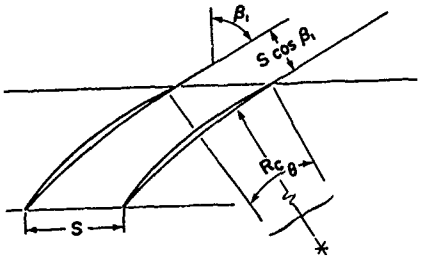

$$\theta = \tan^{-1}\left[\frac{S \sin \beta_i}{R_c + S\cos\beta_i}\right] + (i - i^*)$$

The correction to the total pressure loss coefficient assumes the following variation,

$$\bar{\omega} = \bar{\omega} \left[\frac{Re_{datum}}{Re}\right]^x , \qquad (9)$$

where Re_{datum} is the Reynolds number at which the loss begins to be affected (ie. 2.5×10^5) and x is the exponent which describes the variation in loss (typically 0.2).

The blade chord Reynolds number, Re, is given by:

$$\underline{Re} = \frac{\rho V_1' c}{\mu} , \qquad (10)$$

where the viscosity is given by Sutherlands relation,

$$\mu = \frac{(2.22 \times 10^{-8}) g_o \sqrt{T}}{(1.0 + \frac{180}{\sqrt{T}})} . \qquad (11)$$

Both the datum and exponent are input quantities.

3.4 Blade Passage Choking

After encountering problems in the off-design prediction of choked flow in transonic compressors, using the model described above, we decided to attempt to model the choking of the flow within the blade passage. Specifically, the amount of flow which can be passed through any section of a blade row depends primarily on the throat area of that row, and the upstream conditions. Since, in a quasi-three-dimensional analysis, both stagnation flow conditions and throat area are known, it is possible to calculate the maximum flow rate for each section.

As the actual flow approaches and ultimately reaches the choked flow value for any stream tube, there will be two effects; first, there will be a total-pressure-loss associated with the choking phenomena, and second, the mass flow must be redistributed. By accounting for these effects, it should be possible to better predict the near vertical portion of the compressor characteristic.

3.4.1 Choked Flow Calculation

The computation of the required throat area and of the maximum permissible mass flow can be made for each section by assuming one-dimensional isentropic flow. Thus, we have,

$$\frac{A}{A^*} = \frac{s \cos\beta_1}{d} ,$$

$$\text{or: } \left(\frac{d}{s}\right)_{isen} = \frac{\cos\beta_1}{\frac{A}{A^*}} , \qquad (12)$$

$$\text{where: } \left(\frac{A}{A^*}\right)^2 = \frac{1}{M_1^2}\left[\frac{2}{\gamma+1}\left(1+\frac{\gamma-1}{2} M_1^2\right)\right]^{\frac{\gamma+1}{\gamma-1}} \qquad (13)$$

and d is the throat width, s the blade spacing and β_1 the inlet flow angle. Equations (12) and (13) give the throat area required for the given inlet conditions.

The maximum mass flow is given by:

$$(\rho V)^* = \frac{2\gamma}{\gamma+1}\left(\frac{2}{\gamma+1}\right)^{\frac{1}{\gamma-1}}\left[\frac{P'_o}{\sqrt{\frac{RT'_o}{g_o}}}\right] \qquad (14)$$

3.4.2 Geometric Throat Width

The throat width may be calculated from the cascade geometry, required for the cascade model, if the shape of the mean camber line is assumed to be a circular arc, and the throat is assumed to occur at the leading edge as shown in the sketch below.

The radius of curvature of the mean camber line, R_c, is given by:

$$R_c = \frac{c}{2\sin\frac{\phi}{2}} \qquad (15)$$

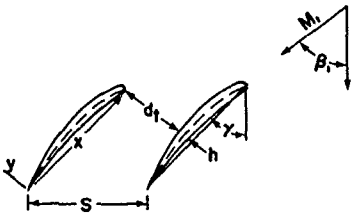

The distance, y, from the chord line to the mean camber line is a function of the distance x,

$$y = \left[R_c^2 - \left(x-\frac{c}{2}\right)^2\right]^{\frac{1}{2}} - R_c\cos\frac{\phi}{2} = f(x). \qquad (16)$$

The distance between the chord lines, d_c, is given by:

$$d_c = s\cos\gamma \qquad (17)$$

and the position of the throat;

$$x_t = s\sin\gamma + r_{l.e.} \qquad (18)$$

If the thickness distribution for the particular blade is given by:

$$\left(\frac{t}{c}\right) = f_1(x),$$

then the throat width can be computed from,

$$d_t = d_c - h - \frac{t}{2c} - r_{l.e.},$$

or

$$d_t = d_c - f(x_t) - \frac{1}{2}f_1(x_t) - r_{l.e.}, \qquad (19)$$

where $f(x)$ is given by Equation (16),

and the thickness function, f_1, must be given for double-circular-arc, 65-Series, and C-Series blades.

3.4.3 Implementation

Equations (12) to (19) permit the calculation of the maximum permissible flow rate, the throat area required to pass that flow, and the geometric (actual) throat area. As mentioned earlier, these parameters must be monitored, and if a choked flow condition is approached, action must be taken. The details of this action depend on the computation method, and at this point in time, the blade passage choking model has been implemented on our streamline curvature program only. The shifting of mass flow by limiting the flow through choked streamtubes is handled very nicely by the streamline approach, and it is anticipated that the matrix approach could model the same behavior.

The increase in loss due to choking is relatively arbitrary as we know of no available data in this area. However, it seems reasonable that the loss would gradually increase in some fashion as shown in the sketch to the right.

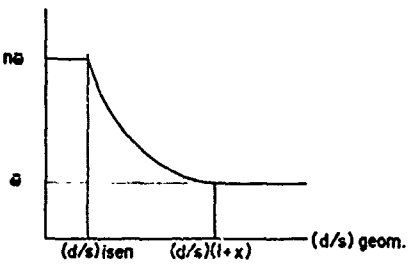

Typical values for n and x are 4 and 0.05 respectively. It has been our experience that this approach is more successful in predicting the steep portion of the characteristic than by increasing the negative incidence profile loss.

3.5 Distribution of Loss and Deflection Through the Blade Row

The cascade model was originally developed for the Streamline Curvature Program (11), and was used essentially unchanged for the Matrix Program. However, the former did not have axial stations within the blade row, whereas the latter does, and it is necessary to apportion the loss and turning to each internal station. The first calculations assumed a linear distribution between inlet and outlet of the blade row. However, this distribution has only the advantage of simplicity, and it would be worth investigating the effect of other distributions. The turning should be distributed on the assumption that the flow follows the camber line of the blade. The loss, on the other hand, probably should be distributed downstream of the blade row which causes it, since it will be caused by the mixing of the wake with the mainstream flow, taking place between the blade row, or even in the subsequent blade row.

Unfortunately, time has not permitted us to study the effect of more rational distributions of turning and loss.

3.6 Cascade Model Tuning

Various features of this cascade model lend themselves to adjustment or tuning from compressor to compressor. The exponent, n, on the off-design loss correlation, section 3.2.2, is the most effective in adjusting the slope of the speed lines. Currently, we input a value of n for $i>i^*$ which is usually different from that for $i<i^*$, so that an asymmetric loss-incidence curve can be simulated.

The effect of Mach number on deviation can be adjusted by changing the critical Mach number, or the factor 8. We have not tried this as yet, but this would have a significant effect on the high speed lines, while not affecting the low ones of a compressor map.

4. END-WALL BOUNDARY-LAYER INTERACTION

The calculation of the end-wall boundary-layers is essential to an accurate prediction of axial compressor performance. For internal flow situations which may be represented by a two-layer model, (that is, the inviscid core and the end-wall boundary-layers) both the individual parts and their interaction must be considered since changes in either layer will, in most cases, significantly alter the other layer.

The blockage due to the end-wall boundary-layers, i.e., the meridional mass defect, ($\rho_s UR\delta_m^*$) must be allowed to influence the inviscid-flow computation. One manner in which this is commonly accomplished is to redefine the end-walls using the calculated displacement thickness, that is, new fictitious physical boundaries are employed for another inviscid-flow computation. Continued iteration of the two solutions will then yield the complete solution.

The inviscid-flow computation technique solves a stream-function equation, in which the values of the stream-function are specified on the boundaries. It has been shown (12) that great benefit with respect to computation time is derived by adopting an alternative method, to that described above, to account for the boundary-layer blockage. This technique essentially places a series of equivalent sources along the end-walls whose strength is dependent on the boundary-layer mass defect, that is,

$$S = \frac{d}{dm}[\rho_\delta UR\delta_m^*] \ .$$

The new fluid emitted from the sources would fill a region adjacent to the body of thickness δ_m^*. Since the stream function, ψ, is a mass flow function, we wish to alter the boundary values by an amount equal to the local boundary-layer mass defect, $\rho_\delta UR\delta_m^*$, to correctly influence the inviscid flow.

Of course, the new boundary values, due to the end-wall blockages, will yield a new estimate of the inviscid flow field. The stagnation streamlines will no longer follow the physical boundaries, but will be displaced by the amount δ_m^*. Since the entire inviscid flow field is known, the flow properties along the stagnation streamline can be found by interpolation. These edge conditions may be used to compute a new estimate of the end-wall boundary layers, and the iterative procedure continued until an acceptably small change occurs between iterations.

In many instances, this iterative procedure converges rapidly and is essentially self-damping; that is, increased blockage accelerates the inviscid core flow, which in turn decreases the blockage on the next pass. However, if one (or both) of the end-wall boundary-layers separates, the predicted blockage may grow extremely large and cause such a large acceleration as to cause the separation to disappear, only to reappear next iteration.

The boundary-layer calculation technique which is currently used in our model is that suggested by Stratford (13), although more recent work by one of the authors has indicated that the three-dimensional boundary-layer effects may be significant.

5. EXTENSIONS TO THE TECHNIQUE

It has been stated repeatedly that the approach described here may be most readily improved by substituting superior cascade correlations. The extensions discussed in this section should be considered in that context.

Since the leading and trailing edges of the blades when viewed in the meridional plane will not generally be radial lines, it becomes desirable for the grid lines of the inviscid-flow technique to be aligned with these edges. This would save the necessity of interpolation at the leading and trailing edges, although at the expense of some additional complexity in the finite-difference method. Of course, if one is also concerned with centrifugal machinery, this extension is necessary since the leading and trailing edges are generally perpendicular to each other.

The end-wall boundary-layer computation currently used is quite simple. Although a sophisticated three-dimensional boundary-layer calculation is probably unrealistic at this time, at least for performance prediction of multi-stage compressors, it is possibly worthwhile to implement an improved end-wall boundary-layer computation technique which tries to account for known three-dimensional phenomena. Even a crude approach, such as using an axisymmetric model of the type developed by one of the authors (14) could prove of value.

6. DISCUSSION OF RESULTS

The cascade model described in this paper was used in conjunction with both the matrix and streamline curvature techniques to predict the performance of both the single stage, and the three stage, transonic compresscrs supplied for the 47th PEP Meeting. These compressors were denoted as test case numbers three and four respectively.

The streamline urvature program was run, as a check on the matrix program, and also since the blade passage choking model is not operational in the latter. As mentioned earlier, since the cascade model has a dominating influence, we did not expect, and did not see, any significant difference in the overall performance prediction of the two programs. The results for the two compressors are shown in Figures (6) and (7).

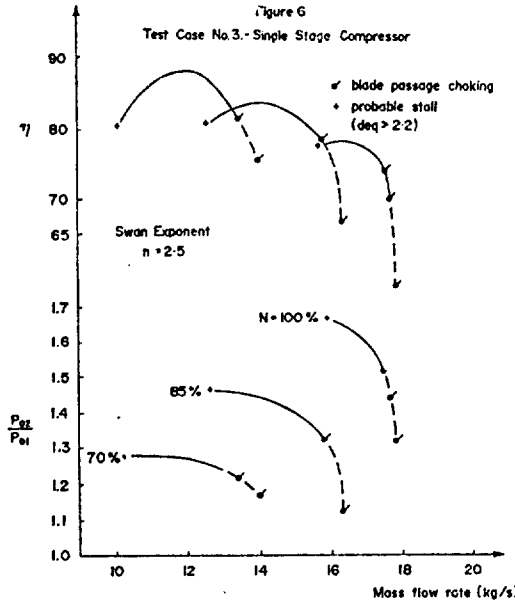

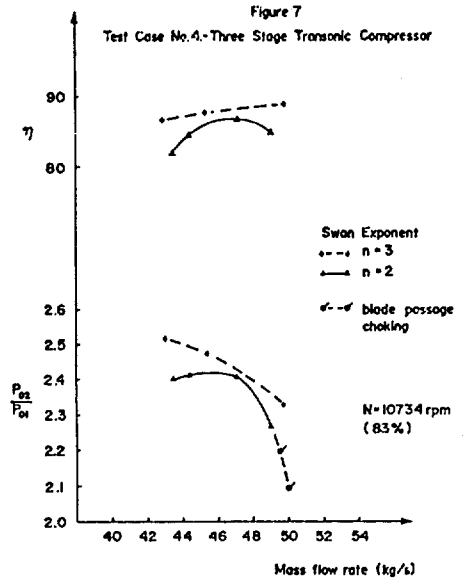

Figure (6) presents the predicted pressure ratio and efficiency, for the single stage compressor, for three constant speed lines. Neither program will predict surge as such, but by examining the output for high diffusion factors (ie. $D_{eq} > 2.2$), one may judge (approximately) the probable area of potential surge. The prediction of choked flow, as shown by the dashed line in Figure (6), was achieved using the blade passage choking model. The matrix program was used up to the maximum mass flow rate for which convergence could be obtained, at which time the streamline curvature program was used. These choked flow points are shown as flagged.

The matrix program permits the use of calculation stations within the blade row passage, and thus the effect of blade blockage may be taken into consideration. This was done initially, but the high relative inlet velocities were increased within the passage to Mach numbers greater than unity. When this occurs, the matrix program becomes unstable, and one cannot obtain convergence. It was necessary to ignore the effect of blade blockage on the internal stations to obtain the results which have been presented. This is a serious assumption if one is interested in the velocities within the blade passage. It was possible to obtain a solution, including blade blockage for a few points, and these results are presented in the detailed test results available at this conference.

Another effect, which has been examined, is the variation of the exponent used in the calculation of the off-design total pressure loss coefficient. This has been described

earlier, and is referred to in the Figures as the Swan exponent. Since decreasing the exponent produces more severe losses, the effect on the characteristics is predictable. For example by decreasing the exponent from 3 to 2, the efficiency of the single stage compressor at 14.3 kg/s and 85% speed dropped from 89% to 84%. In addition the range (predicted) is decreased. The effect is more noticeable in a multi-stage compressor, as shown in Figure (7).

Figure (7) shows one speed line which was predicted for the three stage compressor (test case #4). Similar to test case three, both programs were used to predict the compressor performance, and as before, it was necessary to neglect the effect of blade blockage. The effect of the loss exponent is clearly seen here, with the value of 2 providing the more realistic appearing characteristic.

This compressor was extremely difficult to model, and the authors were simply not able to obtain convergence at the design speed, in spite of repeated efforts. This lack of success was true for both the streamline curvature, and matrix programs. The reason for this, is not readily apparent, and may be due to a data error which was not picked up in the short time available. When the output from converged cases is examined, the problem is seen to be in the hub region, originating with the first blade row.

The large velocity gradient at the exit of the first rotor, produces a very low velocity at the hub relative to the inlet velocity, and thus a high diffusion factor ($D_{eq}>2.2$). This phenomena occurred regardless of the inlet velocity, that is, it was a function of the design (it seems) and not of an off-design problem. The hub contour at the inlet was altered to produce a higher inlet velocity at the hub, but the effect was not significant. This type of inviscid flow model, unfortunately makes the original problem worst, in that the low inlet velocity into the next row produces a large off-design loss which produces a low exit velocity and so on.

Blockage factors were used throughout these analyses, in place of boundary-layer calculation. The extremely large diffusion across the first rotor would certainly have caused problems for most boundary-layer calculation techniques, since it would probably cause separation of the end-wall boundary-layer.

Another phenomena was examined briefly on both compressors using the matrix program. Ordinarily, the total pressure loss for a blade row is distributed linearly through the blade row. It was hypothesized earlier that a more realistic approach would be to dump the loss at the exit of the blade row. The appropriate change was made and the results are inconclusive at this time. The velocity distributions within the blade row are affected slightly, but there is no effect on the overall performance.

7. CONCLUSIONS

The authors have presented a model for predicting the off-design performance of axial compressors, and the results for a single stage, and three stage transonic axial compressor. The model is composed of an inviscid-flow computation technique (matrix through-flow), and a cascade loss and deviation model. At this time, the cascade model appears to be the area still requiring the most attention, although transonic turbomachines point up weaknesses in the inviscid-flow model as well.

We feel that the following areas are worthy of further study:

- the effects of Mach number, axial velocity ratio, and incidence at off-design conditions
- the development of a practical three-dimensional end-wall boundary-layer technique
- a model to incorporate inter-streamline shear and energy transfer effects, by means of effective turbulent mixing parameters
- a means of coping with transonic relative velocities within a blade passage, and integration of this technique with a shock loss model and a blade passage choking model
- further work to more accurately identify the quantitative increase in loss as blade passage choking occurs.

REFERENCES

(1) Marsh, H.; "A Digital Computer Program for the Through-Flow Mechanics in an Arbitrary Turbomachine Using a Matrix Method"; A.R.C. R&M No. 3509, 1968.

(2) Davis, W.R.; "A Matrix Method Applied to the Analysis of the Flow in Turbomachinery"; Carleton University Report No. ME/A 71-6, 1971.

(3) Davis, W.R. and Millar, D.A.J.; "A Comparison of the Matrix and Streamline Curvature Methods of Axial Flow Turbomachinery Analysis, From a User's Point of View"; ASME Paper No. 74-WA/GT-4, 1974.

(4) Davis, W.R. and Millar, D.A.J.; "Axial Flow Compressor Analysis Using a Streamline Curvature Method"; Carleton University Technical Report No. ME/A 76-3, 1976

(5) Johnson, R.A. and Bullock, R.O.; "Aerodynamic Design of Axial Flow Compressors"; NASA SP-36, 1965.

(6) Moffatt, W.C. and Jensen, W.; "The Off-Design Analysis of Axial Flow Compressors"; ASME Transaction, Journal of Engineering for Power, Vol. 89, Series A, No. 4, October 1967, pg. 454.

(7) Monsarrat, N.T. Keenan, M.J., and Tramm, P.C.; "Design Report-Single Stage Evaluation of Highly-Loaded High-Mach No. Compressor Stages'; NASA CR-72562, 1969.

(8) Swan, W.C.; "A Practical Method of Predicting Transonic-Compressor Performance"; Journal of Engineering for Power, July 1961, pg. 322-330.

(9) Lieblien, S.; "Analysis of Experimental Low Speed Loss and Stall Characteristics of 2D Compressor Blade Cascades"; NACA RM E57A28.

(10) Miller, G.R., Lewis, G.W. and Hartmann: "Shock Losses in Transonic Compressor Blade Rows'; Journal of Engineering for Power, July 1961, pp. 235-242.

(11) Davis, W.R. and Millar, D.A.J.; "An Axial Flow Compressor Performance Analysis Computer Program"; Carleton University Report No. ME/A 76-1, 1976.

(12) Davis, W.R.; "A General Finite Difference Technique for the Compressible Flow in the Meridional Plane of Centrifugal Turbomachinery"; ASME Paper No. 75-GT-921, 1975.

(13) Stratford, B.S.; "The Use of Boundary Layer Techniques to Calculate the Blockage From the Annulus Boundary in a Compressor"; ASME Paper No. 67-WA/GT-7.

ACKNOWLEDGEMENT

This work has been supported by National Research Council Contract #OSR5-0103 and this help is gratefully acknowledged. The original program development was carried out under a National Research Council Grant, #A1676, and this support is also most appreciated.

COMMENTS

Comment by K.Papailiou, E.C.L., France

We have used Millar's and Davis' program for several compressors. We have found out that convergence is much easier when applying a weight factor on the losses and not only on the stream function. We also found that going up in Mach number inside the blading and accounting for profile blockage, we get into trouble and the program diverges. For secondary flows, when their effects are taken into account, there is an inconsistency in the radial equilibrium, when going inside the boundary layer region, as pointed by Horlock.

Comment by T.McKain, Detroit Diesel Allison, USA

We have based our correlation on the NASA SP36 as most industries do. What we have found is that in the early stages of a multistage machine, the deviation rules are close to truth, but, in the last stage, due to the combined effects of secondary flows and boundary layers, the prediction starts to deviate quite a lot.

THROUGH-FLOW CALCULATIONS: THEORY AND PRACTICE IN TURBOMACHINERY DESIGN

John E. Caruthers
Senior Project Engineer
Detroit Diesel Allison Division, GMC
P. O. Box 894
Indianapolis, Indiana, 46206, USA

and

Theodore F. McKain
Senior Project Engineer
Detroit Diesel Allison Division, GMC
P. O. Box 894
Indianapolis, Indiana, 46206, USA

SUMMARY:

The through-flow calculation is an integral and vital element of any effective turbomachinery design and development process. This paper reviews the through-flow calculation from both a theoretical and an applications viewpoint. The assumptions involved with typical formulation of the basic equations and the solution techniques employed in such areas as boundary condition specification, numerical evaluation of derivatives and numerical stability are presented. Experimental verification of the theory, using turbomachinery applications, is presented to demonstrate the accuracy of the calculation. Finally, the normal compressor design and development cycle is reviewed to stress the importance of the through-flow calculation in this process.

LIST OF SYMBOLS

$\bar{a}_m$	Meridional acceleration vector (Eq. 9)
B	Streamsheet thickness ratio
D_f	Diffusion factor
f_d	Damping factor
H	Total enthalpy
I	Rothalpy ($H-\omega rV_\theta$)
L	Distance along streamline
M_n	Mach number
N	Distance along calculating station
P	Pressure
R.F.	Thermocouple recovery factor
R_m	Streamline radius of curvature
r,z,θ	Cylindrical coordinates
S	Entropy
T	Temperature
$\bar{V}$	Velocity (inertial frame)
$\bar{W}$	Velocity (blade relative frame)
α	Angle of attack
η	Adiabatic efficiency
ρ	Density
φ	Streamline angle
ψ	Stream function
ω	Blade rotational speed

Subscripts

c	calculating station
m	meridional
r	radial
t	stagnation
θ	tangential

THEORY

It is necessary in the analysis of flow through a turbomachine to introduce certain simplifying assumptions concerning the unsteady three-dimensional viscous flow characteristic of such machines in order to reduce the original problem to a tractable mathematical model. Once accomplished, it is often desirable to further reduce the level of sophistication of the model to obtain one which is practical and which may be solved relatively efficiently with available computing techniques. The latter consideration is of particular importance when such calculations are intended to form the basis of a highly iterative design system.

An assumption pertaining to both the former and latter considerations is the assumption of weak three-dimensional flow which allows analysis of the flow field by consideration of separate 2-D flows in intersecting surfaces which are only partially coupled. The theory of flow through a turbomachine under the above approximation with varying degrees of coupling between the surfaces constitutes what has come to be known as through flow theory, although the term is usually meant to apply more specifically to flow in the hub-to-shroud surface. The theory of the through flow calculation is reviewed in the following development.

Neglecting viscosity, the vector momentum equation can be written in the inertial reference system as

$$\frac{D\bar{V}}{Dt} = -\frac{\nabla p}{\rho} \tag{1}$$

The flow field will be assumed steady relative to the blade row in question (i.e., there is no unsteady interaction between moving and stationary blade rows) so that the momentum equation can be written in the blade fixed system as

$$(\bar{W} \cdot \nabla)\bar{W} + 2\bar{\omega} \times \bar{W} - \omega^2\bar{r} = -\frac{\nabla p}{\rho} \tag{2}$$

Using the relationship

$$T\nabla S = \nabla\left(H - \frac{V^2}{2}\right) - \frac{1}{\rho}\nabla p \tag{3}$$

equation (2) may be written in the form

$$-\bar{W} \times (\nabla \times \bar{W}) + 2\bar{\omega} \times \bar{W} = -\nabla I + T\nabla S \tag{4}$$

where I is a quantity (sometimes called rothalpy) defined by

$$I = H - \omega r V_\theta \tag{5}$$

and $\omega = 0$ for a fixed blade row.

Taking the component of Eq.(4) along a direction N tangent to an arbitrary curved line "C" (Figure 1) gives for the equilibrium equation in this direction

$$\begin{aligned} \frac{1}{2}\frac{dW_M^2}{dN}\bigg|_C = {} & \frac{dI}{dN}\bigg|_C - T\frac{dS}{dN}\bigg|_C - \frac{1}{2}\frac{dW_\theta^2}{dN}\bigg|_C \\ & + \left[W\frac{dWr}{dL}\bigg|_\psi - \left(\frac{W_\theta^2}{r} + 2\omega W_\theta\right)\right]\frac{dr}{dN}\bigg|_C \\ & + W\frac{dWz}{dL}\bigg|_\psi \frac{dz}{dN}\bigg|_C + \left(W\frac{d(rW_\theta)}{dL}\bigg|_\psi + 2\omega r W_r\right)\frac{d\theta}{dN}\bigg|_C \end{aligned} \tag{6}$$

Equation (6) will be referred to as the stream derivative form of the equilibrium equation. The equation is in a form suitable for numerical computation without further reduction. It is notable that slope and curvature expressions do not appear explicitly

in this form, but are contained implicitly in the stream derivative terms. These terms are readily expanded to show the equivalence of the stream derivative form to the more familiar streamline curvature forms. For example

$$W \frac{dWr}{dL}\bigg|_{\psi} = Wm \frac{d(Wm \sin\phi)}{dm}\bigg|_{\psi} \tag{7}$$

$$= \cos\phi \frac{Wm^2}{R_m} + \sin\phi \; Wm \frac{dWm}{dm}\bigg|_{\psi}$$

and

$$W \frac{dWz}{dL}\bigg|_{\psi} = -\sin \frac{Wm^2}{R_m} + \cos\phi \; Wm \frac{dWm}{dm}\bigg|_{\psi} \tag{8}$$

which represent the radial and axial components, respectively, of the meridional acceleration vector

$$\bar{a}_m = \frac{Wm^2}{R_m} \hat{N}m + Wm \frac{dWm}{dm}\bigg|_{\psi} \hat{L}m \tag{9}$$

so that the sum

$$W \frac{dWr}{dL}\bigg|_{\psi} \frac{dr}{dN}\bigg|_{C} + W \frac{dWz}{dL}\bigg|_{\psi} \frac{dz}{dN}\bigg|_{C} \tag{10}$$

appearing in Eq. (6) represents the component of the meridional acceleration, $\bar{a}_m$, along curve "C".

Since all derivatives appearing in the stream derivative form of the equilibrium equation lie along "C" or along streamlines passing through "C", this leads naturally to the consideration of flow within the stream surface so defined. To complete the momentum specification within this surface, an additional equilibrium equation is required. A particularly simple and useful form of the needed equation is obtained by considering equilibrium along the stream direction. The desired equation can be obtained by taking the component of Eq. (4) along the stream direction giving

$$\frac{dI}{dL}\bigg|_{\psi} = T \frac{dS}{dL}\bigg|_{\psi} \tag{11}$$

For effectively adiabatic flow (heat transfer + viscous dissipation = 0)

$$\frac{dI}{dL}\bigg|_{\psi} = 0 \tag{12}$$

so that from Eq. (11)

$$\frac{dS}{dL}\bigg|_{\psi} = 0 \tag{13}$$

In the practical application of the through-flow calculations, Eq. (13) is usually considered to be accurate in the blade-free regions. It is usally desirable and necessary in the bladed regions to introduce dissipative or "loss" mechanisms so that

$$\frac{dS}{dL}\bigg|_{\psi} = f(L) \tag{14}$$

which may be integrated to give

$$\Delta S\bigg|_{\psi} = F(L) \tag{15}$$

where F(L) is specified by the designer from a knowledge of the blade element loss characteristics and is taken as zero in the blade-free space. Eq. (15) is then used instead of Eq. (13) to express the equilibrium condition along the streamline direction. The fact that this substitution is inconsistent with the inviscid assumption used in the development of the momentum equation has been pointed out by Horlock[1], who suggested that a nonconservative body force acting opposite to the stream direction be added to the momentum equation to produce the specified entropy variation. If curve "C" is not normal to the stream direction, then this force has a component which must be included in the equilibrium equation along "C". It is obvious that if this term is neglected in the "C" momentum equation, then the curve should be chosen as nearly normal to the stream direction as possible to reduce the resulting error. In this development the dissipative force component is neglected in the equilibrium equation along "C" but its major effect is retained by inclusion in the streamwise component equation (Eq. (15)).

A final assumption is needed in order to evaluate the tangential velocity terms in the stream derivative equation. The three models most commonly used for this purpose are reviewed by Horlock and Marsh[2]. The models consist of replacing the actual cascade with a cascade containing an infinite number of blades, simulating the blade action by an axisymmetric flow with distributed body forces, and by considering the flow on a suitably defined "mean stream surface". Each of the models is shown to lead to only a first order approximation to the circumferentially averaged flow within the actual cascade, accurate only for low blade loading. The overall changes across the blade row, however, were found to be properly represented. With the proper choice of the mean stream surface the three models yield identical results for the equilibrium equation, with the last term of Eq. (6) interpreted as the equivalent blade or body force.

If a particular stream surface is known a priori, the tangential velocity is uniquely determined by the axial and radial velocities so that equations (6), (15), (12), and the continuity equation (which may allow for stream tube convergence) may be used (along with the boundary conditions and state equation) to solve exactly for all pertinent flow and thermodynamic variables within the stream surface. Wu[3] has proposed a fully 3-D scheme whereby a number of such surfaces are solved from hub to tip and from blade to blade with the solutions iteratively coupled through the stream surface shapes. Such solutions have been achieved for duct flows[4] but are time consuming and presently considered impractical to serve as the basic through-flow calculation without further approximation. Some reasonable reductions of Wu's more general method have recently been advanced[5,6].

Normally, a single stream sheet is chosen to be as representative as possible of the mean flow properties. Within the blade row the shape of the mean stream surface is often taken as the mean camber surface of blade passage. A more laborious approach consists of defining the mean stream surface from the middle streamlines of a sequence of blade to blade solutions along the blade span. In view of the approximation already made in choosing a single hub-to-shroud stream surface, the additional calculations required for this approach hardly seem justified.

For the unbladed portion of the flow path, the flow is considered periodic but generally cannot be considered axisymmetric. The total angular momentum flux, however, must remain constant through the annulus even though changes in angular momentum along the streamlines may occur locally. The "mean stream surface" should thus be selected ahead and behind the blade row so that the angular momentum is conserved along the streamlines in that surface. This choice of the stream surface is tantamount to assuming axisymmetric flow from the outset so that the axisymmetric assumption and a choice of the mean stream surface compatible with the conservation of total angular momentum lead to identical results.

The assumption of axisymmetric flow in the blade-free regions thus allows calculation of the tangential velocity terms from

$$\left.\frac{d(rV_\theta)}{dL}\right|_\psi = 0 \tag{16}$$

In the bladed regions the tangential velocity is obtained either from the stream surface specification

$$\bar{W} \cdot \hat{N}_{ss} = 0 \tag{17}$$

where $\hat{N}_{ss}$ is the unit vector normal to the assumed stream surface, or the tangential velocity may be specified directly by the designer in a number of equivalent forms.

Solution Method

The iterative solution procedure used to solve the governing equations presented above is straight forward in principle and is described step by step in the procedure which follows:

1. The geometry of the flow path is specified and the calculating stations are defined within it along which the equilibrium equation (Eq. (6)) is to be satisfied.

2. The inlet and exit boundary conditions are specified (e.g. flow angle, mass flow distribution, or stream curvature). Inlet values of P_o, T_o, and V_θ are also required input.

3. A number of streamlines which bound a specified amount of mass flow are chosen and initially distributed through the flow path.

4. An initial estimate is made of all velocities, the total temperature and the total pressure.

5. The right hand side of Eq. (6) is evaluated at each streamline and calculating station intersection.

6. Starting at the first calculation station inside the inlet station, the equilibrium equation is integrated numerically from hub to tip assuming an initial value at the hub. A weighted average is taken between the old and new velocities with the old velocities heavily weighted.

7. The resulting mass flow distribution is then integrated to obtain the total mass flow which is compared to the desired mass flow. The velocity distribution is then scaled by desired flow/calculated flow and the streamline positions are adjusted to satisfy continuity locally. The effect of blade or strut blockage is easily included in this step.

8. Steps (5) through (7) are repeated for each calculating station up to the exit station.

9. The inlet and exit stations are solved using the input boundary conditions.

10. Steps (5) - (9) are repeated until the maximum percent velocity change is less than some specified amount.

In the above procedure the continuity equation is satisfied by explicit treatment. This step may be avoided and the continuity equation satisfied identically by introduction of the stream function defined within the stream surface by

$$\frac{\bar{\partial}\psi}{\partial r} = \rho r B W_z; \quad \frac{\bar{\partial}\psi}{\partial z} = -\rho r B W_r \tag{18}$$

where the bars indicate derivatives taken within the relative stream surface. The equilibrium equation then takes the form of

$$\left(\frac{\bar{\partial}^2}{\partial r^2} + \frac{\bar{\partial}^2}{\partial z^2}\right) \psi = f(r,z) \tag{19}$$

where $f(r,z)$ is actually a nonlinear function of ψ, r, and z, but is considered as a known function of r and z for each iteration in a solution scheme defined by

$$\left(\frac{\bar{\partial}^2}{\partial r} + \frac{\bar{\partial}^2}{\partial z^2}\right) \psi^{i+1} = f^i(r,z) \tag{20}$$

This is basically the method used by Marsh[7]. In this method Eq. (20) is expressed in finite difference form for a fixed grid network within the flow path. The fixed grid network and the automatic satisfaction of the continuity equation are the primary differences between this solution method and the one described previously. Each iteration results in a linear algebraic system of equations which may be solved by a number of direct or iterative methods. In fact, the solution of Eq. (20) may be made closely analogous to the stream derivative and stream curvature solution methods by choosing a successive line relaxation algorithm for solution of the matrix equation. A comparison between the stream function method and the stream curvature method has been presented by Davis and Millar[8].

The method used to evaluate the streamwise derivative terms appearing in the equilibrium equation (Eq. (6)) has a significant influence on both the accuracy and stability of the method. Wilkinson[9] has given a study of the various methods available for calculating these derivatives in terms of their influence on the efficiency, accuracy, and stability of the computation. He concludes generally that the finite difference methods are the best and that the spline methods are the worst. Numerical experiments performed at Detroit Diesel Allison support this conclusion. Consequently, the streamline derivatives which appear in the equilibrium equation are evaluated using a second order central difference approximation. This method has given quite satisfactory results over a wide range of turbomachinery application.

As mentioned in Step(6)of the solution procedure, it is necessary to damp the velocity change from iteration to iteration during the solution process in order to assure the stability of the calculation. Generally, the calculation may be stabilized by using sufficiently strong damping although a premium is paid in terms of computing efficiency. For a typical turbomachine calculation, the optimum choice of the damping factor, f_d, usually occurs very near the convergence limit (a typical case is shown in Figure 2.) The optimal damping factor as well as the maximum value for convergence are functions of the particular flow path geometry, Mach number, number of computing stations, and the method used to calculate the stream derivative (or curvature) terms. Wilkinson[9] has developed an expression for the optimal damping factor as well as the convergence limit using a simple parallel flow model. He found the optimal damping factor to be given by

$$f_d = \left(1 - \frac{5}{96} K_{min} (1-M_m^2)A^2\right)^{-1} \tag{21}$$

where A is the grid aspect ratio and K_{min} is a factor dependent on the method of evaluating the stream curvature.

It should also be pointed out that the total number of iterations required to obtain a solution is influenced significantly by the particular iteration method used. For example, the equilibrium equation may be solved simultaneously along each of the calculating stations rather than consecutively, as suggested in the previous outline of the solution procedure. The interaction of the blade element models and the end wall boundary layer calculations with the main through-flow calculation also affects the optimal damping factor as well as its stability limit. Some improvement in computational efficiency can also be achieved by reducing the damping during the iterative process as the solution is approached. An accurate initial guess can also considerably improve the efficiency of the calculation.

A source of common error in the practical application of through-flow calculations concerns the inlet and exit boundary conditions. The proper posing of the elliptic boundary value problem requires that some boundary condition be specified along the closed boundary of the solution domain. For the through-flow problem, the boundary condition along the hub and shroud contours are automatically satisfied by requiring that these be streamlines of the flow. In addition to the total mass flow rate and the inlet input quantities of stagnation temperature, pressure and tangential velocities,

inlet and exit boundary specifications are required. It is sufficient (and necessary) that only one quantity be specified along these boundaries. Typically, this might be the flow angle (streamline slope), the mass flow distribution (streamline position), streamline curvature, or either of the meridional velocity components. Even though any of the above physical specifications translate into proper mathematical constraints for the problem, the arbitrary application of these conditions too near the region of interest can lead to an improper physical result. It is important that the boundary conditions be specified at a location where they can be stated accurately from physical considerations. This often requires that the inlet and exit boundaries be removed somewhat from the actual domain of interest where the physical conditions of the desired flow may be made more consistent with the imposed boundary conditions and where any remaining inaccuracy has little influence at the far removed stations.

EXPERIMENTAL VERIFICATION OF THEORY

For any theoretical analysis to be useful, it must be calibrated against data in problem situations typical of intended usage. It is important, for any useful comparison, that the data be such as to clearly test the theory with underlying assumptions held to a minimum. The through-flow calculation used in turbomachinery applications is composed of two basic elements:

1. Inviscid equations of motion with attendant solution techniques
2. Secondary calculations for real fluid effects.

The comparisons which follow have been chosen to test the validity of the basic equations of motion and the numerical solution techniques. Two examples have been selected for relevance to turbomachinery application, complexity of the problem, and adequacy of defining instrumentation.

The first example, Figures 3 through 7, investigates the flow field in the vicinity of the flow splitter of a low bypass ratio turbofan compressor as the mass flow split is varied. This problem is a very difficult one in that it is a case of swirling flow from the upstream rotor with total pressure and temperature gradients, extremely high flow-field-induced streamline curvature and high local Mach numbers. The comparison is made at three different levels of tip back pressure from near choke to near surge. The comparison between theory and test is exceptionally good, especially at Points B and C where the local Mach numbers are relatively low. The calculation was made with fixed wall boundaries with no provisions to account for boundary layer phenomena.

The second example shown in Figures 8 through 9 is a case of high flow path induced curvature with total pressure and temperature gradients. The stator discharge flow is designed for zero exit swirl and is assumed to be so. Again, excellent agreement between theory and data is seen to exist.

Many comparisons similar to those just described have been reported in the literature and, in general, verify the technical adequacy of the basic equation formulation and solution techniques.

The real fluid effects such as endwall boundary layers, tip clearance leakage, wake mixing, blade element losses and others are neither well documented nor truly understood. Nevertheless, they are just as important to the success of the final product as the basic through-flow calculation. These effects deserve a great amount of future effort.

APPLICATION

In this discussion, the general compressor design and development process is reviewed with emphasis upon the role of the through-flow calculation.

Detroit Diesel Allison's approach to compressor design and development is enumerated below:

1. Design with the best analytical techniques and empirical data available,
2. Instrument the compressor adequately to evaluate the validity of the design theory and assumptions,
3. Obtain sufficient test data to completely define the compressor characteristics, both aerodynamically and structurally,
4. Reduce and interpret the data in a consistent manner, and
5. Perform a comprehensive analysis of the data to determine areas of possible performance improvement.

One complete cycle of this process for a multistage axial flow compressor generally takes about a year to complete with a majority of this time consumed in fabrication. Considering the length of time involved, a high premium is placed upon a technically sound approach in each of the five areas listed above.

Normally, the development process takes more than one cycle to complete due to inadequacies in the design theory and assumptions. A consistent and technically sound approach which builds upon previous experience has proven to be the best method of reducing the number of development cycles. The validity of this approach is exemplified by the development history of one of Detroit Diesel Allison's modern multistage compressors shown below:

	First build	Second build	Third build
Pressure Ratio*	14.55	15.00	15.00
Adiabatic Efficiency*	80.15%	80.50%	82.00%
Surge Pressure Ratio	14.55	17.3+	17.3+

*On engine operating line.

With just two blading modifications, the operating line efficiency was increased nearly 2% and the surge pressure ratio increased by 3 atmospheres.

The through-flow calculation is an integral and vital element in this overall design and development process. In addition to the obvious use of the calculation in the design phase, the calculation provides information for locating instrumentation, aids in determining the true pressure or temperature from measured data, and supplements the measurements to obtain a meaningful flow field definition

Design

In the design phase, the best analytical techniques and empirical data available are used to accomplish the two basic parts of the final design specification, namely:

1. Establish the desired aerodynamic flow field definition,
2. Design blading to produce the conditions established in Part 1.

The flow path shape, number of required stages, Mach number levels, work distribution, and blade element loading and efficiency requirements are determined in the first phase of the design. These variables are chosen to provide maximum assurance of meeting design goals. In this phase, the through-flow calculation is the designer's primary tool. In this calculation the inviscid equations are coupled directly with secondary computations which account for real fluid effects such as aerodynamic blockage, blade element losses and tip clearance leakage. These viscous effects are based on theoretical analyses, but are tempered by past experience with similar configurations.

The purpose of the second phase is to define the detailed blade geometry which will generate the flow field conditions established in Phase 1. To satisfactorily accomplish Phase 2, the following design variables must be correctly defined:

- o Incidence angle
- o Blade element flow capacity
- o Deviation angle
- o Blade shape consistent with Phase 1 loss characteristics.

In both phases,the designer is guided by experience gained from previous compressor development programs. His detailed experience in terms of such items as acceptable loading limits, blade element losses, and incidence and deviation rules is tied directly to the design and analysis system and the consistency in which data was acquired and processed.

Instrumentation

The general requirements for an adequate yet economically tractable instrumentation plan are:

- o Provide adequate instrumentation to minimize assumptions required for flow field definition,
- o Minimize flow field disturbance, and
- o Minimize the additional test time required for data acquisition.

The item of overriding importance is the acquisition of data which is truly representative of the compressor characteristics and not influenced by the measuring instrument. To reduce the blockage and resulting flow field disturbance associated with a conventional cantilevered probe, Detroit Diesel Allison practice is to mount the sensing element directly on the vane surface for all interstage data. A sketch of a typical installation is shown in Figure 10 along with a photograph of an actual vane with leading edge total pressure elements attached. The sensing element is suspended from the pressure surface of the airfoil to minimize the disturbances to the suction surface which is more sensitive due to higher Mach numbers and velocity gradients. To minimize the leading edge incidence effects, the sensing element is surrounded by a ventilated shroud and positioned as far forward of the leading edge as possible. Interference with the preceding rotating blade row determines the maximum stand off distance. In some instances, leading edge effects cannot be eliminated.

In order to ensure accurate interpretation of the data, the instrumentation is calibrated prior to the test to quantify the effects of Mach number and angle of attack on the recovery characteristics of the probe. This calibration is usually accomplished with an isolated airfoil and a two dimensional air jet. An example of the calibration results is shown in Figure 10, where the recovery characteristics of a leading edge mounted thermocouple display assymetry due to the airfoil leading edge effect. This result is the rule rather than the exception in multistage axial flow compressors where the typically small axial gaps between rotating and stationary blade rows would preclude the forward extension of the probe. In order to interpret the data accurately, the true flow Mach number and air angle must be ascertained. This is an extremely vital part of the data reduction effort and requires iterative use of the through-flow calculation for completion. A more detailed discussion of this process is given in a following section of this paper concerned with data reduction.

A typical instrumentation plan which has been used and fulfills the above stated requirements is shown in Figure 11. The instrumentation includes stator leading edge mounted total pressure and temperature sensing elements for interstage data, conventional shrouded total pressure and temperature probes at compressor inlet and exit and a multi-element wake rake behind the exit guide vane in the outer duct. A large contingent of wall static pressure taps is included to define the Mach number distribution over the flow splitter.

The radial locations and angular alignments of the individual elements are determined from the flow field solution defined by the through-flow calculation in the design phase. Increased instrumentation is included in areas of expected high gradients such as around the flow splitter in the above example to evaluate the validity of the through-flow calculation in these areas.

Data Reduction

The instrumentation plan described in Figure 11 is typical of the type and extent of instrumentation incorporated in a development build of a compressor. The limitations of this instrumentation coverage relative to defining the entire flow field are also typical.

The purpose of the data reduction process is to take measured data, apply calibration factors in a consistent and correct manner and then reconstruct the entire flow field definition for comprehensive analysis relative to design intent.

Typically, for interstage data, the stage work input and loss characteristics are well defined from stator leading to rotor trailing edges, Figure 12. Measurements of total pressure and absolute air angle are usually not made at stator exits and, therefore, some assumptions must be made concerning these variables before a complete flow field definition can be constructed. Even with the assumptions on stator loss and detailed measurements of rotor exit total pressure and temperature, the flow field definition is not complete and not in a usable form for detailed analysis. The velocity distribution is not known and, therefore, the key aerodynamic parameters such as incidence, deviation, Mach number and blade element loading cannot be determined. The through-flow calculation with data input in terms of total pressure and temperature at rotor exits and with consistent assumptions on stator loss and deviation is used to provide this required information. The flow field defined for the test point is completely consistent, in terms of stator assumptions and solution methods, with the design flow field and can be compared directly. Once the velocity distribution is known, then the Mach number and angle of attack of the air onto the measuring element (P_t or T_t) can be determined and the appropriate calibration factors applied. The adjusted data changes the velocity distribution and further iterations are required. This process, Figure 13, is obviously iterative and continues until the flow field variables (P_t, T_t, M_n, and air angle) are consistent with the measured interstage data and calibration information. A final important consideration in the data reduction process is the method by which remotely obtained data, Figure 13, is streamlined back (or forward) to the blade trailing (or leading) edges for detailed blade element analysis. The streamlines along which the data is repositioned are determined iteratively for each data point instead of using the streamline definition from the design solution.

The final result of the data reduction process is a complete definition of the entire flow field including blade element conditions. This definition is then compared directly to the design flow field description and areas of performance improvement identified. Once hardware modifications are identified, the cycle starts over again.

Conclusions

The importance of an accurate and flexible through-flow calculation is evident. It is one of the key elements in an effective compressor design and development process and is the primary tool with which the detailed design is accomplished, the data interpreted and analysis performed.

The techniques expounded upon in this paper have lead to significant advances in the state-of-the-art in compressor design. If these advances are to continue, better understanding of the basic fluid mechanics of compressor operation must be incorporated into a usable design and analysis system. Some areas where further improvements are needed are:

- o Intrablade analyses
- o Tip clearance effects
- o Secondary flow and streamline communication
- o Endwall boundary layer development.

Much effort has already been expended in these areas, and some techniques have been incorporated into the design and analysis systems. Data correlations and individual experience remain, however, the prime methods of accounting for these effects.

The primary emphasis of future research efforts should be focused on elements of flow behavior such as those above. Recognizing this need, Detroit Diesel Allison has designed and fabricated a large low speed test rig incorporating a single stage axial compressor designed for loading levels typical of advanced state-of-the-art compressors. Current effort is being directed toward the better understanding of endwall boundary layer development as the flow proceeds through alternating stationary and rotating blade rows. As each of these elements of flow behavior are better understood, improved models will be developed and incorporated into the basic design and analysis system

REFERENCES

1. Horlock, J. H., "On Entropy Production in Adiabatic Flow in Turbomachines", ASME Paper No. 71-F3-3, 1971.

2. Horlock, J. H., and Marsh, H., "Flow Models for Turbomachines", Journal of Mechanical Engineering Science, Vol. 13, No. 5, 1971.

3. Wu, Chung-Hua, "A General Theory of Three-Dimensional Flow in Subsonic and Supersonic Turbomachines of Axial, Radial, and Mixed Flow Types", NACA TN 2604, 1952.

4. Allran, R. R., Fagan, J. R., and Haley, P. J., "Elements of Three-Dimensional Flow", Proceedings of a Workshop for Prediction Methods for Jet V/STOL Propulsion Aerodynamics, Editor - M. F. Platzer, Vol. 1, 1975.

5. Novak, R. A., and Hearsey, R. M., "A Nearly Three-Dimensional Intrablade Computing System for Turbomachinery - Part I: General Description", ASME Paper No. 76-FE-19, 1976.

6. Bosman, C., and El-Shaarawi, M. A. I., "Quasi-Three-Dimensional Numerical Solution of Flow in Turbomachines", ASME Paper No. 76-FE-23, 1976.

7. Marsh, H., "A Digital Computer Program for the Through-Flow Fluid Mechanics in an Arbitrary Turbomachine Using a Matrix Method", Aeronautical Research Council R. & M. No. 3509, 1968.

8. Davis, W. R., and Millar, D. A. J., "A Comparison of the Matrix and Streamline Curvature Methods of Axial Flow Turbomachinery Analysis, From a User's Point of View", ASME Paper No. 74-WA/GT-4, 1974.

9. Wilkinson, D. H., "Stability, Convergence and Accuracy of Two-Dimensional Streamline Curvature Methods Using Quasi-Orthogonals", Institution of Mechanical Engineers - Thermodynamics and Fluid Mechanics Convention, Paper No. 35, 1970.

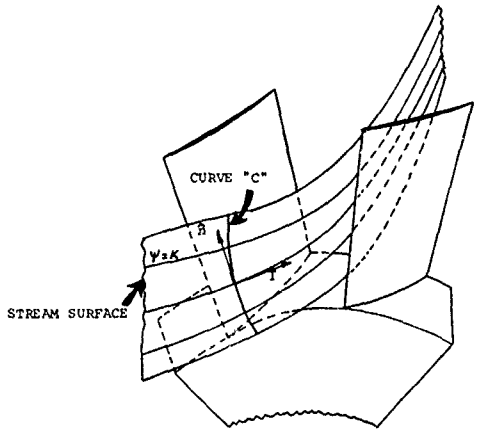

Figure 1. Stream Surface and Coordinate System

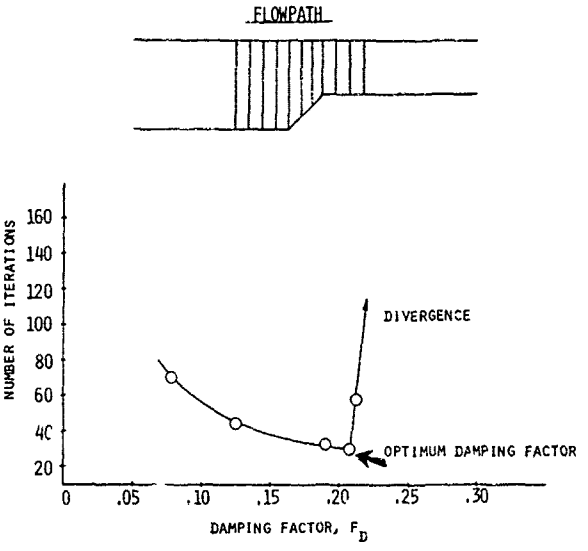

Figure 2. Damping and Convergence

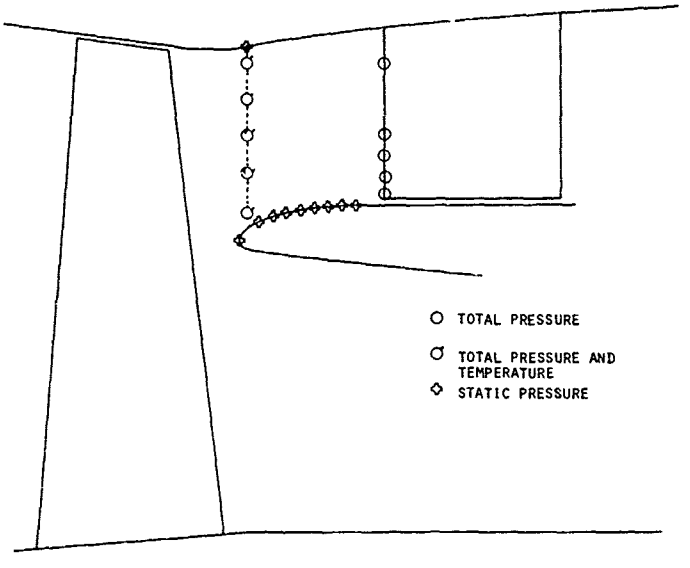

Figure 3. Example 1 - Instrumentation

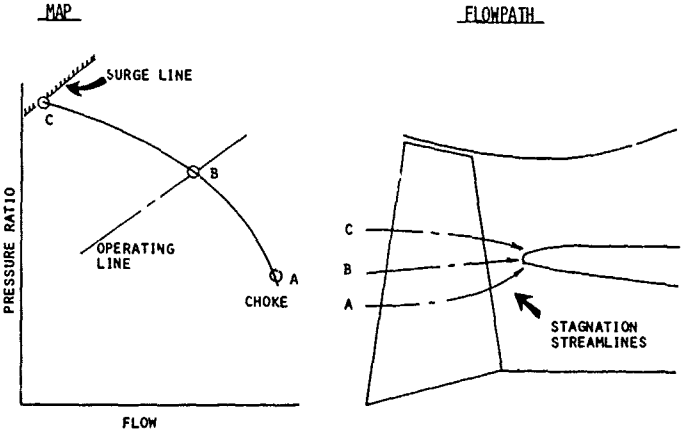

Figure 4. Example 1 - Data Point Locations

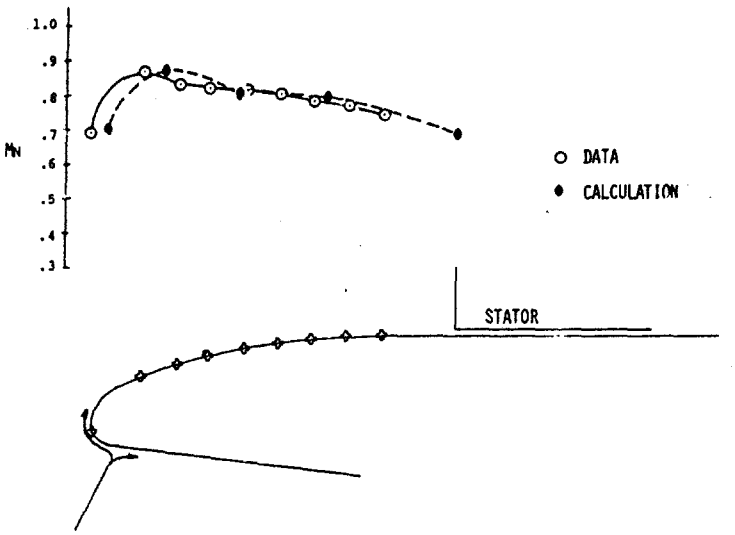

Figure 5. Example 1 - Near Choke Data Point

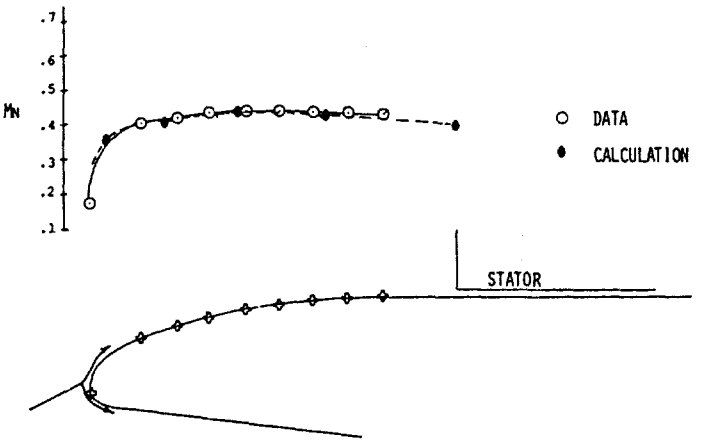

Figure 6. Example 1 - Operating Line Data Point

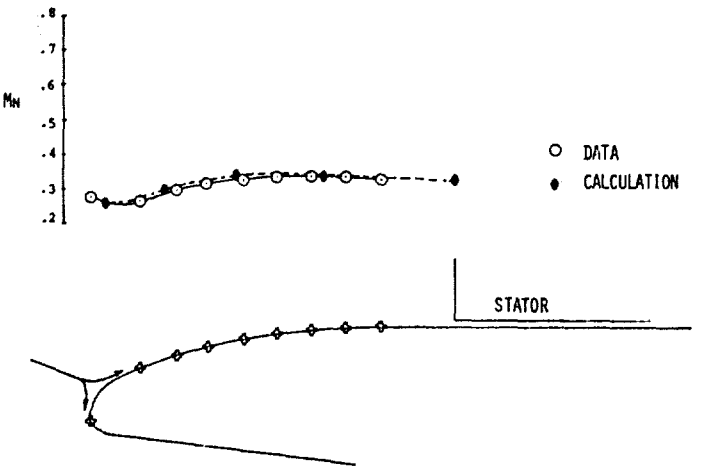

Figure 7. Example 1- Near Surge Data Point

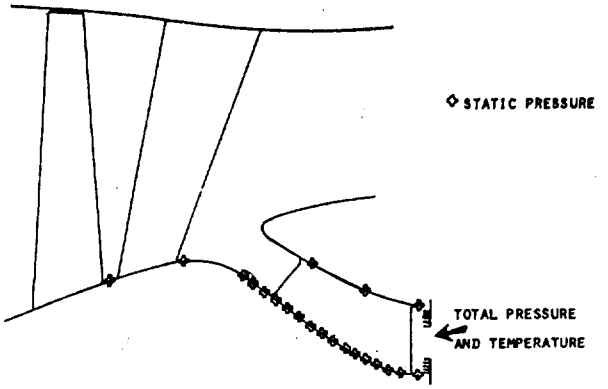

Figure 8. Example 2 - Flowpath and Instrumentation

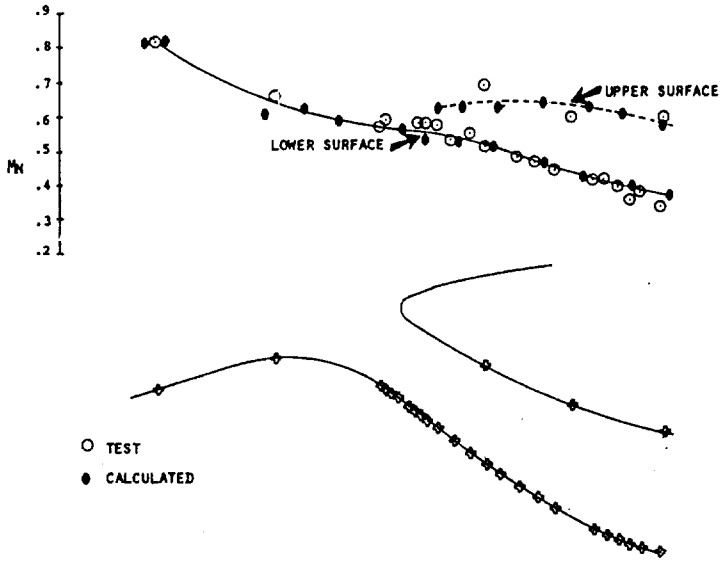

Figure 9. Example 2 - Data Comparison

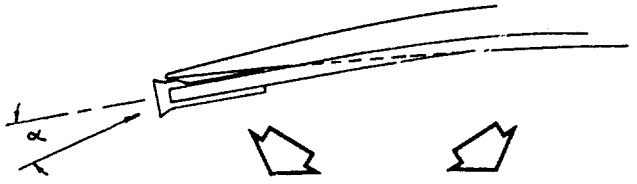

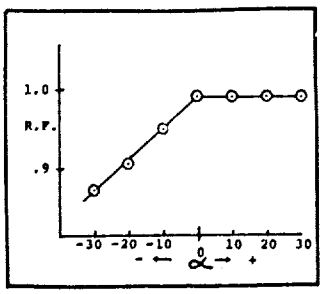

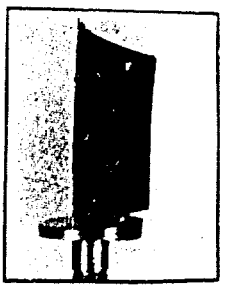

Figure 10. Stator Leading Edge Instrumentation Schematic and Characteristics

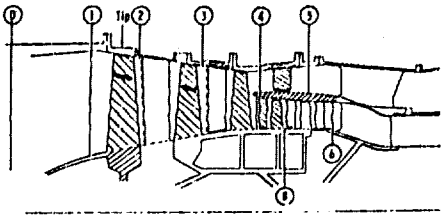

	Plane Number						
	0	2	3	4	5	6	8
Total pressure (vane leading edge)		3-14 element	2-11 element				2-5 element
Total temperature (vane leading edge)		2-14 element	2-11 element				2-5 element
Total pressure (fixed probe)	4-4 element			2-10 element	5-5 element	3-5 element	
Total temperature (fixed probe)	4-4 element			2-10 element	3-5 element	3-5 element	
Dynamic pressure					3-3 element	3-3 element	
Static pressure	4 tip	4 tip	4 tip 4 hub	6 tip 6 split OD 6 split ID 18°	6 tip 6 hub	6 tip	4 tip
Wake rake					3-15 element		

* A double row of wall static pressure probes were located from splitter leading edge to bypass exit vane inlet.

Figure 11. Instrumentation Plan

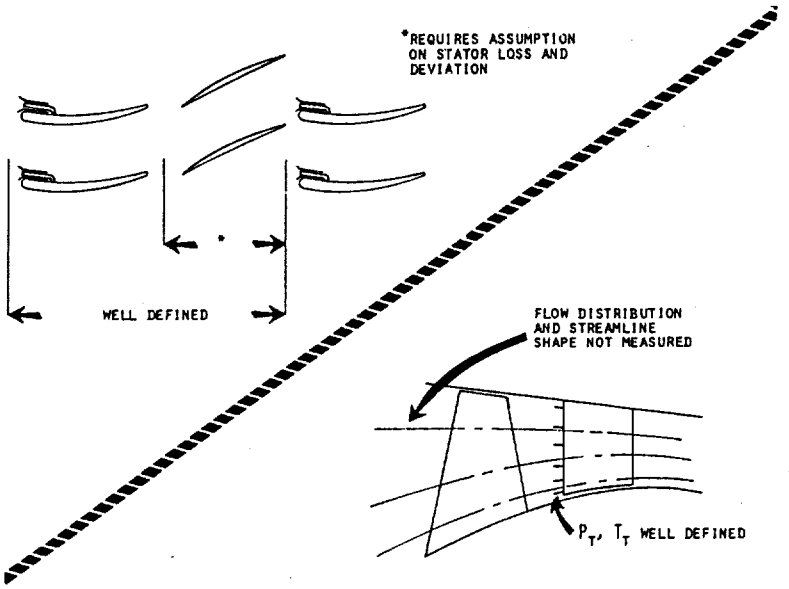

Figure 12. Instrumentation Limitations

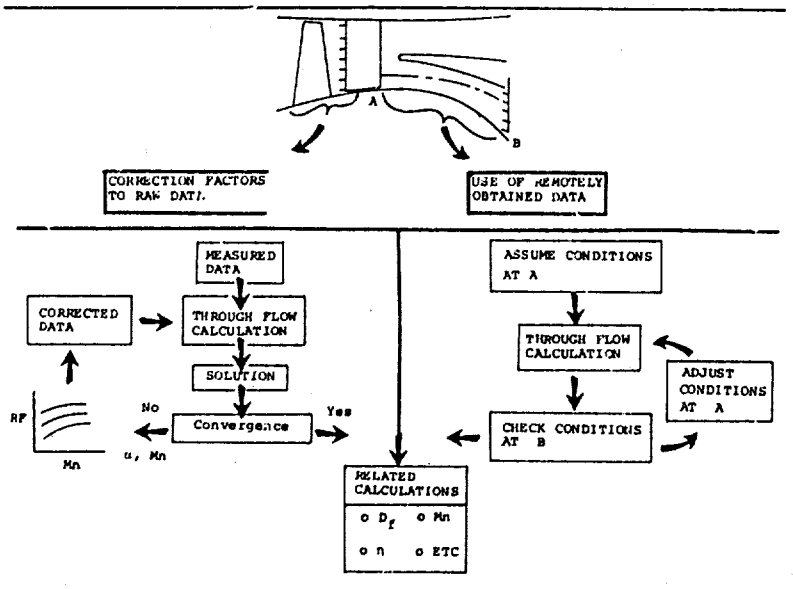

Figure 13. Data Reduction Process

COMMENTS

Comment by D.Millar, Carleton University, Canada

Do you use outer wall (casing) wall tappings for comparison with calculation, especially to separate rotor from stator performance within the stage? I would think this would be quite useful for a compressor which has essentially axial flow between rotor and stator, where there is little radial pressure gradient.

Authors' response:

Outer wall static pressures are used for comparison, but it is hard to break out the combined effects of loss, blockage and whirl.

FINITE ELEMENT METHOD FOR THROUGH-FLOW CALCULATIONS

by

Ch. Hirsch

Professor, Dept. of Fluid Mechanics

Vrije Universiteit Brussel

1050 Brussels

Belgium

SUMMARY

A description is presented of the application of the Finite Element method to the radial equilibrium equation in the form obtained after introduction of the streamfunction. A short presentation of the basic features of the F.E.M. is given and the particular aspects of its application to the through-flow problem in turbomachines are described.

A comparison with an analytic solution for an axisymmetric transitional annulus with swirl allows an estimation of the numerical accuracy of the method. Other examples of results include a transonic axial compressor and an axial turbine. The coupling with an end-wall boundary layer calculation for axial compressors is also briefly described and some results are presented.

INTRODUCTION

The calculation methods for the through-flow in turbomachines developed in recent years have mainly been concentrated on two numerical techniques, the streamline curvature method and the so-called matrix method, which is essentially a finite difference scheme. Although these methods have achieved satisfactory results, they still suffer from certain difficulties. Estimations of the curvature of a streamline which is defined by a discrete number of points can create large errors [1], [2] while the correct simulation of curved end-wall in the matrix method requires complicated "computational stencils" [3].

A Finite Element method is presented in this paper for the calculation of the meridional through-flow in a turbomachine which doesn't suffer from these difficulties. Quadrilateral curved (isoparametric) elements are used which can simulate accurately the curvature of boundaries while estimations of streamline curvature do not appear in the calculation.

After deriving the equation for the stream function which is solved in its quasi-harmonic form, the finite element technique is described. The calculation method can handle any geometry, axial or radial, and examples of results are presented. Comparison with an analytical solution for the downstream part of an annular transition with swirling flow gives indications on the accuracy of the computation method. Examples are also shown of a transonic axial compressor and an axial turbine calculation. Besides, the coupling of the main flow with an end-wall boundary layer calculation method for axial compressors is briefly described and some results are presented.

1. BASIC EQUATIONS

Starting from the three-dimensional flow equations in the relative system, with the introduction of the energy equation in the form of the first principle of thermodynamics and the definition of the rothalpy I

$$\frac{\partial \vec{W}}{\partial t} - \vec{W} \wedge (\vec{\nabla} \wedge \vec{V}) = T \vec{\nabla} s - \vec{\nabla} I + \vec{F}_f/\rho \qquad (1)$$

$$\frac{\partial \rho}{\partial t} + \vec{\nabla} \rho \vec{W} = 0 \qquad (2)$$

$$I = h + \vec{W}^2/2 - \omega^2 r^2/2 = H - U V_\theta \qquad (3)$$

where $\vec{W}$ and $\vec{V}$ are the relative and absolute velocities, h the static enthalpy, s the entropy, $U = \omega r$, and $\vec{F}_f$ the sum of viscous and turbulent shear stresses, one can derive the meridional through-flow equations in different ways.

Following C.H. Wu's S1, S2 surfaces approach [4], equ. (1) is projected on a meridional type of stream surface S2 with derivatives along this surface and the introduction of body forces replacing the blades. This requires the knowledge of this surface or a more or less arbitrary assumption of its shape. Another approach consists in integrating equ. (1) and the continuity equation (2) over a pitch, from pressure side of a blade to the suction side of the following blade [5], [6]. In this way equations are obtained for the pitch-averaged equations, whose projections in cylindrical coordinates (r, θ, z) contain the projections of the terms of equ. (1) (for the pitch-averaged quantities) plus a blade force term and a certain number of terms describing the deviations from axisymmetry. These terms, which are neglected in the axisymmetric approximation, could be estimated within the blades from the knowledge of the blade-to-blade flow. However, as shown in ref [5], these terms are generally small and proportional to the loading inside a blade row. Outside a blade row, the main contribution comes from the wakes and an estimation based on a simplified wake model [7], shows that the contributions from the non-axisymmetry to the meridional through-flow are proportional to the total pressure loss coefficients and are generally small, except maybe in the end-wall regions.

Therefore, neglecting the non-axisymmetric contributions, one obtains in cylindrical coordinates

$$\frac{1}{r}\frac{\partial}{\partial r}(b\, r\, \rho\, W_r) + \frac{\partial}{\partial z}(b\, \rho\, W_z) = 0 \tag{4}$$

$$W_z\left[\frac{\partial}{\partial z} W_r - \frac{\partial}{\partial r} W_z\right] = T\frac{\partial s}{\partial r} - \frac{\partial I}{\partial r} + \frac{W_\theta}{r}\frac{\partial}{\partial r}(r\, V_\theta) + (F_{b,r} + F_{f,r})/\rho \tag{5}$$

$$W_r\left[\frac{\partial}{\partial r} W_z - \frac{\partial}{\partial z} W_r\right] = T\frac{\partial s}{\partial z} - \frac{\partial I}{\partial z} + \frac{W_\theta}{r}\frac{\partial}{\partial z}(r\, V_\theta) + (F_{b,z} + F_{f,z})/\rho \tag{6}$$

$$\frac{1}{r}\frac{\partial}{\partial m}(r\, V_\theta) = (F_{b,\theta} + F_{f,\theta})/\rho \tag{7}$$

where all variables are pitch-averaged quantities, b is the tangential blockage factor

$$b = 1 - t/s \tag{8}$$

with t the blade thickness and s the pitch; m is the coordinate along a meridional streamline and F_b is the blade force.

Introducing a stream function in order to satisfy the continuity equation (4), through

$$\frac{\partial \psi}{\partial r} = \rho\, r\, b\, W_z \tag{9a}$$

$$\frac{\partial \psi}{\partial z} = -\rho\, r\, b\, W_r \tag{9b}$$

and introducing equ. (9a) and (9b) in the radial component of the momentum equation [5], one obtains

$$\frac{\partial}{\partial r}\left(\frac{1}{\rho r b}\frac{\partial \psi}{\partial r}\right) + \frac{\partial}{\partial z}\left(\frac{1}{\rho r b}\frac{\partial \psi}{\partial z}\right) = \frac{1}{W_z}\left[\frac{\partial I}{\partial r} - T\frac{\partial s}{\partial r} - \frac{W_\theta}{r}\frac{\partial}{\partial r} r\, V_\theta - F_{b,r}/\rho - F_{f,r}/\rho\right] \tag{10}$$

This well known form for the radial equilibrium equation is however not applicable to radial geometries where the axial velocity W_z will go to zero. One could then use the axial component of the momentum equation (6), but a more unified approach is obtained, following Bosman & Marsh [8], if the equations are projected along the direction of $(\vec{F}_f \wedge \vec{W})$ taking advantage from the relations

$$\vec{F}_b \cdot \vec{W} = 0 \qquad \text{and} \qquad \vec{F}_f \wedge \vec{W} = 0 \tag{11}$$

In this way, the r.h.s. of equ. (10) becomes for a rotor

$$\rho\, r\, b \frac{dI}{d\psi} - \frac{T}{W^2}\frac{\partial s}{\partial r}(W_z + W_\theta \operatorname{tg}\beta) + \frac{T}{W^2}\frac{\partial s}{\partial z}(W_r - W_\theta \operatorname{tg}\beta) - \frac{1}{r}\frac{\partial}{\partial r}(r V_\theta)\cdot \operatorname{tg}\beta - \frac{1}{r}\frac{\partial}{\partial z}(r V_\theta).\operatorname{tg}\beta \tag{12}$$

with

$$\operatorname{tg}\beta = W_\theta / W_m \tag{13}$$

and

$$W_r \operatorname{tg}\beta + W_\theta - W_z \operatorname{tg}\beta = 0 \tag{14}$$

It is interesting to note that the forces do not appear anymore although they are not neglected.

An analogous expression is obtained for a fixed blade row and outside a blade row in a duct region, the r.h.s. becomes

$$\rho\, r \left[\frac{dH}{d\psi} - T\frac{ds}{d\psi} - \frac{V_\theta}{r}\frac{d}{d\psi} r V_\theta\right] \tag{15}$$

where H is the stagnation enthalpy.

2. THE FINITE ELEMENT METHOD

The basic principles of the Finite Element method can be summarized through the three following steps

a) Division of the physical domain into subdomains of simple geometrical forms (triangles, quadrilaterals, rectilinear or curvilinear). Each subdomain $\mathcal{D}^{(e)}$ is called a finite element and contains nodes on its boundaries or inside the subdomain (fig. 1). Moreover the elements may not overlap and have to cover the whole physical domain

$$\cup \mathcal{D}^{(e)} = \mathcal{D} \tag{16}$$

$$\mathcal{D}^{(e)} \cap \mathcal{D}^{(e')} = 0 \tag{17}$$

The fact that the form of the elements need not be of regular shape allows easily to take into account the presence of irregular or curved boundaries.

b) Definition of interpolation functions whereby the field variables are locally approximated in each finite element by a combination of continuous interpolation functions and by the nodal values of the unknown functions (which, by the way, may also be values of the derivatives of the field variables).

Denoting by $\phi^{(e)}$ the approximation of the unknown field variables in element e and by $\phi_j^{(e)}$ the values at the node j, one assumes the form

$$\phi^{(e)}(\underset{\sim}{x}) = \sum_{j=1}^{s^{(e)}} N_j^{(e)}(\underset{\sim}{x})\, \phi_j^{(e)} \tag{18}$$

where $N_j^{(e)}$ are the shape functions in element (e) depending on the coordinates $\underset{\sim}{x}$ ($\underset{\sim}{x}$ denotes a set of coordinates) and $s^{(e)}$ is the number of nodes in element (e).

In a two-dimensional domain (r, z), $N_j^{(e)}(\underset{\sim}{x}) \equiv N_j^{(e)}(r, z)$

From the definitions (18), for each node i within the element e

$$N_j^{(e)}(\underset{\sim}{x}_i) = \delta_{ij} \quad \text{and} \quad N_j^{(e)}(\underset{\sim}{x}) = 0 \quad \text{if } \underset{\sim}{x} \notin \mathcal{D}^{(e)} \tag{19}$$

where $\underset{\sim}{x}_i$ are the coordinates of node i.

The explicit form of the interpolation functions N_j depends on the form of the elements, the number of nodes and on the order of the differential equations to be solved.

The most effective form for the shape functions are polynomials. The FE method then amounts to a piecewise continuous polynomial approximation for the field functions.

c) The definition of a basic integral functional equation equivalent to the field equations to be solved. This is probably the most essential and particular step of the formulation of a finite element approximation since it allows, after replacement of the field variables by the approximation (18) for each element to obtain an algebraic system of equations for the unknown nodal values $\phi_j^{(e)}$. Indeed, if the functional equation is written as

$$I \equiv \int_{\mathcal{D}} h\,(\phi,\ \partial\phi,\ \ldots)\ d\underset{\sim}{x} + \int_{\partial\mathcal{D}} g\,(\phi,\ \partial\phi,\ \ldots)\ d\underset{\sim}{x} = 0 \tag{20}$$

insertion of equation (18) and consideration of equation (17), allows to write

$$I = \sum_e I_e = 0 \tag{21}$$

leading, in each element, to an algebraic system for the ϕ_j^e of the form

$$k_{ij}^{(e)}\ \phi_j^{(e)} = F_i^{(e)} \tag{22}$$

or with usual notations

$$[k^{(e)}]\ \{\phi^{(e)}\} = \{F^{(e)}\} \tag{23}$$

whereby $k_{ij}^{(e)}$ and $F_i^{(e)}$ are integrals of combinations of products of shape functions and their derivatives and can therefore be calculated at least numerically.

The assembly rule

$$I = \sum_e I_e \tag{24}$$

leads to the final algebraic system

$$[K]\ \{\phi\} = \{F\} \tag{25}$$

The matrix K is calles the "stiffness matrix" (with analogy to elasticity problems).

The assembly rule implies certain continuity conditions along the inter-element boundaries in order that the sum of the integrals on the inter-element boundaries cancels in the sum (21).

Expressed from an engineering point of view, see ref. [9], this leads to certain continuity conditions for the shape functions. If one denotes by r the order of the highest derivative accuring in the integral equation (20), then the criterion states that the field functions must satisfy to the continuity of all derivatives up to order (r - 1) accross the element boundaries. For r = 1, this implies continuity of the function while for r = 2, continuity of the function and the first derivative are imposed accross the element boundaries. This appears to be a sufficient but not always necessary condition.

We may add a this stage, that a sufficient (but not always necessary) condition for convergence of the F.E.M. when the size of elements tends to zero, is that the set of shape functions must be able to represent any constant value of the field variables and derivatives up to order r within an element. This implies

$$\sum_{j=1}^{s^{(e)}} N_j^{(e)}(\underset{\sim}{x}) = 1 \qquad \underset{\sim}{x} \in \mathcal{D}^{(e)} \tag{26}$$

More rigorous formulations can be found in [10].

An integral formulation for equ. (10) can be obtained by the Galerkin method of weighted residuals. Writing this equation under the general form

$$R_v(\psi) \equiv \frac{\partial}{\partial r}\left(k \frac{\partial \psi}{\partial r}\right) + \frac{\partial}{\partial z}\left(k \frac{\partial \psi}{\partial z}\right) + f(r, z, \psi) = 0 \tag{27}$$

where $k = 1/\rho\, b\, r$ and f is minus the r.h.s. equ. (13) - (15).

The boundary conditions are $\psi = 0$ at the hub wall, $\psi = \dot{m}/2\pi$ where $\dot{m}$ is the mass flow rate at the tip wall, $\frac{\partial \psi}{\partial n} = 0$ or ψ imposed at the entrance section and $\frac{\partial \psi}{\partial n} = 0$ at the outlet section.

If $\tilde{\psi}$ is an approximation to ψ, satisfying the boundary conditions along the parts of the boundary where ψ is fixed, then the residual

$$R_v(\tilde{\psi}) \neq 0 \tag{28}$$

and a "best approximation" will be defined as the one which cancels a weighted average of R_v plus a weighted contribution on the boundary when Neumann conditions are present. Therefore, the following integral formulation is obtained which is equivalent (in the weak sense) to the original differential equation

$$-\int_{\mathcal{D}} W \cdot R_v \, d\Omega + \int_C W \cdot \frac{\partial \tilde{\psi}}{\partial n} \, dC = 0 \tag{29}$$

where C is the contour enclosing the domain $\mathcal{D}$.

Replacing R_v by its definition, equ. (27) and integrating by parts the following form is obtained

$$\int_{\mathcal{D}} \left[k \left(\frac{\partial \tilde{\psi}}{\partial r} \cdot \frac{\partial W}{\partial r} + \frac{\partial \tilde{\psi}}{\partial z} \frac{\partial W}{\partial z}\right) - f(r, z, \tilde{\psi}) \cdot W \right] d\Omega = 0 \tag{30}$$

where the weight functions W can be arbitrarily chosen.

3. CALCULATION PROCEDURE WITH FINITE ELEMENTS

The meridional section of the machine is divided into finite elements which are chosen to be 8-node quadrilateral isoparametric (curved) elements (fig. 2). The reason for the choice of these elements is twofold : it enables to handle accurately curved boundaries and complicated geometries like in radial machines with simple meshes and at the same time provides a high order of accuracy (probably third order based on linear theory [10]). The corresponding shape functions N_j are biquadratic in the local coordinates ξ, η (fig. 2).

Calculation stations are chosen and disposed in the duct part of the machine and at the edges and center line of the blades (fig. 3). The number of grid points on each station is fixed while the element distribution is generated in the program.

With the FE approximation in each element

$$\psi = \sum_{i=1}^{8} \psi_i N_i \tag{31}$$

where ψ_i are the unknown values at the nodes, and the Galerkin procedure where the weight functions W are chosen equal to the shape functions N_j, equ. (30) takes the matrix form, in each element E ,

$$[K]^e \{\psi\}^e = \{f\}^e \tag{32}$$

where $\{\psi\}^e$ is the vector of the unknown nodal values and

$$[K]^e_{ij} = \int_E k \left(\frac{\partial N_i}{\partial r}\frac{\partial N_j}{\partial r} + \frac{\partial N_i}{\partial z}\frac{\partial N_j}{\partial z}\right) d\Omega \tag{33}$$

$$\{f\}_j^e = \int_E f\, N_j \, d\,\Omega \tag{34}$$

Assembling equations (32) for all elements, the complete system of equations

$$[K]\ \{\psi\} = \{f\} \tag{35}$$

is obtained.

Equation (35) is a non-linear system of algebraic equations, which has to be solved iteratively. The whole calculation procedure amounts therefore to the estimation of the matrix elements (33) and (34) ; this requires the computation of the flow variables at all nodes in order to estimate k and f, the integration being performed numerically through Gauss-point quadrature formula's. After this step, the algebraic system (35) is solved with an elimination method adapted to the banded, symmetric nature of the matrix [K] and an iterative procedure is established to handle the non-linear character of the system (35). More details about these parts of the calculation can be found in [11] and [6]. It is however worthwhile to mention that an underrelaxation coefficient has to be introduced in order to obtain convergence, through

$$\{\psi\}_{n+1} = \{\psi\}_n + \mu\, [\{\tilde{\psi}\}_{n+1} - \{\psi\}_n] \tag{36}$$

where $\{\tilde{\psi}\}_{n+1}$ is the solution of (35) obtained at iteration (n+1) while $\{\psi\}_{n+1}$ is used to start the next iteration.

4. APPLICATIONS

The computer code based on the finite element method has been applied to various situations. Separate codes have been developed for axial compressors and axial turbines and the codes can handle also any ducting configuration axial, radial or mixed with a representation of the end-wall curvature by second-order polynomials within each element as a consequence of the use of isoparametric elements.

4.1 Comparison with an exact solution

An axisymmetric transition ducting with swirling flow super-imposed on an uniform axial velocity distribution has been calculated for an incompressible flow.

The geometry of this configuration consists of two cylindrical annuli at different radii connected by a transition - fig. 4. The inlet flow is composed of a uniform axial velocity U (flow from left to right) superposed on a solid body rotations $V_\theta = \Omega\, r$. The hub radius is 0.25 m at inlet and 0.10 m at outlet while the tip radious changes from .35 m to .2 m. The mass flow is 10 kg/sec and $\Omega = 100\ \text{sec}^{-1}$.

As shown by Batchelor [12] an analytic solution exists in the downstream region which can be expressed as a combintation of Bessel function's for an incompressible flow

$$\psi/\rho = \frac{1}{2}\ U\ (r^2 - a_h^2\ ) + r\,[A\ J_1\ (k\ r) + B\ Y_1\ (k\ r)] \tag{37}$$

where $R = \dfrac{2\ \Omega}{U}$

The coefficients A and B are obtained in a straigh forward way by expressing that the walls of the downstream part are streamfunctions at the same value as the corresponding upstream part. This leads to

$$A = \frac{U}{2 b_t b_h}\ \frac{b_h\ (a_t^2 - b_t^2)\ Y_1\ (k\ b_h) - b_t\ (a_h^2 - b_h^2)\ Y_1\ (k\ b_h)}{J_1\ (k\ b_t)\ Y_1\ (k\ b_h) - J_1\ (k\ b_h)\ Y_1\ (k\ b_t)}$$

and B is obtained by interchanging J_1 with Y_1, while a_h and b_h denote resp. the upstream and down-

stream hub radii and a_t and b_t the corresponding tip radii.

The downstream velocity profiles are obtained by

$$V_z = U + A\,k\,J_o(k\,r) + B\,k\,Y_o(k\,r) \tag{39}$$

$$V_\theta = \Omega\,r + k\,A\,J_1(k\,r) + B\,k\,Y_1(k\,r) \tag{40}$$

Figure 4 shows the element distribution (dashed lines) and the calculated streamlines while fig. 5 shows the calculated velocity profiles in the dowstream region compared with the theoretical values. Excellent agreement is achieved as shown on fig. 6 where the relative error in percent of the actual value is plotted in function of radius for ψ, V_z and V_θ. As can be seen from fig. 6 the maximum error on the streamfunction is less than .006 % while the error on the axial velocity, is everywhere below . 05 %. As for V_θ the error remains below .002 %.

It is to be noted that no underrelaxation is needed for incompressible flows. This case converged in two iterations obtaining root mean square convergence level of .05 % and required 30 sec CP time on a CDC 6500 for 406 nodes.

4.2 Axial Turbine

The three stage turbine of test case 2 has been calculated with the finite element method, fig 7.

The losses and deviations are calculated with the Ainly-Mathieson correlations. Although, as seen on fig. 8, the pressure ratios are generally too high, except at the higher mass flow of 7.58 kg/sec (at design speed), the radial distributions at outlet of the plotted variables, flow angle, total temperature ratio, axial and relative Mach numbers agree quite well with the data, as can be seen on fig 9 to 12. The calculated total pressure ratio profiles at outlet, although shifted, are of the correct shape, fig. 13. On all figures the dashed lines are the experimental results and the line with the dots are the calculated values.

4.3 Axial compressors

Various axial compressors have been calculated [6], [11] with the FE method. The loss model included in the code is based on the correlations used by Davis [13].

Runs performed on a two highly loaded axial flow fan [14] and on other cases show that the correlation is generally acceptable although the stator losses have a tendency to be overestimated, especially at lower speeds. The deviations are in general fairly well predicted.

Fig. 14 shows the calculated losses and cascate angles for this 2-stage fan at 70 % of design speed for the second stator while fig. 15 shows the corresponding results for the first rotor at design speed compared to experimental data. Examples of calculated radial distributions of relative flow angles and Mach numbers are shown on fig. 16 and 17 for the design point at inlet and outlet of the two rotors together with experimental results.

4.4 End-wall boundary layers in axial compressors

The blockage introduced by the end-wall boundary layers has a non-negligible influence on the whole flow and performance of an axial compressor, and blockage factors are always introduced in a way or in another in through-flow calculations. Either they are introduced more or less arbitrarily in the calculations or boundary layer theories can be used for this purpose. An interesting model has been proposed recently by Mellor & Wood [15] which enables the prediction of blockage and end-wall losses. An extension of this model has been developed in ref. [16], [17] in order to predict complete velocity profiles. Although much progress is still necessary, the explicit introduction of boundary layer velocity laws (like the Mager law for the cross-flow e.g.) allows the calculation, besides blockage, of wall skewing angles, shape factors and skin-friction coefficients of the three-dimensional end-wall layer . An example of calculated boundary layer parameters is shown here for the

four stage compressor of test case 5. Fig. 18 shows the geometry of the compressor while fig. 19 and 20 show the axial variation at hub and tip of axial displacement thickness and wall skewing angle for a reduced mass flow of 13.5 kg/s at 60 % design speed. The resulting complete velocity profiles behind rotors is also shown in fig. 21 for the same point. Also shown on fig. 19, is the axial displacement thickness as calculated with the original Mellor & Wood theory which assumes constant shape factor and provides no means of estimating the wall skewing angle. Inherent in the theory is also the influence of efficiency due to end-wall losses. Calculated efficiencies for this mass flow are 87.1 % without these losses and 82.3 % when the end-wall losses are taken into account.

CONCLUSIONS

The application of the Finite Element Method to through flow calculations appears to have the advantage of being able to handle arbitrary geometries in a straightforward way without the uncertainties connected to estimations of curvatures. Besides high accuracy can be obtained with simple computational meshes.

Examples of a swirling flow in a ducting configuration as well as axial turbine and compressor calculations illustrate the accuracy and versatility of the method, which appears therefore to present a valid alternative to the other existing numerical techniques for through-flow calculations in axial turbomachinery.

REFERENCES

[1] Wilkinson D.H. "Stability, Convergence and Accuracy of Two-Dimensional Streamline Curvature Methods using Quasi-Orthogonals", Proc. Inst. Mech. Eng. Vol 184, p 108 (1970).

[2] Howard, J.H.G., Osborne, C. "A Centrifugal Compressor Flow Analysis employing a Wake-Jet Passage Flow Model", ASME Paper 76 - FE - 21, (1976).

[3] Davis, W.R. "A General Finite Difference Technique for the Compressible Flow in the Meridional Plane of a Centrifugal Turbomachine", ASME Paper 75 GT 121, (1975).

[4] Wu, C.H. "A General Theory of Three-Dimensional Flow in Subsonic and Supersonic Turbomachines of Axial-, Radial-, and Mixed Flow Type", NACA TIN 2604, (1952).

[5] Smith, L.H., Jr. "The Radial Equilibrium Equation of Turbomachinery" Trans. ASME, Journal of Engineering for Power, 88A, 1, (1966).

[6] Hirsch, Ch, Warzee, G. "A Finite Element Method for Through-Flow Calculations in Turbomachines" ASME Paper 76 FE 12, (1976).

[7] Hirsch, Ch. "Unsteady Contributions to Steady Radial Equilibrium Flow Equations" AGARD PEP meeting on "Unsteady Phenomena in Turbomachinery", Sept. 1975, Monterey (U.S.A.).

[8] Bosman, C. & Marsh, H. "An Improved Method for Calculating the Flow in Turbomachines, including a consistent Loss Model", Jour. Mech. Eng. Science , 16, 25, (1974).

[9] Zienkienicz, O.C. "The Finite Element Method in Engineering Science", Mc Graw Hill, London, (1971).

[10] Strang, G. & Fix, G.J. "An Analysis of the Finite Element Method" Prentice Hall, (1973).

[11] Hirsch, Ch. & Warzee, G. "A Finite Element Method for Flow Calculations in Turbomachines" Vrije Universiteit Brussel, Dept. of Fluid Mechanics, Report VUB-STR-5-July 1974.

[12] Batchelor, G.K. "An Introduction to Fluid Dynamics", Cambridge University Press, London, (1967).

[13] Davis, W.R. "A Computer Program for the Analysis and Design of Turbomachinery" Univ. of Carleton, Rep ME/A - 71 - 5, (1971).

[14] Ruggeri, R.S. & Benser, W.A. "Performance of a High loaded Two-Stage Axial Flow Fan" NASA TM-X-3076 (1974).

[15] Mellor, G. & Wood, G. "An Axial Compressor End-Wall Boundary Layer Theory" Trans. ASME, 93D, 300, (1971).

[16] Hirsch, Ch. "End-Wall Boundary Layers in Axial Compressors" Trans. ASME, 96A, 413, (1971).

[17] Hirsch, Ch. "Flow Prediction in Axial Flow Compressors including End-Wall Boundary Layers" ASME-Paper 76 GT 72, (1976).

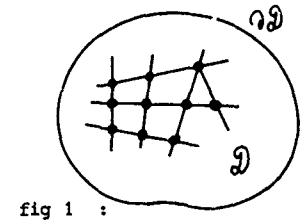

fig 1 :
Finite element subdivision

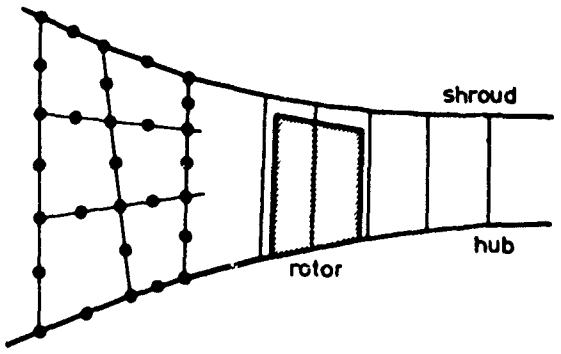

Fig. 3 Element and node distribution.

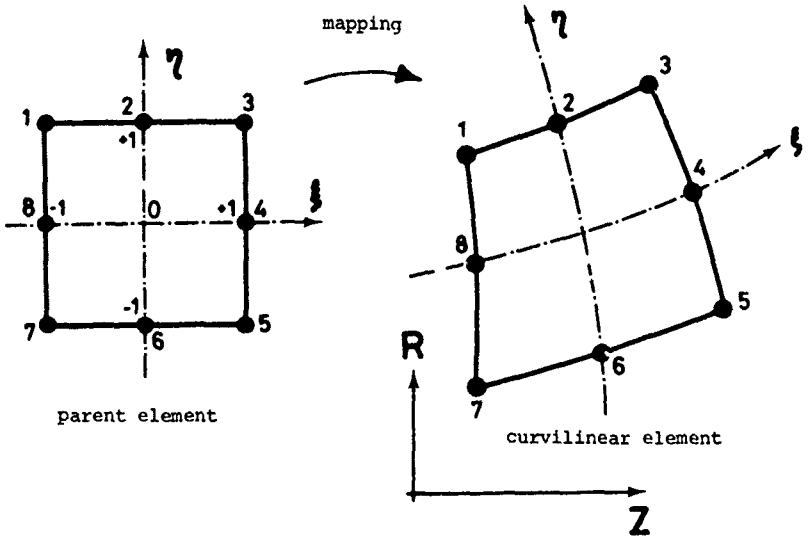

Fig. 2 Isoparametric quadrilateral element.

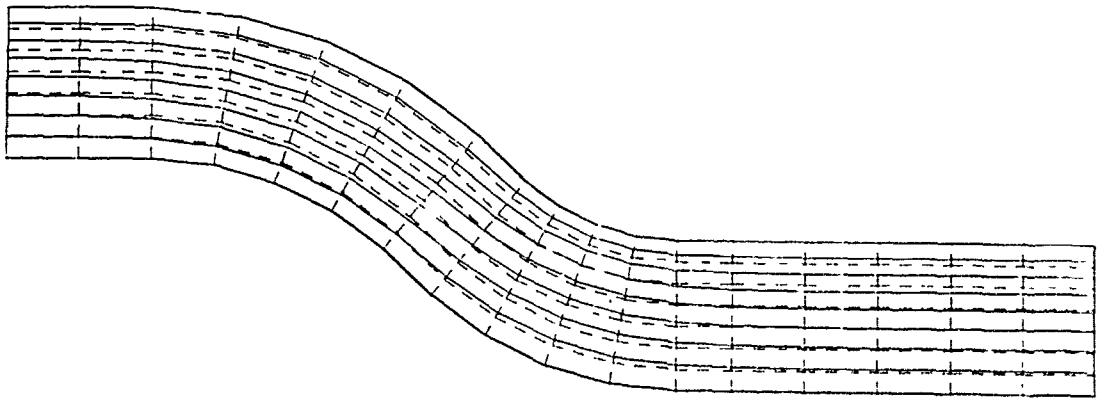

AXISYMMETRIC TRANSITION WITH SWIRL

Fig. 4 Geometry, element distribution and calculated streamlines.

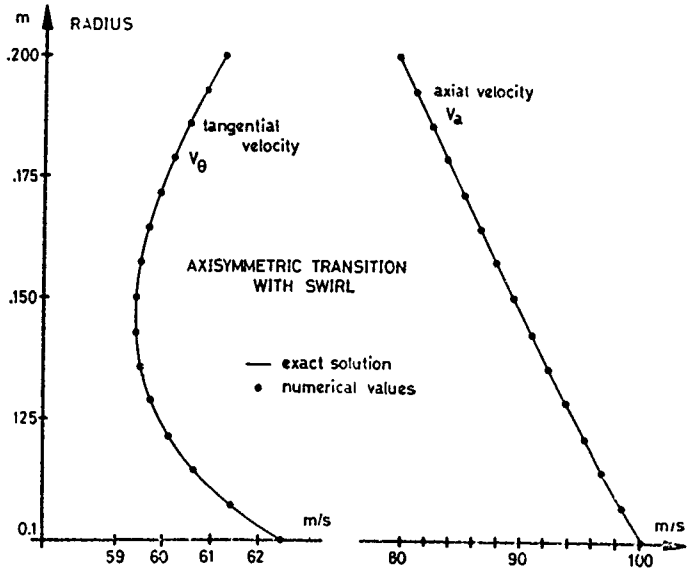

Fig. 5 Comparison between analytical and calculated solutions.

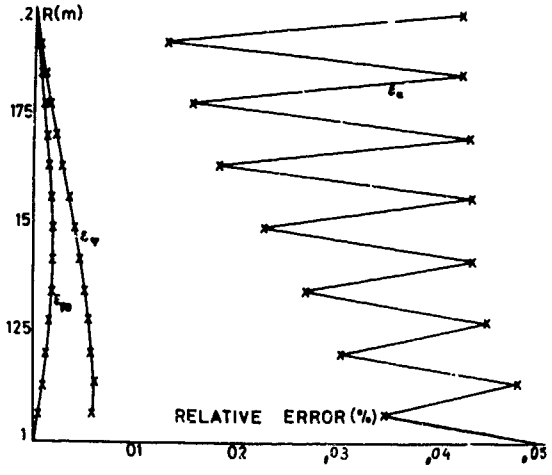

Fig. 6 Radial variation of relative error.

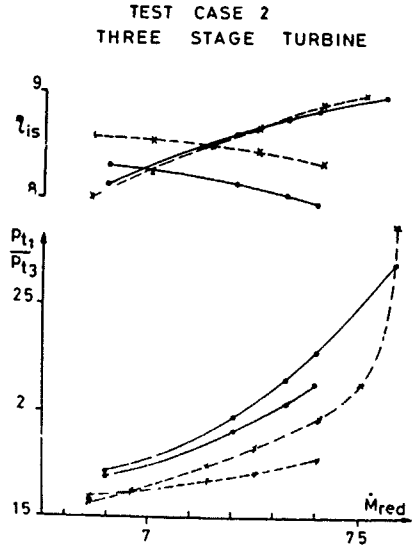

Fig. 8 Test case 2 : Performance curves at 60 % and 100 % of design speed.

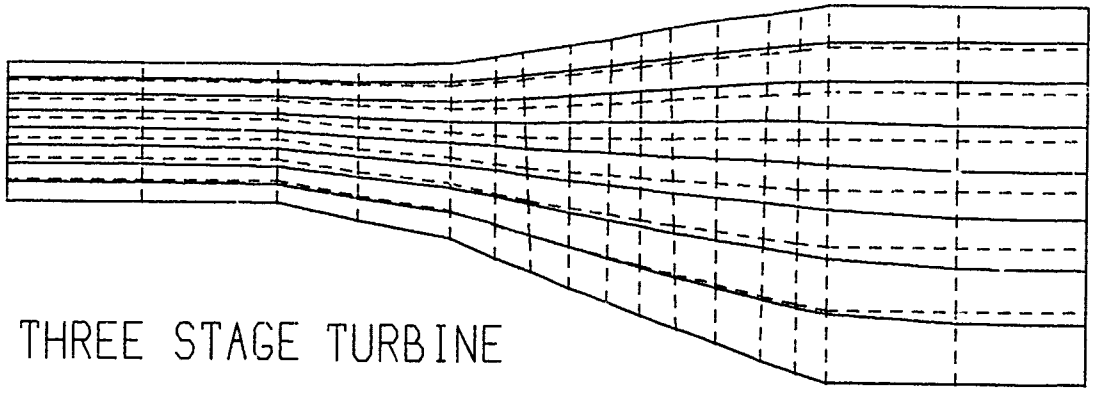

Fig. 7 Test case 2 : Geometry, element distribution and streamlines at design speed and $\dot{m}_{red}$ = 7.58kg/s

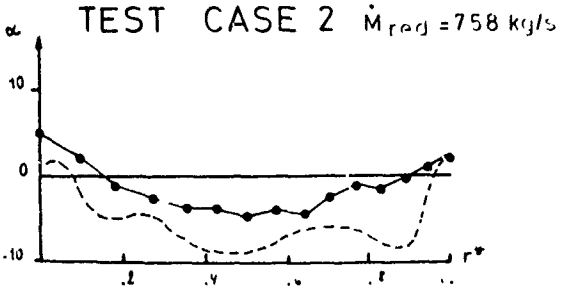

Fig. 9 Outlet flow angle profile at $\dot{m}_{red}$ = 7.58kg/s for test case 2.

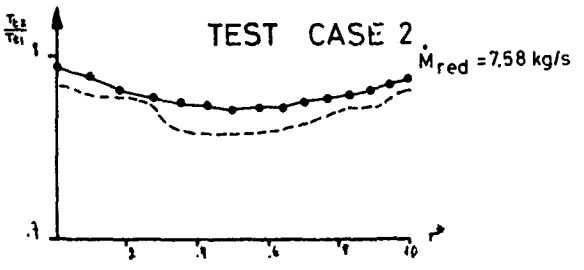

Fig. 10 Outlet total temperature profile at $\dot{m}_{red}$ = 7.58 kg/s for test case 2.

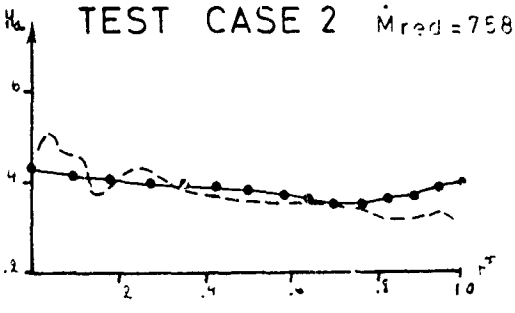

Fig. 11 Outlet axial Mach number distributicn at $\dot{m}_{red}$ = 7.58 kg/s for test case 2.

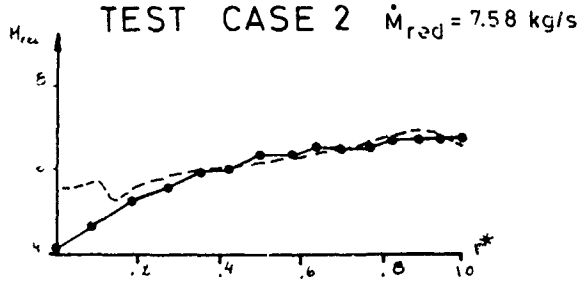

Fig. 12 Outlet relative Mach number distribution at $\dot{m}_{red}$ = 7.58kg/s for test case 2.

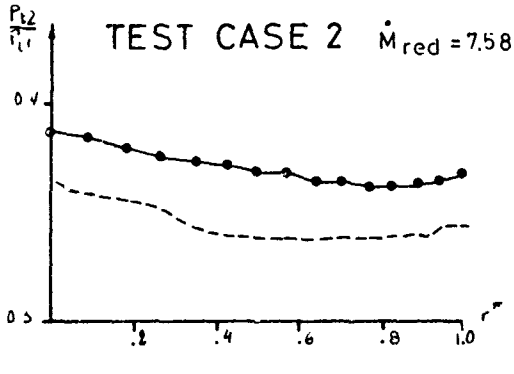

Fig. 13 Outlet total pressure profile for $\dot{m}_{red}$ = 7.58kg/s for test case 2.

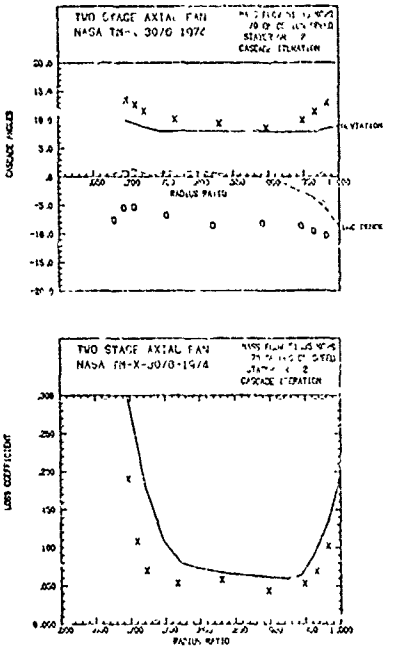

Fig. 14 Two-stage fan : deviations, incidence and loss coefficient distributions at second stator outlet at 70 % of design speed. O : experimental incidence, X : experimental deviations and losses.

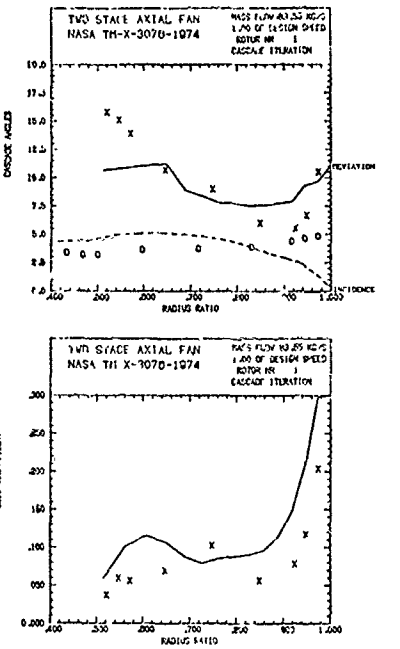

Fig. 15 Two-stage fan : deviations, incidences and losses at first rotor at design speed. O : experimental incidence, X : experimental deviations and losses.

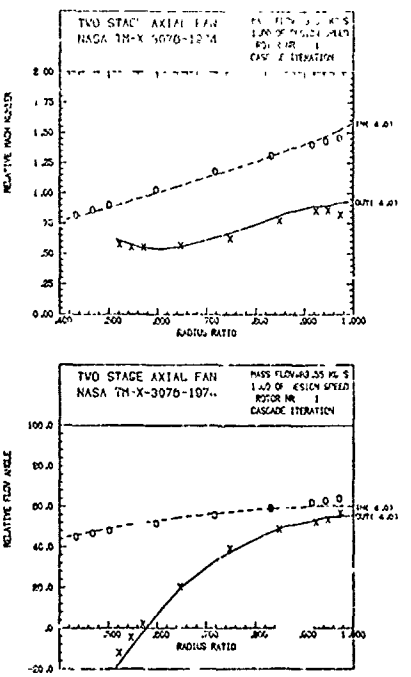

Fig. 16 Two-stage fan : relative Mach number and flow angles distribution at first rotor outlet at design speed. O : experimental values at inlet, X : experimental values at outlet.

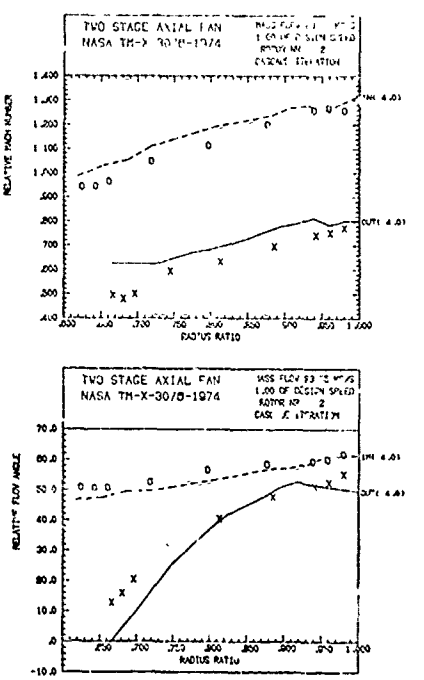

Fig. 17 Two-stage fan : relative Mach number and flow angles distribution at second rotor outlet at design speed. O : experimental values at inlet, X : experimental values at oulet.

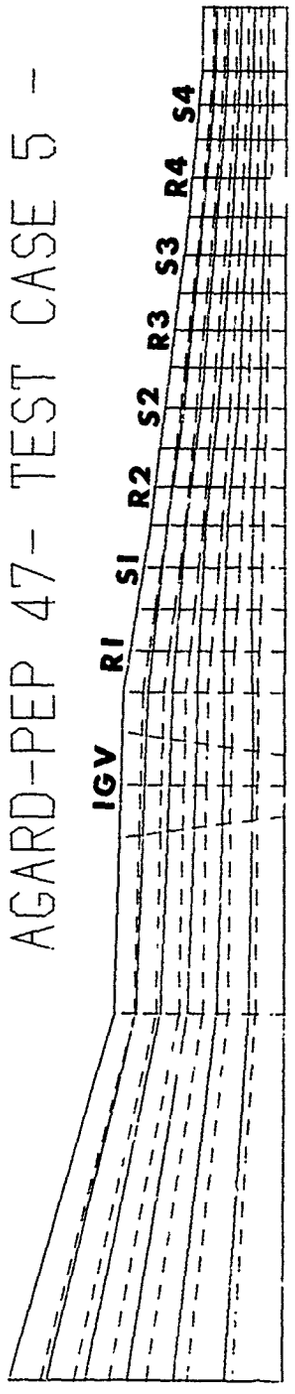

Fig. 18 Geometry, element distribution and calculated streamlines for the 4 stage compressor of test case 5.

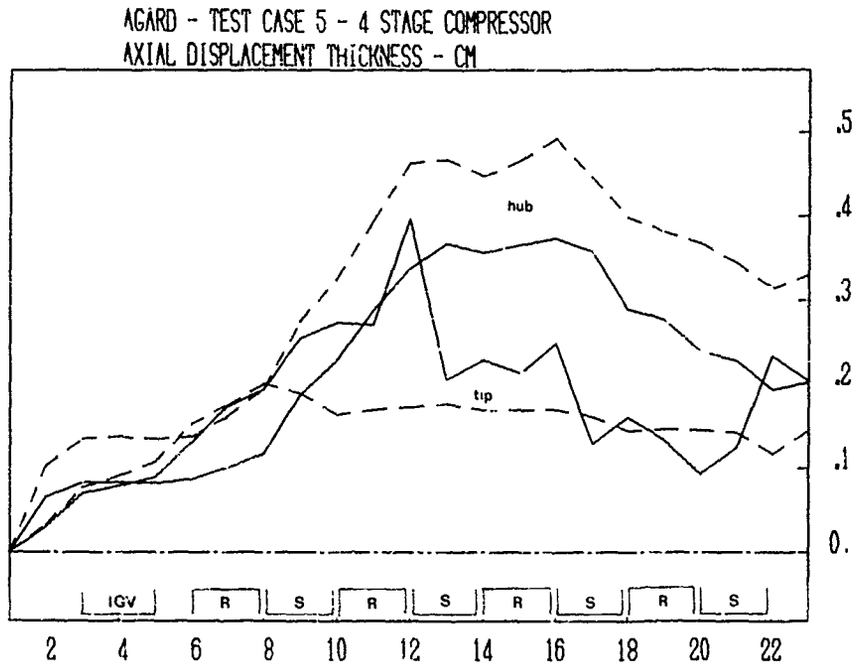

Fig. 19 Axial displacement thickness of end-wall boundary layers at $\dot{m}_{red}$ = 13.5 kg/s and 60 % design speed for test case 5.

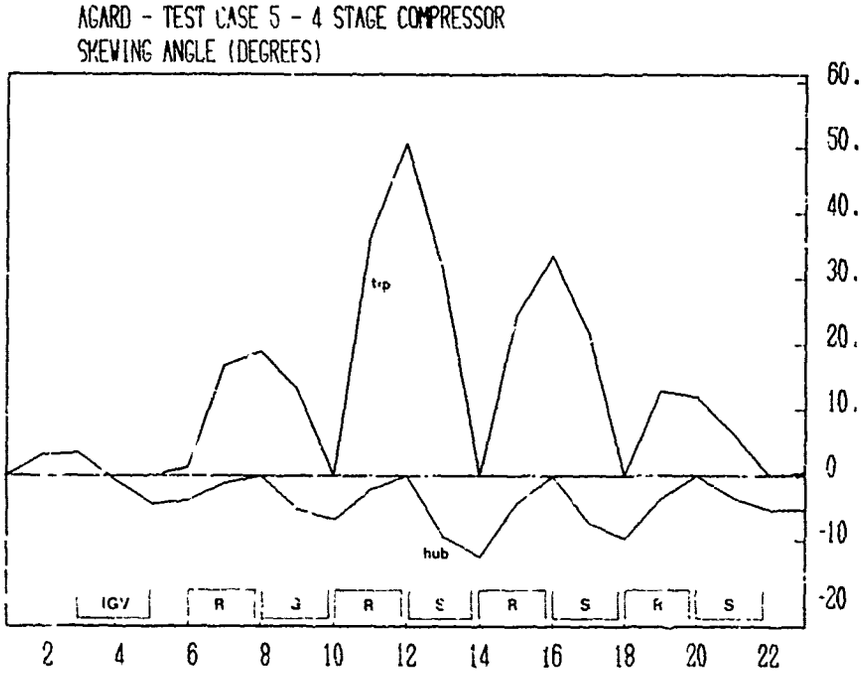

Fig. 20 Wall skewing angle of end-wall boundary layers at $\dot{m}_{red}$ = 13.5 kg/s and 60 % design speed for test case 5.

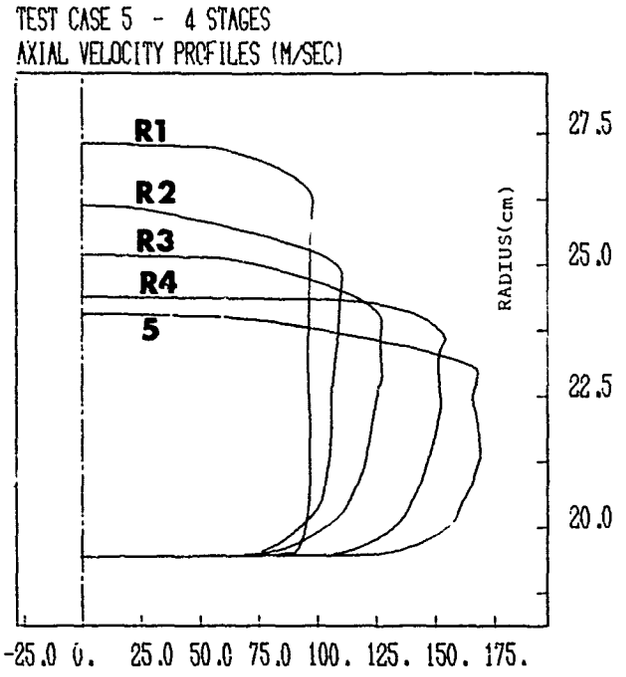

Fig. 21 a Test case 5 : Axial velocity profile including the end-wall boundary layer velocity distribution for $\dot{m}_{red}$ = 13.5 kg/s and 60 % of design speed at outlet of all rotors and at compressor outlet (curve 5)

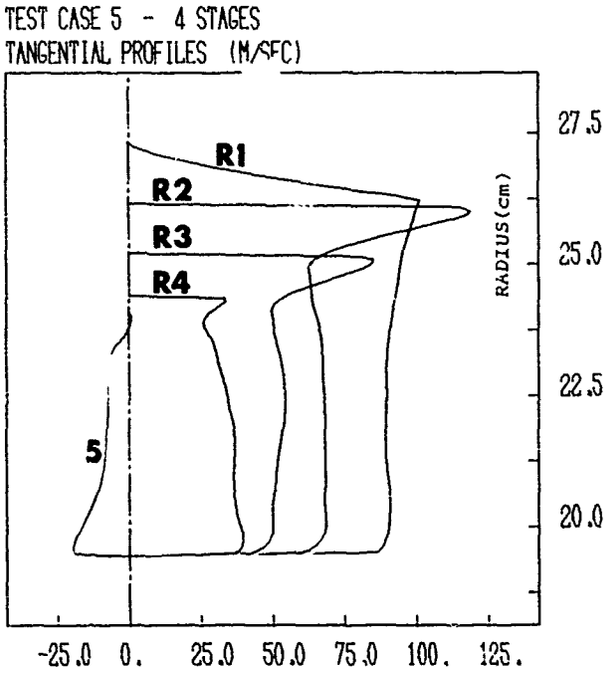

Fig 21 b Test case 5 : Tangential velocity profile including the end-wall boundary layer velocity distribution for $\dot{m}_{red}$ = 13.5 kg/s and 60 % of design speed at outlet of all rotors and at compressor outlet (curve 5)

COMMENTS

Comment by H.Marsh, University of Durham, UK

(a) The matrix through-flow method has Mach number limitations. Is the finite element method subject to the same restrictions on Mach number?

(b) Since the time of computation is of the same order as for the streamline curvature and matrix methods, it would appear that the main advantage of the finite element approach is that it can be extended to three dimensions. Is this correct?

Authors' response:

(a) The Mach number limitation is defined by subsonic meridional velocity when the tangential velocity is imposed instead of the flow angle. So even when the blade angles are given and flow angles defined through correlation for the deviation, one can work in the iterative process as if the tangential velocity were given. Figure 16 of the paper shows a case where the inlet Mach number at tip of the first rotor is 1.5 and which was run without any problem.

(b) One of the advantages of finite element method is indeed the ease with which it can be extended to three dimensions. However, we feel that even in two dimensions there should be some advantages with respect to streamline curvature and matrix method. In particular, the approach with isoparametric elements allows a simulation of curved boundaries, even in strongly curved (e.g. mixed or radial) geometries without loss in accuracy and without any modification in the computer coding. Besides, the order of accuracy of the 8-nodes elements (with biquadratic shape functions) is third order for the corresponding linear problem (see Reference 10 of the paper), while an equivalent accuracy can only be achieved in a matrix method for a centrifugal type of geometry, e.g. by a computational "stencil" of 11 to 15 points as shown by W.R.Davis[3]. This implies that an equivalent accuracy could be obtained in a FE approximation with a coarser mesh. Another point would also lie in the generality with which the elements can be distributed in the calculation domain by only defining calculation stations (which can be curved in order to match a curved leading edge e.g.) without the necessity of having to define a complete calculation mesh by some particular distorted mesh for a given geometry.

Comment by A.Neal, National Engineering Laboratory, UK

(a) How do you evaluate the Ψ derivatives in the RHS of the "Poisson" equation?

(b) What level of Ψ continuity do you use?

(c) Will you use a stram function formulation or primitives for three-dimensional work?

Authors' response:

(a) The Ψ derivatives are evaluated through the FE approximation since.

$$\Psi = \Sigma \Psi_i N_i(r, z)$$

$$\frac{\partial \Psi}{\partial r} = \sum_i \Psi_i \frac{\partial N_i}{\partial r}, \quad \frac{\partial \Psi}{\partial r} = \sum_i \Psi_i \frac{\partial N_i}{\partial z}.$$

(b) The continuity, sufficient to insure convergence, is continuity of the function values only at the inter-element boundaries. It is therefore not necessary to insure continuity of the derivatives of the shape functions at interelement boundaries, which gives a broader possibility of choice for the shape functions.

(c) In a fully three-dimensional calculation, you cannot use a stream function which is only defined in two-dimensional. One can therefore use either a potential function or the primitive variables. Actually, the most straightforward way would be a potential function formulation since this requires only one unknown at each node and the extension from the actual two-dimensional code to a three-dimensional variable formulation is feasible and probably more appropriate for calculation of transonic flows with shock capturing.

Comment by J.Fabri, ONERA, France

Could you give some ideas how the computation time compared with other methods?

Authors' response:

For the axisymmetric transition with swirl, which is an incompressible calculation, we have a 406 nodes and the case convergence in two iterations with a computation time of about 30 sec on a CDC 6400. For the highly loaded two-stage fan of NASA, we showed, the calculation time depends on the Mach number level due to the under-relaxation factor with decreasing Mach number. At 70% design speed, the calculation requires about 45 sec while at design need with inlet relative Mach numbers at tip of 1.5, the computation time is around 85 sec.

We feel that these computation times are comparable to the times required by the other methods.

Comment by T.McKain, Detroit Diesel Allison, USA

(a) When you go inside the blade row, how do you specify the stream surface that you are calculating on, or the work input on that surface?

(b) In the inner blade station, do you do a blade to blade analysis?

(c) Do you find much different outlet diagrams if you use different assumptions?

Authors' response:

(a) As I said, we do not define a stream surface as we are working on pitch average values. We use an axisymmetric approximation.

(b) No, it is why we use the axisymmetric assumption. If we did, we could estimate the inner blade variation. At the moment, we use a linear assumption of turning and losses.

(c) It has an influence on the total pressure ratio and some influence on the radial distribution. This is certainly one weak point of all the through-flow to have to estimate the loss and turning evolution inside the blading.

THREE-DIMENSIONAL FLOW CALCULATION FOR A TRANSONIC COMPRESSOR ROTOR

by
William T. Thompkins, Jr.
Research Assistant
and
David A. Oliver
Research Associate
Department of Aeronautics and Astronautics
Massachusetts Institute of Technology
Cambridge, Massachusetts 02139
USA

SUMMARY

A numerical calculation of the steady, inviscid, three dimensional flow in a isolated transonic compressor rotor has been completed using MacCormack's second order accurate time-marching scheme. This rotor has a tip Mach number of 1.2, an overall diameter of 2 feet, and inlet hub/tip ratio of 0.5. The computed rotor total pressure ratio is 1.82. Comparisons between the numerical solution, measurements of the intra-blade static density field obtained by gas fluorescence, and time resolved exit flow measurements showed that the inviscid computation accurately models transonic rotor aerodynamics and rotor blade pressure distributions in the upstream portions of the blade passages, the viscous effects influencing mainly the downstream flow.

INTRODUCTION

Analysis of flow in high speed compressor stages has usually been limited to inviscid solutions for either the axisymmetric or the "gap-wise" averaged through-flow. These solutions typically depended on experimental cascade correlations to provide required blade forces or flow turning. Quasi-three dimensional inviscid solutions for realistic geometries are now being developed for use in highly loaded stages where the axisymmetric solutions are inadequate, for examples see references (1,2). These procedures typically consist of an iteration between different two dimensional flow solutions: an axisymmetric solution along a mean meridional streamsurface and solutions along several blade to blade surfaces at different radii. Blade forces needed for the axisymmetric solution are determined from the blade to blade solutions; while, the blade to blade solutions attempt to include three dimensional flow effects like meridional streamline curvature and convergence as determined from the axisymmetric solutions.

For compressor rotors with transonic inlet Mach numbers, neither pure axisymmetric or quasi-three dimensional solutions are expected to yield accurate results due to the strong coupling between different sections of the flow field. It is the purpose of this paper to report on a fully three dimensional solution procedure which has been used to study the flow in a highly loaded transonic axial compressor rotor. This procedure utilizes MacCormack's time-marching finite-difference method to compute a steady state solution to the inviscid flow equations or Euler equations. A computed flow solution will be compared to intra-blade static density measurements obtained by gas fluoresence, reference 3, and to time resolved exit plane flow measurements obtained for the rotor's design point.

NUMERICAL PROCEDURES

Full details of the numerical procedures used are contained in references (4,5) and only a summary of these methods will be presented in this paper. The governing partial differential equations solved in this study were the three dimensional Euler equations which are the inviscid momentum equations plus the continuity equation. Since only weak shock waves were expected to appear in the solution, the energy equation was replaced by the isentropic flow assumption. Implementation of the blade surface boundary condition, that the flow be tangent to the blade, is simplest in a reference frame rotating with the rotor. The Euler equations for this frame and in cylindrical coordinates become:

$$\frac{\partial U}{\partial t} + \frac{\partial F}{\partial r} + \frac{\partial G}{\partial \theta} + \frac{\partial H}{\partial Z} = K$$

where

$$U = \begin{matrix} \rho \\ r\rho u \\ r\rho v_{abs} \\ r\rho w \\ r\rho w \\ r\rho uw \\ r\rho w v_{abs} \\ r(\rho w^2 + P) \end{matrix} \qquad F = \begin{matrix} r\rho u \\ r(\rho u^2 + P) \\ r\rho v_{abs} \\ r\rho w \end{matrix} \qquad K = \begin{matrix} 0 \\ \rho v_{abs}^2 + P \\ r\rho u v_{abs} \\ 0 \end{matrix}$$

$$G = \begin{matrix} \rho(v_{abs} - \Omega r) \\ \rho(v_{abs} - \Omega r)u \\ \rho(v_{abs} - \Omega r)v_{abs}^2 + P \\ \rho(v_{abs} - \Omega r)w \end{matrix} \qquad (1)$$

$$v_{abs} = v_{rel} + r\Omega$$

The physical flow domain is illustrated by figure 1 which shows the test rotor as seen looking radially inward. Especially important geometric features are the 35° hub surface slope and the 25° blade twist from hub to tip. The domain is bounded at the blade tips by a cylindrical casing. By symmetry the domain is reduced to one blade passage bounded by the hub and tip casing and the suction and pressure surfaces of two adjacent blades.

This complexly shaped domain is transformed to one which is geometrically simple by a coordinate stretching. The stretching maps the blade surfaces onto untwisted planes and maps the hub surface onto the Z axis. The stretched or computational domain is shown in figure 2.

Solutions to these equations were obtained in the computational domain using MacCormack's method, see reference (6). It is a two-step, explicit, second order accurate, conditionally stable method. This method is used because it is relatively simple, easily adapted to various coordinate transforms, and easily handles mixed subsonic and supersonic flows. The shock capturing nature of this method is also essential since the location and strength of shock waves appearing in the flow are unknown. The addition of artificial viscosity terms was necessary to stabilize the solution procedure along sonic surfaces and near blade leading and trailing edges.

The blade surface boundary condition for inviscid flow, $\bar{V}_{rel} \cdot \bar{n} = 0$, is applied with second order accuracy through the use of a body centered coordinate system. In this orthogonal coordinate system, defining sketch shown below, derivatives of fluid quantities in a direction normal to the blade surface are found and used to predict the fluid state at an auxiliary point. MacCormack's method is used at the boundary point as if they were interior points.

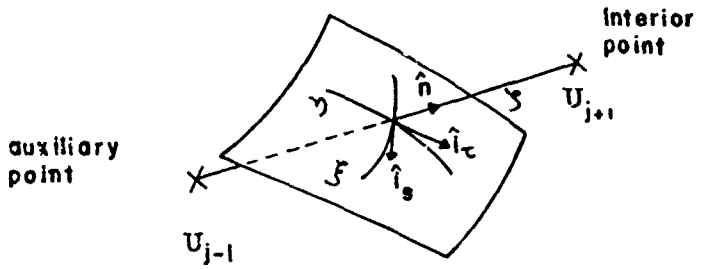

In these coordinates the normal momentum equation becomes:

$$\frac{\partial u_n}{\partial t} + \frac{u_s}{h_s}\frac{\partial u_n}{\partial \xi} + \frac{u_\tau}{h_\tau}\frac{\partial u_n}{\partial \eta} + \frac{u_n}{h_n}\frac{\partial u_n}{\partial \zeta} + \frac{u_n u_s}{h_n h_s}\frac{\partial h_u}{\partial \xi}$$

$$+ \frac{u_\tau u_n}{h_\tau h_n}\frac{\partial h_\tau}{\partial \eta} - \frac{u_s^2}{h_s h_n}\frac{\partial h_s}{\partial \zeta} - \frac{u_\tau^2}{h_\tau h_n}\frac{\partial h_\tau}{\partial \zeta} = \frac{-1}{\rho h_n}\frac{\partial P}{\partial \zeta} \qquad (2)$$

$$+ \Omega^2 r(\hat{i}_r \cdot \bar{n}) - 2\Omega(\hat{i}_z \times \bar{V}_{rel}) \cdot \bar{n}$$

For simplicity the centrifugal and coriolis accelerations are expressed in terms of the base (r,θ,Z) coordinate system. Since $u_n \equiv 1$ this equation reduces to

$$\frac{\partial \rho}{\partial n} = \frac{\rho}{a^2}\left[\frac{u_s^2}{R_s} + \frac{u_\tau^2}{R_\tau} - \frac{2\rho}{a^2}\left[\Omega(\hat{i}_z \times \bar{V}_{rel}) - \Omega^2 r \hat{i}_r\right]\right] \qquad (3)$$

where $\frac{1}{R_s} = \frac{1}{h_s h_n}\frac{\partial h_s}{\partial \zeta}$ and $\frac{1}{R_\tau} = \frac{1}{h_\tau h_n}\frac{\partial h_\tau}{\partial \zeta}$ are the surface radii of curvature along the ξ and η coordinate lines. Expressions for $\frac{\partial u_s}{\partial n}$ and $\frac{\partial u_\tau}{\partial n}$ can be determined from the components of the vorticity vector.

$$\frac{\partial u_s}{\partial n} = \omega_\tau - \frac{u_s}{R_s} \qquad (4)$$

$$\frac{\partial u_\tau}{\partial n} = \omega_s + \frac{u_\tau}{R_\tau} \qquad (5)$$

For the case of irrotational transonic flow when the principle radii of curvature are not small, it was

shown in reference (4) that a second order accurate approximation for $\frac{\partial u_n}{\partial n}$ is provided by reflection in the blade normal direction, i.e. $(u_n)_{j-1} = -(u_n)_{j+1}$. These conditions were fulfilled for the test rotor.

The upstream and downstream boundary conditions which guarantee a unique stable solution are not known in general for this problem, and we must be guided by experience and intuition in formulating these conditions. For the highly loaded rotor calculation, conditions similar to those imposed during a compressor test were found to be adequate. That is, the inlet stagnation state of the fluid and the mean outlet static pressure were specified. The rotor mass flow rate was determined as part of the solution. Fluid state variables were calculated at these boundaries using an unsteady analysis for the axisymmetric flow. For the test rotor geometry, this analysis reduces to one dimensional unsteady flow along the meridional stream surfaces.

This simplification does imply some inconsistencies at the boundaries. In particular, at the upstream boundary the transmission of acoustic disturbances is falsified; at the downstream boundary vorticity convection is distorted. The acoustic disturbances carry very little energy and their falsification can have little influence on the flow over the rotor. At the downstream boundary the specified axisymmetric flow is potentially inconsistent with the blade flow solution if that solution requires a significant amount of radial vorticity to be present at the computational boundary. For the present calculations, this inconsistency does not appear to be important even though some radial vorticity is shed by the rotor. This vorticity is considerably modified by the cumulative action of the artificial viscosity terms and by the inherent dissipation and dispersion of the numerical scheme.

Limitations of computer time and storage prevent detailed flow resolution near leading and trailing edges. These points are dealt with by the expedient of placing them between grid points or by considering the edges to be infinitely thin. The Kutta condition is imposed at the trailing edge by requiring that the suction and pressure surface flow angles, in a plane normal to the blade axis, and the pressure be equal at the last grid point on the blade. This procedure allows a slip surface to form in a plane tangent to the trailing edge. The movement of this surface is not explicitly followed in the calculation.

RESULTS

The techniques outlined in the previous section have been used to compute the flow in a transonic compressor rotor whose design and performance are representative of modern stages. This rotor has a tip Mach number of 1.2, a total pressure ratio of 1.65, an inlet hub to tip ratio of 0.5, and an inlet axial Mach number of 0.5. The computed solution has a rotor total pressure ratio of 1.82 with an inlet Mach number of 0.46. Because of the large expenditure of computer time necessary for a three dimensional solution, this calculation was terminated when the solution was further from steady state than would normally be desired. A residual unsteadiness of 5 percent is present at some points in the domain, but the major features of the solution, such as rotor total pressure ratio and shock wave strength, have been stable for over 80 time steps.

The mixed subsonic and supersonic flow inherent in a transonic compressor rotor is clearly shown by figures 3 through 6, which show contour plots of the relative coordinate system Mach number. These contour plots are projected into viewing planes from blade to blade surfaces of revolution which are equally spaced in the radial direction. Figure 3 indicates that a strong passage shock exists at the tip radius and that it is nearly normal to the flow. A weak oblique shock stands in front of the rotor. The approximate location of the computed shocks is shown as dashed lines in figure 3. For the passage shock, this dashed line follows the Mach number equal 1.0 contour which is at about the midpoint of this shock. The importance of the entrance region geometry is shown by the expansion of the flow up to a Mach number of 1.7 on the suction surface. In figures 4 and 5 the passage shock can be seen to weaken and move forward relative to the blades as the radius decreases. The oblique shock in front of the rotor weakens and then disappears. Figure 6 shows the Mach number contours along the hub surface. A patch of supersonic flow appears on the suction surface in an otherwise subsonic flow. The angle of attack at this radius is about 15° larger than the design intent. A sharp recompression terminates the supersonic patch and extends across the blade passage.

The flow field illustrated by these figures at first sight appears qualitatively as might be expected if the flow were quasi-two dimensional. One illustration, however, that this flow is in fact strongly three dimensional is shown in figure 7. This figure shows the position of three computed blade to blade streamsurfaces, which are normally called S1 surfaces. The coordinates of these surfaces were determined by integration along fluid particle paths originally through a constant inlet radius line. The projected view of these surfaces is the one which is seen by an observer facing directly downstream. Near the tip radius these surfaces approximate a surface of revolution; however, at smaller radii they cannot be approximated as surfaces of revolution. The middle streamsurface has an inlet radius ratio 0.772. At the rotor exit, the streamline on the blade suction surface has a radius ratio of 0.80; while, the streamline on the blade pressure surface has an exit radius ratio of 0.85. This radial displacement is 16 percent of the blade height. At a slightly lower radius the streamline radial displacement reaches a maximum value of 20 percent. This warpage or streamline radial displacement is one manifestation of the streamwise vorticity being shed by the rotor. The intricate nature of the flow kinematics is illustrated by the S1 surface nearest the hub. Along the suction surface the flow is converging in the radial direction while the streamlines are diverging in the azimuthal direction. The reverse situation is occuring on the pressure surface.

Streamsurfaces with a different orientation, called S2 surfaces, are shown in figure 8. These surfaces are determined by fluid particles which initially lay on three radial lines near the blade pressure surface, at mid-gap, and near the blade suction surface. The angular distance between these surfaces has been exaggerated to allow each surface to be seen but otherwise they are to the same scale and viewed as figure 7. This figure shows, perhaps more clearly than figure 7, the blade to blade and hub to tip variation in streamline shape. Of particular importance is the fact that while the radial slope of the streamlines is near zero at the suction surface it generally is several degrees positive along the pressure surface and near mid-gap. This difference is crucial in transonic flows.

Comparison to Fluorescent Density Measurements

A comprehensive series of measurements of the flow in the test rotor have been carried out in the M.I.T. Blowdown Compressor Facility. This facility, which is described in reference 7, allows time resolved aerodynamic testing of full scale compressor stages at low cost. In a blowdown experiment, the rotor is brought up to speed in a vacuum, a diaphragm is opened, and the test gas allowed to flow for a time of the order of one tenth second, during which time the rotor is driven by its own inertia. A "steady-state" test time of approximately 40 milliseconds is provided during each test run.

A unique flow visualization study of the flow in through the test rotor has been reported by Epstein (3). He was able to visualize the instantaneous static density field using a flourescent gas, 2, 3 butanedione, as a tracer. In this technique, the flow is illuminated along a plane using a dye laser. When illuminated at the proper wavelength, 425nm, the tracer gas fluoresces within 10^{-8} seconds. The intensity of the fluorescent emission, when photographically recorded, indicates the density variation in the illuminated plane. Quantitive density maps are obtained by correcting the images for distortion and non-linearities in the illumination and imaging systems.

The visualized density in a plane with a radius ratio of 0.88 is shown in figure 9a; the fully corrected density map is shown in figure 9b. The computed density contour map along the same plane is shown in figure 10. The gas fluorescence technique determines only the relative density between points in the flow and not the absolute density. For comparison with the computed density field, the upstream density in the fully corrected maps has been set to the computed value at that radius. The measured density gradients are, of course, independent of the upstream density value. Comparison of figures 9b and 10 shows that the flow expansion on the suction surface is accurately predicted both in magnitude and shape. The flow expands to about 90 percent of the upstream density at a point midway between the leading edge and the passage shock. The spatial resolution of the passage shock is of course much finer in the optical density measurements, but the shock strength is about the same in both cases, density ratio of 1.35, and the shock falls at nearly the maximum blade thickness. The flow visualization also shows the passage shock to terminate in a lambda shock formation typical of a laminar shock-boundary layer as would be expected for a shock of this strength. A density ratio of about 1.1 is predicted for the oblique shock standing in front of the rotor while the measured value is about 1.2. In addition the flow visualization shows the bow shock to be detached. The computed shock strength is correct for an attached oblique shock; however, a small decrease in the upstream Mach number would require that the computed shock be detached as it is in figure 9a.

Experimental and computed densities in the $r/r_t = 0.80$ plane are shown in figures 11 and 12. This plane is at a slightly larger radius than the design sonic radius. The passage shock remains strong in both cases, density ratio of 1.3, and the flow expands on the suction surface to a density nearly equal to the upstream density. The measured strength of the oblique shock is large, density ratio of 1.25; while, the computed shock strength is again smaller, about 1.05. No evidence of boundary layer separation is found at this radius. The important three dimensional nature of this flow is illustrated by the fact that the suction surface expansion does not continue from the blade leading edge up to the passage shock as it would if the flow were two dimensional. The predicted minimum density point also occurs in this same area although this fact is not clear from figure 11.

At a radius ratio of 0.70, figures 13 and 14, the character of the flow has markedly changed. In the visualized flow, the bow shock has been replaced by a diffuse compression region. The computed inlet Mach number is 1.08. The computed flow expands to a density ratio of 0.80, relative to the upstream flow, at about the 35 percent chord point, as does the visualized flow. In both cases, the density rise across the blade passage is 1.3.

These comparisons demonstrate that the inviscid computation accurately predicts the intra-blade density field upstream from obvious viscous phenomena like the passage shock - boundary layer interaction. The only important difference is the consistent under prediction of the oblique shock strength. To determine if this difference is due to insufficient grid resolution at the leading edge, the difference in rotor total pressure ratio, or some other factor such as an unstarted blade passage will require further work.

Comparison to Measured Rotor-Outlet Flow

Time resolved measurements of total pressure, static pressure, radial flow angle and pitchwise flow angle behind the compressor rotor were determined using probes based on the miniature silicon-bonded transducer diaphragms produced by the Kulite Corporation. Probes which can be used to resolve highly unsteady three dimensional flow fields can be produced by combining several of these diaphragms into one probe body. The particular design used in these measurements is shown in schematic form in figure 15. This probe functions much like a five-hole wedge probe. While the Kulite diaphragms have a high natural frequency, up to 150 KHZ, mechanical and aerodynamic phenomena limit the useful frequency responses to no more than 10 times blade passing frequency or about 30 KHZ. The use of this probe is fully described in reference (4).

The average performance of the test rotor was well predicted within the limitations of an inviscid flow analysis. Radial profiles of the computed and experimental total and static pressure ratio, theta averaged, are shown in figure 16. This figure shows that the average profiles are accurately predicted even though the computed total pressure ratio is higher than the expermental value. A contour plot of the computed total pressure ratio in an $r - \theta$ plane immediately downstream of the rotor is shown in figure 17. Small deviations from periodicity with blade passing period in this map are artifacts from the contour plotting routine. Figure 18 shows an experimentally determined total pressure map for the same axial location. The basic radial gradient in this map is predicted accurately, but local details particularly near the blade wakes are not predicted well. One unusual feature of the flow, the paired spikes in total pressure ratio near an r/r_t of 0.89, does appear to have an inviscid origin since they appear in both experimental and computed maps.

The computed average flow angles in the relative reference frame are compared to the experimental angles in figure 19. For $r/r_t < 0.90$, the predicted angles are generally one to two degrees lower than the measured values. For $r/r_t > 0.90$, the predicted angles are generally six to seven degrees lower than the measured values. Both the time resolved pressure measurements and the gas density measurements indicated that an unsteady boundary layer separation is occurring at these radii.

Figure 20 shows the pitchwise variation of the computed velocity components at a radius ratio

of 0.75. Figures 21 and 22 show time resolved Mach number components at a comparable location. In figure 21, the areas of low axial Mach number are the viscous blade wakes. These wakes also have a large excess of pitchwise velocity. Between these wakes the structure of the velocity field is reasonably well predicted by the inviscid computation. In particular, the computed radial velocity has a large outward component at the pressure surface. The measured radial velocity, figure 22, also has a large outward component at the edge of the pressure side of the wake. Across the wake, its radial Mach number decreases by 0.20 to 0.25 which means that a large cross flow velocity exists inside the wake. Pitchwise and axial Mach numbers between the wakes are generally consistent with figure 20. As the radius ratio increases, the actual flow becomes more and more dominated by the blade wakes and the separations produced by the shock-boundary layer interaction. As this transition occurs, the agreement between the computed and the experimental exit velocities becomes progressively poorer.

DISCUSSION

The comparisons in the previous section indicate that the inviscid three dimensional computation accurately models the flow through the test rotor upstream of obvious viscous phenomena like the shock-boundary layer interaction. Where an inviscid core flow exists downstream of the rotor, its details are generally consistent with the computed solution, but significant interaction between the core flow and the wakes occurs. Where boundary layer separation and flow unsteadiness are important flow features, the inviscid computation does not accurately predict flow details as would be expected. A detailed prediction of the rotor exit flow will require accurate calculation of the three dimensional separation region behind the passage shock as well as the movement of the shed viscous wakes. However, much of the rotor aerodynamics and blade pressure distribution upstream of important viscous phenomena can be understood with a purely inviscid analysis.

The cost of a three dimensional rotor calculation while large is not prohibitive. It is estimated that a fully converged solution for the test rotor would require approximately 25 hours of CPU time on an IBM 370/168. Such an expenditure, while inappropriate for preliminary design studies, is a small fraction of the resources expended by the major engine companies on new fan or compressor stage designs. It is entirely possible that the increased understanding of the flow will enable performance improvements which will fully justify the expense of the computation. This is yet to be demonstrated.

Time-marching methods such as MacCormack's method have received considerable criticism because of large solution times compared to relaxation methods or implicit methods, for typical relaxation solutions see references 8 and 9. In general the time marching methods appear to be as much as 2 or 3 orders of magnitude slower than relaxation methods for the same problems. However, general relaxation methods for the Eulerian equations are not available; where as, the full Eulerian or Navier-Stokes equations can be solved by time marching, hyperbolic, methods. If accurate solutions to problems such as the highly loaded transonic compressor rotor are required, the time-marching methods are perhaps the only available methods. Their total solution costs can be reduced by providing an initial condition guess as close to the true solution as possible, perhaps provided by relaxation or implicit solutions for linearized or irrotational flow fields.

REFERENCES

1. Bosman, C., and El-Shaarawic, M.A.I., "Quasi Three Dimensional Numerical Solution of Flow in Turbomachines," ASME Paper No. 76-FE-23, 1976.

2. Novak, R. A., and Hearsey, R. M., "A Nearly Three-Dimensional Intrablade Computing System for Turbomachinery - Part I: General Description," ASME Paper No. 76-FE-19, 1976.

3. Epstein, A. H., "Quantitative Density Visualization in a Transonic Compressor Rotor," Ph.D. Thesis, M.I.T., September 1975.

4. Thompkins, W. T., "An Experimental and Computational Study of the Flow in a Transonic Compressor Rotor," Ph.D. Thesis, M.I.T., May 1976

5. Sparie, Panagiotis, "A Computational Study of the Three Dimensional Flow in a Single Stage Transonic Compressor," Ph.D. Thesis, M.I.T., February, 1974.

6. MacCormack, R. W., and Paullay, A. J., "Computational Efficiency Achieved by Time Splitting of Finite Difference Operators," AIAA Paper No. 72-154, 1972.

7. Kerrebrock, J. L., Epstein, A. H., Hainis, D. M., and Thompkins, W. T., "The M.I.T. Blowdown Compressor Facility," J. Engr. for Power, 96, 4, October 1974, pp 394-405.

8. Martin, E. D., and Lomax, H., "Rapid Finite-Difference Computation of Subsonic and Transonic Aerodynamic Flows," AIAA Paper No. 74-11.

9. Jameson, A., "Iterative Solution of Transonic Flows Over Airfoils and Wings Including Flows at Mach 1," Comm. of Pure and Applied Math., Vol. 27, 1974, pp. 283-309.

ACKNOWLEDGEMENTS

This work was supported by the NASA Lewis Research Center under Grant NGL-22-009-383 supervised by Mr. W. D. McNally. The author is indebted to Prof. J. L. Kerrebrock for his overall guidance and wisdom

and to Mr. Thorwald Christensen and Dr. Allan H. Epstein, who also contributed figures 9, 11, and 13, for their help in the experimental work.

SIDE VIEW OF BLOWDOWN COMPRESSOR ROTOR

FIGURE 1

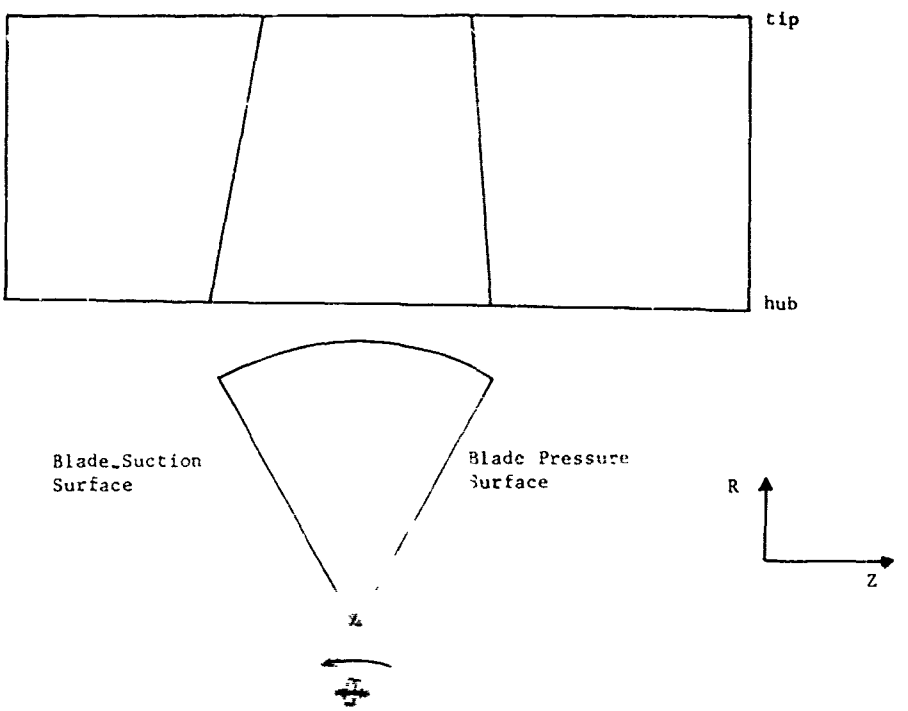

Axial - Radial Views of Computational Domain

FIGURE 2

Mach Number Countours for Computational
Blade to Blade Surface
Radius Ratio = 1.0

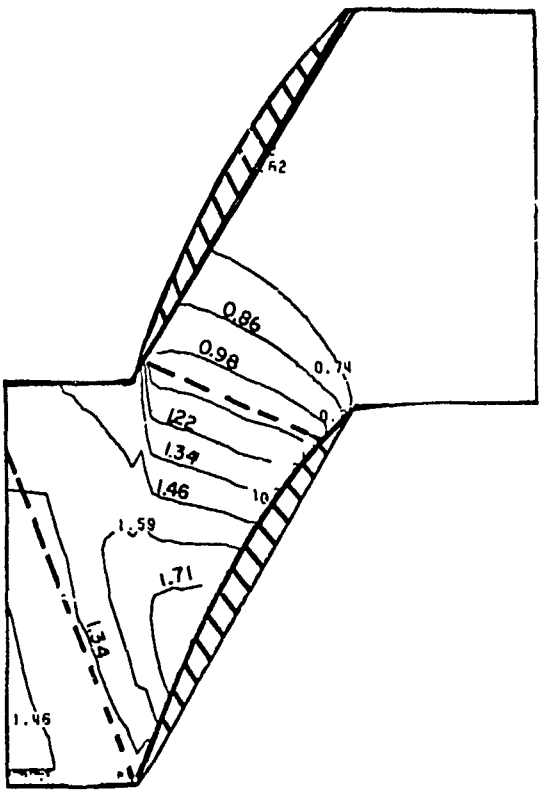

FIGURE 3

Mach Number Contours for Computational
Blade to Blade Surface
Radius Ratio = 0.86

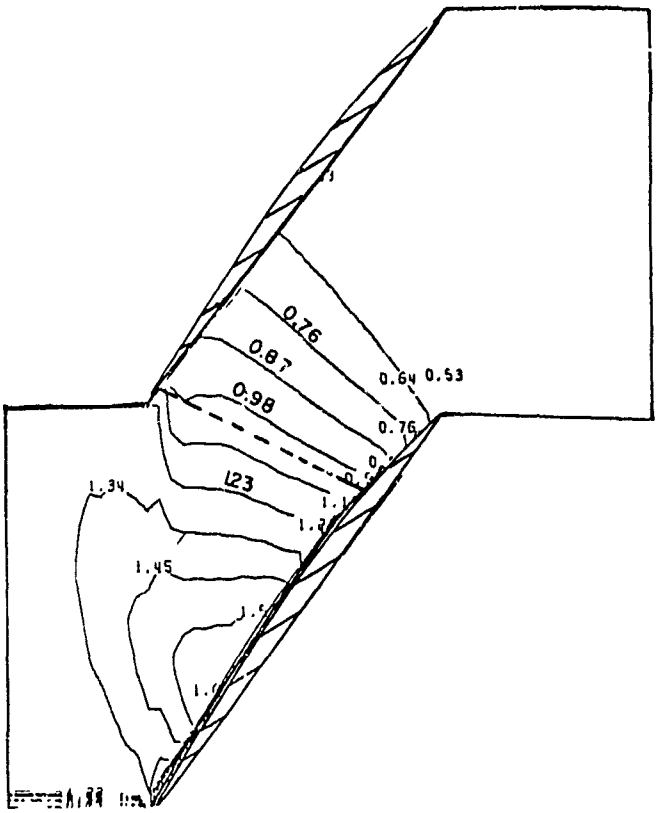

FIGURE 4

Mach Number Contours for Computational
Blade to Blade Surface Radius Ratio= 0.75

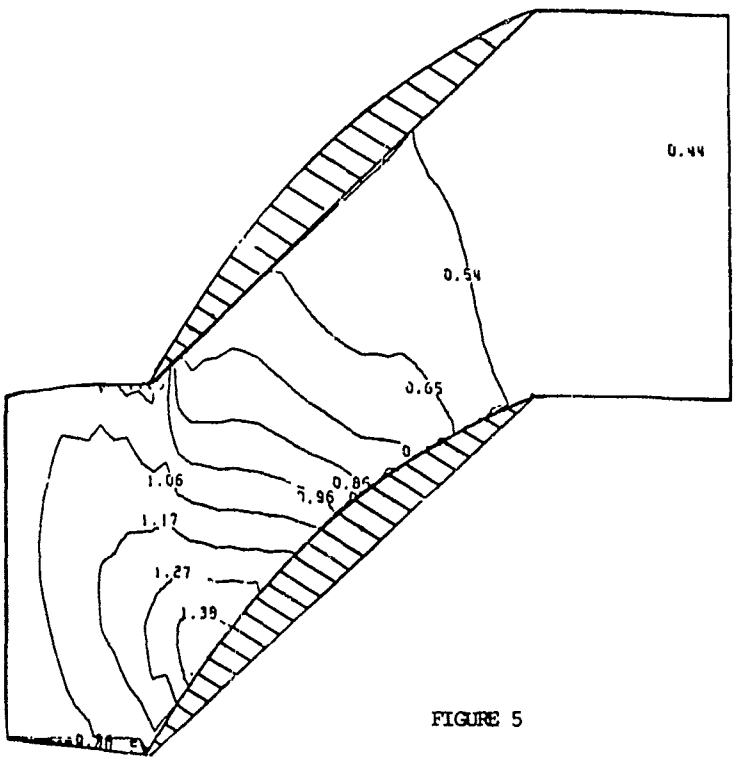

FIGURE 5

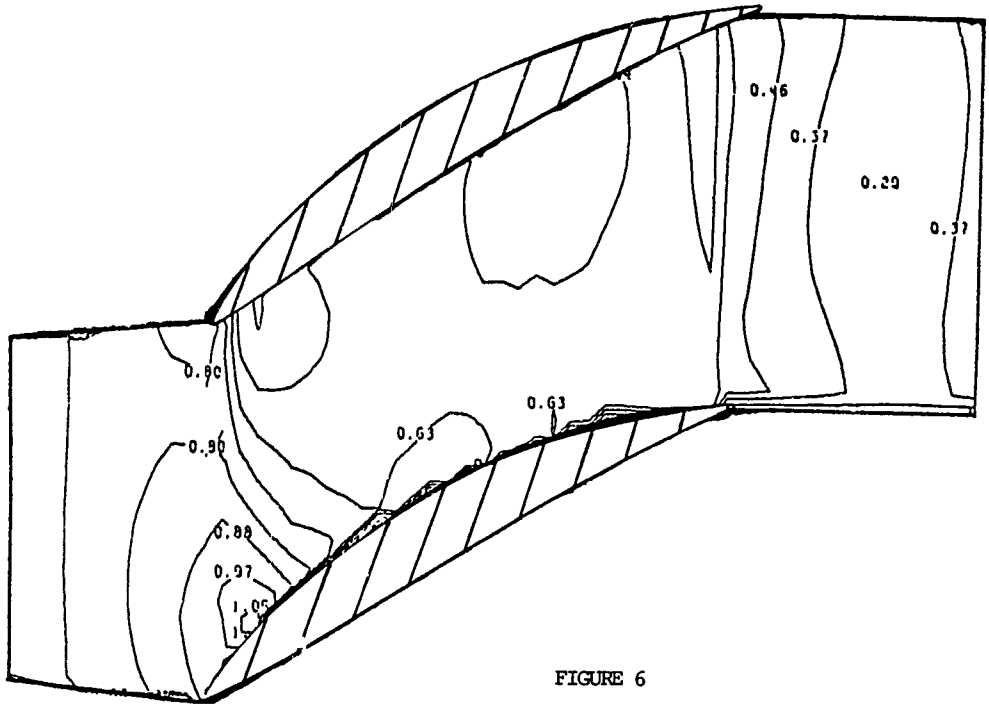

FIGURE 6

Computed Blade to blade Stream Surfaces

View as Seen Looking Downstream

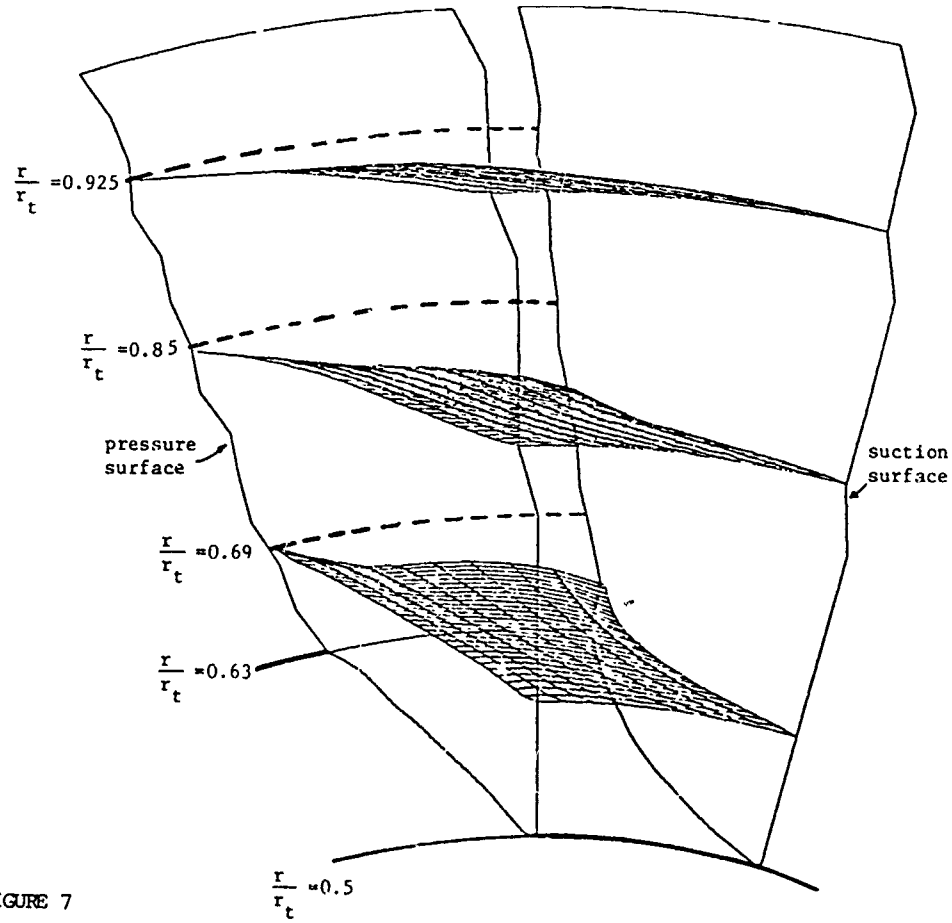

FIGURE 7

Computed S2 Surfaces

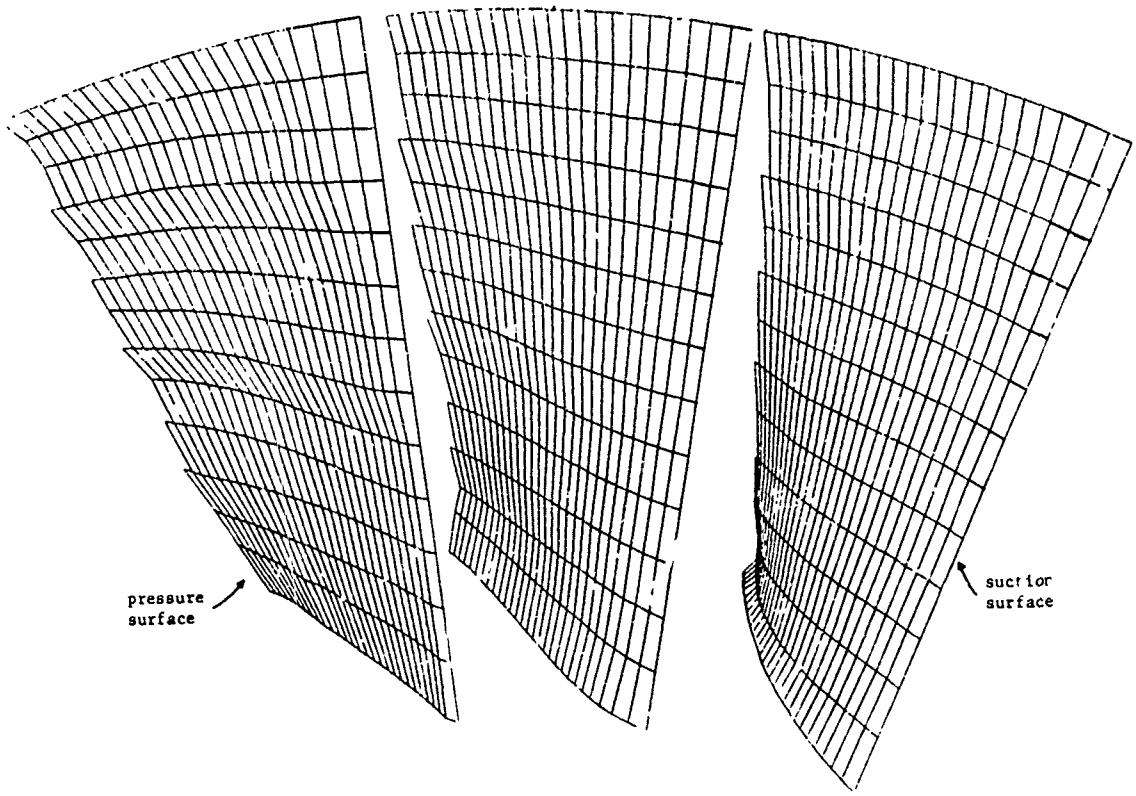

FIGURE 8

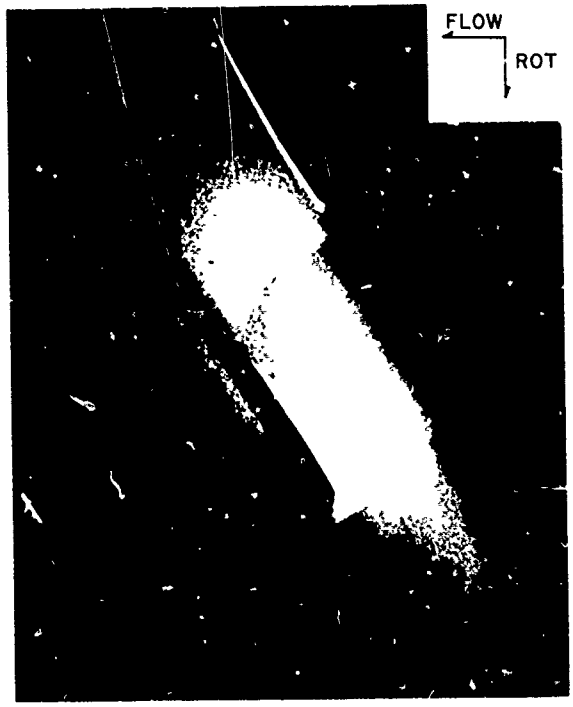

UNPROCESSED

VISUALIZED FLOW AT r/r_t = 0.6

FIGURE 9a

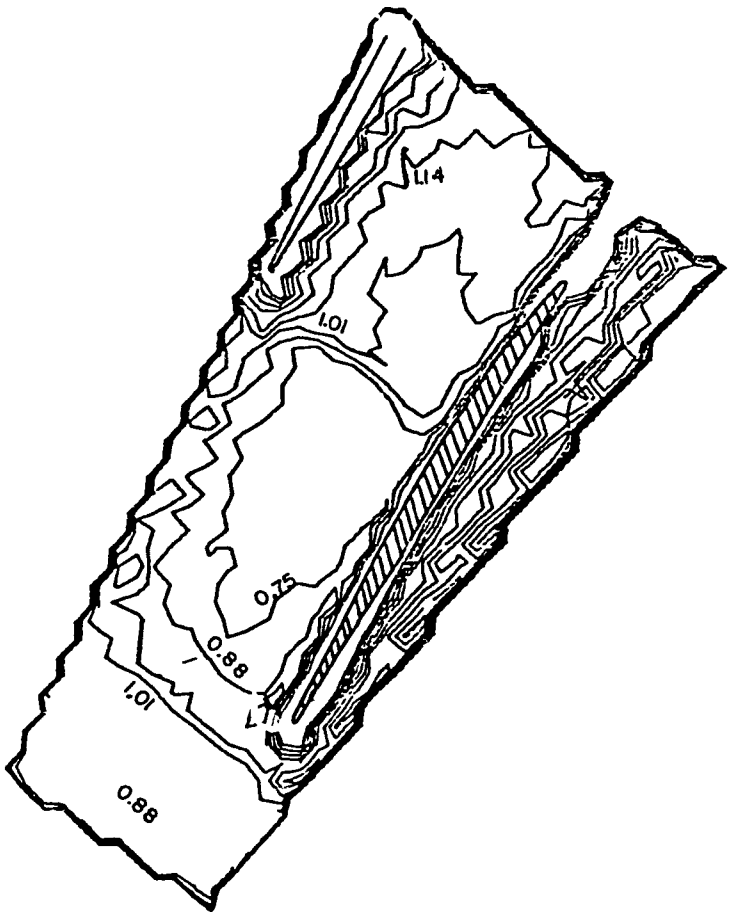

FULLY CORRECTED

FIGURE 9b

Computed Density Contour Map
Radius Ratio = 0.88

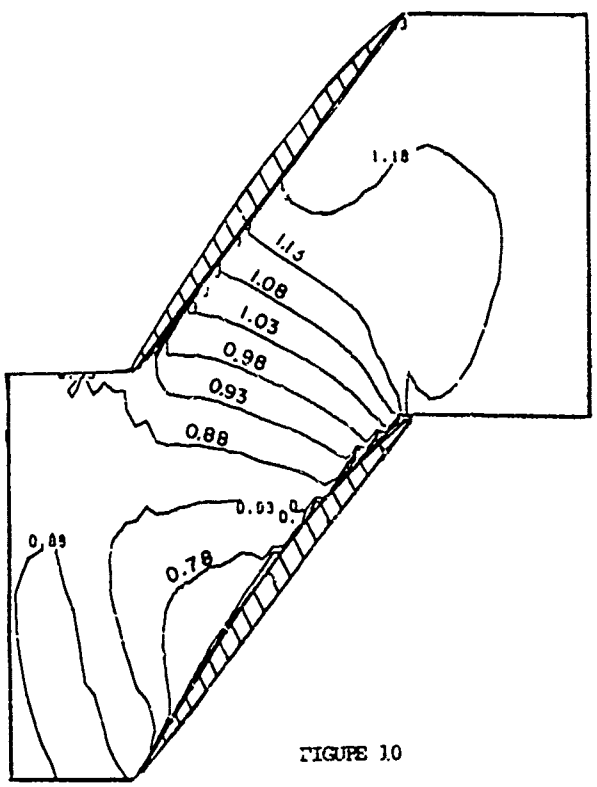

FIGURE 10

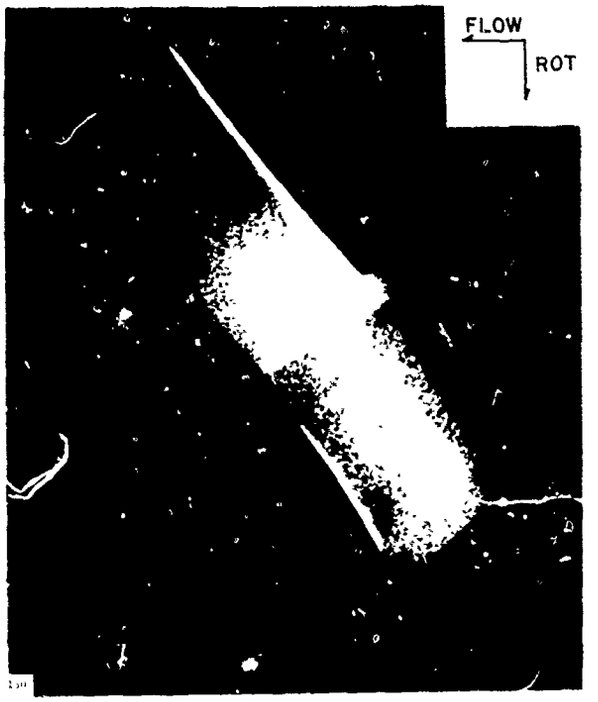

UNPROCESSED

VISUALIZED FLOW AT $r/r_t = 0.80$

FIGURE 11a

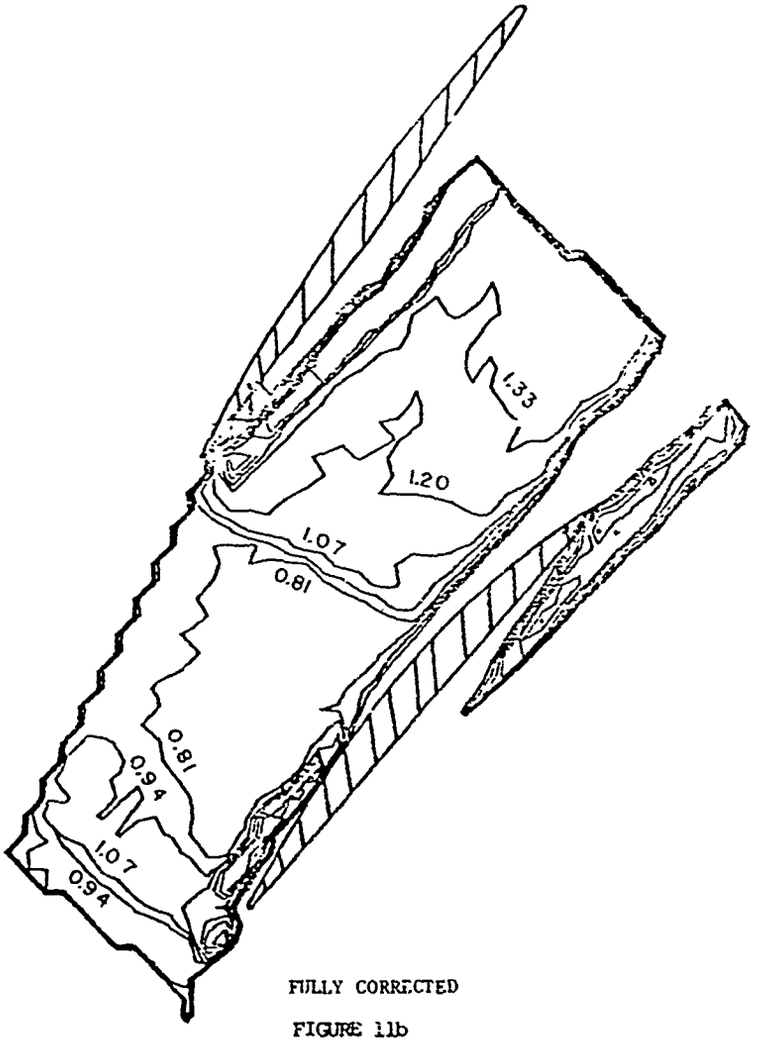

FULLY CORRECTED

FIGURE 11b

Computed Density Contour Map
Radius Ratio = 0.80

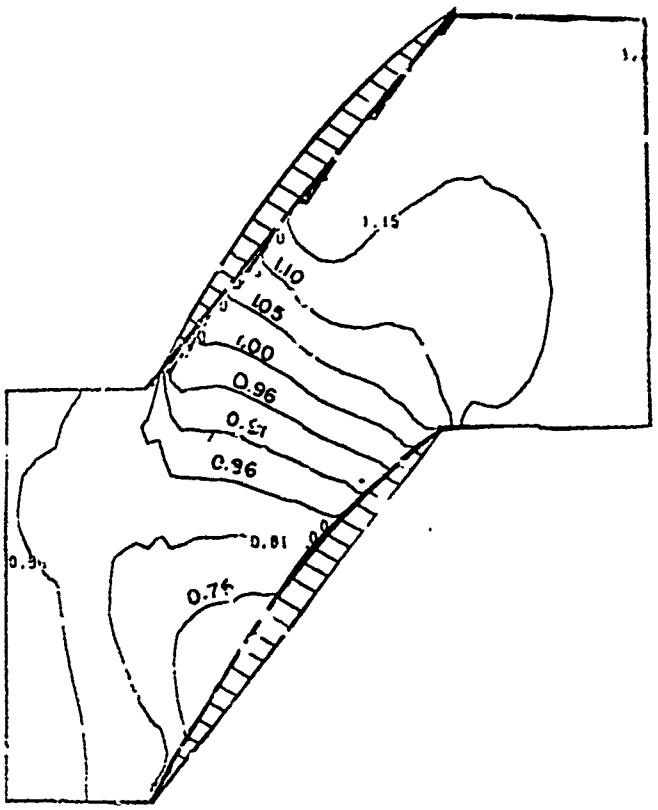

FIGURE 12

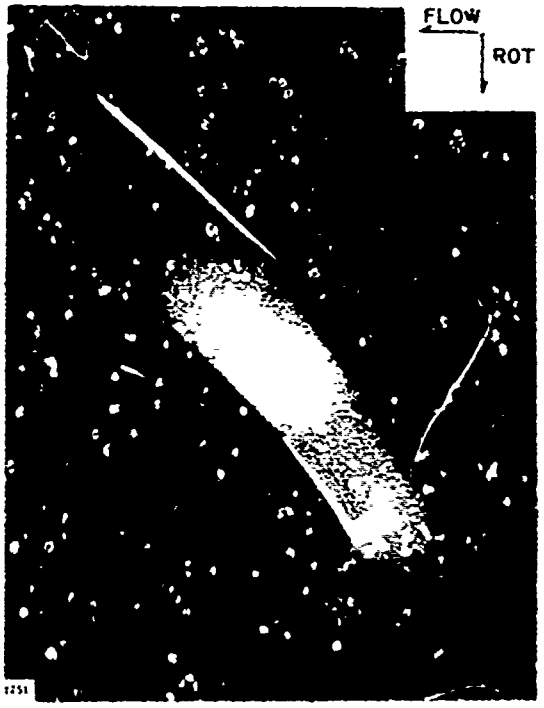

UNPROCESSED

VISUALIZED FLOW AT $r/r_t = 0.70$

FIGURE 13a

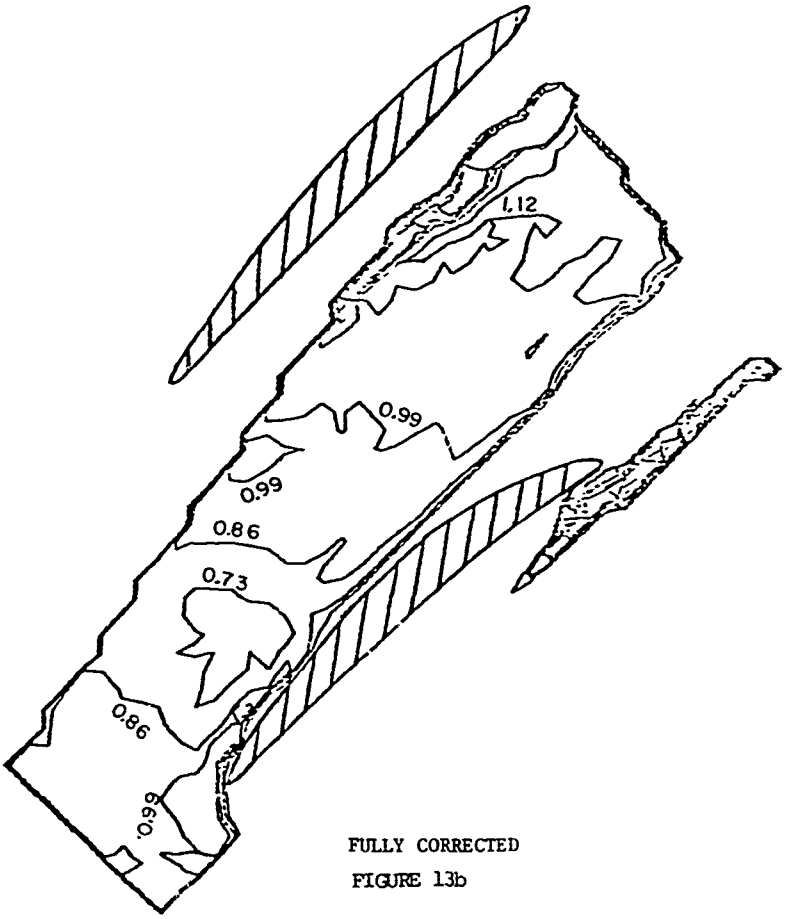

FULLY CORRECTED

FIGURE 13b

Computed Density Contour Map
Radius Ratio = 0.70

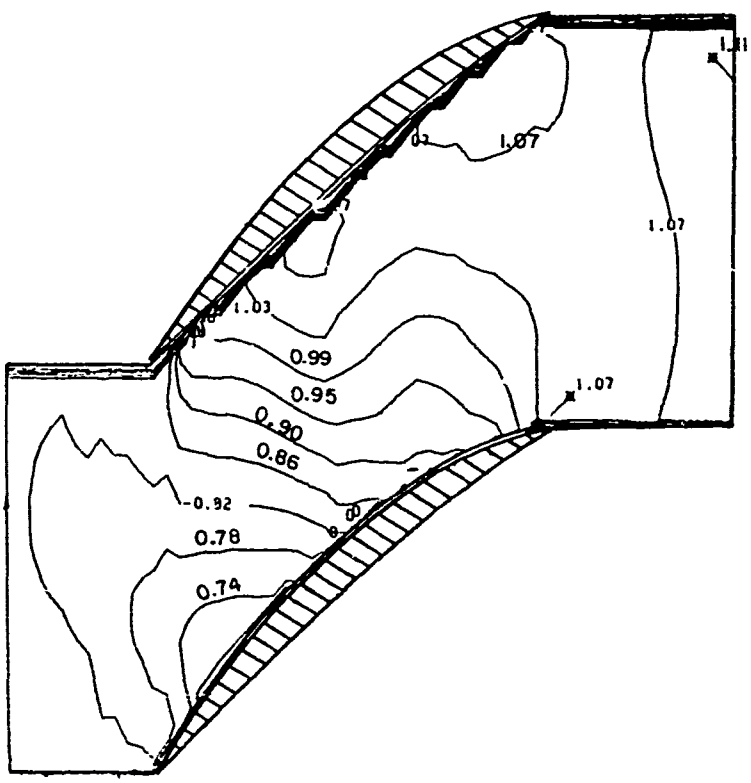

FIGURE 14

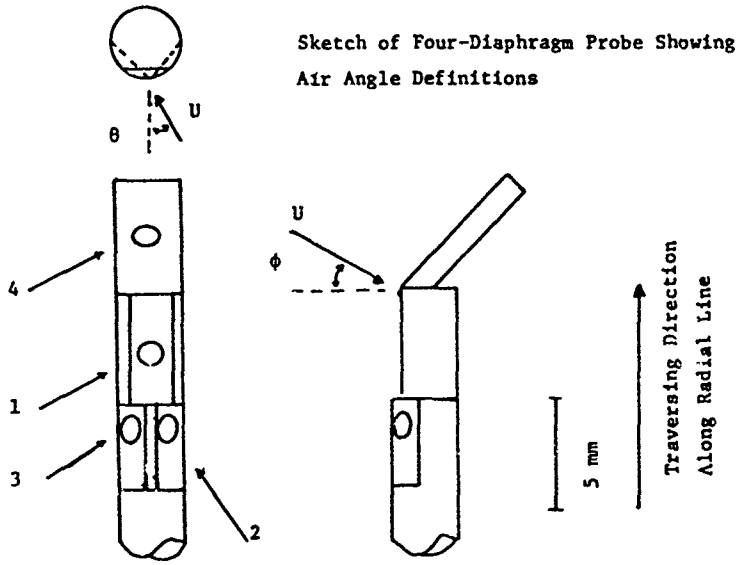

Sketch of Four-Diaphragm Probe Showing
Air Angle Definitions

FIGURE 15

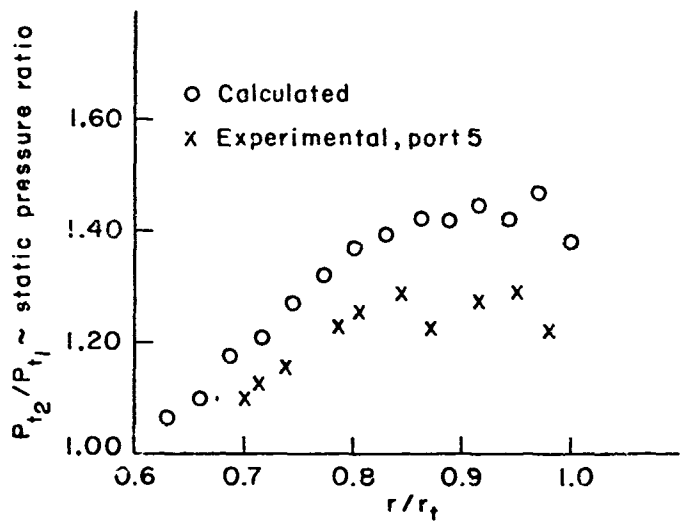

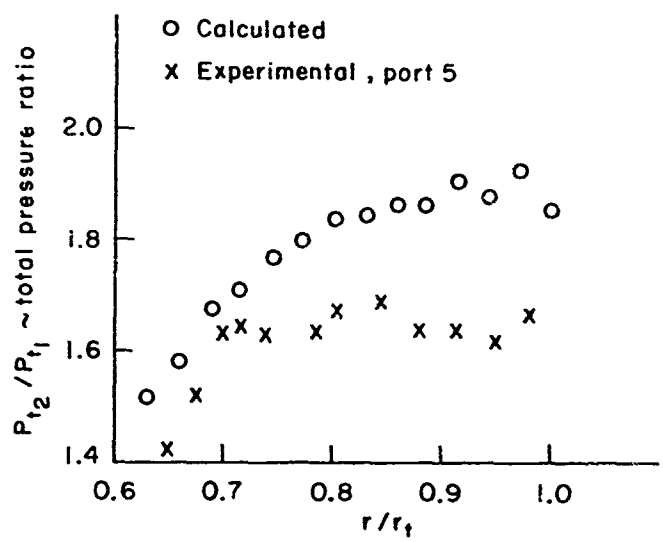

Rotor Total and Static Pressure Ratios
Theta Averaged Values

FIGURE 16

Computed Total Pressure Ratio Map
At Blade Trailing Edge

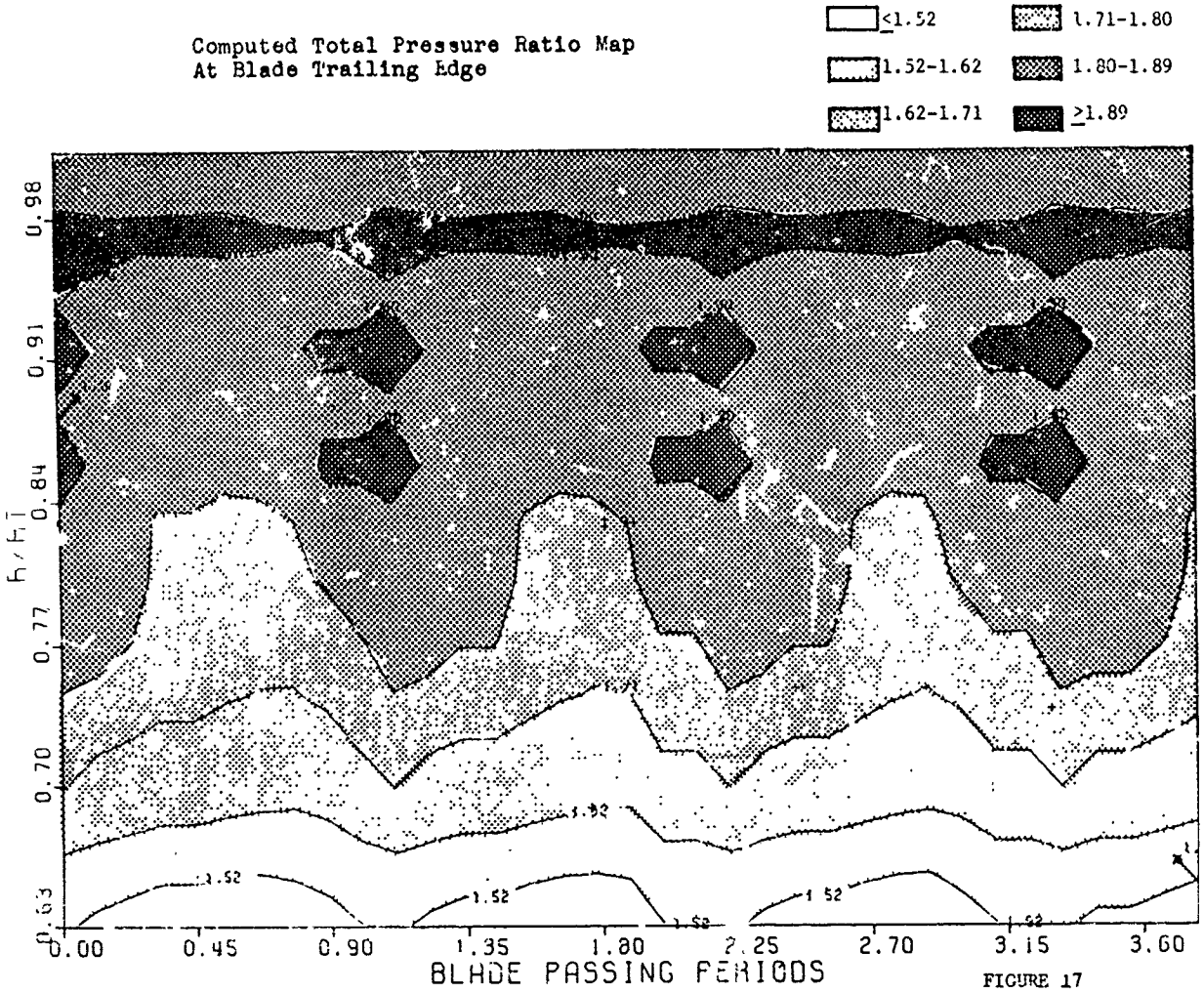

FIGURE 17

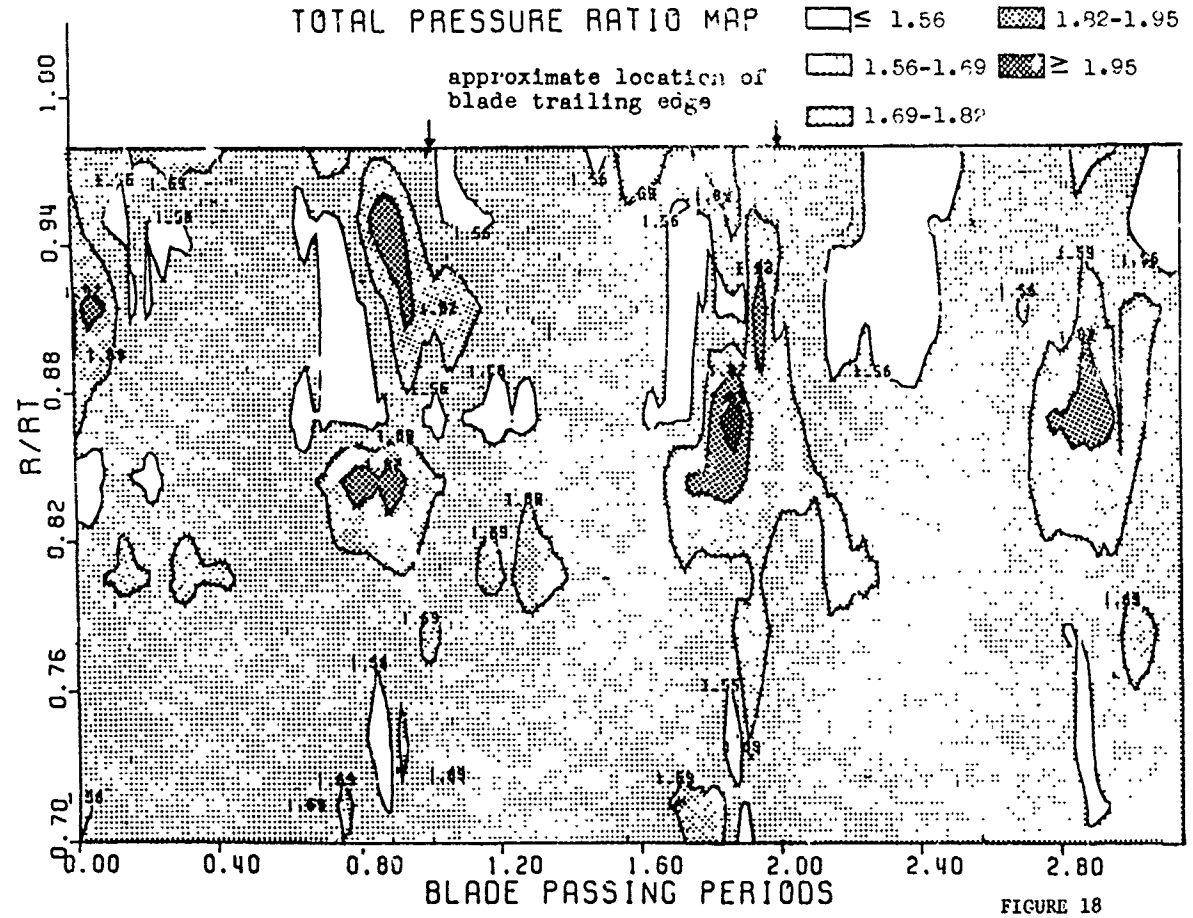

FIGURE 18

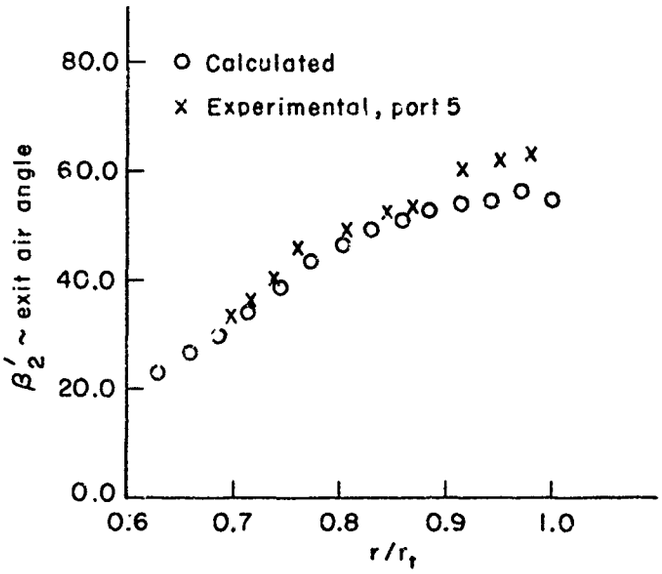

Rotor Exit Air Angles Relative Coordinate Frame Theta Averaged Values

FIGURE 19

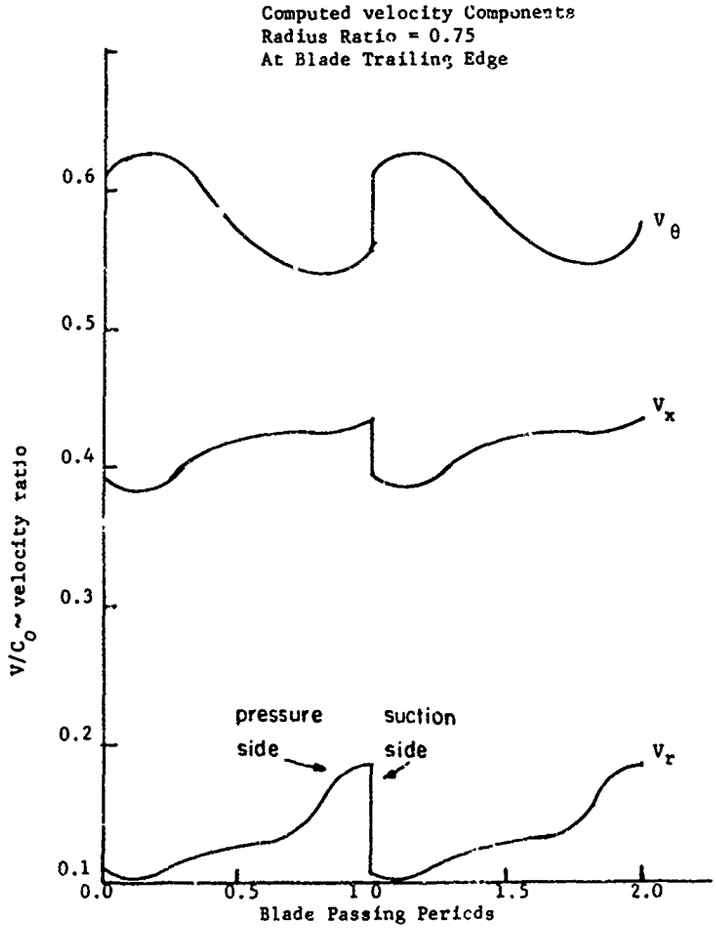

FIGURE 20

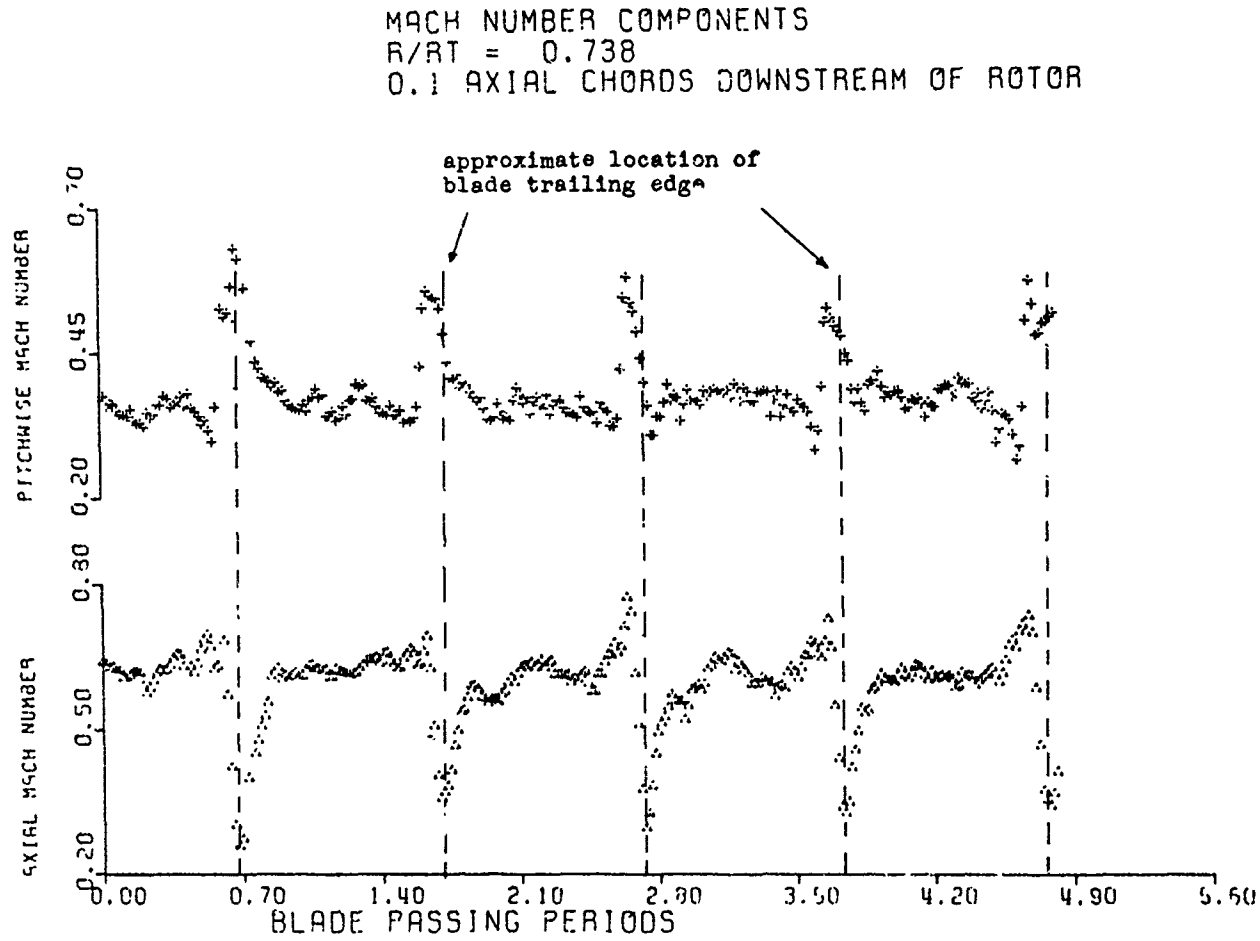

FIGURE 21

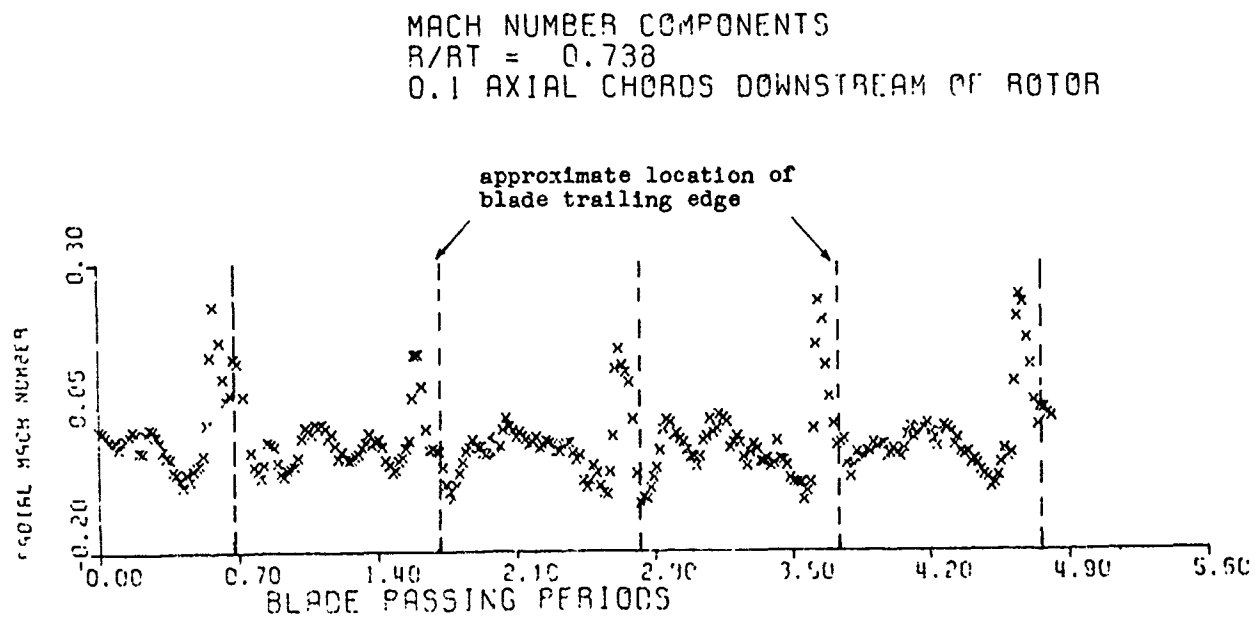

FIGURE 22

COMMENTS

Comment by Ch.Hirsch, V.U.B., Belgium

(a) Did I understand you correctly when you said that your calculation is not isentropic? How do you calculate the entropy variation across the shock?

(b) What are your boundary conditions at the upstream and downstream boundaries of the passage?

(c) Have you to impose flow angles or tangential velocities at these boundaries?

Authors' response.

(a) The calculation procedure does assume isentropic flow as the expected shocks are weak.

(b) Upstream boundary conditions are that the fluid stagnation state is specified that the inlet swirl velocity is zero. At the downstream boundary, a mean, θ averaged, static pressure is imposed on the hub surface.

(c) The axial velocity at both boundaries is allowed to float as the calculation proceeds, thus no flow angles are imposed.

Comment by D.Miller, Carleton University, Canada

Have you considered how one could include viscous effects into this method?

Authors' response:

There are no present plans to produce a fully three-dimensional viscous code at M.I.T. The present code is now being adapted to add a boundary layer analysis and adapt the blade geometry to calculated displacement thickness.

THROUGH-FLOW CALCULATION PROCEDURES FOR APPLICATION TO HIGH SPEED LARGE TURBINES

by
H.J.A. COX

Head of Theoretical Aerodynamics Group,
GEC Turbine Generators Ltd.,
Barton Dock Road, Urmston, Manchester, M31 2 JD, England.

SUMMARY

Major difficulties arise in the evaluation of through flow solutions relevant to conditions existing within the rear stages of large modern low pressure steam turbines. The highly loaded stage designs in which convergent-divergent profiles are used require computation procedures which can accurately allow for supersonic Mach numbers at both guide and runner blade outlet, high values of streamline slope in the meridional plane and varying quantities of mass flow tapped off between stages. The consequent effect of these conditions on turbine performance and various methods by which they can be incorporated into a streamline curvature computation process are discussed together with the use of steam thermodynamic data. Procedures which can be employed to obtain numerical stability and convergence in the computation process are suggested and further problems concerned with the evaluation of off-design solutions are briefly considered.

NOMENCLATURE

a	local acoustic velocity.	r	radius.
Ccrit	critical acoustic velocity.	δr	distance between adjacent stream surfaces ψ and $\psi+\delta\psi$
B	fluid outlet angle relative to tangential direction on stream surface.	s	blade pitch
β	projection of B on cylindrical surface.	T_T	total temperature.
C	fluid absolute velocity.	t	static temperature.
$C_u C_r C_z$	tangential, radial, axial component.	U	blade peripheral velocity.
C_r, C_v	throat flow coefficients.	v	specific volume.
C_r^*, C_v^*	choking values.	W	relative velocity.
G	mass flow along streamtube.	X	loss factor.
H_T	total enthalpy.	X_p, X_s	profile, secondary loss factors.
H_R	relative total enthalpy.	X_g, X_R	guide, runner, duct and interspace
ΔH_T	total enthalpy drop across blading.	X_D X_i	loss factors.
h	static enthalpy.	z	axial distance.
M	Mach number.	δ	deviation.
M′	isentropic Mach number.	ϵ	inclination of computing station.
Me	exit value.	η	efficiency.
M_m, M_z	meridional and axial components.	η_p	profile efficiency.
P_T	total pressure.	$\Delta\eta$	efficiency debit - power loss.
p	static pressure.	ρ	density.
ψ	stream function.	σ	stream line slope in merid. plane. (C_r/C_z)
q	leakage flows	γ	ratio of specific heats.

1.0 INTRODUCTION

A cross section defining the meridional plane of the last stage of an L.P. steam turbine is shown in the diagram of Fig.1. Here the pronounced wall flare shown in the duct interspace between the upstream runner exit and the guide inlet is typical of last stages and, to some extent, the penultimate stages of modern highly loaded low press' cylinder designs. The geometry illustrated will give rise to large computed values of streamline slope and curvature in the region near to the flared wall with consequent effects on the resultant radial static pressure distributions. Some care must thus be taken to establish a valid flow boundary, (outer streamline), which may or may not be coincident with the geometric boundary of the duct interspace.

Application of through-flow computing methods to stages of this type are additionally complicated by a number of other factors some of which are specifically related to steam turbine application.

(i) Presence of significant bleed-off flows between stages and complicated root leakage flow patterns.
(ii) Equation of state must allow for real steam properties (imperfect gas laws), both in the dry and the two-phase thermodynamic flow regimes.
(iii) Flow solutions must allow for outlet Mach numbers which can have high supersonic values both at the rotor outlet (relative to the blade) and at the guide outlet. For highly loaded stages the exit isentropic Mach number, Me′, at the rotor tip (relative) or at the guide root can be of the order Me′ = 2.0; the rotor relative outlet Mach number in this situation being supersonic over most of the blade height.

Specific procedures can be developed to account for these effects and items (ii) and (iii) above are discussed in detail in subsequent sections, the latter item particularly in respect of convergent-divergent profile design where the efficiency variation with Mach number exhibits a completely different form from that shown by convergent blading.

While blade row computation stations are generally located at axial positions coincident as far as possible with blade leading and trailing edges, note must also be made of the mean axial location of the blade passage at inlet and outlet (throat). From this information account can then be taken within the computer program of any annular streamtube area variation and its subsequent effect on the overall passage geometry and position of the choking throat, both of which can vary considerably from their nominal plane flow (specified input) values. Allowance for changes in streamtube area downstream of the effective throat must also be made in the computation of outlet flow angle.

A general computational procedure is first briefly defined in section 1 followed in section 2 by the specification of a simple thermodynamic procedure which will allow use of steam data, or that of any non perfect gas, in relation to the method of allocation of interstage losses discussed in some detail in section 3. The basic radial equilibrium and energy equations are defined in sections 4 and 5 while the associated computational problems of convergence and stability are covered in sections 6 and 7. Procedures which will allow for supersonic flow and streamtube diffusion effects, both on outlet angle and blade profile efficiency (for convergent and convergent-divergent profiles), are covered in sections 8 and 9 while in the final section the problems of off-design prediction are briefly discussed.

2.0 CALCULATION PROCESS

The calculation process is based on an iterative procedure in which the radial equilibrium equation and energy equation are applied successively to each axial station within the turbine using a previously determined streamline flow pattern to define the slope and curvature terms. These calculations are carried out in each iterative cycle by using set values of some suitable flow parameter at a specified reference point (i.e. on the root or mean streamline); these reference parameters being assigned for the first calculation and then updated to satisfy continuity in each succeeding iteration. Once the reference parameter is defined, the radial equilibrium equation may then be solved iteratively in conjunction with the energy equation, working station-by-station successively downstream through the turbine. From the radial flow solutions established at each station the implied mass flow can be obtained by integration and the differences between the calculated and the required value used to adjust each reference parameter for the succeeding iteration. The above process is then repeated until the integrated mass flow at each station agrees with the locally required value.

A simple realistic procedure that can be used to handle the varying leakage flows is illustrated diagrammatically in Fig.2. where the take-off flow is shown locally subtracted from the flow through the tip and root annular streamtubes. With this procedure the tip and root take off quantities cannot exceed the corresponding streamtube flow upstream of the leakage points. Root flow quantities must be automatically evaluated within the iteration process using a flow balance between guide and balance hole flow while the take-off flow (to reheater, drainage, etc.) can generally be specified in the input data. The rotor tip leakage flow should be excluded from the blading through-flow, the outer streamline boundary being adjusted at guide exit to allow the computed leakage flow to pass through the available guide opening external to the tip streamline defining the flow boundary.

3.0 THERMODYNAMIC STATE LINE

For steam application, thermodynamic fluid properties are usually obtained from stored tabulated data corresponding to that shown graphically by a Mollier chart. Local conditions may then be obtained by reference to a computed state line defined by values of inlet pressure and enthalpy and the local static-to-static efficiency from inlet to the particular station considered. Strictly separate state-lines are required for each streamline in order to allow for any radial variation in efficiency but sufficient accuracy can usually be obtained by adopting a mean state line for each stage.

If we consider the loss build up within a stage, we can subdivide the sum total of losses into three constituent parts:

a) blade losses
b) duct losses between runner outlet and the downstream guide inlet and annulus losses in the guide exit-runner inlet interspace
c) power losses arising from flow leakage, windage loss etc.

It then seems plausible to assume that the state line across the blading from guide inlet to runner outlet incorporates all the blade and duct interspace losses and the state line efficiency is identical to the static-to-static blading efficiency evaluated from guide inlet to runner outlet, this being represented by a line B-C on Fig.4. It is then convenient to ensure that the computed stage efficiency derived within the through-flow program is exactly compatible with standard prediction procedures and this can be achieved if we assume that the duct losses (b) and power losses (c) above are both totally absorbed within the duct region between runner outlet and the downstream guide entry. Strictly the power losses arise by consideration of work/lb of total flow and the precise axial distance over which they effectively mix into the main through flow is unknown. Each downstream guide inlet condition is thus defined to include the power losses incurred by the upstream stage which together with the associated duct losses, gives the resultant state line over the duct region indicated by the line CB in Fig. 4.

Thermodynamic data within the blading can then be evaluated in each iterative cycle by interpolation of stored property data evaluated at a number of fixed values of static pressure and enthalpy which include the updated pressures and enthalpies on the reference streamline at guide inlet and runner exit. In its simplest form this procedure is then consistent with interpolation along a constant efficiency state line where the state line efficiency is defined by the blading static-to-static efficiency evaluated in the previous cycle. Interpolation is usually carried out using parameters log p, pv, t and d (dryness fraction) as functions of the isentropic heat drop evaluated in cumulative form relative to the static enthalpy at inlet to the first stage. For the downstream duct region it is preferable to interpolate property values at the required pressure

from data obtained using both the upstream and downstream blading statelines. Direct interpolation of property values along the line CB′ is not recommended as any pressure variation outside the specified terminal values could lead to unacceptable density extrapolation errors. A typical cumulative heat drop curve for pressure (log p) is illustrated in Fig.3, the overlap region between successive stages incorporating the effects of the total enthalpy increase resulting from the upstream stage power losses.

3.1 Stage Loss Breakdown

The primary break-down of the stage losses used in the subsequent discussion is based on the following definitions of blading and stage efficiencies

$$\eta_{\text{blade}} = \frac{\Delta H_T}{\Delta H_T + \sum \text{blade losses} + \sum \text{interspace losses}}$$

$$\eta_{\text{stage}} = \frac{\Delta H_T - \sum \text{power losses}}{\Delta H_T + \sum \text{blade losses} + \sum \text{interspace losses}}$$

$$\overline{\eta}_{\text{stage}} = \frac{\Delta H_T - \sum \text{power losses}}{\Delta H_T + \sum \text{blade losses} + \sum \text{interspace losses} + \sum \text{duct losses}}$$

where ΔH_T denotes the total enthalpy drop from guide inlet to runner outlet along each streamline. All the above losses are derived from computed loss coefficients in enthalpy form, this being the most convenient definition for use in conjunction with the state line procedure discussed above. Then for each loss constituent we have:

a) blade losses:- derived via loss factors X_G and X_R (guide and runner respectively) where, following the notation in the blading enthalpy/entropy diagram of Fig.4, we have $\sum X_G = 2gJ\,\delta h_G / C_1^2$ and $\sum Y_R = 2gJ\,\delta h_R / W_3^2$; where δh_G and δh_R denote the enthalpy equivalent loss debits incurred by the guide and runner respectively. We can then write

$$\sum \text{blade losses} = (\Sigma X_G C_1^2 + \Sigma X_R W_3^2)/2gJ$$

The normal definition of blade section kinetic efficiency is simply related to these loss coefficients since by inspection of the diagram in fig. 4 it follows that:-

$$\eta_G = (1 + \Sigma X_G)^{-1} \quad ; \quad \eta_R = (1 + \Sigma X_R)^{-1}$$

By implication the terms ΣX assume that each blading loss factor is given by the algebraic sum of a number of constituent parts; thus $\Sigma X = \Sigma X_p + X_s$ and ΣX_p includes separate contributions due to Reynolds No., blade roughness, incidence, trailing edge thickness, stream-tube diffusion and Mach number. All these terms plus the secondary loss factor, X_s, can be obtained from some standard algebraic loss correction such as that reported in (10) for example. For incompressible flow the definition ΣX reduces to the usual form of total pressure loss coefficient.

b) Duct and interspace losses - expressed in a similar manner to the blade losses, using an enthalpy equivalent loss debit, but in this case expressed as a proportion of the enthalpy drop equivalent to the inlet velocity. Then considering conditions across the duct region between stage inlet (upstream runner exit) and the guide inlet station in the enthalpy/enthalpy diagram of Fig. 4 we can define an annulus duct loss factor $(\Sigma X_a)_D$

$$(\Sigma X_a)_D = 2gJ\delta h_D / C_A^2 = 2gJ \sum \text{duct loss} / C_A^2$$

which for incompressible flow reduces to the usual definition of total pressure loss coefficient. The annulus duct loss factor is assumed to be made up of the algebraic sum of separately estimated factors $(\Sigma X_a)_D = X_{a_1} + X_{a_2} + X_{a_3}$, where: X_{a_1} = lap loss, X_{a_2} = wall cavity loss and X_{a_3} = diverging annulus loss. In situations where the duct region contains a number of separate stations the simplest procedure is to split $(\Sigma X_a)_D$ into discreet values representing the loss coefficient over the axial zone from runner outlet to each individual duct station.

The same definitions apply to the guide exit/runner inlet interspace losses where the annulus loss coefficient for this zone is defined, in terms of the notation in Fig.4, by the expression $(\Sigma X_a)_i = 2gJ\,\delta h_i / C_1^2$ and $\sum$ interspace losses = $(\Sigma X_a)_i C_1^2 / 2gJ$

c) Power losses are most conveniently derived from a sum of individual direct efficiency debits relative to the blading efficiency. Thus $\eta_{\text{blade}} - \eta_{\text{stage}} = \Sigma \Delta\eta_{\text{power}}$ where $\Sigma\Delta\eta_{\text{power}}$ is made up of separate contributions due to: tip leakage, gland leakage, balance hole leakage, power windage loss and wetness loss in wet steam. These losses enter the calculation through the definition of the state line and are represented by the enthalpy overlap of successive blading state lines. The overlap for each stage can be derived by ensuring that the conditions at successive guide inlet stations are compatible with the computed overall stage efficiency $\overline{\eta}_{\text{stage}}$. In the detailed calculation procedure each loss constituent should be applied across the respective zones in which they arise. One possible method of incorporating these losses is illustrated in Fig. 4; each loss constituent being applied, via the corresponding energy equation, across the zone shown in the table below:

	Stage Exit / Guide Inlet	Guide Inlet / Guide Outlet	Guide Outlet / Runner Inlet	Runner Inlet / Runner Outlet
Profile and secondary loss	-	$\Sigma X_{p_G} + X_{s_G}$	-	$\Sigma X_{p_R} + X_{s_R}$
Lap and cavity losses	$(X_{a_1} + X_{a_2})_R$	-	$(X_{a_1} + X_{a_2})_G$	-
Annular loss	$(X_{a_3})_R$	-	negligible	-

Normally all losses other than profile loss are evaluated on average overall conditions and used as a constant coefficient at all radii. Some improvement to this procedure can be applied to the secondary loss component based on an analysis of test data which shows secondary loss to vary inversely with aspect ratio for aspect ratios greater than 2.0. Within this range of aspect ratio separate root and tip secondary losses can then each be applied over a height range

equal to one chord, using a variation giving zero loss at one chord distance in from the tip and root respectively with a maximum value adjusted to give an integrated loss equivalent to that obtained by applying a constant mean coefficient over the complete height. Some restriction to this procedure has to be applied in multi-stage applications since the root and tip losses cannot simply accumulate in the end regions but must gradually diffuse into the main stream flow. No allowance for an accumulated annulus wall boundary layer is made, the general impression at present is that with the high deflection blading employed in steam turbine stages the end wall boundary layers separate within the blade passage; the boundary layer thickness at entry to each blade row resulting only from the growth downstream of the separation point in the upstream blade.

4.0 RADIAL EQUILIBRIUM EQUATION

The overall calculation procedure considers the flow at a number of axial stations within the turbine, a radial equilibrium equation together with energy and continuity equations being used at each station to determine the radial distribution of flow properties across the annulus. Each distribution is adjusted such that the radial acceleration imparted to a fluid particle passing from station-to-station is accounted for in the local radial equilibrium equation; the radial acceleration being derived from the slope and curvature of the meridional streamlines computed from continuity considerations.

Simplification of the fundamental momentum equations given in (1) is obtained by considering the flow to be axi-symmetric and thus all derivatives with respect to the tangential co-ordinate, θ, can be neglected. Errors in this assumption are discussed to some extent in (2). Application in this form is then usually restricted to stations outside the blade rows to which the above approximation is only strictly relevent. On the assumption of steady, inviscid and axi-symmetric flow, the basic equations governing the flow in the annular duct regions between blade rows may be derived from the fundamental Euler momentum equations and the continuity equation. It is usually convenient to transform these equations from the normal cylindrical (r, z) system of co-ordinates to a (ψ, z) system by the introduction of a stream function ψ. In this form the Euler equations can be written in the form:

$$2\pi r\left(\partial p/\partial \psi\right)_z = \frac{C_\omega^2}{C_{zr}} - C_z\left(\partial\sigma/\partial z\right)_\psi - \sigma\left(\partial C_z/\partial z\right)_\psi$$

$$C_z\left(\partial C_\omega/\partial z\right)_\psi + \frac{C_r C_\omega}{r} = 0$$

$$\frac{1}{\rho}\left(\partial p/\partial z\right)_\psi + \frac{1}{2}\frac{\partial}{\partial z}\left[C_z^2\left(1+\sigma^2\right) + C_\omega^2\right] = 0$$

$$\frac{\partial}{\partial z}\left(\rho C_{zr}\right)_\psi + 2\pi\rho^2 r^2 C_z^2\left(\partial\sigma/\partial\psi\right)_z = 0$$

where the streamline slope in the meridional plane, $\sigma = C_r/C_z = \left(\partial r/\partial z\right)_\psi$ has been introduced to replace the radial velocity term and where the stream function ψ is defined by the equations:-

$$\left(\partial\psi/\partial r\right)_z = 2\pi r\rho C_z \quad ; \quad \left(\partial\psi/\partial z\right)_r = -2\pi r\rho C_r$$

The first of the Euler equations above, usually referred to as the full radial equilibrium equation, is used to establish the static pressure gradients at each station. The term $\left(\partial\sigma/\partial z\right)_\psi$ appearing in the second term on the right hand side of the radial equilibrium equation is directly evaluated at each station from the local streamline curvature. The determination of the third term is rather more complicated and is usually derived from the continuity equation eliminating $\partial\rho/\partial z$ by use of the third momentum equation. Then with some algebraic manipulation we can obtain

$$\left(1-M_m^2\right)\frac{1}{C_z}\left(\partial C_z/\partial z\right)_\psi = \sigma M_z^2\left(\partial\sigma/\partial z\right)_\psi - \frac{\sigma}{r}\left(1+M_z^2\cot^2\beta\right) - \left(\partial\sigma/\partial r\right)_z$$

where the axial Mach number, M_z $(= C_z/a)$ and the meridional Mach number Mm $(= C_z\sqrt{1+\sigma^2}/a)$ have been introduced together with the flow angle β on the cylindrical surface, defined by $\cot\beta = C_\omega/C_z$. Substituting this equation into the first of the Euler momentum equations above will give the normally quoted isentropic axi-symmetric radial equilibrium equation:-

$$2\pi\rho C_z\left(\partial p/\partial\psi\right)_z = \frac{1}{\rho}\left(\partial p/\partial r\right)_z = \left[\left(1-M_z\right)^2\left(\frac{C_\omega^2}{r} - C_z^2\left(\frac{\partial\sigma}{\partial z}\right)_\psi\right) + C_z C_r\frac{1}{r}\frac{\partial}{\partial r}\left(\sigma r\right)_z\right]\left(1-M_m^2\right)^{-1}$$

Analysis of the equation for $\left(\partial C_z/\partial z\right)_\psi$ in (2) shows that values of the axial velocity gradient are finite at the meridional sonic condition Mm = 1.0. This condition obviously implies that at this Mach number the right hand side of the equation $\left(\partial C_z/\partial z\right)_\psi$ must reduce to zero, giving an equivalent situation to that represented by zero streamtube area gradient in plane flow. It follows from this analysis that in situations where the meridional Mach number approaches unity, the axial velocity gradient is indeterminate and an alternative equation is required.

One simple procedure is to over-ride the equation for $\partial C_z/\partial z$ over some specified range, say $.90 \leq$ Mm ≤ 1.10, with an auxiliary relation such that $\left(\partial C_z/\partial z\right)_\psi = 0$ when Mm = 1.0, although this may introduce convergence problems if at some stage in the iteration process the value of Mm exceeds unity. An alternative stable method is to replace the complete equation with a difference calculation, deriving $\left(\partial C_z/\partial z\right)_\psi$ directly from the previously computed values of the axial velocity, but there are some reservations concerning the accuracy of this procedure in situations where large changes in axial velocity take place across the blade stations.

Finally allowance must be made in these equations to incorporate non-radial stations, since it is desirable to align these as far as possible with blade leading and trailing edges, or with interduct traverse planes. Then defining each station by a mean straight line inclined at an angle ϵ to the horizontal, z, axis we can obtain with some algebraic manipulation:

$$2\pi r\left(1-\sigma\tan\epsilon\right)\left(\partial p/\partial\psi\right)_{\epsilon'} = \frac{C_\omega^2}{C_{zr}} - \left(\sigma+\tan\epsilon\right)\left(\partial C_z/\partial z\right)_\psi - C_z\left(\partial\sigma/\partial z\right)_\psi$$

where ϵ' denotes differentiation along the new sloping axis and

$$\left(\frac{\partial\sigma}{\partial r}\right)_z = \left[\left(\frac{\partial\sigma}{\partial r}\right)_{\epsilon'} - \tan\epsilon\left(\frac{\partial\sigma}{\partial z}\right)_\psi\right]\left(1-\sigma\tan\epsilon\right)^{-1}$$

Complete solutions in the ducting interspace regions between blade rows then follows from the second and third momentum equations. The second equation can be written in the form $\partial(C_\omega r)/\partial z = 0$ which simply states that angular momentum is conserved along a streamline in inviscid irrotational flow. Integration of the third momentum equation along the appropriate streamline in the duct region would

yield an inviscid energy equation comparable with the radial equilibrium equation derived above, but with the method described in section 3.0 the integrated energy equation is implicit in the application of the state line procedure, localised losses being additionally smeared along the flow path.

5.0 ENERGY EQUATIONS

The radial variation of the fluid velocity at any station can be calculated for each streamline starting at the reference line along which the assigned fluid parameters are defined. Thus considering a particular stage in which, say, values of reference static pressures have been fixed from the previous iteration and upstream data at the previous runner exit has been fully computed, the calculation process can then proceed as follows:-

(i) Duct Regions:- previous stage exit up to guide inlet. The absolute velocity at any intermediate station can be directly computed from the change in cumulative heat drop, corresponding to the upstream and local static pressures, together with the known upstream velocity and the corresponding enthalpy loss factor. The relevant equation is quoted in the diagram of fig. 4. This procedure is computationally simple to apply since cumulative heat drop and static pressure are directly related to each other in the state line procedure discussed above. Application of the constant angular momentum equation and known streamline slope will then yield all three velocity components. The overall radial distribution at any one station can then be computed iteratively; first evaluating $\partial P/\partial \psi$ from a difference approximation and then using a curve fit integration procedure to obtain a second approximation to the static pressure and so on. When this procedure has converged a full radial equilibrium solution has been established relative to the reference pressure and streamline geometry and the calculation process can then proceed on to the next station. In the final computation cycles the initial pressure distribution can be obtained by straight scaling of the previously computed values.

(ii) Guide Exit:- The velocity at the reference streamlines is directly computed using the cumulative heat drop as shown in the diagrams of figs. 3 and 4. the loss through the guide blading being accounted for by use of the enthalpy loss coefficient $\bar{Z}X_G$. Then for a known fluid outlet angle β_2 interpolated from the outlet angle routine described in section 8.0, the velocity components can be evaluated from the known streamline slope. The complete solution procedure then follows that discussed for the duct regions above.

(iii) Runner Inlet:- Procedure follows exactly that laid down for the duct regions using the respective interspace enthalpy loss coefficient.

(iv) Runner Exit:- The relative velocity at outlet is obtained by applying the Euler work equation along the computed streamline, the resulting equation and associated enthalpy-entropy diagram being given in fig. 4. The full solution follows similarly to that discussed above, absolute velocities and velocity components being derived from the usual velocity triangle relationships together with the interpolated fluid outlet angle.

All the equations quoted in fig. 4 and the definitions of efficiency in section 3.1 are based on an approximation which is equivalent to assuming the constant pressure lines on the Mollier Chart to be parallel over small ranges of enthalpy and entropy. Correction to these equations can be made by using the general expression relating the isentropic enthalpy change between two pressures p_1 and p_2 usually given in the form $1 - (p_2/p_1)^{\frac{\gamma-1}{\gamma}} = h_1 - h_2/h_1 - \lambda$ where λ takes values of the order of 800 and 535 in BTU/lb for superheated and wet steam respectively. Differences between the two methods are marginal and certainly within the accuracy of prediction of the losses.

A comparison with single stage data obtained by N.G.T.E. using a simplified form of the computation process described above is shown in fig. 5. Reasonable agreement with the measured data is shown comparable at least with that computed using the method reported in (8).

6.0 CONVERGENCE PROCEDURE

At each axial station the value of the stream function at the outer diameter of the flow annulus, which is identically equal to the total computed mass flow crossing each station, is calculated by integrating $(\partial\psi/\partial r)\epsilon'$ numerically. The difference between this integrated value and the required value, either specified in the input data or averaged can then be used as a basis for the correction procedures described below. Where the mass flow is not specified, a required value can be determined for each calculation cycle from the average of all the implied values computed at blading exit stations.

First, equivalent streamline positions corresponding to the flow solution just computed are obtained by integrating the stream function gradient. New values of the streamline positions required for the succeeding iteration can then be derived using an input specified damping factor discussed in the subsequent section. Secondly the reference parameter at each station has to be corrected to bring the implied values of mass flow ψ_t, into line with either the specified value or the averaged value obtained on the previous cycle, adjusted in each case to allow for any computed leakage. Pressure adjustments along the reference streamline can be carried out by using some form of approximation to the equation for the local mass flow parameter. This procedure is easiest to apply in situations where the relation between static pressure and mass flow can be written in the form $(\psi \text{ tip actual}/\psi \text{ tip required})^2 = (p'^2 - p^2)\text{ actual}/(p'^2 - p^2)\text{ required}$, where $p' - p$ denotes the meridional velocity head. Thus in conditions where the outlet static pressure from the last stage is specified, a modified value of p' can be deduced which will correct the exit value of ψ tip to the required value. The upstream station static pressure may then be adjusted using the above equation to compensate both for the corresponding (ψ) tip error at that station and the change in p' resulting from the (ψ) tip error downstream. In this manner each reference pressure can be successively modified station-by-station backwards through the machine.

This backward correction procedure has been found to give considerable advantages over the usual method of proceeding from the inlet in cases where the mass flow is not specified. If a forward adjusting procedure is used, considerable computing time has to be employed to determine the choking

or limiting value of the inlet mass flow parameter whereas the above procedure, which essentially looks at the exit mass flow parameter, is not subject to any critical limiting condition.

7.0 STABILITY PROBLEMS

The principal method of ensuring stability of convergence is through the use of a damping factor f, where for any parameter ϕ being iterated we have for the required, $(n+1)^{th}$ value:- $\phi_{n+1} = \phi_n + f(\phi_{n'} - \phi_n)$ and the damping factor f is generally assigned a value between 0.1 and 0.5. Parameters involved in this process include the reference parameter and all streamline positions at each station.

There appears to be no relevant analysis by which optimum damping factors can be derived or any method from which it is possible to determine whether absolute convergence can be achieved in any geometric situation. Following the analysis of (11) it appears to be essential to limit the streamline curve fit (from which the slope and curvature terms in the radial equilibrium equation are evaluated) to some fairly simple form in order to eliminate any possibility of introducing numerical distortion. Generally a simple second order equation is used to define each streamline in relation to the upstream and downstream stations and to obtain the slope and curvature at the central station via successive differentiation. A modified spline curve procedure which makes some allowance for upstream and downstream effects can be obtained by using a similar second order curve fit to the computed slopes and to differentiate this expression to obtain the curvature. Numerous other versions of curve-fit routines have been published. (4) for example; in all cases boundary values of slope and curvature along the first and last computing stations have to be specified as input data.

Experience in the application of through-flow procedures to the analysis of stage designs of the type illustrated in fig.1, has shown that the relative positioning of each computing station can have a considerable effect on convergence. Although the original streamline curvature procedures were limited to computing stations coincident with the leading and trailing edges of each blade, it is now recommended that as far as possible, near equal axial pitching between succesive stations should always be used. The following axial station locations are suggested for the following situations to ensure stability of convergence:

(i) Close axial spacing between guide exit and runner inlet:- use one intermediate station only.
(ii) Guide blading with large axial width:- use intermediate stations (non choked) within the blade row. In this case it is recommended that these stations should be treated similarly to a blade exit station i.e. on the blading stats line, assuming zero blade blockage and an input specified distribution of flow angle.
(iii) Wide axial spacing between runner exit and guide entry:- use a number of intermediate ducting stations.

For final stage calculations at least two downstream duct type stations should be included in order to remove the required input specified boundary conditions of slope and curvature away from the runner exit station.

8.0 OUTLET ANGLE PROCEDURE

In general deviation appears to be insensitive to incidence variations at constant Mach number in the low loss range, rising sharply to a peak value at positive incidence near to the stall value and then reducing with further increase in incidence. This type of incidence variation appears to be similar at other values of subsonic Mach number, the general level varying as the outlet Mach number approaches unity. In application to a general through-flow analysis, if first order effects only are included, it is usually safe to assume that incidence effects on deviation are negligible and deviation may thus be considered to be a function of Mach number and streamline slope and diffusion only. At low values of outlet Mach number, Me, deviation can be assumed to be constant up to values of $Me \simeq 0.4$ and thence to vary up to a sonic value which can be greater or less than the low speed value. Under supersonic conditions a considerable variation in outlet angle will arise from the re-adjustment of flow conditions required to satisfy continuity downstream of a choked throat. From this continuity condition, it is possible to theoretically relate conditions at the throat to uniform mixed values downstream where it is obvious that as the Mach number at outlet from the cascade increases, the flow angle B must become increasingly larger than the angle given by $\sin^{-1} o/s$; this effect being consistent with the flow expansion properties by which supersonic flow is established within the blade passage. Since this theoretical relation can be applied at the condition where the outlet Mach number is unity, the subsonic region can then be adequately defined in the through flow program by some specified curve fit between the input low speed value and the computed sonic value, this resulting in the type of relation between outlet angle and Mach number illustrated diagrammatically in fig. 6.

In addition to the plane flow deviation obtained from correlated cascade test data, a further correction to the outlet angle in the subsonic Mach number range is required to allow for streamline slope and diffusion effects. A fairly simple theoretical procedure has been given in (12) assuming the stream surfaces to remain conical and axi-symmetric within the blade passage; computed values of deviation of the order of - 5° at high values of streamline slope being roughly consistent with measured values. The procedure quoted above can easily be adjusted to give plane flow deviation values consistent with an existing cascade correlation.

8.1 Theoretical Outlet Angle Equations

A theoretical supersonic outlet angle in plane flow situations can be derived from application of the one-dimensional continuity equation applied along the streamtube illustrated in fig. 7. By considering the flow between adjacent stream surfaces for each blade passage and equating the mass flow at the throat (suffix t - defined in terms of integrated mean values over the full throat area) and downstream (suffix o - defined in terms of momentum mean values), the following expression for the downstream angle B measured on the stream surface can be obtained:

$$\text{Sin B} = C_F \frac{o}{s}\left[1 - \frac{\delta-1}{2} Me^2 \left(\frac{1}{\eta} - 1\right)\right]^{-\frac{\gamma}{\delta-1}} \quad \text{and} \quad C_F = \left(\overline{F P_T / P_{T_o}}\right)_t \bar{E}_e^{-1} \frac{\delta r_t}{\delta r_e} \left(\frac{1+6e^2}{1+6t^2}\right)^{1/2}$$

In this equation F denotes the ratio of the local mass flow parameter to its theoretical maximum value, i.e. $F = \frac{G\sqrt{T}}{P}\Big/\left(\frac{G\sqrt{T}}{P}\right)_{max} = \left(\frac{\delta+1}{2}\right)^{\frac{\delta+1}{2(\delta-1)}} M\left(1 + \frac{\delta-1}{2}M^2\right)^{-(\delta+1)/2(\delta-1)}$

and η represents the local blading efficiency evaluated between inlet and the downstream station. Then defining a downstream sonic condition where Me = 1.0 with corresponding values of outlet angle B^* and efficiency η^*, the theoretical value of B^* can be obtained from an equivalent inviscid flow model where $(\overline{rV}_T/R_{T_0})^*_t = C_V(1-\Sigma\delta^*/o)$ and C_V denotes the flow coefficient computed with an effective throat width equal to the geometric width less the sum of the displacement thicknesses, $\Sigma\delta^*$, of the boundary layers at the throat. Values of $(1-\Sigma\delta^*/o)\,C_V$ of the order of .985 appear typical of plane parallel flow cascade test data obtained for normal guide blade sections. Alternatively C_F^* (C_F at Me = 1.0) can be computed from specified input data of B^* and η^* if known.

For supersonic conditions we can assume the throat is continuously choked and the equation defining the supersonic outlet angle measured on the stream surface can then be written in the form:-

$$\text{Sin } B = C_F^* \frac{o}{s} M_e^{-1}\left(\frac{2}{\gamma+1} + \frac{\gamma-1}{\gamma+1}M_e^2\right)^{\gamma+1/2(\gamma-1)}\left(1-\frac{\gamma-1}{2}Me^2\left(\frac{1}{\eta}-1\right)\right)^{-\gamma/\gamma-1}$$

For subsonic flow conditions the outlet angle has to vary with outlet Mach number between the low speed (incompressible) value and the sonic value B^*. For a fixed stream surface geometry the inlet mass flow parameter can be expressed in the following form $(G\sqrt{T_{T_0}}/P_{T_0})/(G\sqrt{T_{T_0}}/P_{T_0})^* = F_{Me}C_F/C_F^*$. Then if we assume the inlet mass flow parameter to vary monotonically with outlet Mach number up to a maximum value when Me = 1.0 we require $C_F/C_F^* \leq F_e$ and $d(F_e C_F/C_F^*)\,d(Me) = 0$ when Me = 1.0, both of which can be satisfied by the relation $C_F/C_F^* = 1 + (C_{F_{LS}}C_{F^*}^{-1} - 1)(F_e^{-1}-1)(F_{e_{LS}}^{-1}-1)$. Here for convenience the low speed condition is defined at Me = 0.5, and the corresponding value of $(C_F)_{LS}$ can be evaluated from the equation for C_F given above using the known low speed section efficiency η_{LS}. Substituting the above expression for C_F into the general equation for sin B given initially will then give the required variation of sin B over the range $0.5 \leq Me \leq 1.0$.

The general form of the overall variation of outlet angle with outlet Mach number is illustrated diagrammatically in fig. 6 where the ratio: sin $B/(C_F^* o/s)$ is shown as a function of Me and η. The subsonic interpolation given above then provides one possible variation between (B) low speed (specified) and B^* (computed) with the important property that there is no gradient discontinuity at the sonic condition. By this procedure the inlet mass flow parameter along each individual streamtube will rise to a peak value with zero slope at Me = 1.0 and remain constant for further increases in outlet Mach number.

Corrections to these equations can be made fairly easily for annular flow conditions if we assume the stream surfaces to remain axi-symmetric within the blade passage. The annular streamtube normal depth $\delta r/(1+\sigma^2)^{1/2}$ will then vary across the throat and an integrated mean value should be used. At the same time the consequent variation of the radius of the stream surface across the runner blade throat will give a rise to a net change in relative total enthalpy from throat to outlet. This effect can then be incorporated into the equation above using a correction term derived in a similar manner to that given in (12).

It should finally be noted that for all procedures of the type discussed above, where the continuity condition is used to define the outlet flow angle in the supersonic flow regime, some assumption must be made concerning the shape of the streamline surfaces within the blade. Once a plausible surface geometry has been assumed, the non-uniqueness problem discussed in (13) is effectively eliminated although the use of an alternative surface geometry will of course lead to an equally consistent but different flow solution.

9.0 EFFICIENCY INTERPOLATION FOR CONVERGENT-DIVERGENT BLADING.

The following analysis of convergent-divergent blade profile loss is based on the assumption that the efficiency at some specific condition is known, either by calculation or from test data. For convenience in calculation this reference condition can be selected at the point where the expansion fan centred at the pressure side trailing edge just covers the complete suction surface. At this condition any further increase in the overall pressure ratio across the blade will not materially affect the local surface conditions and the outlet tangential velocity has reached its maximum value. For design calculations this fully loaded condition, numerically defined by values of the blade profile efficiency and the corresponding tangential velocity ratio, can preferably be obtained from a characteristic blade-to-blade solution together with the associated boundary layer parameters at exit. Once this reference limit load condition is known, the efficiencies at other conditions can be evaluated within the through-flow program using an interpolation procedure similar in type to that discussed below.

In Fig. 7 a typical set of cascade test data for a convergent-divergent blade is shown superimposed of a one-dimensional blade performance chart. Here the outlet tangential velocity ratio C_ω/C_{crit} is shown plotted as a function of the outlet isentropic Mach number for specified values of blade efficiency. The parameter C_ω/C_{crit} is directly derived from the supersonic outlet angle analysis discussed in the previous section, the tangential velocity ratio being given by:

$$C_\omega/C_{crit} = Me\cos B\sqrt{\frac{\gamma+1}{2}\left[1+\frac{\gamma-1}{2}M_e^2\right]^{-1/2}}$$

and C_{crit} denotes the critical acoustic velocity at the point where the local Mach number is unity. The typical test values of C_ω/C_{crit} are shown increasing up to a maximum value at the limit load condition which lies to the left-hand side of the loci of the peaks of the one dimensional curves. Over the region of constant C_ω/C_{crit}, one-dimensional continuity then implies that for a limit loaded blade there is a unique relation between blade efficiency and outlet Mach number for a given blade geometry.

Operation in the region to the right-hand side of this peak loci is associated with meridional Mach number Mm in excess of unity and this condition can only arise in situations where there is an associated divergence of the annular streamtube. Values of Mm just in excess of unity ($Mm \simeq 1.1$) can be established in cylindrical flow situations following expansion of the flow into the base region downstream of the trailing edge. Further increase in overall pressure ratio in this situation will then be accompanied by a continuous system of ring shocks (located at varying axial distances downstream of

the blade trailing edge) which are required to satisfy continuity and energy conditions along the streamtube. Under these conditions the preceding analysis has to be modified for computing downstream flow conditions, the flow process has to be examined in two stages - limited expansion down to the exit condition at the trailing edge followed by a separate analysis of the downstream flow situation. The absence of complete circumferential periodicity in linear cascade models prohibits the establishment of this type of flow situation which has been visualised in rotating cascade tests reported in (14). Due to the upstream influence of the downstream blade row in existing turbine situations it is doubtful whether meridional Mach numbers much in excess of unity can exist even in conditions where there is considerable divergence of the annular streamtube.

Typically the blade profile efficiency may be assumed constant in the low subsonic Mach number regime, this being consistent with normal convergent blading loss analysis. For convenience the point at which Mach number effects are introduced can be taken at a value of isentropic outlet Mach number $M_2' = .75$; this being approximately the same point at which compressibility effects first appear on curved-back convergent blading. The blade efficiency may then be assumed to drop sharply to a minimum value at $M_2' \simeq .95$, rise subsequently in the supersonic range to a maximum value $(\eta_p)_{max}$ and finally fall slightly to its specified limit load value $(\eta_p)_{LL}$. For outlet Mach numbers in excess of the limit load value, the unique relation implied by the one-dimensional continuity equation can be used up to the condition where the meridional Mach number just exceeds unity. The general form of this efficiency variation is shown diagrammatically in fig. 8 where suffices .75; .95; η_p max; LL are used to denote the corresponding values of the tangential velocity ratio. This form of loss variation is typical of convergent-divergent blading; the high loss at low supersonic flow conditions resulting from the high shock loss and the associated flow distortion just downstream of the throat in the internal divergent passage.

An interpolation procedure may then be based on a unique curve fit in the range: $(C_\omega/C_{crit})_{.95} \leq C_\omega/C_{crit} \leq (C_\omega/C_{crit})_{\eta_{pmax}}$ in the form $(\eta_p - \eta_{p_{min}})/\delta\eta_p$ as some function of $C_\omega - (C_\omega)_{.95} / (C_\omega)_{\eta_{pmax}} - (C_\omega)_{.95}$. Over the remaining segments of the efficiency curve simple second order interpolation equations can be used. Input data to the efficiency interpolation routine must then supply information to derive the following parameters:

(i) $\delta\eta_p$ - difference between the maximum efficiency and the minimum value (at $M_2 \simeq .95$). This parameter is largely a function of the internal passage divergence expressed geometrically by the internal area ratio defined in the upper diagram of fig. 8. Typically this efficiency debit is of the order of 8% for internal area ratios equivalent to a one-dimensional Mach number equal to 1.4.

(ii) $(C_\omega/C_{crit})_{\eta_{pmax}}$, $\eta_{p_{max}} - \eta_{p_{LL}}$:- both of these parameters can be correlated in terms of the int'l area ratio and the mean passage angle, θ, (Fig.8).

(iii) $(C_\omega/C_{crit})_{LL}$, $\eta_{p_{LL}}$:- evaluated by calculation.

For situations where considerable streamtube slope and diffusion are present, correction factors must be applied to the plane flow value of the limit load tangential velocity ratio.

10.0 EFFECT OF STREAMTUBE AREA VARIATION ON LOSS.

For subsonic flow conditions, fairly simple correction procedures can be derived to allow for the effect of streamtube height variations. A particularly simple method is available in conditions where the blade passage contraction ratio (10) is involved in the profile loss correlation. In this case the corrected loss can be evaluated from a standard correlation using an effective contraction ratio which incorporates the computed area variation of the annular streamtube across the blade passage. Alternatively use can be made of a loss correlation using a blade surface diffusion parameter such as that published in (15). The diffusion parameter corresponding to the predicted plane flow loss is first evaluated from this correlation and then adjusted to incorporate the effects of any stream tube area variation. The corrected loss can then be evaluated from the same diffusion loss correlation but now using the adjusted value of the surface diffusion parameter. Both of these procedures give very similar values of profile loss correction and are in good agreement with test values; published loss data for widely flared guide blade cascades being given in (16).

For flow conditions at high outlet Mach numbers, alternative procedures have to be employed in situations where the passage geometry is so modified as to change its mode of operation. The most serious problem is introduced on convergent blading with small passage contraction where the effect of streamtube divergence can be to effectively produce a convergent-divergent profile. At low supersonic outlet Mach numbers this can result in large increases in profile loss resulting from flow breakdown downstream of the effective throat which is displaced upstream away from its nominal plane flow position. Test data on high deflection blading tested in flared cascades has confirmed that this change in the mode of operation does actually take place. Within the limitations of a through flow procedure, using computing stations at blade inlet and outlet only, the precise location of the true throat can only be estimated by assuming some simple relation between passage width and streamtube height variation across the blade row. Once this value has been estimated, an equivalent internal area ratio may be computed and convergent-divergent loss procedures used to evaluate the blade performance at outlet conditions where the isentropic Mach number exceeds 0.75. For impulse type sections near to the root operating with considerable streamtube diffusion this procedure will predict considerable excess losses at sonic outlet conditions.

11.0 APPLICATION TO PART-LOAD CONDITIONS

For stage designs of the type illustrated in fig. 1, a streamline curvature technique of the form discussed above can only be applied over a relatively narrow band of operating conditions. At stage pressure ratios much lower than the nominal design value the flow characteristics within the stage are considerably modified; zones of reverse flow appearing first at the hub downstream of the runner blade and then, with a further reduction in stage pressure ratio, additionally at the tip within the inter-

space region between guide and runner. Once these zones of reverse flow become established the associated streamline flow pattern in the meridional plane is severely distorted with resulting slopes and curvatures of much higher order than the values existing under design conditions.

A typical stage power diagram is given in fig. 9 where a number of non-dimensional power/speed curves each at constant mass flow are illustrated. Thus at constant peripheral velocity the stage output power reduces with decreasing mass flow rate, is zero at some intermediate value of mass flow and reaches a maximum negative value at the zero flow condition. Data given in (17) and (18) state that three distinct types of flow regime can be distinguished each of which can be positively located within specific areas of the power speed diagram as shown in fig. 9. These three flow regimes are then defined by the following stage operating characteristics.

I - uniform streamline flow without hub or tip separation.

II - zone of reverse flow existing downstream of the runner blade. The flow at guide exit fills the annulus but there is considerable streamline distortion at the inlet to the runner blade which is operating with high negative values of incidence.

III - zone of reverse flow in the guide exit - runner inlet interspace as well as the reverse flow zone existing in II above. Severe streamline distortion exists at all points within the stage.

The streamline flow characteristics and reverse flow zones of flow regimes II and III above are illustrated diagrammatically in fig. 9.

In order to compute flow solutions in either of the two flow regimes II and III above, a procedure defining the radial extent of the hub and interspace recirculation zones must be included in the overall computation process. Data given in (17) and (18) suggest means by which the extent of each recirculating zone can be established but even then it is doubtful whether a full streamline curvature technique can be used to evaluate a solution. From analysis of turbine test data it is suggested (18) that flow conditions in regime II can be computed by assuming the tip axial velocity at runner exit to be invarient with change in flow rate. No specific means are given for determining the onset of hub separation but published data (19) indicates that this condition cannot be far removed from the point at which zero root reaction is obtained. For conditions in regime III the tip flow is controlled by the formation of an inlet shock system to the runner blading, the onset of this shock being taken (17) at the point at which the tip static pressure at inlet to the blade passage becomes equal to the total pressure at guide exit.

REFERENCES

1. Chung-Hua-Wu, Wolfenstein. Application of Radial Equilibrium Condition to Axial Flow Compressor and Turbine Design. NACA Report 955 (1950).

2. Smith, L.H. The Radial Equilibrium Equation of Turbomachinery. Trans. ASME. Journal Engineering Power. January, 1966.

3. Novak, C.A. Streamline Curvature Computing Procedures for Fluid Flow Problems. Trans. ASME Paper 66-WA/GT-3 1966.

4. Renaudin, A, Somm, E. Quasi-Three-Dimensional Flow in a Multi-stage Turbine Calculation and Experimental Verification.

5. Horlock, J.H., Marsh, H. The use of Averaged Flow Equations of Motion in Turbomachinery Aerodynamics. A.R.C. 34132 November, 1972.

6. Horlock, J.H., Marsh, H. Flow Models for Turbomachines. Journal Mech. Engg. SD Vol. 13(5) 1971.

7. Horlock, J.H. Approximate Equations for the Properties of Superheated Steam. Proc. Inst. Mech. Engg. 173(1951)

8. Horlock, J.H., Perkins, H.J. Annulus Wall Boundary Layers in Turbomachines. AGARDograph No.185 May, 1974.

9. Ainley, D.G., Mathieson, G.R. A Method of Performance Estimation for Axial-flow Turbines. N.G.T.E. Report R111

10. Craig, H.R.M., Cox, H.J.A. Performance Estimation of Axial-flow Turbines. Proc. Inst. Mech. Engg. 185 (1970/71).

11. Wilkinson, D.H. Stability, Convergence and Accuracy of Two-Dimensional Streamline Curvature Methods using Quasi-orthogonals. Proc. Inst. Mech. Engg. 184 (1969-70).

12. Traupel, W. Prediction of Flow Outlet Angle in Blade-rows with Conical Stream Surfaces. ASME 73-GT-32.

13. Perkins, H.J., Horlock, J.H. Computation of Flows in Turbomachines. International Symposium on Finite Element Methods in Flow Problems, University of Wales, Swansea, January, 1974.

14. Rhomberg, F. — Investigations into Rotating Blade Cascades for Transonic Flow. B.B. Review December, 1964.

15. Stewart, W.L. Whitney, W.J. Wong, R.Y. — A Study of Boundary Layer Characteristics of Turbomachine Blade Rows and their relation to Overall Blade Loss. Trans. ASME Journal Basic Engg. 83-D(1960)588.

16. Deich, M.E. et al. — A Study of a Sharply Divergent Annular Turbine Blade Row. Teploenergetika 1964(11).

17. Emin, O.N. Lysenko, G.N. — Investigating the Characteristics of a Stage of a Reaction Turbine in the region of Compressor-type Modes. Teploenergetika 1972(19)3.

18. Emin, O.N. Lysenko, G.N. — An approximate Method of Calculating the Characteristics of a Turbine Stage in the Region of Greatly Off-design Modes of Operation. Teploenergetika 1973 20(3).

19. Troyanovski, B.M. et al. — Designing Steam Turbine Last Stages. Teploenergetika 1970(17)2.

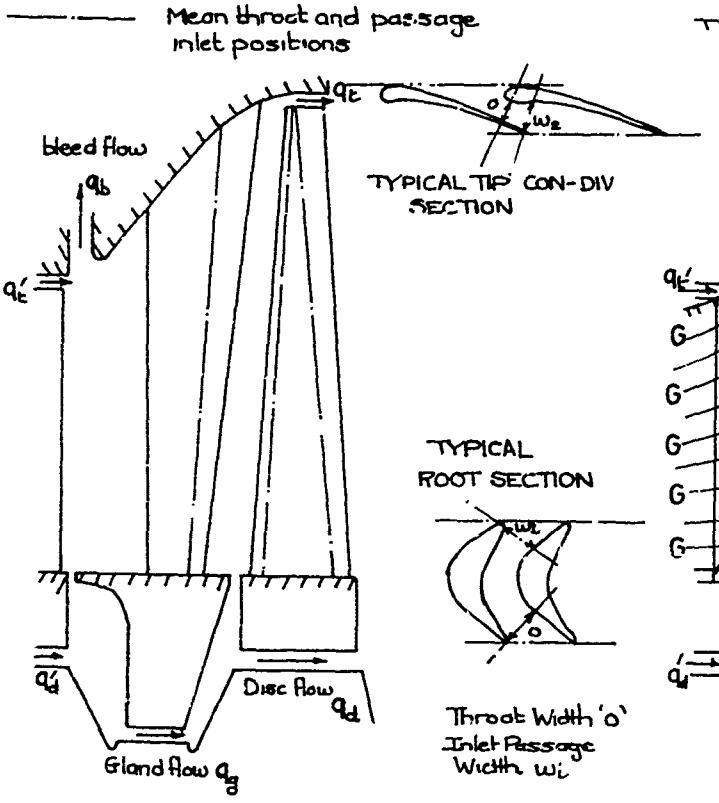

CROSS SECTION OF TYPICAL L.P. TURBINE STAGE

FIG 1

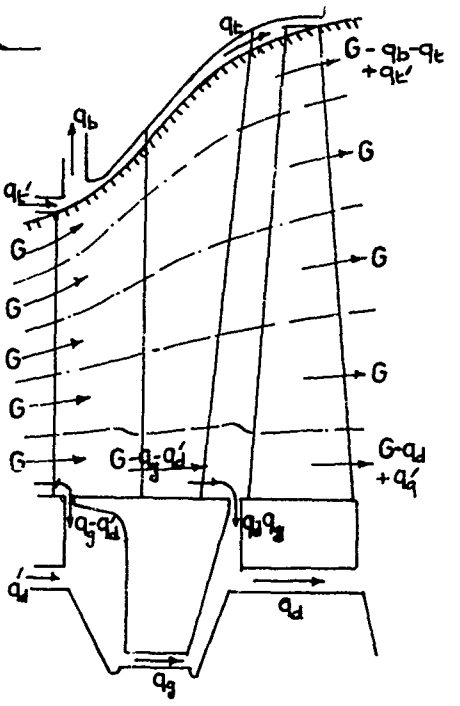

LOCAL DEBIT OF LEAKAGE FLOWS FROM MAIN THROUGH FLOW

FIG 2

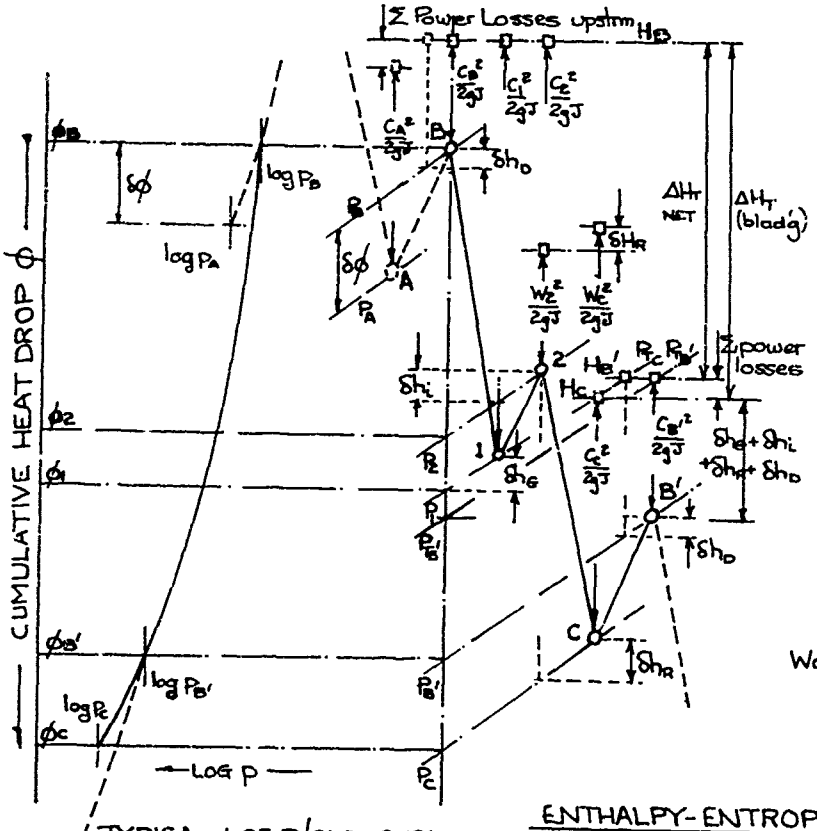

TYPICAL LOG P/CHD CURVE

FIG 3

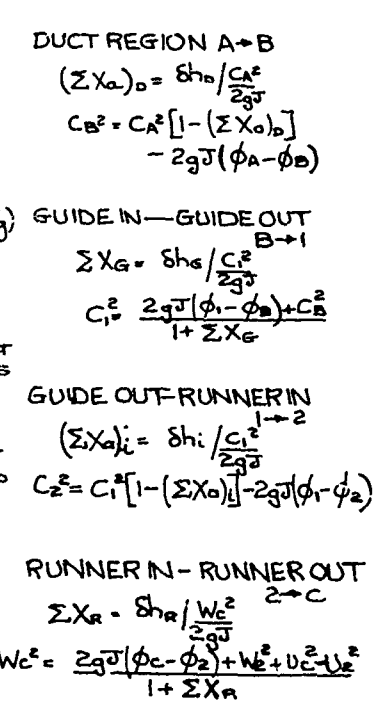

ENTHALPY-ENTROPY DIAGRAM ALONG STREAMLINE

FIG 4

DUCT REGION A→B

$$(\Sigma X_o)_D = \delta h_o / \frac{C_A^2}{2gJ}$$

$$C_B^2 = C_A^2\left[1-(\Sigma X_o)_D\right] - 2gJ(\phi_A - \phi_B)$$

GUIDE IN—GUIDE OUT B→1

$$\Sigma X_G = \delta h_G / \frac{C_1^2}{2gJ}$$

$$C_1^2 = \frac{2gJ(\phi_1 - \phi_B) + C_B^2}{1+\Sigma X_G}$$

GUIDE OUT-RUNNER IN 1→2

$$(\Sigma X_o)_i = \delta h_i / \frac{C_1^2}{2gJ}$$

$$C_2^2 = C_1^2\left[1-(\Sigma X_o)_i\right] - 2gJ(\phi_1 - \phi_2)$$

RUNNER IN - RUNNER OUT 2→C

$$\Sigma X_R = \delta h_R / \frac{W_C^2}{2gJ}$$

$$W_C^2 = \frac{2gJ(\phi_C - \phi_2) + W_2^2 + U_C^2 - U_2^2}{1+\Sigma X_R}$$

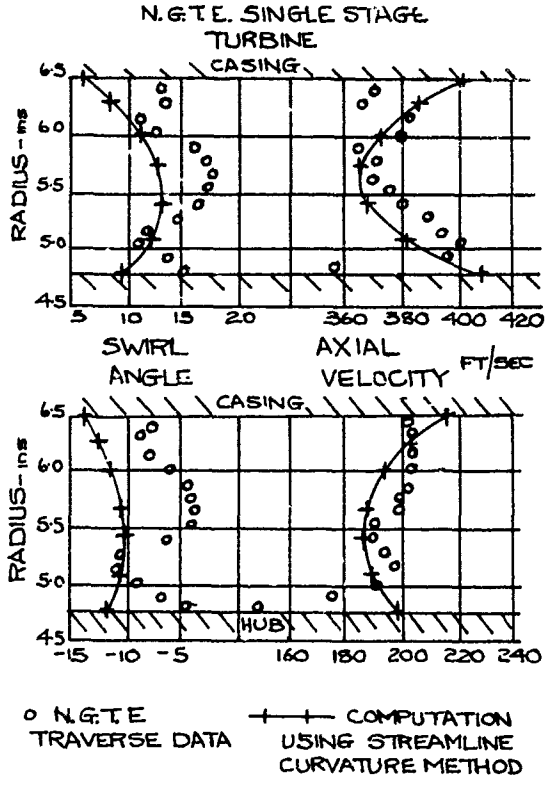

COMPARISON OF MEASURED AND CALCULATED DATA FIG 5

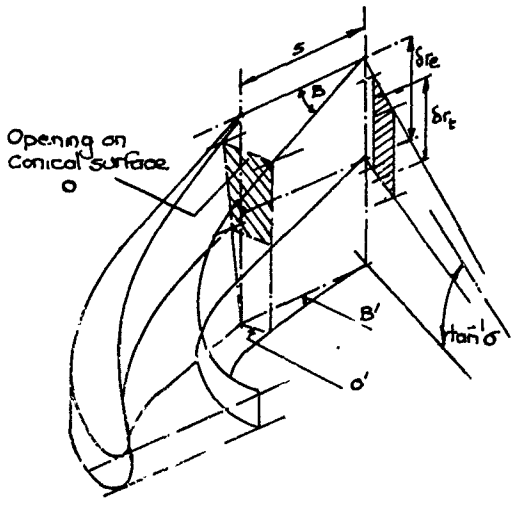

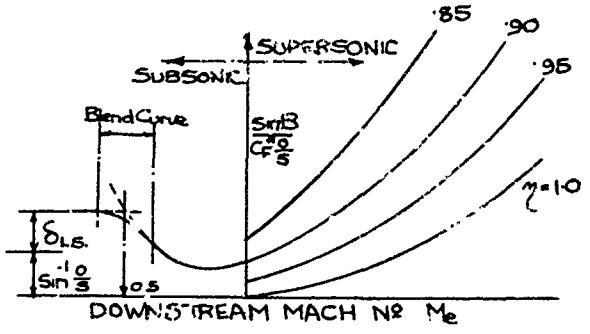

MACH Nº EFFECTS ON DEVIATION FIG 6

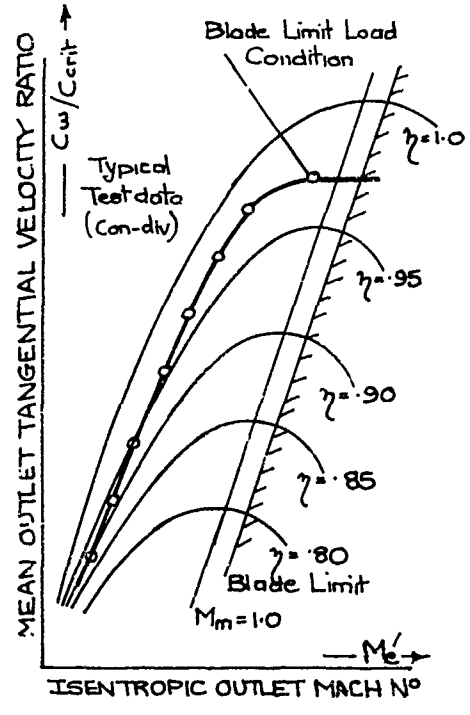

ONE-DIMENSIONAL SUPERSONIC BLADE PERFORMANCE CHART FIG 7

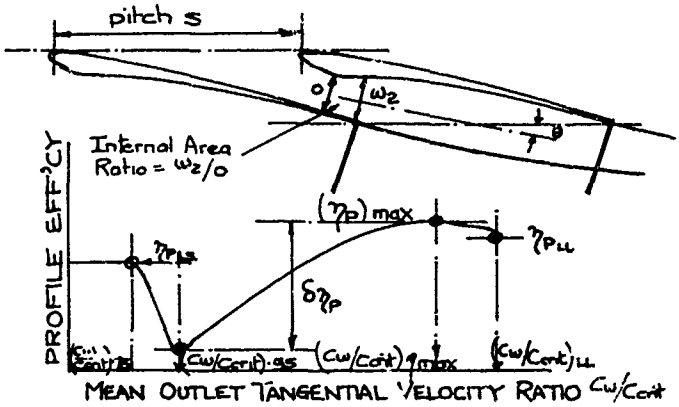

TYPICAL VARIATION OF PROFILE EFFICIENCY WITH MEAN OUTLET TANGENTIAL VELOCITY RATIO FIG 8

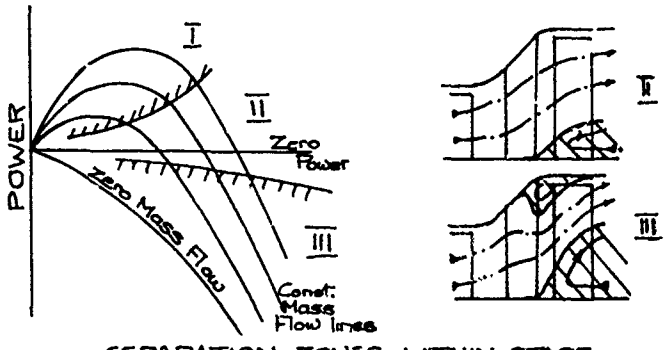

SEPARATION ZONES WITHIN STAGE UNDER PART-LOAD OPERATION FIG 9

COMMENTS

Comments by R.Lewis, University of Newcastle, UK

This paper and several others have brought out the importance of paying attention in future to the intensity of fluid processes which occur within the actual blade row. I would make particular mention that most of the rapid density changes occur between leading and trailing edges although their effects both upstream and downstream may be major, as illustrated by the work of Hawthorne and Kingrose and later by Lewis and Horlock.

My second point in relation to the present paper is the strong casing flare and radial flows needed to accommodate density changes. Has the author incorporated design rules to correct S1 outlet angles for these strong sweep effects? In my experience swirl velocities, based upon two-dimensional cascade tests, could be up to 10% in error. The corrections originally proposed by Smith and Yeh have proved to work well for highly swept high deflection turbine cascades tested in my own laboratories in both parallel wall swept cascades and conical flow annular cascades.

Authors' response:

As far as the first point is concerned, if you are pressing for much more complicated solutions then as far as accuracy is concerned I can only agree with you that this kind of effect should be taken into account. As far as doing design work, I am absolutely horrified that people would contemplate using highly complicated blade to blade programs which require a couple of weeks to sort out the data before getting an answer. The comparison with data that we have got does not suggest that we compute massive errors. We evaluate the kind of situation that tends to be produced in the turbine, and we can in fact predict the efficiency of our turbines. For the second point, you are asking if we are taking into account the flaring in the design of our blade profiles. We would check the effect of streamline shape for a particular profile design, but we would hope that there is such an acceleration through the guide blade that the effect of slope or diffusion terms on the streamline itself would not introduce serious diffusion effects on the blade surface. The blades we are talking about have got an inlet angle of 90° and an outlet angle of around 15°. There is thus a very large acceleration across the blade, and providing that the profile is properly designed in the two-dimensional sense, i.e. accelerates uniformly from inlet to outlet, then local diffusion regions even in the presence of streamline diffusion can be avoided. The other problem that I mentioned earlier is that in a design of this sort, the blade and stator combination has to provide a range of duties. We are not just designing a blade but an LP stage operating over a range of different volume flows at exit. This leads to different streamline patterns, and designing a profile for just one streamline may not be particularly advantageous.

Comment

Concerning the radial flow part of the section, I have done cascade tests with cascade swept to 45° with heavy loading. I find that there is a considerable reduction in the turning property of the fluid.

Authors' response:

We are using Traupel's method which corrects for that effect. The method gives around 6° negative deviation for a convergent blade for a 45° flare. This arises from the variation of radius across the throat and from the change in slope and streamtube height between throat and the trailing edge.

Comment by C.Sieverding, von Kármán Institute, Belgium

You defined as limit loading condition the one for which the trailing edge shock for one blade hits the trailing edge of the next one. I would suggest that the limit loading is reached when the trailing edge shock falls behind the reattachment point which is behind the trailing edge of the other blade.

Authors' response:

I accept this point, But when you have to take into account the radial flow effects on deviation, this also will affect the computation of the tangential velocity distributions. What I suggest is that we drop this definition and simply use the maximum value of C_w/C_{crit} which comes out of the deviation equation which includes all the radial flow effects. You can differentiate the equation and find the maximum value within the through-flow program. Otherwise, you will get an inconsistency between specifying one set of two-dimensional conditions and evaluating the deviation from another set of equations.

Comment by J.Dunham, N.G.T.E., UK

What radial distribution of losses was assumed in calculating Figure 5? Were the secondary losses uniformly distributed across the blade height, or concentrated towards the hub and tip as outlined in Section 3.1?

Authors' response:

Solutions quoted assumed constant secondary loss across the blade height, profile losses are evaluated locally at each radius. General method of concentrating secondary losses at root and tip would not be applied since aspect ratio of the blading is less than 2.0. Parabolic distributions of secondary loss were in fact introduced which slightly improved correlation between tests and calculated distributions, but did not of course predict the overturning effects at root and tip.

DESIGN OF TURBINE, USING DISTRIBUTED OR AVERAGE LOSSES; EFFECT OF BLOWING

D. K. Mukherjee
Gas Turbine Department
Brown Boveri/Baden
Switzerland

SUMMARY

The design of a multi-stage turbine begins with one-dimensional calculations. Flow field computations which then follow are invaluable as they allow to determine velocity triangles at different radii and to design the blades. In these calculations, aerodynamic losses and outlet angle deviations due to secondary and tip clearance flow, as well as the influence of coolant on the main stream expansion are taken into account.

NOMENCLATURE

A	area
C	specific heat
C	absolute velocity
c	chord length
e	proper work by the fluid
h	blade height, enthalpy
K	kinetic energy
$\dot{m}$	mass flow rate
n	polytropic exponent
o	throat
p	pressure
$\dot{q}$	heat flow to coolant
R	gas constant
r	radius
s	entropy
s	spacing
T	temperature
t	trailing edge thickness
u	circumferential speed
v	specific volume
W	relative velocity
y*	critical distance from boundary wall for secondary loss
y**	critical distance from boundary wall for tip clearance loss
α, α'	absolute flow angle measured from tangential direction
α	coolant blowing angle
β, β'	relative flow angle measured from tangential direction
$\Delta\beta$	angular deviation
Δh	enthalpy drop
ε	slope angle of meridional stream line
ζ	loss coefficient
η	polytropic efficiency
γ	isentropic exponent
π	pressure ratio
τ	tip clearance

Subscripts

0	two-dimensional
1	inlet to blade row
2	outlet from blade row
3	inlet to next blade row
c	coolant
eff.	effective
i	inlet to turbine
m	measured value
n	meridional component
o	turbine outlet
p	profile
p	pressure side
r	radial
r	rotor
s	secondary
s	suction surface
s	stator
τ	tip clearance
t	trailing edge

y just after trailing edge
* stagnation
- mean value

INTRODUCTION.

The design of a multi-stage turbine starts with a one-dimensional calculation at reference radii. For this purpose stage characteristics are used, these data are usually taken from an experimental turbine for a particular blading. However, aspect ratio, channel end wall inclination, Mach number, Reynolds number etc. may differ to that of the experimental turbine. Thus, although the load coefficient at reference radii is same, the radial distribution and therefore the turbine performance may be quite different. In a turbine with high inlet temperature certain blade rows are cooled. The effect of coolant from a blade row is of course considered in the one-dimensional calculation by modifying the inlet data of the following stage. In case the coolant is discharged from a vane, a part of this is accounted for at the stage inlet and the rest at the outlet.

Once the main dimensions of the hot gas channel, and, as a first approximation the number of blades and chord length in each row have been fixed, a radial equilibrium calculation is started. The three-dimensional flow in a multi-stage turbine is of course very complex. The energy dissipation and flow angle vary along the circumference and also spanwise. Our calculation model is however simple as it is axissymmetric, thus neglecting all variations of data along the circumference. The coolant, usually a part of compressor air, is blown out from blades or end walls, expanding in the turbine from a comparatively low pressure and temperature, fig. 1. The exhaust coolant velocity is usually different to that of main stream. There is a spanwise distribution of coolant mass flow and thus a radial variation of mixing loss and outlet angle. The aerodynamic losses - profile and secondary losses - vary spanwise as well. Tip clearance losses and losses due to uneven rotor or casing boundaries are regional and should be considered accordingly. These losses have further an effect on the outlet angle of a row.

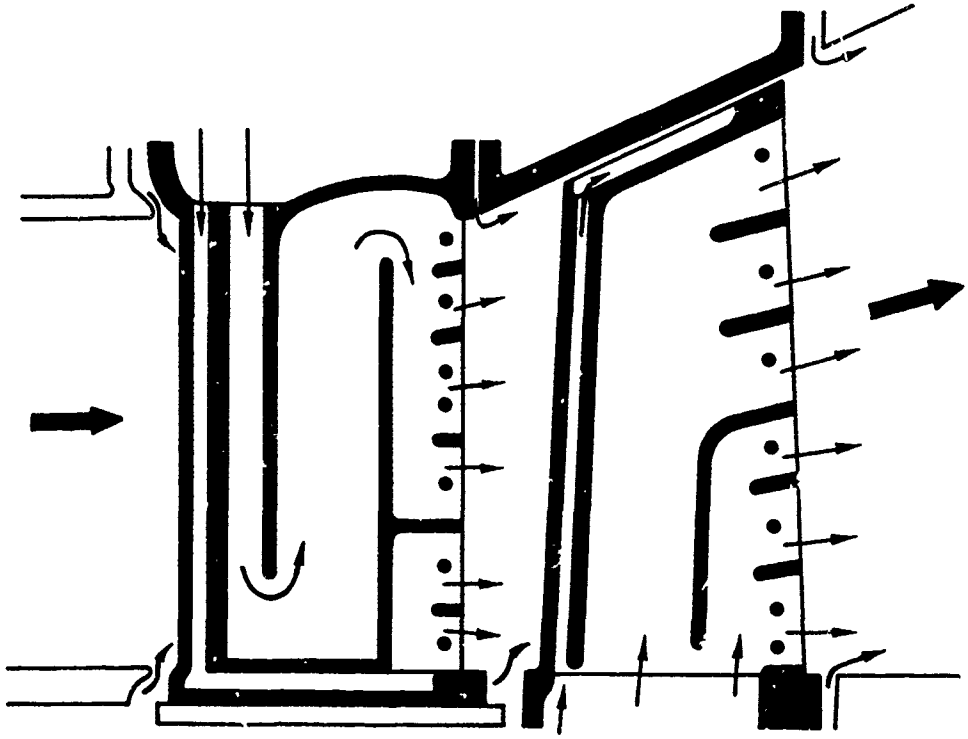

FIG. 1 - FIRST STAGE OF A TURBINE SHOWING COOLING SYSTEM AND SECONDARY AIR FLOWING INTO MAIN STREAM CHANNEL

AERODYNAMIC LOSSES

The primary loss in a two-dimensional flow around the blade profile consists of friction losses, trailing edge losses and after mixing losses. These have been given in several literatures [1, 2, 3, 4, 5]. In [1] these losses are determined as a function of inlet angle (β_{10}), outlet angle (β_{20}), solidity (c/s) and trailing edge thickness t. In case of coolant exhausting at the trailing edge, its thickness is modified to an effective value in a simplified calculation. The actual flow behaviour is probably quite complicated due to the lower pressure and wake, [3, 4, 5]. The influence of Mach number, Reynolds number, surface roughness on profile losses should of course be considered.

Using data of [1] one can feed a spanwise distribution of these losses into the radial equilibrium calculation. Several boundary layer calculation programs are available [6, 7] which calculate profile losses. This calculation is of course done to design an optimum profile for a given inlet and outlet angle.

Theoretical and experimental investigations have been published in [8] on secondary losses. These interesting lecture series demonstrated the complexity of secondary flow [9]. In order to feed a spanwise distribution of secondary loss in a flow field calculation, it is necessary to know the critical aspect ratio $(h/c)_{crit}$, [10, 11, 12]. Based on data of [11] and [13] Traupel suggests for critical blade height:

$$(h/s)_{crit} = 7...10\sqrt{\zeta_p}$$

This formula (lower value for reaction blading) is being used by us as it agrees with results of our experimental turbine. Thus the distance y* from the boundary walls from where the secondary loss no more exists is known. In choosing the chord length of a blade, every effort is made to achieve an aspect ratio higher than the critical value. Systematic tests in an experimental turbine allow us to correlate the mean secondary loss as a function of load coefficient and blade geometry. In absence of similar test data, mean secondary loss data of [1, 14, 15] are suggested. Instead of a spanwise distribution according to [10], a simple parabolic distribution whose mean agrees to our experimental data is considered. The profile loss curve is tangent to this parabola at y*. In case of rotor or casing walls having a high angle of inclination, extra secondary losses are given in [16]. Data on tip clearance losses for shrouded and nonshrouded blades are available in [1, 17, 18]. The position of the tip clearance vortex, and thus the critical distance y** from the end wall up to where the radial distribution of tip clearance loss exists, is known from [18]. A radial distribution similar to [18] whose average over the blade span satisfy our experimental data is used. Extra losses like end wall friction loss and those due to uneven boundary walls etc. are given in [1] and should be used for boundary stream tubes.

OUTLET ANGLE

When the blade geometry of a row is known, the outlet angle along the conical stream surface at different radii for each row is required. This is determined according to [19] in which of course a few assumptions are made. In some instances, like very small outlet angle or large pitch this method or those given by [1, 20] may not be accurate enough. These integral methods are not universal. If possible it is better to check the outlet angles according to more basic calculating methods like [21].

The radial distribution of the outlet angle due to secondary flow superimposed on the spanwise two-dimensional outlet angle is given by [10, 18]. In most of the literatures the change in outlet angle due to secondary flow and tip clearance, as a mean value over blade height, has been investigated. The experimental results in the Institut für thermische Turbomaschinen, ETH Zürich, [13] and Traupels correlation for a mean outlet angle correction due to secondary and tip clearance flow are used. A radial distribution at the end wall regions due to secondary flow and tip clearance is superimposed on the calculated angles due to two-dimensional flow to satisfy the mean correction. In case the flow outlet angles are known from a radial equilibrium calculation the blade can be designed.

INFLUENCE OF COOLING AIR ON MAIN STREAM PROPERTIES

The effect of secondary air, blown out in the main stream channel, should be considered in the axis-symmetric radial equilibrium calculation. The expansion of main stream is not adiabatic. The coolant is usually ejected in the form of discrete jets from holes or slots, fig. 2. We assume, similar to [22], that, in case of pressure surface blowing the coolant further expands. However if the coolant is ejected on the suction surface it has to be pumped to the pressure existing at the trailing edge. However the coolant exhausting from trailing edge of a blade row or from boundary walls of intermediate passages between the blades is assumed to have mixed completely with the main stream up to the inlet of next row. The coolant from hub or casing is mixed only in the boundary stream tubes. A spanwise distribution of coolant and its effect on the main stream properties is thus considered. The calculating stations being the trailing edge of a blade row and inlet to next row. In the appendix, the effect of coolant on the main stream data is analysed.

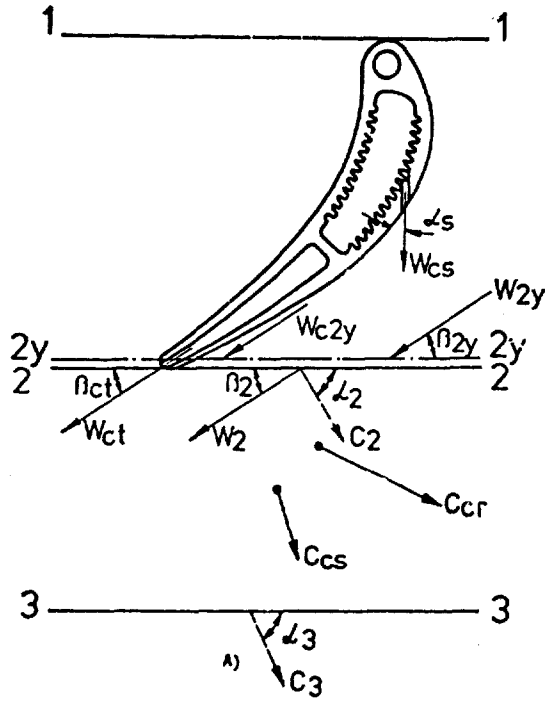

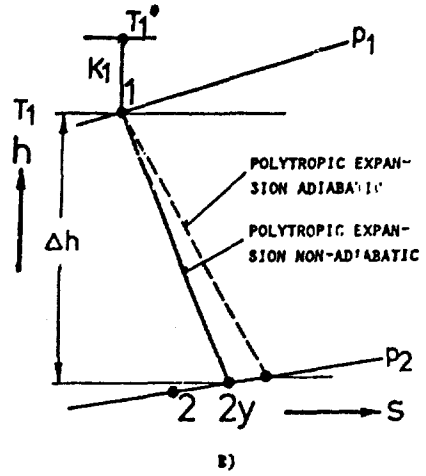

FIG. 2 - A) COOLANT FROM BLADE SURFACE, TRAILING EDGE AND BOUNDARY WALLS WITH MAIN STREAM AT DIFFERENT STATIONS, S. APPENDIX

B) MAIN STREAM EXPANSION INFLUENCED BY COOLING AIR IN h-s DIAGRAM

RADIAL EQUILIBRIUM COMPUTATION

A computer program based on the stream line curvature approach is used for gas turbine design. The calculations of the flow field consider, primarily, the conservation laws of momentum and mass. In addition the energy equation in the form often used in turbomachinery and the equations defining the fluid properties are required.

For high temperature gas turbine design the computing system has been further developed to handle coolant flow. The influence of coolant is considered in the computing procedure by using secondary programs together with the main radial equilibrium program. The following secondary programs, (subroutines to the main program), are used, s. fig. 3.

A.: Coolant mass flow and radial distribution of coolant from a blade row

B.: Change in aero-thermodynamic data at outlet of a row (s. Appendix)

C1): Mean aerodynamic loss coefficient and spanwise outlet angle distribution (due to varying pitch and blade stagger) including an average angle deviation due to secondary and tip clearance flow, i.e.:

$$\zeta(r) = \bar{\zeta}; \qquad \beta_2(r) = \beta_{20}(r) + \overline{\Delta\beta}_{s,\tau}$$

2): Radial aerodynamic loss distribution and outlet angle distribution due to secondary and tip clearance flow

$$\zeta(r) = \zeta_p(r) + \zeta_{s,\tau}(r); \quad \beta_2(r) = \beta_{20}(r) + \Delta\beta_{s,\tau}(r)$$

To save computing time, a preliminary calculation is conducted in which the total mass flow $\dot{m}_o$ at the last computing station in the exhaust diffusor is taken as inlet mass flow $\dot{m}_i$. An inlet temperature called "mixed flow inlet temperature $\bar{T}_i$ corresponding to the mean proper wirk $\bar{e}$ (s. Appendix and fig. 4) is used. These data are known from the one-dimensional calculation. The channel annulus is modified at each station to achieve minimum change in boundary wall curvatures and correct inlet velocity. The computing stations are: outlet of each row, a few stations in the axissymmetric part of inlet and in the exhaust diffusor. The outlet angles $\beta_{20}(r)$ at each row are assumed and supplied to program C1 as input. A constant polytropic efficiency calculated from mixed flow inlet temperature $\bar{T}_i$ and mean proper work $\bar{e}$ is used, s. fig. 4. The radial equilibrium calculation of the so-called "mixed turbine" is then conducted to satisfy the outlet pressure and mass flow for a given inlet pressure. The consistent mean values of the fluid at any station according to Dzung [23] are of course decisive. This computation allows to find suitable outlet angle distribution satisfying degree of reaction in each stage, proper inlet flow condition to exhaust diffusor etc.. Although this computation is simplified, the intermediate pressures of this calculation could be used to determine the one-dimensional expansion of the main stream and coolant, s. fig. 4. For this purpose, the annulus

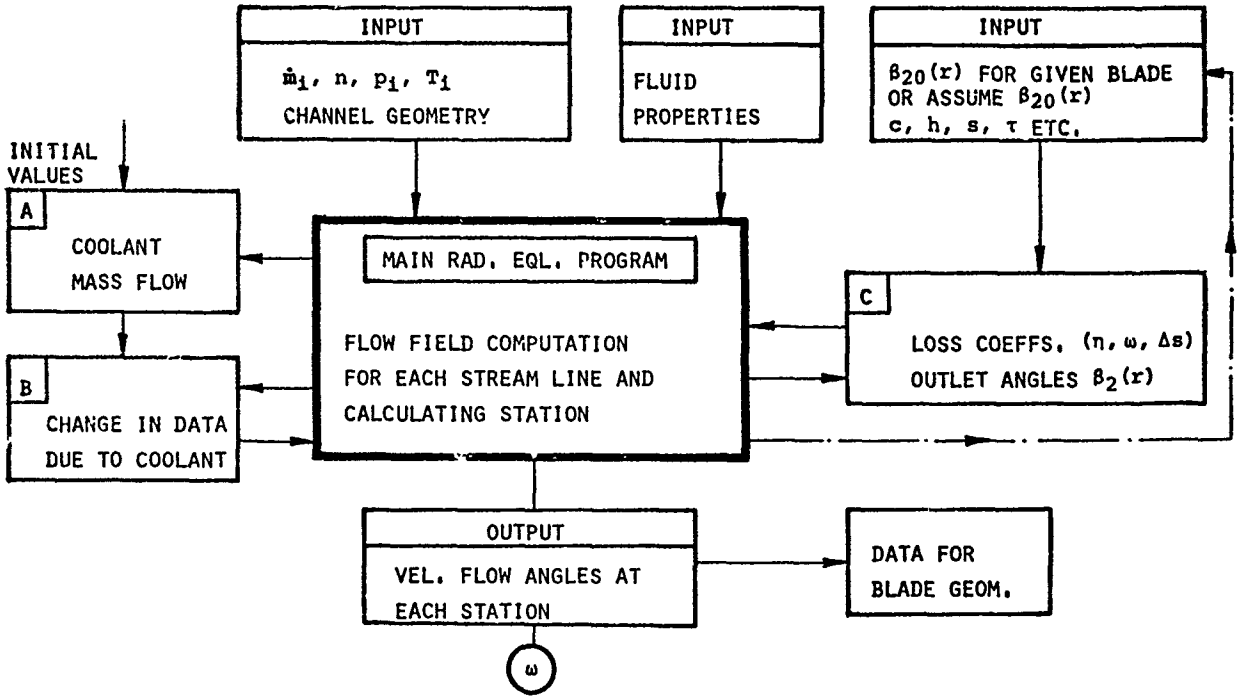

FIG. 3 - PROGRAM-SYSTEM FOR TURBINE FLOW FIELD COMPUTATION

COMPUTER PROGRAM A: CALCULATES COOLANT MASS FLOW AND ITS RADIAL DISTRIBUTION FROM A ROW

COMPUTER PROGRAM B: CALCULATES CHANGE IN AERO-THERMODYNAMIC DATA AT OUTLET OF A ROW, S. APPENDIX

COMPUTER PROGRAM C: CALCULATES AERODYNAMIC LOSS COEFFS. AND OUTLET ANGLES DUE TO SECONDARY AND TIP CLEARANCE FLOW

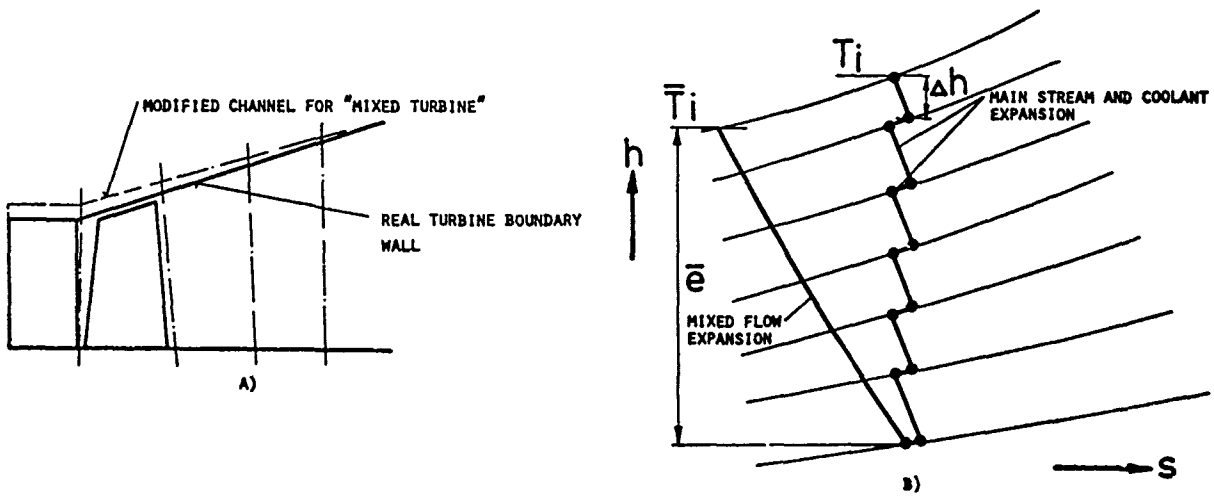

FIG. 4 - A) MODIFIED TURBINE CHANNEL FOR PRELIMINARY MIXED FLOW CALCULATIONS AND REAL CHANNEL

B) EXPANSION OF MAIN STREAM AND COOLANT IN h-s DIAGRAM FOR REAL TURBINE AND FOR AN EQUIVALENT MIXED FLOW EXPANSION

may even be subdivided into a number of concentric channels as suggested by Traupel and distributed loss coefficients and regional losses can be considered to determine power output of the turbine.

A second flow field computation is then started with the real annulus, real inlet flow, assumed coolant flow for different blade rows and with the main stream inlet temperature and pressure, corresponding to the previous calculation. The aerodynamic losses and outlet angles are determined for each row in program C1, based on the previous calculation. Recently spanwise distribution of losses and spanwise modification in outlet angle due to three-dimensional flow is being considered in program C2. The coolant mass flow in each row is calculated in Program A based on the main stream data of the row. The modified main stream data at the computing stations from program B are then considered in the flow field computation.

CALCULATION AND COMPARISON WITH EXPERIMENT

For a five stage low temperature, low Mach number experimental turbine, examples of radial equilibrium calculations are presented below. These have been done using

a) . mean aerodynamic losses $\bar{\zeta}$, s. fig. 5 (according to program C1)

. spanwise outlet angle variation along the conical stream surface $\beta_{20}(r)$ according to (1) Traupel [19]
(2) $\beta_{20}(r) = \arcsin o/s$, fig. 5
with a constant additional deviation due to secondary and tip clearance flow, (program C1)

b) . spanwise distribution of aerodynamic losses and outlet angle influence by secondary flow and tip clearance, (according to program C2) with $\beta_{20}(r) = \arcsin o/s$, fig. 5

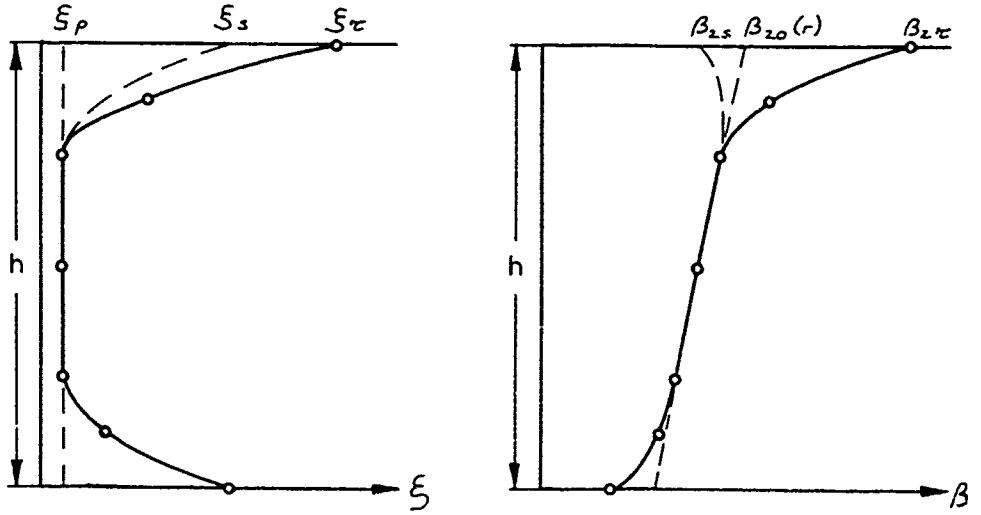

FIG. 5 - LOSS AND OUTLET ANGLE DISTRIBUTION

The computations of the flow field have been conducted for a turbine blade geometry with two different clearances

$$\tau/c = 0.015 \text{ and } 0.062$$

The stages are repeating stages with a degree of reaction 0,5 and cylindrical blades and vanes. The outlet angles of the blades vary from hub to casing approximately 15° to 25° radially. As this turbine was measured extensively the results of the calculations can be compared with the test data. The measurements consist of mass flow (which remains unchanged from inlet to outlet), inlet pressure and temperature. At turbine outlet, approximately 0,5c distant from the last row, pressure, velocity and angles with five hole probes have been taken. These probes were traveresed radially. Tables below show the results of the calculations compared with the experimental data. As shown in the tables 1 and 2 the calculated data of a(2) with $\beta_{20}(r) = \arcsin o/s$ agree well with measured mass flow and pressure ratio. In the through flow calculation of b (tables 1 and 2) with spanwise distribution the basic angles $\beta_{20}(r)$ were therefore taken from a(2).

Figs. 6 and 7 show the calculated angle and velocity distributions for the example a(2), compared with the measured data for blades with low tip clearance $\tau/c = 0.015$. Similar calculation for blades with high tip clearance $\tau/c = 0.062$ and experimental data are shown in figs. 8 and 9. For the high tip clearance blading with loss and angle distribution, (example b), figs. 10 and 11 show the calculated and measured values. Better agreement in the calculated angle and velocity distribution with measurements compared to the data of a(2) can be seen. The computation with distributed losses allows a better

agreement in the end wall regions. However, the strong gradient in loss and outlet angle input probably causes numerical problems in the radial equilibrium calculations which creates a wavy character of the plotted results in the mid-span region.

TABLE 1

Relative clearance $\tau/c = 0.015$

	Calculation a(1)	Calculation a(2)	Calculation b	Measurement
$\dot{m}/\dot{m}_m$	1.2168	1.002	0.9420	1.000
π^*/π^*_m	1.0182	0,9998	0.9881	1.000

TABLE 2

Relative clearance $\tau/c = 0.062$

	Calculation a(2)	Calculation b	Measurement
$\dot{m}/\dot{m}_m$	0.9877	0.9868	1.000
π^*/π^*_m	0.9993	0.9921	1.000

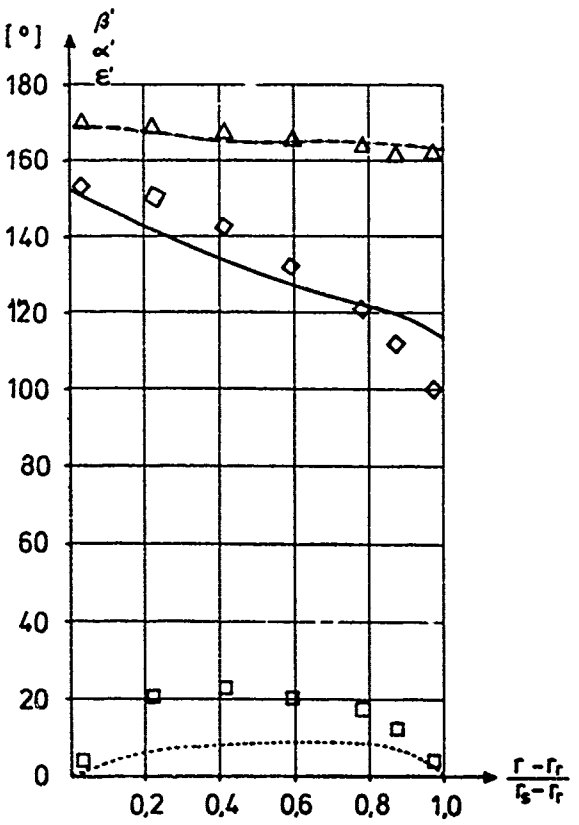

FIG. 6 - CALCULATED FLOW ANGLES COMPARED WITH MEASUREMENT FOR EXAMPLE a(2) WITH REL. CLEARANCE 0,015

Measured		Calculated
△	β'	----
◇	α'	——
□	ε	.....

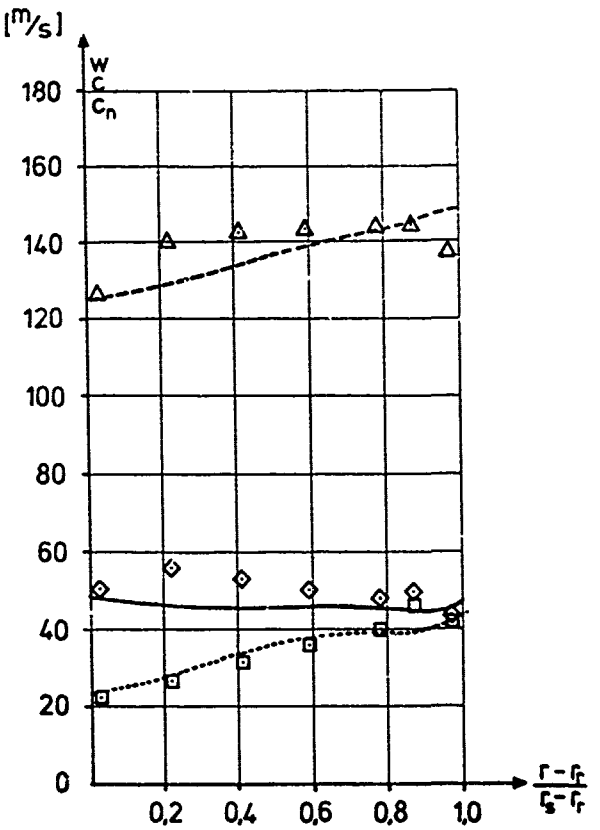

FIG. 7 - CALCULATED FLOW VELOCITIES COMPARED WITH MEASURED VALUES FOR EXAMPLE a(2) WITH REL. CLEARANCE 0,015

Measured		Calculated
△	w	----
◇	c	——
□	c_n	.....

FIG. 8

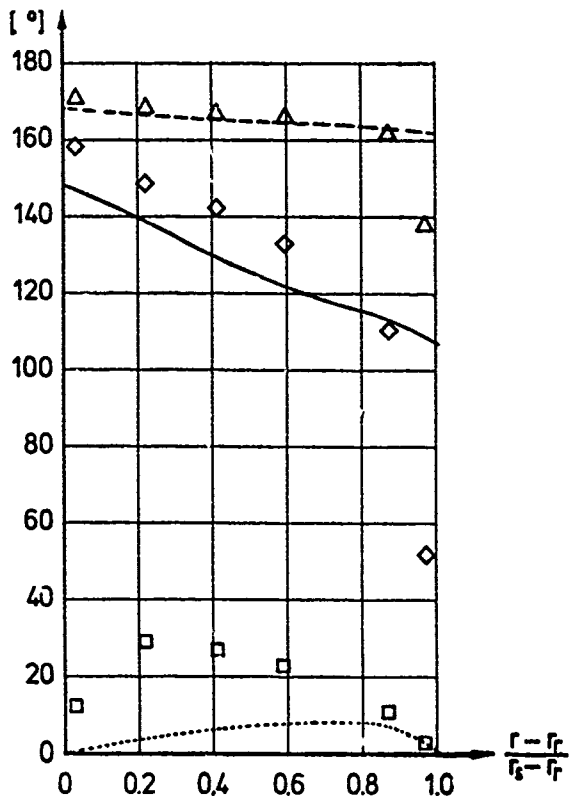

FIG. 9

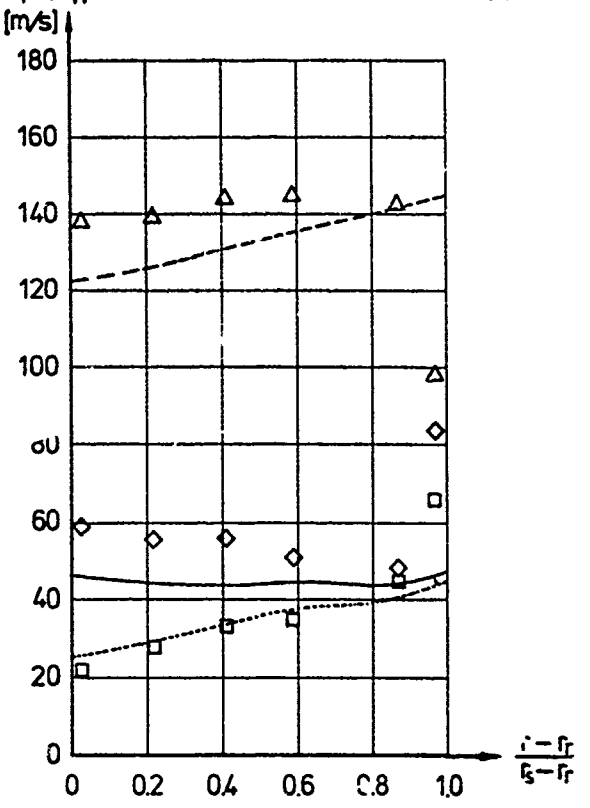

FIG. 10

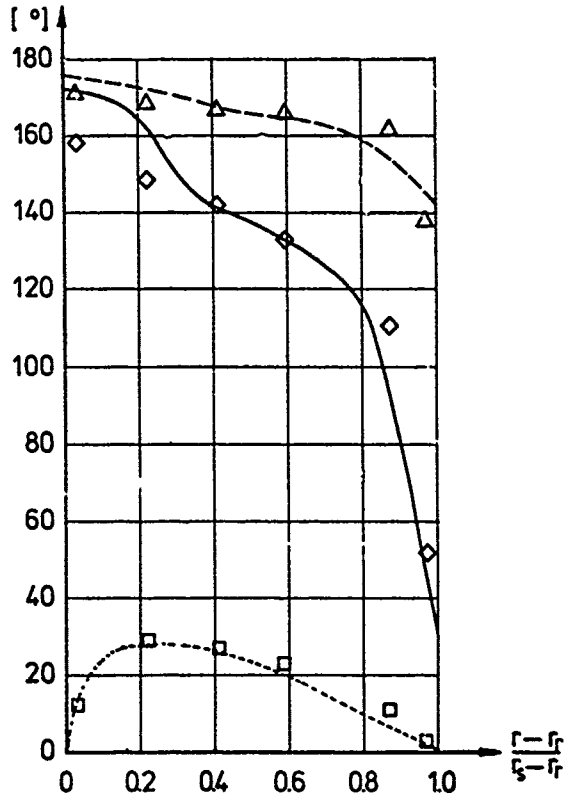

FIG. 11

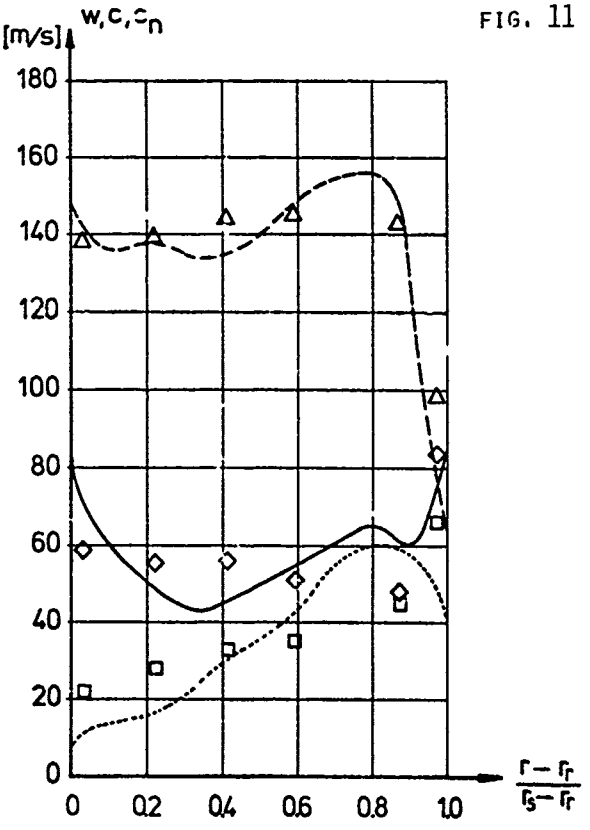

FIG. 8 - CALC. a(2); FIG. 10 - CALC. b
CALCULATED AND MEASURED FLOW ANGLES
WITH REL. CLEARANCE 0,062

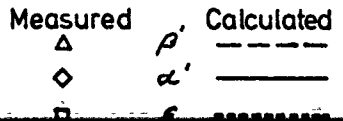

FIG. 9 - CALC. a(2); FIG. 11 - CALC. b
CALCULATED AND MEASURED FLOW VELOCITIES
WITH REL. CLEARANCE 0,062

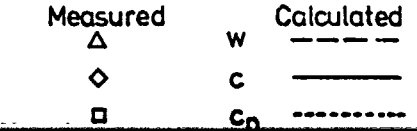

BLADE DESIGN

Once the radial equilibrium calculation ends to satisfaction, the blade profiles are developed along the conical stream surface to achieve optimal aerodynamic behaviour. Fig. 12 shows the calculation steps involved. The blade development starts with an assumed optimum velocity distribution; the profiles are then modified at the leading and trailing edge manually. Further profile modification to achieve required outlet angle is conducted at the CAD-station (computet aided design procedure). For cooled blades the coolant passages are designed and the hollow blade geometry is used for further investigation. The mechanical, thermal and vibrating stresses (natural frequency) have to be investigated to achieve desired blade life.

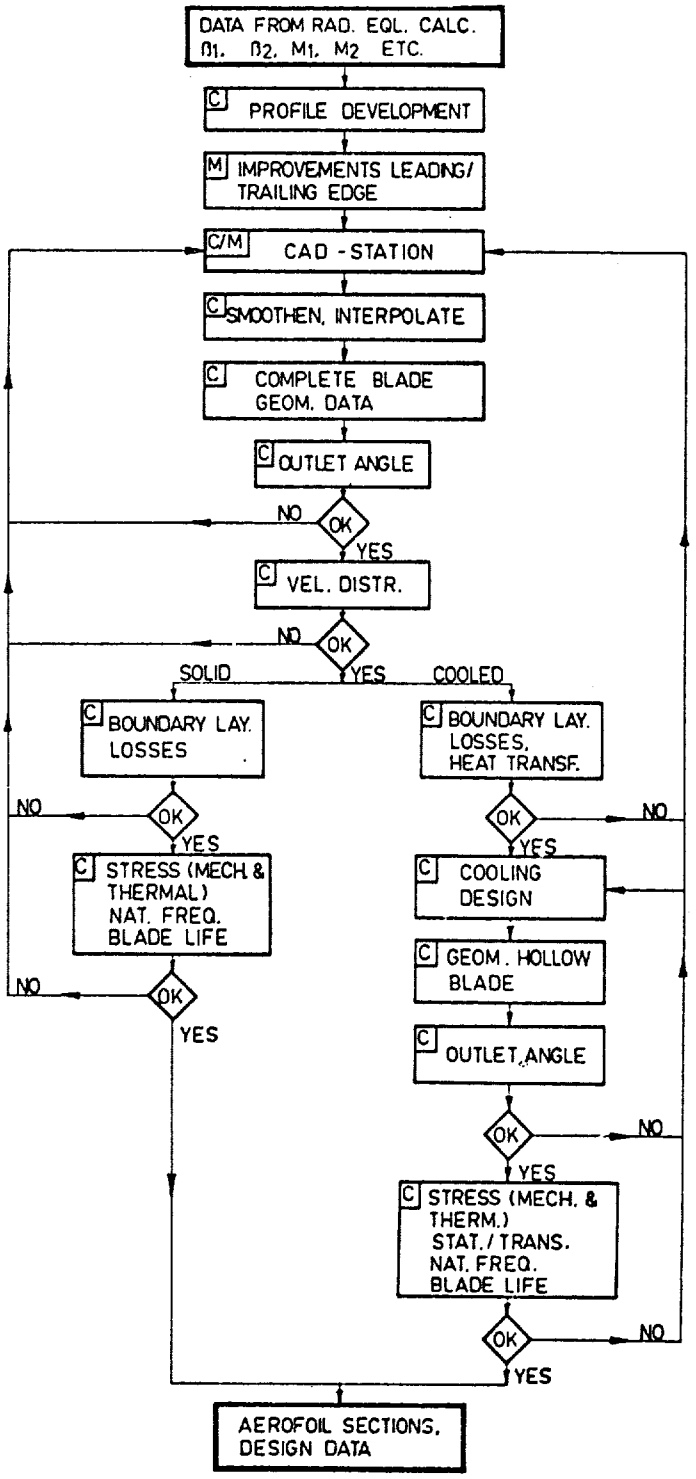

FIG. 12 - CALCULATION STEPS TO DEVELOP BLADE PROFILES FOR GIVEN FLOW CONDITIONS
C: COMPUTER PROGRAMS M: MANUAL STEP

CONCLUSION

In the radial equilibrium calculation the influence of coolant blown into main stream are considered. The aerodynamic losses and outlet angle deviations, even radially distributed, can be considered. For quick computation of the flow field, a mean loss coefficient and a mean angular deviation can be used as well. Stronger emphasis should be given in determining the outlet angles of a blade row along the meridional planes for two-dimensional flow by using exact solutions or by determining these data from experiment.

REFERENCES

1. Traupel, W.: Thermische Turbomaschinen, Bd. I Springer Verlag, Berlin, Heidelberg, New York, 1966.

2. Prust, H.W.: Boundary Layer Losses, Turbine Design and Application, Vol. 2 Edited by A.J. Glassman, Lewis Research Center, NASA SP-290, 1973.

3. Dzung, L.S.: Schaufelgitter mit dicker Hinterkante, Technical Note BBC, (unpublished)

4. Dibelius, G.: Mischverluste insbesondere bei Schaufeln mit dicker Hinterkante, Technical Note BBC, (unpublished).

5. Bammert, K. und Fiedler, K.: Hinterkanten- und Reibungsverlust in Turbinenschaufelgittern, Forsch. Ing.-Wes. 32, (1966) 5.

6. Imbach, H.E.: Die Berechnung der kompressiblen reibungsfreien Unterschallströmung durch räumliche Gitter aus Schaufeln auch grosser Dicke und starker Wölbung, PhD Thesis, ETH Zürich, 1964.

7. Dibelius, G.: Reibungseffekte in geraden Schaufelgittern, in [1], S. 276-282.

8. v.K.I. for Fluid Dynamics: Secondary Flows in Turbomachines, Lecture Series 72, Jan. 13-17, 1975.

9. Chauvin, J.: Turbine Cascade End Wall Losses, A Review, Secondary Flows in Turbomachines, Jan. 13-17, 1975, v.K.I. for Fluid Dynamics, Lecture Series 72.

10. Salvage, J.W.: A Review of Cascade Secondary Flow Effects, Secondary Flows in Turbomachines, Jan. 13-17, 1975, v.K.I. for Fluid Dynamics, Lecture Series 72.

11. Holliger, K.: Weiterentwicklung von Dampfturbinenschaufelungen, Escher Wyss Mitt. 33 jg., 1960.

12. Balje, O.E.: Axial Cascade Technology and Application to Flow Path Designs, Part I. ASME Trans., Series A, Vol. 90, Oct. 1968.

13. Utz, C.: Experimentelle Untersuchung der Strömungsverluste in einer mehrstufigen Axialturbine, Diss. Nr. 4894, ETH Zürich, 1972.

14. Wegel, S.: Strömungsuntersuchungen an Beschleunigungsgittern in Windkanal und in der Axialturbine, Diss. T.H. Darmstadt, 1970.

15. Wolf, H.: Die Randverluste in geraden Schaufelgittern, Wissenschaft. Z. der TH Dresden, 10, Heft 2, 1961.

16. Dejc and Trojanovskij: Untersuchung und Berechnung axialer Turbinenstufen, VEB Verlag, Technik Berlin, 1973.

17. Traupel, W.: Ergebnisse von Turbinenversuchen am Institut für Thermische Turbomaschinen an der ETH Zürich, in L.S. Dzung: Flow Research on Blading, Elsevier Publishing Co. Amsterdam-London-New York, 1970.

18. Lakshminarayana, B.: Methods of Predicting the Tip Clearance Effects in Axial Flow Turbomachinery, ASME Paper No. 69-WA/FE 26.

19. Traupel, W.: Predicting of Flow Outlet Angle in Blade Rows with Conical Stream Surfaces, ASME Publication 73-GT-32.

20. Ainley, D.G. and Mathieson, G.C.R.: An Examination of the Flow and Pressure Losses in Blade Flow of Axial Flow Turbines, ARCR. & M. 2891 (1955).

21. Ribaut, M.: Three-Dimensional Calculation of Flow in Turbomachines with the Aid of Singularities Trans., ASME J. of Engg. for Power. July 1968, p. 258-264.

22. Prust, H.W.: An Analytical Study of the Effect of Coolant Flow Variables on the Kinetic Energy Output of a Cooled Turbine Blade Row, NASA TMX-67960.

23. Dzung, L.S.: Consistent Mean Values in the Theory of Turbomachines for Compressible Media, Brown Boveri Review, 58 (1971) 10, S. 485-492.

24. Dzung, L.S. Seippel, C.: Aerodynamic Aspects of Blading Research, in L.S. Dzung: Flow Research on Blading, Elsevier Publishing Co. Amsterdam-London-New York, 1970.

ACKNOWLEDGEMENT

The author expresses his thanks to Mr. C. Jacobi and to Mr. H.J. Graf, for their help in calculating the examples presented. Finally, the author would like to acknowledge the support of the management of the Gas and Steam Turbine Departments of BBC for this work.

APPENDIX

EFFECT OF COOLANT ON MAIN STREAM DATA

The cooling air, ejected into the hot gas channel, creates a change in aero-thermodynamic data with entropy production due to mixing. This secondary air, blown out from blade surface or from trailing edge, has often a radial distribution. The coolant from rotor or blade carrier exhausting in the intermediate passage between the blades effec s in the first instance the boundary stream tubes. A calculation method is presented below to determine the radial change in the main stream properties. In the calculating s ations following assumptions are made.

Station 1: Inlet to a row with homogeneous flow along the circumference, fig. 2.

Station 2y: Just after the trailing edge; no mixing of coolant (exhausted at pressure or suction surface) with main stream takes place. Furthermore $p_{2y} = p_{c2y}$ and $\beta_{2y} = \beta_{c2y}$.

Station 2: Just after plane 2y; complete mixing of main stream and coolant (from pressure or suction surface) takes place without any change in flow angle and pressure, i.e. $\beta_2 = \beta_{2y}$ and $p_2 = p_{2y}$. No mixing of coolant from trailing edge with main stream takes place. We assume further $p_{ct} = p_2$ and $\beta_{ct} \gtreqless \beta_2$.

Station 3: Inlet to next row; complete mixing of main stream with coolant from trailing edge of proceeding row, from hub or casing takes place, $p_3 \neq p_2$ and $\beta_3 \neq \beta_2$.

A radial distribution of the main stream properties (changed due to coolant flow) at plane 2 and 3 (identical to station 1 of the next row) is calculated along the meridional plane.

A.1 Expansion of main stream

In case of cooled blade the main stream expansion is not adiabatic. The heat flux from main stream into the blade, i.e. absorbed by the cooling air is denoted by $\dot{q}_c$ for unit main stream mass flow. In case of a combined convective-film cooled blade we assume however no heat transfer between coolant film on blade surface and main stream up to station 2y. Furthermore let η be the polytropic efficiency, n the polytropic exponent and ζ_c the coolant coefficient. We define proper work [24]

$$e = \Delta h - \dot{q}_c \tag{1}$$

with

$$\Delta h = (\eta + \zeta_c)\ \left(\frac{n}{n-1}\right) RT_1 \left[1 - \left(\frac{p_2}{p_1}\right)^{\frac{n-1}{n}}\right] \tag{2}$$

and

$$\dot{q}_c = \zeta_c\ \left(\frac{n}{n-1}\right) RT_1 \left[1 - \left(\frac{p_2}{p_1}\right)^{\frac{n-1}{n}}\right] \tag{3}$$

In the above equations we have according to [1]

$$\zeta_c = \frac{d\dot{q}_c}{v dp} \tag{4}$$

$$\eta = \frac{de}{v dp} \tag{5}$$

$$\left(\frac{n-1}{n}\right) = (\eta + \zeta_c)\left(\frac{\gamma - 1}{\gamma}\right) \tag{6}$$

and dp is the infinitesimal pressure-drop along the flow paths.
η and ζ_c are assumed to remain constant during the expansion; p_{2y} has been replaced by p_2.

The velocity of main stream at station 2y:

for the fixed blade $$W_{2y} = \sqrt{2(K_1 + e)} \tag{7a}$$

for rotating blade $$= \sqrt{2(K_1 + e + \frac{\Delta u^2}{2})} \tag{7b}$$

with $$K_1 = W_1^2/2 \tag{8}$$

As will be shown later the effective main stream velocity is different to that given by eq. (7) when the coolant is blown out on the suction surface. The equations in relative system are also valid for a vane in absolute system with velocity W replaced by C.

A.2 Expansion or compression of coolant

From the blade cooling preliminary calculation following data $\dot{m}_c$, W_c, p_c, p_c^*, T_c^*, α (s. fig. 2) at different blowing holes or slots are known. It is assumed that the effective velocity of coolant is $W_c \cdot \cos\alpha$. The velocity normal to blade surface is thus neglected. In case the coolant is blown out on pressure surface the coolant expands downstream up to plane 2y.
Its velocity at 2y is:

vane $$W_{c2yp} = \sqrt{2(K_{cp} + e_{cp})} \tag{9a}$$

blade $$= \sqrt{2(K_{cp} + e_{cp} + \frac{\Delta u^2_{cp}}{2})} \tag{9b}$$

In the above equation

$$K_{cp} = \frac{1}{2}(W_{cp} \cos\alpha_p)^2 \tag{10}$$

$$e_{cp} = \eta_{cp} \frac{n_{cp}}{n_{cp}-1} RT_{cp} \left[1 - (\frac{p_2}{p_{cp}})^{\frac{n_{cp}-1}{n_{cp}}} \right] \tag{11}$$

with $$\frac{n_{cp}-1}{n_{cp}} = (\eta_{cp}) \cdot (\frac{\gamma_{cp}-1}{\gamma_{cp}})$$

If the cooling air exhausts on the suction surface we assume its effective velocity at plane 2y to remain unchanged, i.e.

$$W_{c2ys} = W_{cs} \cdot \cos\alpha_s \tag{12}$$

However the coolant is pumped from its exhaust pressure to that at plane 2y. This pumping work is supplied by the main stream. Compared to the main stream velocity given by eq. (7) the effective velocity therefore reduces to

$$\frac{W^2_{2yeff}}{2} \cdot \dot{m} = \frac{W^2_{2y}}{2} \cdot \dot{m} - \sum e_{cs} \cdot \dot{m}_{cs} \tag{13}$$

For fixed blade $$e_{cs} = \frac{1}{\eta_{cs}} (\frac{n_{cs}}{n_{cs}-1}) RT_{cs} \left[(\frac{p_2}{p_{cs}})^{\frac{n_{cs}-1}{n_{cs}}} - 1 \right] \tag{14a}$$

For rotating blade $$= \frac{1}{\eta_{cs}} (\frac{n_{cs}}{n_{cs}-1}) RT_{cs} \left[(\frac{p_2}{p_{cs}})^{\frac{n_{cs}-1}{n_{cs}}} - 1 \right] - \frac{\Delta u^2_{cs}}{2} \tag{14b}$$

For the coolant stream we have

$$\frac{n_{cs}-1}{n_{cs}} = (\frac{1}{\eta_{cs}}) (\frac{\gamma_{cs}-1}{\gamma_{cs}}); \tag{15}$$

The γ_c is a function of coolant temperature. (We assume the polytropic efficiency of coolant η_c to be same as that of main stream.)

A.3 Data at station 2

The velocity at station 2 after complete mixing is calculated from the momentum equation:

$$W_2 = \frac{\dot{m} \cdot W_{2yeff} + \sum \dot{m}_c \cdot W_{c2y}}{\dot{m} + \sum \dot{m}_c} \tag{16}$$

The outlet angle β_2 can be calculated from the continuity equation

$$A_2 \cdot W_2 \cdot \left(\frac{p2}{RT_2}\right) \sin \beta_2 = \dot{m} + \sum \dot{m}_c \tag{17}$$

with

$$h_2 = h_2^* - \frac{W_2^2}{2} \tag{18}$$

The stagnation enthalpy h_2^* can be calculated from the energy equation

$$h_2^* = \frac{(\dot{m} \cdot h_1^* - \dot{q}_c \cdot \dot{m}) + \sum \dot{m}_c h_c^*}{(\dot{m} + \sum \dot{m}_c)} \tag{19}$$

from which we have the stagnation and static temperature T_2^* resp. T_2.

A.4 Data at station 3

At this station we consider the coolant from trailing edge, from rotor or blade carrier completely mixed with the main stream. The equations in absolute system are written for inclined meridional stream plane. The coolant from hub or casing exhausting in the intermediate passage between the blade rows (i.e. between plane 2 and 3) is mixed at plane 3 in the boundary stream tubes. Angular momentum equation between plane 2 and 3:

$$\dot{m}_3 \cdot C_3 \cdot \cos \alpha_3 \cdot r_3 = \dot{m}_2 \cdot C_2 \cdot \cos \alpha_2 \cdot r_2 + \sum \dot{m}_c \cdot C_c \cdot \cos \alpha_c \cdot r_c \tag{20}$$

The momentum equation along the meridional plane:

$$m_3 \cdot C_3 \cdot \sin \alpha_3 + p_3 \cdot A_3 = m_2 \cdot C_2 \cdot \sin \alpha_2 + \sum \dot{m}_c \cdot C_c \cdot \sin \alpha_c + p_2 \cdot A_2 + \frac{1}{2}(p_2 + p_3)(A_3 - A_2) \tag{21}$$

The equations of continuity, energy and the relationship between static and stagnation temperature together with the above two equations allow to calculate all the unknown data at plane 3. These data at station 3 can be transformed to be used for station 1 of the next row.

A.5 Proper work of the row

The proper work of the row between station 1 and 2 resp. 3 is given by the following equation

$$(\dot{m} + \sum \dot{m}_c)\bar{e} = \dot{m} \cdot e + \sum \dot{m}_{cp} \cdot e_{cp} - \sum \dot{m}_{cs} \cdot e_{cs} \tag{22}$$

$\bar{e}$ can be used to determine the mixed flow inlet temperature $\bar{T}_i$. We are as well interested in the product of mass flow and proper work, i.e. in the right hand side of the eq. 2.

COMMENTS

Comment by M.Moore, C.E.G.B., UK

The problems of introduction of cooling air highlights a difficult area in turbine calculations, where to introduce losses in a stage. The profile losses in a turbine fixed blade do not mix with the main flow within the stator, but are distributed in the following gap and moving blades. Should the stator losses from correlations therefore be applied in the rotor? Similarly, at stations, for example, following the stator trailing edge, what is the appropriate fluid velocity to be used in radial momentum equations? Should it be the main stream (inviscid case) value or some mean value averaged to incorporate the wake deficit? The author's opinion on these two aspects would be appreciated.

Authors' response:

It is true, that the wakes due to boundary layers and trailing edge from the blade do not mix with the main flow immediately at the trailing edge. The mixing occurs downstream in the bladeless passage and in the following row. The assumption that the complete mixing occurs at the trailing edge is thus pessimistic.

Traupel in his profile loss analysis, distinguishes between the energy dissipation inside the blade row and that due to mixing of the wake outside. Similarly, he gives a relationship between the outlet angle at the trailing edge and that far downstream after complete mixing. Assuming complete mixing of the wake in the bladeless passage (i.e. up to the inlet to next row) one could compute the flow field accordingly. In the radial equilibrium calculation the computing stations are then, outlet of each row and inlet to next row. Proper losses and outlet angles have of course to be used as described above. The fluid velocities at these stations computed from the radial equilibrium calculation are then appropriate to this loss distribution.

The axial distance between the bladeless passage is chosen such that the following row is not excited from the wake. Sufficient equalisation of the wake thus takes place in this passage. The entropy production due to momentum equalisation follows a parabolic rule. According to Traupel a 50% resp. 75% equalisation of velocity causes 75% resp. 93.8% of the total entropy production. Thus the above assumption that the losses due to complete mixing of the wake occur in the bladeless passage is not far from reality.

In my presentation similar assumption has been made for coolant stream. Cooling air discharged from the blade surface (pressure or suction surface) for film cooling is assumed to be mixed completely upto the trailing edge of the blade. However coolant blown out at the trailing edge of the blade is mixed completely with the main stream up to the inlet of next row

A CRITICAL REVIEW OF TURBINE FLOW CALCULATION PROCEDURES

A. F. Carter, Manager, Fluid Dynamic Systems Group,
Northern Research and Engineering Corporation, Cambridge, Massachusetts 02139

SUMMARY

Computational techniques developed for modern computers have provided engineers with basically sound tools for turbine design and analysis. However, the current analytical methods do not necessarily lead to improved turbine performances or more reliable predictions of the quantities of interest. Unfortunately, the blade-row performance parameters, such as total-pressure-loss coefficients and flow deviations, remain the weak assumptions in most of the otherwise sophisticated calculations of turbine flow conditions. This paper reviews some of the areas in which further efforts are needed. Since a turbine's performance ultimately depends on the detailed design of the blading, the paper concentrates on this aspect of turbine design and analysis.

INTRODUCTION

Given as many equations as there are unknowns, it is usually possible to solve the equations and to determine the unknowns. The availability of computers has made it possible to solve quite complex equations encountered in design and analysis problems. There is no doubt that the solution of the complex flows within a turbine requires sophisticated computer programs. However, I personally doubt that current analytical procedures have made many contributions to improved performances of turbines. Engineers have been provided with powerful tools in the form of computer programs for their design and analysis tasks. Large piles of computer output, however, do not necessarily mean better turbines or significantly more reliable predictions of the quantities of interest.

I work for a company which has been responsible for a wide range of computer-aided design and analysis procedures. One example of our efforts is the TD2 program of References 1, 2, and 3. Nevertheless, for the purpose of this paper I intend to play the role of a devil's advocate. Specifically, I intend to point out that many of the calculations currently performed are of little real value if they do not directly tackle the problem of blade-row performance and its dependence on the detailed design standard of the blading.

MISCELLANEOUS PROBLEMS

In the days of the slide rule, very simple procedures were used for design and analysis. Free-vortex, constant-work designs were readily completed. Simple performance correlations were developed and readily applied. Turbines frequently performed quite well and more often than not met their design requirements and objectives.

When I was first confronted with a nonfree-vortex design, it was because someone had decided it would be much simpler to use constant section blading for a stator than to manufacture the more complex shape which resulted from the usual free-vortex design. The problem to be addressed then was to determine the magnitude of the performance penalty associated with this mechanically simpler design. The problem I have today is to find anyone who has a quantitatively valid model for the higher performances achieved in the various "nonfree-vortex" designs which are used by many turbine manufacturers. Later in the paper I question the validity of attempts to control reaction or to use controlled-vortex aerodynamics as an explanation of the improved performance of turbines of the type considered in Reference 4.

Once it had been established that designs having a common mean radius standard, but differing in detail across the annulus from hub to casing, performed differently, it became necessary to consider losses at various radial locations. Immediately, the engineers developing analytical tools met a basic problem. Losses are related to boundary layers; boundary layers migrate across streamlines defined by the core flow; and losses are measured at radial locations significantly different from those at which the low-momentum flows originated. A problem with the streamline curvature approach to turbine design and analysis is that detailed calculations of the core flows usually make assumptions concerning the losses which significantly affect the validity of the calculations.

The flow conditions for a first stator row are quite complex, but as soon as the design or analysis problem involves a later row, there is an increase in the complexity. It has been shown experimentally that the performance of a rotor row depends on the quality of the flow entering the row. The replacement of a stator row of a poorly performing stage by an improved design of slightly lower loss has on several occasions increased the stage efficiency level by an amount far greater than that which could be attributed to the lowered stator-row loss. One simple approach to the problem of correctly modelling the performance of a rotor would be to treat the entering flow as consisting of a core flow and a wake. Thus, each transit of a rotor blade across the pitch of a stator blade would yield a variation of inlet flow condition for the rotor. Detailed analyses of flow conditions within a rotor, or for a section of the rotor blading, are interesting. However, if these calculations ignore the time-varying flow conditions, they address only part of the real problem.

One of the programs developed by NREC is for the analysis of turbines of a given geometry. The analysis which preceded the development of the program (Program TOD3D) considered in detail the possibility that there would be cases in which there is a deterioration of the stage exit flow profile to the point that

there is a reversed flow region at the hub of low hub-to-tip diameter ratio stages. Provisions were made for handling the occurrence of negative meridional velocities. However, in none of the cases investigated did these negative velocities occur. The underlying reason was that we assigned total pressure losses using loss coefficients based on relative exit dynamic heads. Hence, as velocities decreased near the hub, the total pressure loss also decreased in the calculations. The computational scheme, therefore, imposed limits on the deteriorations of the flow profile. Since experimental data have shown very poor flow profiles in many of the low hub-to-tip diameter ratio turbines, there is a question whether or not the conventional loss coefficient approach will ever properly predict the flow fields of these turbines.

Engineers working to develop analytical procedures face yet another basic dilemma. The question to be resolved is how much effort should be devoted to accurately analyzing poor performance designs. There is a strong correlation between poor performance and blading standards which impose separated flows. The computational problems increase when separated flows have to be considered. It would probably be better to direct analytical efforts towards improving blading design standards rather than towards the development of computational procedures to tackle poorly designed turbines. One approach to the problem of flow calculations and performance predictions, in the presence of separated flows, might be to develop the "least resistance theory" frequently quoted in the older text books on hydraulic machinery. In effect, the flow through turbines could be considered in terms of what flow situation corresponds to the most efficient passage of the flow through the stage or stages.

Before completing this brief recital of problems not, to my knowledge, currently tackled by analytical methods, there are two very important questions to be considered: one, how much greater complexity should be introduced into the analytical methods?, and two, how are the various analytical procedures dealing with the aerodynamics of turbines best integrated with the equally important mechanical aspects of turbines? I do not know the answers to these questions, but I have opinions. I believe we will be reaching the point of diminishing returns, when the cost of engineering time and computer usage approaches the cost of obtaining model tests of candidate designs. With respect to the second question, I believe turbine technology is already at the point where the challenge is no longer to achieve predictably high efficiencies but to maintain efficiency levels in turbines which are more reliable, more readily manufactured, lighter, and less expensive.

SPECIFIC DESIGN PROBLEMS

Programs such as NREC's Program TD2 (and its equivalents which have been developed by most of the aircraft engine companies) provide engineers with great design freedom. It is possible to generate many design alternatives which satisfy the specific design requirements. However, there is still the problem of deciding which of the many alternatives should be selected. Clearly, it is impractical to carry each of many parallel design efforts to a detailed blading standard before making a choice. Hence, there is a need to relate alternative sets of blade inlet and exit flow data to probable performance. A wide variety of blading types can be selected to satisfy the required power output and flow capacity.

The program developed by NREC assigns a "consistent" set of losses to design alternatives, but to date, this "consistent" set of losses has failed to properly predict the efficiency level increase which has occurred for some of the nonfree-vortex designs when compared with the free-vortex equivalent. The governing equations at stator-exit/rotor-inlet and rotor-exit planes can be solved for a variety of possible tangential velocity or meridional velocity profiles. The radial variations of flow angles can be tailored to meet specific requirements. If the calculations are performed with assumed total pressure losses assigned to various streamtubes, there is little reason to believe significant changes in performance will be achieved compared with a free-vortex design. Stator exit flows are found to be primarily a function of the average tangential velocity. Consequently, the static pressures at hub and casing do not vary significantly from design alternative to design alternative, provided the average stage reaction is maintained. Various streamline patterns can be generated in which rotor relative flow angles change as the distance between adjacent stream surfaces defining equal flow increments change. If we use loss coefficients that depend heavily on local reaction, it is not possible to claim reaction control as the means by which stage efficiency is improved. Similarly, attempts to extract more work from the more efficient sections of the turbine lead to relatively small predicted efficiency improvements. Here again, there is only a relatively narrow band of possible solutions of the row exit flow fields.

It must be concluded that one design out-performs another, not because of the choice of particular vortex flows, but because the use of that vortex flow has led to the design of blading which is inherently capable of higher performance. Returning to the question of losses, consider the actual flow leaving a blade row. Traverses downstream of stators show that a very high percentage of the flow is loss free. The measured loss is associated with the low-momentum flow originating from the blade surface and annulus wall boundary layers. Mixing of high and low-momentum flows continues over considerable flow distances, and first-stage stator wakes can be measured downstream of two or more stages. The static pressure fields are controlled by the virtually loss-free core flow. The wake flow accounts for a small percentage of the total. In these circumstances, it could be argued that the basic radial equilibrium equation should be solved for the loss-free flow. The low-momentum flow could be considered as circumferential and radial blockages.

In the above model, there would be a problem of assigning these blockages. Boundary-layer migration is an important consideration. If, in the stator row, the static pressure field causes low-momentum flow to migrate towards the hub, the free stream flow will be forced outward. It is because the above is a valid model of the physics of the flow that I have lost enthusiasm for taking part in academic arguments with respect to streamline curvature and axial derivatives of various quantities in solutions of the supposedly governing equations which are now an integral part of most modern computer programs for design and analysis. In effect, I advocate even stronger emphasis on the blade design standard. I believe it makes more sense to select a particular nonfree-vortex design because it will be possible to design more efficient blading rather than to devote considerable efforts to provide accurate predictions of the flow fields in the inter-blade-row spaces. Unfortunately, almost endless varieties are now available to a designer with

access to computer programs. Complex flow fields are solved in order to generate inter-blade row velocity triangle data.

I would carry the above one step further. If, in the detailed blading task, an engineer finds that the detailed aerodynamic and mechanical requirements are not consistent with satisfying criteria related to boundary layer behavior, he should be prepared to respecify the parameters controlling the vortex flows.

SPECIFIC ANALYSIS PROBLEMS

The analysis problem consists of determining the detailed performance of a turbine when blading and over-all operating conditions are defined. Designs can be analyzed before they are manufactured or when experimental data are available. The over-all objective to be set for analysis methods is that the performance of turbines will be accurately predicted in advance of any hardware procurement. There is obviously some advantage associated with the ability to model detailed performance after the fact; that is, when test data become available. However, if the purpose of the analysis is to discover why particular problems exist, it is already too late. Hopefully, the primary purpose of experimental work will be to improve the analytical methods for future application.

Northern Research and Engineering Corporation personnel, like many other engineers, have devoted considerable efforts to the development of analysis procedures. It is possible to construct analytically sound models of the physics of the flow. In the case of centrifugal compressor blading, an attempt was made to analytically treat both the viscous boundary layer flow and the inviscid flow field in a series of computer programs. These computer programs were developed but not to the point that they could be considered engineering tools. However, the work did lead to the formulation of simpler procedures for the quantitative assessment of different impeller design standards. The work was also extended in order to provide improved correlations for use in axial compressor analysis programs employing the multi-streamtube, streamline curvature analysis method. In theory, the method of analysis can also be applied to turbine blade rows.

The migration of boundary-layer flows across streamlines defined by the core flow is the basic problem to be tackled if reliable predictions of stages in detail are to be obtained. There would appear to be two distinct levels to the problem. One is a redistribution of losses under the influence of the strong pressure gradients or blade rotation forces in the case of rotor rows. The second is the additive loss effects which will occur when a net influx of low-momentum flow to a particular region causes a flow separation. When boundary-layer separations occur, the regions of separated flow act to limit the total pressure loss in a blade row as a whole. Hence, there is a limit to how badly any blade row will perform. However, blade rows downstream of rows in which there are significant flow separations have their performances adversely affected. The most probable explanation of why significant improvements in stage performance are achieved when a stator blade row is replaced by one having a very small decrease in row loss coefficient is that rotor row performance is strongly dependent on the time-varying flow conditions.

It would be a tremendous achievement if the analytical methods were developed to the point that all measurable quantities were accurately predicted for all turbines. I think it would be a more significant achievement if methods were developed to the point that design alternatives could be rapidly evaluated in the process of selecting a design which would perform predictably well.

If the objective is to select a design which will perform predictably well, it is only necessary to establish achievable levels and use blade analysis procedures which identify the detailed design standard in a semi-quantitative manner. I fail to see the value of an analysis procedure which will accurately reproduce the performance of designs in which basic criteria related to detailed design standards have not been satisfied. Much can be made of the analysis of the complex secondary flows. However, a better course of action would be to reduce the significance of secondary flows by careful design of blade sections in order to control the growth of boundary layers.

In the absence of experimental data, most analysis methods need to establish flow deviations from the actual blading angles and loss as a function of over-all operating conditions. It is interesting to note that many of the empirical correlations of deviation can be substantiated by potential flow analyses. It is also possible to calculate profile losses following an analysis of the surface velocity and/or pressure distributions. If turbines were to perform with section loss levels equal to those predicted from analyses of individual profiles (or equal to those measured in planar cascade tests), operating point efficiencies would often be in excess of 95 per cent on a total-to-total pressure ratio basis. Loss and deviation correlations for use in the analysis of designs must therefore include significant "secondary" losses and deviations. In the case of stators, it is reasonable to assume that in most stages there is both a redistribution of loss and additional losses created by separation-inducing, low-momentum flow migration. In the case of rotors, there is the added complexity of time variations of inlet flow velocit, and incidence associated with the mixture of high- and low-momentum flows from upstream rows. I believe that the calculations of surface velocity distributions for selected sections of a turbine's blading have become routine now that computer programs have become available. However, I am not aware that much attention is being paid to the fact that all but the first row of a turbine's blading will operate with wide variations of incidence associated with core and wake flows.

Boundary-layer characteristics will be time varying for all rows except a first stator. The time-averaged loss may be a simple average of the loss versus incidence characteristic for the appropriate incidence variation associated with the wakes from upstream rows. However, it is easy to conceive that the effects of a local high incidence would persist and that this provides the explanation of the strong dependence of rotor row performances on upstream blade row performance.

Earlier I stated that empirical correlations for deviation could be substantiated by potential flow analyses. Accepting this to be a true statement, it should be possible to predict flow deviations for sections consisting of both the geometric blading and the associated boundary layer. Such procedures are

not currently advocated, however, because of the boundary-layer migration which occurs in the actual stage environment. Nevertheless, if the analysis of a turbine includes a redistribution of loss, it would be logical to develop correlations in which loss and deviation are related. In essence, an effort should be made to relate both loss and deviation to the boundary-layer behavior and, hence, to the actual blading standard.

SECONDARY FLOWS

Physical models of the flow within turbine blade rows are constructed with relatively little effort if the modelling remains at the qualitative level. It is considerably more difficult to proceed to a quantitative modelling. It is important to note that very large radial forces act on any component of the flow within a turbine.

One simplification of the secondary flow problem is to consider the boundary-layer flow as having one half the free stream velocity adjacent to the boundary layer. If the free stream is in radial equilibrium, it is obvious that the low-momentum flow will follow flow paths which diverge significantly from those of the free stream. At the end walls, there will be large forces acting in the circumferential direction.

Anyone who has investigated the details of the flow downstream of stators is aware that high losses are measured towards the hub end, in particular, at the junction of the end wall and the suction surface. Anyone who has traversed the exit flow of a turbine stage has observed regions of high loss which are difficult to relate directly to flow conditions of the free stream at the corresponding radial location. I think it is important that anyone who attempts to develop correlations for use in turbine design and analysis recognizes the boundary-layer migration problem.

There are a variety of different correlations which attempt to include the effect of blade-row aspect ratio on turbine loss and flow deviation. It is quite possible that each of the alternatives is a valid correlation for a particular series of turbines. However, aspect ratio is just one of the parameters influencing the loss in a blade row. Similarly, there used to be differing correlations for the effect of stage hub-to-tip diameter ratio. It has been experimentally shown that the critical aspect ratio for a stator row differs from that of a rotor row. (Critical in the above sense means a value at which blade-row losses become significantly greater than those of a high aspect ratio design.) Nonradial stacking of stator blade sections is known to affect the performance of a turbine. From the above, it is clear that any future attempts to provide correlations for either the total secondary loss in blade rows or the redistribution of losses (to be used in the analysis of flow conditions across an annulus) should recognize the parameters directly affecting boundary-layer migration. NREC has developed a migration parameter for use in axial compressor analyses, and it should be possible to develop an equivalent one for use in turbine analyses.

I do not mean to discourage efforts to develop analytical methods of treating the complex viscous and inviscid flow interactions. However, I do believe that, for day-to-day utilization by engineers, it will be necessary to simplify the representation of blade-row performances through the development of empirical correlations. Preferably, these correlations will be based on the assumption that the detailed blading can be categorized as well-designed.

BLADE ROW DESIGN

If it is assumed that there is a large over-all acceleration of the velocity for all blade sections, there will be little incentive to be concerned with the detailed design of turbine blading. However, there are considerable advantages associated with increasing the loading of turbine stages. As loadings increase, local diffusion rates can become as large as those experienced in compressors. Simple considerations of surface velocity distributions or pressure distributions will show that adverse pressure gradients become more likely as the ratio of inlet-to-exit velocity approaches unity or attempts are made to achieve the required momentum transfer in lower solidity blading.

Since surface distributions are important, NREC has taken the position that all turbine blading should be undertaken using the direct-design method. Specifically, we chose to develop the Stanitz method of References 5 and 6. It is a direct-design method in that the engineer directly controls the quantities of interest. The engineer selects the surface Mach number distributions and attempts to satisfy criteria with respect to maximum surface Mach numbers and local diffusion rates while satisfying over-all mechanical constraints arising from stress and manufacturing considerations. It could be argued that the actual surface distributions will differ from those assumed at the design stage because of the various assumptions made. However, the actual flow conditions within the row will be closely related to those assumed in the design of the individual sections of the blading.

The use of well-designed profiles in a blade row decreases the importance of secondary flows. Clearly, the less low-momentum flow which is generated, the less is the significance of the migration of these flows. Nevertheless, there will be boundary-layer flow migration, and there is no reason why it should not be taken into consideration at the design stage, at least qualitatively. One first step is to consider the static pressure contours for a complete surface. These contours can be used to obtain first estimates of both the rate of boundary-layer growth and the probable direction of the boundary-layer migration. For stator blades, the designer has some freedom with respect to the stacking of the blade sections, and this freedom should be used. For rotor blading, the highly stressed rows of most aircraft gas turbines limit the freedom to stack sections in order to meet specific aerodynamic requirements. Nevertheless, it is usually possible to redefine blading sections in order to improve the over-all aerodynamic performance without adversely affecting local stresses.

The design of rotor blading should consider its operating environment. Specifically, it should recognize the fact that stator wakes will be present in the inlet relative flow. The fact that most, if not

all, design-point selection programs list single variations of inlet angle and inlet velocity or Mach number with radius for a design point tends to obscure the fact that the rotor will be required to operate with a time-varying inlet flow. The actual magnitude of the variation is difficult to estimate. The decay of wakes is a function of flow distance from the source of wakes and the details of the low-momentum flow at the trailing edge of the upstream row. Nevertheless, there will always be a component of the flow which is at a substantially different incidence than the core flow. It would, therefore, be a mistake to design any rotor section for absolute minimum loss at one particular inlet flow condition.

The operating range requirement of each section will differ. Velocity triangle data of the conventional type can be used to construct velocity triangle data for the wake flows entering the rotor. Obviously, it would be necessary to make assumptions with respect to the ratio of residual wake velocity and the free stream. In some cases it might not be possible to avoid local stalling of the flow, but at least the engineer should be prepared to make some compromises in selecting a "nominal" design-point loading in order to provide some margin for the actual operating conditions.

Existing analysis procedures can be used to establish surface distribution data at various incidences and at inlet velocity levels. It would be useful if these analyses were programmed to yield the variations in loading associated with typical core and wake flows. Wakes from upstream rows are known to play an important part in the excitation of vibrations which can lead to fatigue failures. However, the energy input for a particular vibration mode will depend strongly on the rotor blade's response to the time-varying flow conditions.

In the case of aircraft gas turbines, fatigue failures of turbine blading are now rare events. However, in the case of industrial turbines (both gas and steam), failures excited by unsteady aerodynamic forces still occur. The design of blading to avoid all possible excitations of a large number of natural frequencies over a wide range of operating conditions and speeds is a formidable task. At this time it is not clear whether or not compromises of the aerodynamic design standard to improve mechanical features of a blade-row design is the correct approach. However, one thing is certain, and that is that the aerodynamic and mechanical design of blading should be closely coordinated and not treated as two distinct and separate tasks.

CONCLUDING REMARKS

I apologize to all those who expect to see complex equations and detailed results of analytical or experimental investigations in a paper of this type. On the one hand, I believe that many presentations of turbine calculation procedures have tended to obscure the physics of the problem they address. On the other hand, very little of the efforts of NREC can be presented in the open literature; an overwhelming percentage of our total turbomachinery effort is undertaken for specific industrial clients.

The state-of-the-art of turbine technology is not really as bad as I have made it seem. It is true that the analytical treatment of the turbine design and analysis problem can be very complex. However, I believe that the acquisition of some better insights into the physics of the flow should be the principal objective of those who wish to further develop the analytical models. I believe that much of the work undertaken in the past fifteen to twenty years can be put to good use. The ultimate objective is to put the analytical procedures to work to achieve better and more reliably predicted performances. There is little point in spending high-level engineering efforts and making extensive use of expensive computers if turbine performances do not change or if existing performance levels are not achieved with cheaper, lighter, and more reliable machinery.

REFERENCES

1. Carter, A. F., Platt, M., and Lenherr, F. K., Analysis of Geometry and Design Point Performance of Axial Flow Turbines, I-Development of the Analysis Method and the Loss Coefficient Correlation, (NASA CR-1181), 1968.

2. Platt, M., and Carter, A. F., Analysis of Geometry and Design Point Performance of Axial Flow Turbines, II-Computer Program, (NASA CR-1187), 1968.

3. Carter, A. F., and Lenherr, F. K., Analysis of Geometry and Design-Point Performance of Axial-Flow Turbines Using Specified Meridional Velocity Gradients, (NASA CR-1456), 1969.

4. Dorman, T. E., Welna, H., and Lindlauf, R. W., "The Application of Controlled-Vortex Aerodynamics to Advanced Axial Flow Turbines", J. Eng. Power, vol. 90, no. 3, July, 1968, pp. 245-250.

5. Stanitz, John D., Design of Two-Dimensional Channels with Prescribed Velocity Distributions Along the Channel Walls, (NACA Report No. 1115), National Advisory Committee for Aeronautics, 1953.

6. Stanitz, John D., and Sheldrake, Leonard, Application of a Channel Design Method to High-Solidity Cascades and Tests of an Impulse Cascade with 90° of Turning, (NACA Report No. 1116), National Advisory Committee for Aeronautics, 1953.

COMMENTS

Comments by H.Cox, G.E.C., UK

I have a number of points. First of all, you said that you thought that there would be a correlation between loss and deviation. Do you mean in cascades? To my knowledge, there is no such thing. You have a change of loss with incidence and no change of deviation. We have tried to look at this at optimum incidence and we could not find any correlation between minimum loss and deviation. Low deviation blades can have high losses and conversely high deviation blades can have low losses. I think that this is associated with deviation being composed of two elements, one associated with the boundary layer, one with the potential flow. To do what you suggest, you would have to split the deviation into its two constituent parts.

Authors' response:

I am working with real turbine flow and I do not think that cascades have anything to do with the real world. Anulus cascades are not really the kind of thing we are worried about, but the real flow. If our turbines would operate with the cascade loss, their efficiencies would be up in the 95%. What I meant is that people have demonstrated that the empirical correlation were developed because of the lack of computer, not because people did not know better.

The potential flow calculation will give you a potential flow deviation and a "potential flow losses", i.e. blade pressure distribution that you can use to calculate boundary layer and the associated loss. And there is a relationship between velocity and loss. That I call potential flow solution. If you find that there is a loss redistribution to a certain area, then it would appear that at that station, there are high losses. I am saying that the deviations which are occurring there could also be related back to a potential flow solution. The potential flow solution is related to the blade and the boundary layer around the blade.

Comment

Could I ask another question? You are using different vortex design, you are saying that you obtain different efficiencies according to the design, that you cannot predict. What sort of errors in efficiency are you talking about?

Authors' response:

Sometimes three points; using a conventional loss scheme. This is important if you are between 88% and 91%. We are trying to get to 1% in efficiency.

Comment by J.Railly, University of Birmingham, UK

Regarding the difference between "potential" and real deviation, on the basis of calculation, in which boundary layers are represented by sources, the eventual difference between uncorrected and corrected potential solution is very tiny. You could thus expect, for attached boundary layer, to be very near the prediction by Martensen's method, for instance.

Authors' response:

I agree that the deviation calculated for lightly-loaded, well-designed profiles is not greatly affected by consideration of the boundary layer and the trailing edge wake. The point I was trying to make in the paper was that boundary layers and boundary layer migration effectively redefine the boundaries of the core flow. Hence, there should be a correlation between loss and deviation. If losses are redistributed, flow deviations should also be redistributed with regions of high loss being associated with high deviation values. It is known that local loss coefficients can be several times larger than the pure profile loss for the section. In these circumstances there is no reason to believe that the deviation will not be significantly different from the two-dimensional "profile" value. What is significant will depend on the compressor or turbine being considered. In the case of multi-stage compressors, very small changes in the deviations assigned to the earlier blade rows can greatly affect the predicted performance of the overall machine. In highly loaded, multi-stage turbines small changes in deviation will significantly affect the stage work splits.

Comment by J.Dunham, N.G.T.E., UK

I agree that the radial migration of losses has an important effect on loss distribution. But this migration occurs mainly in the trailing edge wake region, and how do you calculate migration of low energy fluid along the trailing edge?

Authors' response:

In the paper, I was primarily concerned with boundary layer migration within a blade row. However, since the pressure field downstream of a blade row will satisfy the radial equilibrium conditions for the wakefree flow, it is obvious that there will be a radial migration of low momentum flow in the wake region. Although I have not attempted any calculations of the migration of the low momentum flow, I am reasonably certain that the problem will be amenable to treatment by writing and solving the appropriate equations of motion.

For a given radial pressure gradient the radius of curvature of the low velocity flow will depend on the velocity level. I expect that typical flow patterns in both stator and rotor blade row wakes could be estimated with reasonable accuracy once the wake flow is represented by a series of discrete velocity levels.

Comment by M.Denton, C.E.G.B., UK

I agree with your statement about large radial migration. I have made measurements myself showing large movement of low energy flow from casing to hub. However, on the same turbine, the agreement between measured

and calculated (by through-flow) data was very good indeed. I would tend to conclude that the effect of the migration on the through-flow, on the mean flow, is small. Do you agree?

Authors' response:

The better the basic blade design, the smaller the migration should be. I pointed out in my text, that the emphasis should be on keeping the low momentum flow quantities as small as possible. If you have small low momentum flows, you have small secondary flows. Typically, you can design blading where there is no deceleration until very late in the blade. The boundary layer growth on the blade can be very limited. In these circumstances, the amount of flow moved to other radius is small. However, I still see that bad blades are being put into turbines. It is in those poorly bladed turbines that the migration phenomenon is important. In a variety of applications, it is sometimes difficult to avoid migration. For instance, in very small turbines where you have manufacturing constraints, for instance where one cannot tolerate chord smaller than 1/2 inch. The blades have then a low aspect ratio. A good method should handle this as well.

Comments by H.Cox, G.E.C., UK

What makes you believe that the difference between measured and calculated efficiencies is due to migration, and not to unsteady effects?

Authors' response:

In the rotor, the unsteady effects are the very important ones.

Comment

You are getting now to small effects for the migration. Let us say that on your 3% difference in efficiency, 1% is due to unsteady effects, 1% to turbulence level, that leaves you only 1% for the migration. I am speaking for small turbines, presumably in large machines, there is a bigger effect.

Authors' response:

I did not want to blame all on the migration. I just wanted to point out that one has to consider it in the correlations. A lot of correlations have been developed. Some still subsist, some have died away. They took an array of parameters into account. They were, in fact, attempts to explain a particular series of results which is a very desirable objective, but also very constraining. If you decide that turbines in a particular class are inefficient, because of previous experience, you have lost the game. You have to assume that you can make the migration small.

Comment

In fact, we have published a correlation which was tested on a number of small diameter ratio turbines. Our original intention was to use a fudge factor to modify the calculation to suit the measured data, but we did not need it.

Authors' response:

Our objective should be that when we have to design a turbine, before anyone picks up a machine tool, we should know how that turbine will perform. If you have to wait until you try to line up your measurements with your model, this is too late. If you are good it is interesting. If it is bad, you have to modify your model. If you have a bad product you cannot sell it. The objective of the theoretical calculation should be to make the performance of turbomachines predictable.

COMPRESSOR DESIGN AND EXPERIMENTAL RESULTS

by

H.B. Weyer

DFVLR-Institut für Luftstrahlantriebe,
Linder Höhe, 5 Köln 90, W.Germany

INTRODUCTION

After the first day's excellent introduction to the current techniques available to evaluate the axisymmetric flow field in turbomachines at design and off-design conditions, the second day of the meeting was concentrated primarily on proving these calculation methods by comparing the results with corresponding experimental data from real test machines. In preparing this part of the meeting the program committee asked for appropriate test cases, got a limited number of examples, and selected finally five machines - 2 turbines and 3 compressors.

Prime criteria for the selection were:

1. The comparison should cover both compressors and turbines, single-stage as well as multi-stage machines.
2. The flow path dimensions should be such that the effects of gap flow and end wall boundary layers are always present but not dominant.
3. Complete geometrical data and appropriate test results should be available.

DESCRIPTION OF COMPRESSOR TEST CASES

The details of the compressor cases - as far as now available - are included in the following tables and diagrams. Tab.1 gives a survey on the main design parameters of the three compressor test examples, designated by the numbers 3 to 5.

Test Case 3 is a single-stage transonic compressor without inlet guide vanes investigated at DFVLR. It was designed for a total pressure ratio of 1.51 at a mass flow rate of 17.3 kg/s and a tip speed of 425 m/s. The isentropic efficiency was estimated to be about 80.5 %. The rotor inlet diameter of 400 mm was prescribed by the DFVLR axial compressor test rig.

Tab.2 contains additional design characteristics; the stage pressure ratio of 1.51 is predicted to occur at a temperature rise of 15.4 % of the inlet total value. MCA-profiles were selected for the rotor blading from hub to tip. NACA-65 profiles with a circular arc camber line were used throughout the stator blade height. 28 blades with a tip chord length of about 60 mm were selected for the rotor, 60 blades for the stator yielding usual blade solidities between 1.34 and 2.0 for the rotor and 1.5 to 2.4 for the stator. The maximum inlet Machnumbers to rotor and stator blading reach up to 1.37 and 0.76 respectively. The maximum diffusion factor is estimated to be 0.53 for the rotor and 0.48 for the stator. Fig.1(a) demonstrates the compressor annulus geometry. Hub and outer wall are shaped to adapt the flow path to the stage pressure rise, to achieve nearly constant axial velocity over the annulus height, and to balance rotor and stator diffusion factors properly. (Due to contract restrictions detailed geometric data of this machine are not allowed to be published.)

Test Case 4 (MTU, Munich) is a 3-stage transonic compressor without inlet guide vanes, too. It was designed for a total pressure ratio of 2.9 at a corrected mass flow of 61.7 kg/s and at a tip speed of 470 m/s of the first rotor. The overall isentropic efficiency in this case was predicted to be around 83 %.

Tab.3 offers detailed informations on the design characteristics of the different stages. The pressure ratio decreases from 1.44 of the first stage to 1.4 of the last stage; the relative temperature rise behaves - as expected - similarly to the pressure ratio variation. For the rotor blades special wedge type and DCA profiles are selected to achieve the design flow pattern. The stator blades consist of NACA-65 profiles with circular arc camber line. Looking at the Mach numbers it becomes evident, that all three rotors are operating at transonic inlet velocities. The rotor and stator blade solidities are choosen such that the diffusion factors are kept well below critical values. A detailed description of this compressor is given in Ref.(1). Fig.1(b) shows the annulus geometry of this compressor; the location of the rotors and stators, and the position of the instrumentation planes are also indicated. Measurements have been carried out upstream and downstream of the blade rows yielding primarily overall performance data for the comparison. (Permission of publication of the compressor geometry was not achieved.)

Test Case 5 (NGTE, Pyestock) is a 4-stage compressor with inlet guide vanes which was designed for an overall pressure ratio of 2.95 at a mass flow of 24.1 kg/s. The tip speed of the first rotor was set at 362 m/s. The isentropic efficiency was estimated to reach 86 %.

Stage design characteristics as pressure ratio and temperature rise were not available when preparing Tab.4. The average pressure ratio of 1.31 is evaluated from the overall pressure ratio just to give an idea of the energy addition within the stages. All rotors are equipped with DCA-blades, all stators with NGTE-C4-profiles. The relative tip Mach number at the inlet of the first rotor is kept relatively low at 1.22. (All other data including diffusion factors are not available.) The compressor annulus geometry (Fig.1(c)), the 4-stage concept, and the moderate inlet Mach number characterize this machine as a typical JP compressor of a modern turbofan engine (s.Ref.(2)). The instrumentation planes (Fig.3) were located such to provide detailed stage element performance data. +)

EXPERIMENTAL RESULTS - TEST CASE 3

The single stage transonic compressor - Test Case 3 - has been investigated using both conventional and far advanced measuring techniques. The instrumentation planes just upstream and downstream of the stage were equipped with probe rakes or radially traversing probes to analyse the spanwise distribution of the total pressure and temperature, and of the flow direction. A liquid-filled Pitot probe was inserted between rotor and stator to determine well-defined mean total pressures in the strongly fluctuating discharge flow of the rotor. The inaccuracy of the pressure measurements was proved to be about 0.5 % primarily due to the inaccuracy of the today available pressure transducers; the error of the temperature measurements was estimated not to exceed half a degree.

Additionally, the rotor flow field (ahead, within, and behind the blading) was studied in great detail using advanced laser velocimeter (Ref.(3)). These tests carried out at design (20 260 rpm) and off-design speeds yielded quite complete informations on the span- and gapwise velocity profiles, on the 3-dimensional shock waves, on the flow separations, and on the blade wakes.

The overall performance of this compressor is shown in Fig.2. The speed lines are quite typical of a single stage transonic compressor; at design speed a maximum pressure ratio of 1.65 and a maximum efficiency of 85 % - based on temperature rise - are achieved. There is a slight increase in maximum efficiency from 85 to 100 % speed due to long term operation at 85 % speed associated with severe rotor and stator blade contamination. The tests at 100 % speed were carried out with the compressor cleaned up.

The following figures (Fig.3 to 7) give a survey on the spanwise distribution behind rotor and stator of main flow parameters as total pressure ratio, temperature rise, Mach numbers, the absolute flow angles, and flow losses. The experimental data shown represents the flow pattern at design mass flow (17.3 kg/s) and at maximum efficiency with an equivalent mass flow of 16.8 kg/s. The relatively uniform stage total pressure profile satisfies the prime design requirement of a radially constant work addition within the stage. The rotor outlet flow angle - and in consequence the temperature rise-increases near hub and outer wall which is also a design prospect in order to compensate for the additional flow losses occuring near the end walls. This is verified experimentally by the radial distribution of rotor and stator losses shown in Fig.7.

EXPERIMENTAL RESULTS - TEST CASE 4

As already mentioned, in Test Case 4 - that is the 3-stage transonic compressor - measurements were carried out primarily at compressor inlet and outlet using ordinary total pressure and temperature rakes. The static pressure was drawn from wall tap readings and adapted within the flow by fulfilling the radial equilibrium. The accuracy of the pressure and temperature measurement can be assumed to be the same as in Test Case 3.

Interstage measurements are available, however, the experimentator himself believes the results being not as confident as necessary to check with corresponding calculated data. Thus, for Test Case 4 the comparison will be restricted on the overall performance which is shown for this compressor in Fig.8. The isentropic efficiency is based on torque measurements corrected for disc ventilation losses and for bearing friction losses.

At 100 % speed that typical straight speed line is observed which is representative of multi-stage transonic compressors. The pressure ratio exceeds the value of 3 to 1 whereas the maximum isentropic efficiency reaches up to about 84 %.

EXPERIMENTAL RESULTS - TEST CASE 5

The experiments on Test Case 5 - the 4-stage compressor - were carried out with an inlet spoiler incorporated to simulate a typical fan exit pressure profile at this JP-compression-system entrance. The inlet total pressure was taken as the arithmetic mean of several eight-point Kiel rakes which were stationed 0.7 chords upstream of the rotor 1 blade leading edge. Four half shield thermocouple probes located far upstream of the compressor were used to determine the arithmetic average of inlet total temperature. The compressor overall performance is evaluated from arithmetic means of outlet total pressure and total temperature measured by Kiel rakes and half shield thermocouple probes at 2.3 and 5.5 chords downstream of the outlet guide vanes. (For further details - e.g. circumferential probe traversing to cover IGV and OGV wake areas - see Ref.(2).)

Constant speed characteristics were taken at several speeds, and the results obtained are partially presented in Fig.9. The compressor achieves its design pressure ratio, but

+) The geometric data of this compressor are summarized in the appendix.

exceeds the design mass flow by 2.5 %. The isentropic efficiency remains 3 % below the design value.

Interstage measurements are available behind each rotor of this compressor yielding informations on the radial profiles of total pressure and temperature, of static pressure, and of flow angle; wedge type probes and single half shield thermocouple probes were thought to fulfill all these functions satisfactorily. No informations are available on the accuracy of the pressure measurements; the error of temperature measurement however is believed to be 0.1 % of the actual value.

The experimentator has only submitted the total pressure and temperature profiles at the outlet of each rotor, which data are plotted in Fig.10 and 11.

RESULTS OF LASER VELOCIMETER MEASUREMENTS IN TEST CASE 3

As already mentioned a laser velocimeter - the so-called "Two-Focus technique", developed here at DFVLR (Ref.(3)) - was applied for a detailed study of the transonic flow field within the rotor of this single stage compressor. For these measurements in fast moving blade rows the "Two-Focus Velocimeter" was operated as a stroboscope. Up to 15 circumferential measuring positions over one blade spacing were settled in each measuring locus designated by circular symbols in Fig.12. This diagram demonstrates furthermore that measurements could be performed also in the vicinity of the hub and outer casing walls.

As a few examples of this investigation the following figures (Fig.13) illustrate the rotor flow field at three different blade heights. Lines of constant relative Mach number - plotted here over two rotor blade channels - represent the flow pattern at design speed - 20 260 rpm - and maximum efficiency. Near hub a small supersonic flow regime appears - just above M = 1; at 68 % blade height a typical bow shock is located within the blade entrance portion turning over to oblique shocks inside and outside the blades at 89 % annulus height. All data gathered up to now yield a quite complete picture of the transonic rotor flow field, including 3-d shock waves, 3-d flow effects, blade wakes etc.

These few examples should just demonstrate the today's experimental capabilities. The new advanced testing techniques give us great chances to accomplish our theoretical compressor flow model and to develop more realiable hub-to-tip, blade-to-blade or even 3-d calculation methods.

ACKNOWLEDGEMENT

The author gratefully acknowledges the essential contribution of Deutsche Forschungsung Versuchsanstalt für Luft- und Raumfahrt e.V. (DFVLR), Cologne, Forschungsvereinigung Verbrennungskraftmaschinen (FVV), Frankfurt, Motoren- und Turbinenunion (MTU), Munich, and National Gas Turbine Establishment (NGTE), Pyestock, by submitting the complete data of the test compressors. Especially the author wishes to thank Dr. L. Fottner, MTU, and Dr D. Smith, NGTE, for their active support.

REFERENCES

1. Volkmann, H., Fottner, L., and Scholz, N. Aerodynamische Entwicklung eines dreistufigen Transsonik-Frontgebläses. ZfW 22 (1974), Heft 4.

2. Dransfield, D., and Calvert, W. Detailed Flow Measurements in a Four Stage Axial Compressor. ASME-Paper 76-GT-46 (1976).

3. Schodl, R. On Optical Methods for the Flow Measurement in Turbomachines and on the Development of a New Laser-Dual-Beam Technique. in: AGARD-AG-207 (ed.: M. Pianko).

APPENDIX: Geometric Data of Test Case 5

Tab. 1.1: Flow Path Geometry

Z	-546	-351	-160	0	42,3	85,2	124,5	166,0	204,3	243,0
R_{Hub}	0	194,3	194,3	194,3	194,3	194,3	194,3	194,3	194,3	194,3
R_{Tip}	396,1	338,8	284,0	280,2	273,3	266,2	261,5	256,6	252,0	247,4

z	282,5	317,5	350,0
R_{Hub}	194,3	194,3	194,3
R_{Tip}	243,9	240,8	240,8

Tab. 1.2: Location of Instrumentation

z	- 8	47,9	130,0	209,4	287,9	330

All dimensions in mm, z: axial coordinate

Tab. 2.1: Profile Type and Number of Blades

Stage No.	1	1	2	2	3
Blade Row	IGV	Rotor	Stator	Rotor	Stator	Rotor
Prof. Type	C4	DCA	C4	DCA	C4	DCA
Number of Blades	26	47	80	45	74	43

Stage No.	3	4	4
Blade Row	Stator	Rotor	OGV
Prof. Type	C4	DCA	C4
Number of Blades	70	38	72

Tab.2.2 Blade and Cascade Data (on sections parallel to axis)

Radius mm	axial Location Z Leading Edge mm	Trailing Edge mm	Solidity	Stagger Angle deg.	Blade Inlet Angle deg.	Outlet Angle deg.	max Thickness % chord	Leading Edge Radius % chord
Stage No.: 1			Blade Row:	IGV				
194,3	-63,0	-31,7	0,667	1,9	0	3,7	7,0	0,84
215,8	-65,6	-29,0	0,708	3,9	0	7,8	7,0	0,84
237,2	-68,5	-26,2	0,755	6,2	0	12,4	7,0	0,84
258.7	-71,4	-23,3	0,806	8,6	0	17,2	7,0	0,84
280,2	-74,4	-20,2	0,868	11,5	0	22,9	7,0	0,84
Stage No.: 1			Blade Row:	Rotor				
194,3	1,9	41,0	1,905	37,8	52,0	23,5	8,0	0,48
214,1	3,2	39,3	1,686	41,5	51,4	31,6	6,5	0,39
233,8	4,2	38,0	1,511	44,4	51,3	37,5	5,0	0,30
253,6	4,9	36,9	1,370	46,6	51,9	41,2	4,0	0,27
273,3	5,6	36,0	1,253	48,4	52,9	43,8	3,0	0,27
Stage No.: 1			Blade Row:	Stator				
194,3	49,3	79,9	2,083	15,7	42,0	-10,6	5,0	0,60
212,3	48,6	80,0	1,961	15,8	39,4	- 8,1	5,5	0,66
230,2	47,9	80,1	1,852	16,1	38,4	- 6,2	6,0	0,72
248,2	47,3	80,0	1,754	16,9	38,8	-5,0	6,5	0,78
266,2	46,7	79,9	1,667	17,9	40,6	- 4,8	7,0	0,84
Stage No.: 2			Blade Row:	Rotor				
194,3	87,2	123,3	1,733	40,0	54,5	25,5	8,0	0,48
211,1	88,0	121,8	1,600	44,3	54,5	25,5	8,0	0,48
227,9	88,7	120,5	1,484	47,6	54,4	40,8	5,0	0,30
244,7	89,1	119,5	1,385	50,1	54,7	45,5	4,0	0,27
261,5	89,3	118,7	1,299	51,6	55,1	48,1	3,0	0,27
Stage No.: 2			Blade Row:	Stator				
194,3	131,3	160,8	1,852	15,0	40,0	-10,0	5,0	0,60
209,9	130,7	160,5	1,731	14,5	38,0	- 9,0	5,5	0,66
225,5	130,0	160,1	1,623	14,1	36,7	- 8,6	6,0	0,72
241,0	129,3	159,7	1,531	13,8	36,3	- 8,7	6,5	0,78
256,6	128,6	159,3	1,447	13,2	36,3	- 9,9	7,0	0,84

All dimensions in mm or in percent chord (as max. thickness, leading edge radius).
All angles in axial direction and with respect to compressor axis.

Tab.2.2 Blade and Cascade Data (continued)

Radius mm	axial Location Z Leading Edge mm	Trailing Edge mm	Solidity	Stagger Angle deg.	Blade Inlet Angle deg.	Outlet	max. Thickness % chord	Leading Edge Radius % chord
Stage No.: 3			Blade Row:		Rotor			
194,3	167,9	203,1	1,669	42,0	54,4	29,5	8,0	0,48
208,7	168,3	202,4	1,587	45,2	54,7	35,7	6,7	0,40
223,1	168,5	201,7	1,515	47,5	54,8	40,1	5,5	0,33
237,6	168,7	200,8	1,451	50,3	56,2	44,3	4,2	0,25
252,0	168,8	200,2	1,391	52,0	57,4	46,6	3,0	0,25
Stage No.: 3			Blade Row:		Stator			
194,3	211,0	238,0	1,605	15,2	39,7	-9,4	5,0	0,60
207,6	209,7	238,9	1,563	14,3	37,1	-8,5	5,5	0,66
220,9	209,4	238,6	1,515	14,1	36,2	-8,1	6,0	0,72
234,1	208,7	238,9	1,475	14,0	36,4	-8,5	6,5	0,78
247,4	208,0	239,1	1,439	13,9	37,3	-9,6	7,0	0,84
Stage No.: 4			Blade Row:		Rotor			
194,3	245,0	281,2	1,542	43,0	55,5	30,5	8,0	0,48
206,7	245,4	280,7	1,488	46,0	55,9	36,1	6,7	0,40
219,1	245,6	280,6	1,437	47,8	56,2	39,5	5,5	0,33
231,5	246,2	280,0	1,389	50,6	57,7	43,5	4,2	0,24
243,9	246,7	279,5	1,346	52,9	59,1	46,6	3,0	0,23
Stage No.: 4			Blade Row		Stator			
194,3	289,9	315,6	1,568	14,8	39,4	-9,8	5,0	0,6
205,9	288,9	315,7	1,538	14,4	37,5	-8,7	5,5	0,66
217,5	287,9	315,7	1,516	14,5	37,0	-8,0	6,0	0,72
229,2	286,9	315,8	1,493	14,6	37,2	-8,0	6,5	0,78
240,8	285,9	315,8	1,471	14,8	38,0	-8,5	7,0	0,84

All dimensions in mm or in percent chord (as max. thickness, leading edge radius).
All angles in axial direction and with respect to compressor axis.

Tab.1 Prime design characteristics of Compressor Test Cases 3 to 5.

Test Case	Type of Machine	Mass Flow	Design Press.Ratio +)	Data Effic. +)	Tip Speed
3	1-stage trans.compressor	17.3 kg/s	1.51	81 %	425 m/s
4	3-stage trans.compressor	61.7 kg/s	2.9	83 %	470 m/s
5	4-stage trans.compressor	24.1 kg/s	2.95	86 %	362 m/s

+) total to total data

Tab.2 Stage design data of the single-stage transonic compressor (DFVLR - Test Case 3).

Parameter	Stage 1	
Pressure Ratio	1.51	
Temperature Rise	0.154	
Blade Row	Rotor	Stator
Number of Blades	28	60
Profile Type	MCA	NACA-65 1)
Solidity hub tip	2.0 1.34	2.4 1.52
Mach Number (max.)	1.37	0.76
Diffusion Factor (max.)	0.53	0.46

1) Circular Arc Camber Line

Tab.3 Stage design data of the 3-stage transonic compressor (MTU-Test Case 4).

Parameter	Stage 1		Stage 2		Stage 3	
Pressure Ratio	1.444		1.435		1.402	
Temperature Rise	0.13		0.12		0.12	
Blade Row	Rotor	Stator	Rotor	Stator	Rotor	Stator
Number of Blades	21	29	31	53	45	41
Profile Type	wedge type	NACA 65 1)	wedge type	NACA 65 1)	DCA	NACA 65 1)
Solidity hub tip	1.85 1.22	1.85 0.90	1.85 1.25	1.96 1.22	2.00 1.25	1.93 1.23
Mach Number (max.)	1.54	0.71	1.24	0.78	1.08	0.67
Diffusion Factor	0.47	0.31	0.42	0.45	0.47	0.32

1) Circular Arc Camber Line

Tab.4 Stage design data of the 4-stage transonic compressor (NGTE - Test Case 5).

Parameter		Stage 1		Stage 2		Stage 3		Stage 4	
Pressure Ratio		1.31 (average stage pressure ratio)							
Temperature Rise									
Blade Row	IGV	Rotor	Stator	Rotor	Stator	Rotor	Stator	Rotor	OGV
Number of Blades	26	47	80	45	74	43	70	38	72
Profile Type	C4 1)	DCA	C4 1)	DCA	C4 1)	DCA	C4 1)	DCA	C4 1)
Solidity hub tip	0.67 0.87	1.91 1.25	2.08 1.67	1.73 1.30	1.85 1.45	1.67 1.39	1.61 1.44	1.54 1.35	1.48 1.47
Machnumber (max.)		1.22							
Diffusion Factor									

1) Circular Arc Camberline

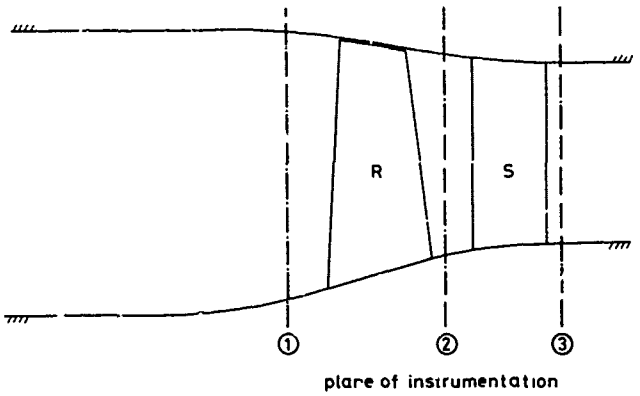

(a) Test Case 3 (1-stage)

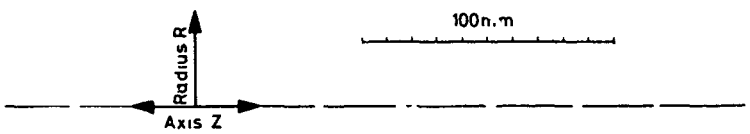

(b) Test Case 4 (3-stage)

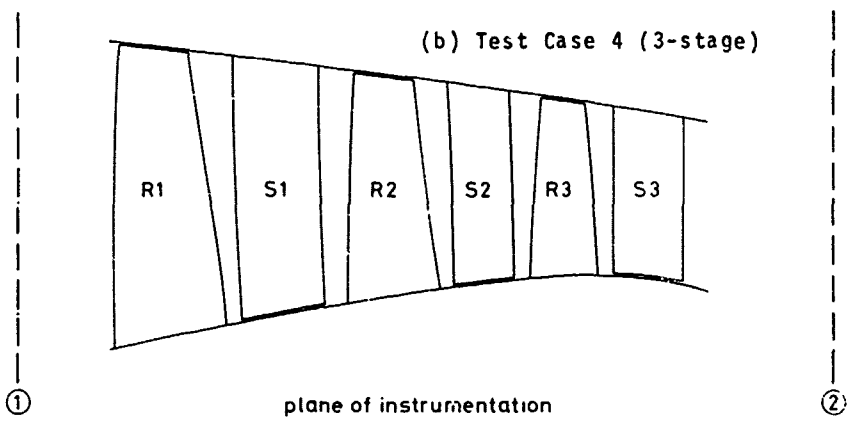

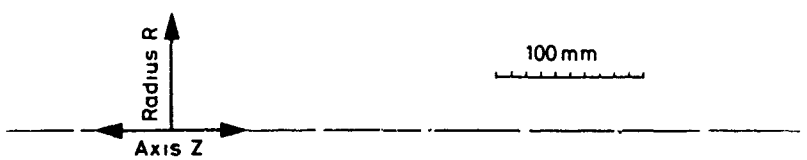

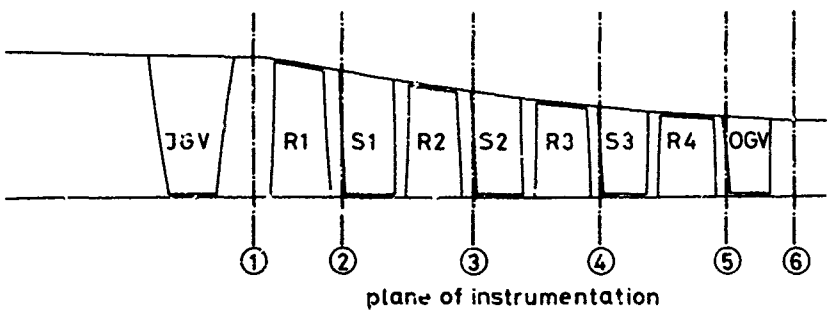

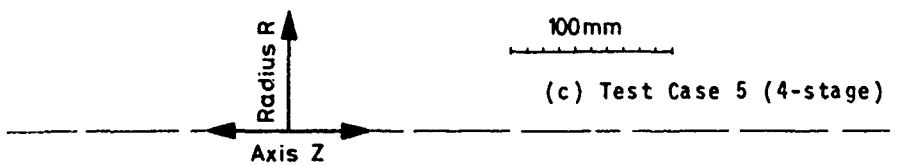

(c) Test Case 5 (4-stage)

Fig.1 Annulus geometry of the test compressors

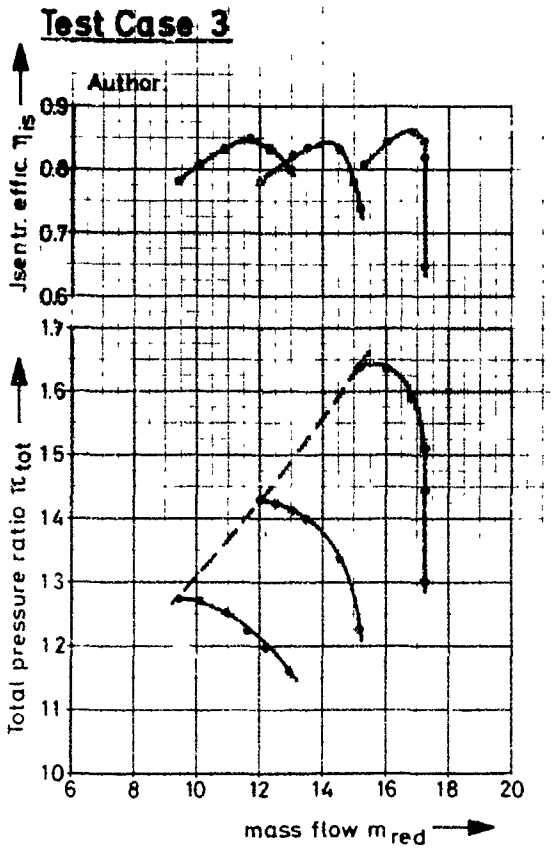

Fig.2 Overall performance of the 1-stage compressor (Test Case 3).

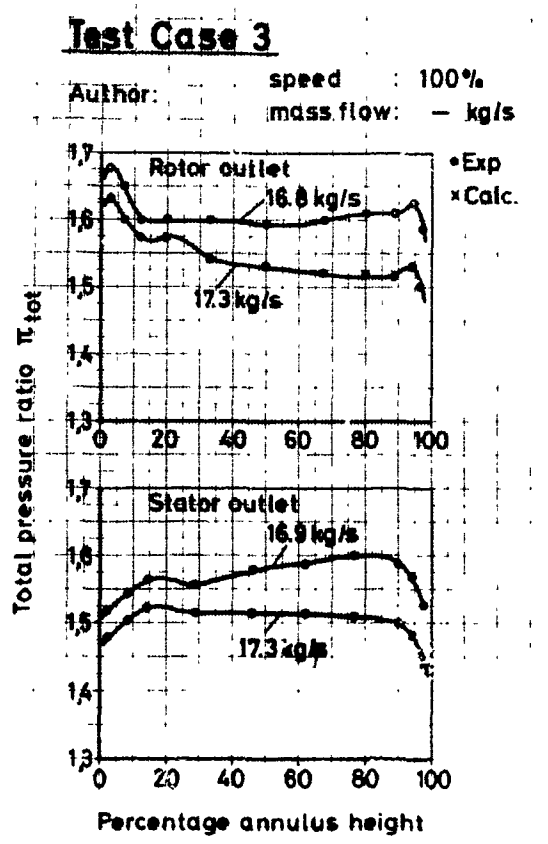

Fig.3 Total pressure ratio of rotor and stage versus radius for Test Case 3

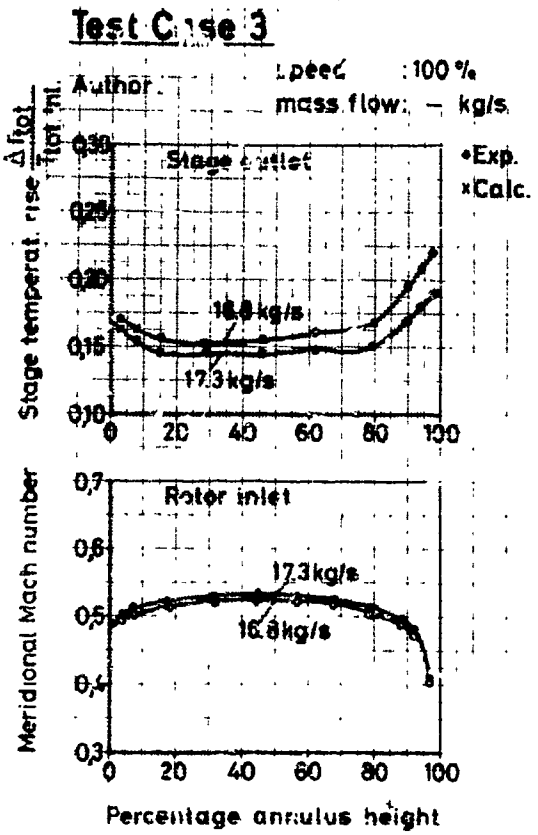

Fig.4 Stage temperature rise and meridional Mach number at rotor inlet versus radius for Test Case 3.

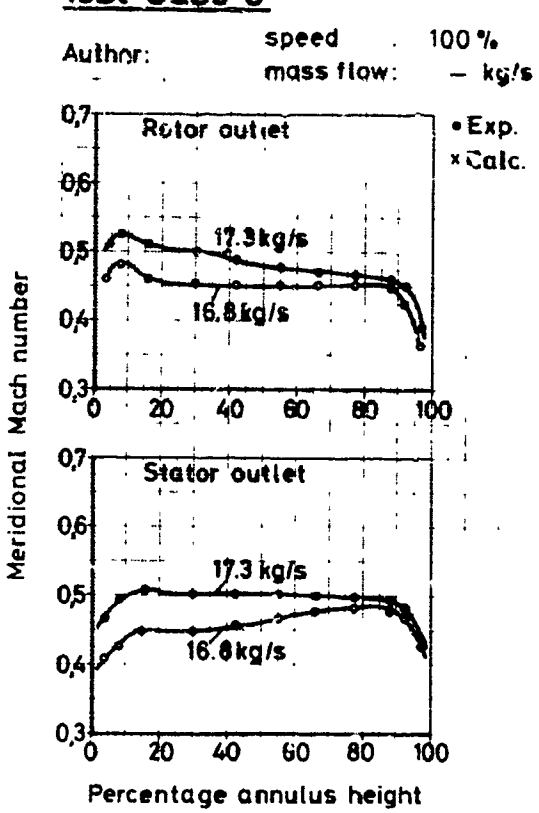

Fig.5 Meridional Mach number at rotor and stator outlet versus radius for Test Case 3

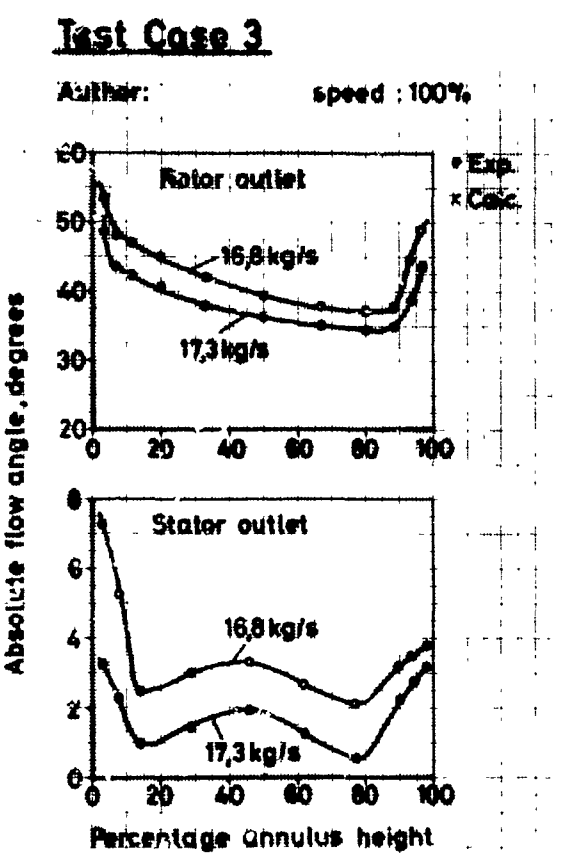

Fig.6 Absolute flow angle at rotor and stator outlet versus radius for Test Case 3.

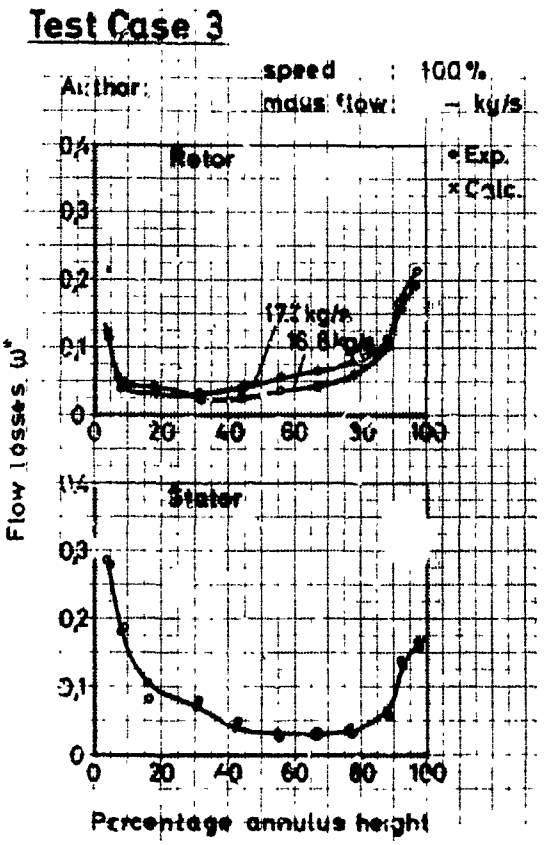

Fig.7 Flow losses of rotor and stator versus radius for Test Case 3.

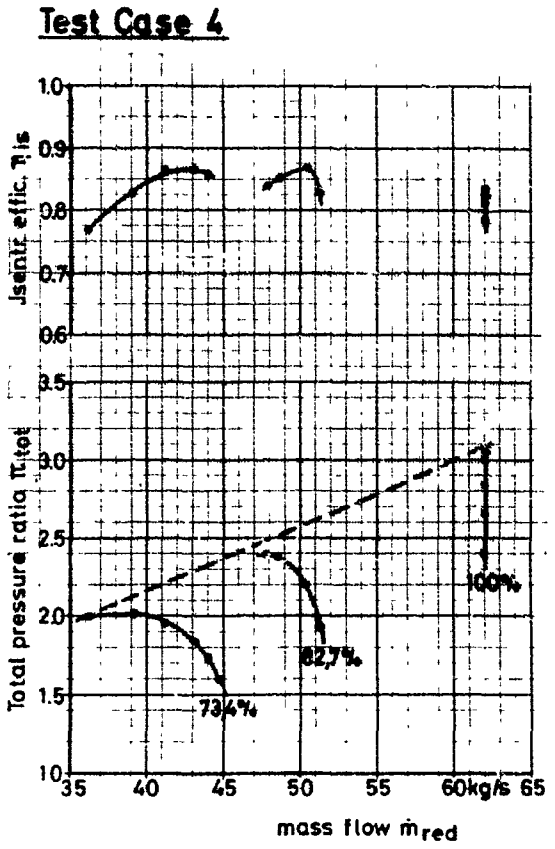

Fig.8 Overall performance data of the 3-stage transonic compressor (Test Case 4).

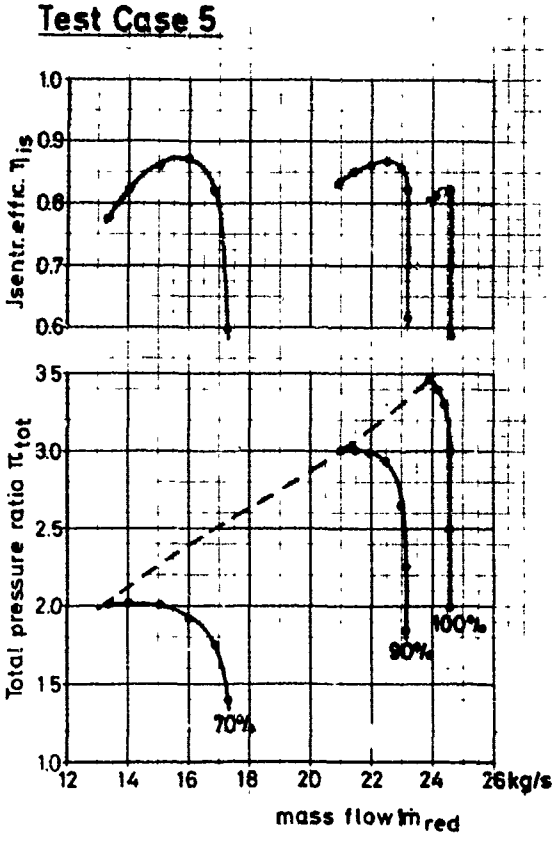

Fig.9 Performance map of the 4-stage transonic compressor (Test Case 5)

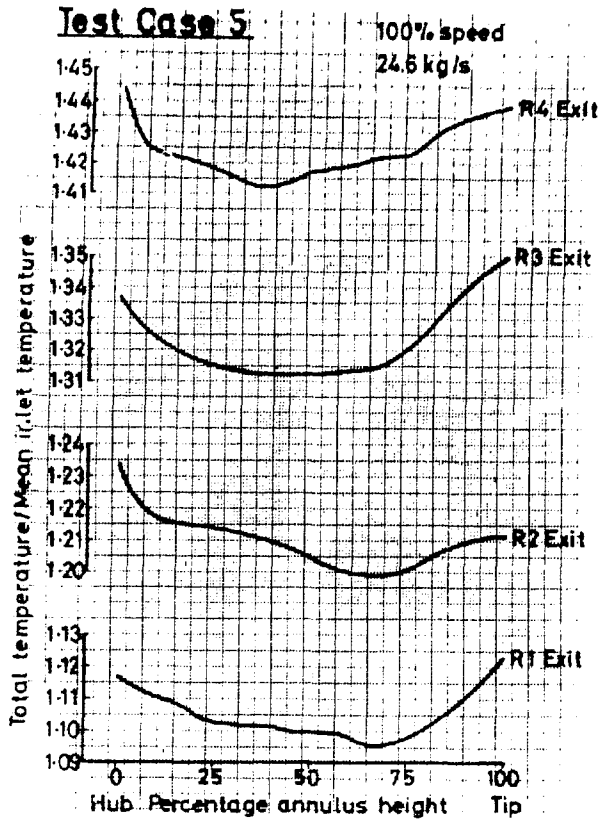

Fig.10 Total temperature ratio at the exit of each rotor versus radius for Test Case 5.

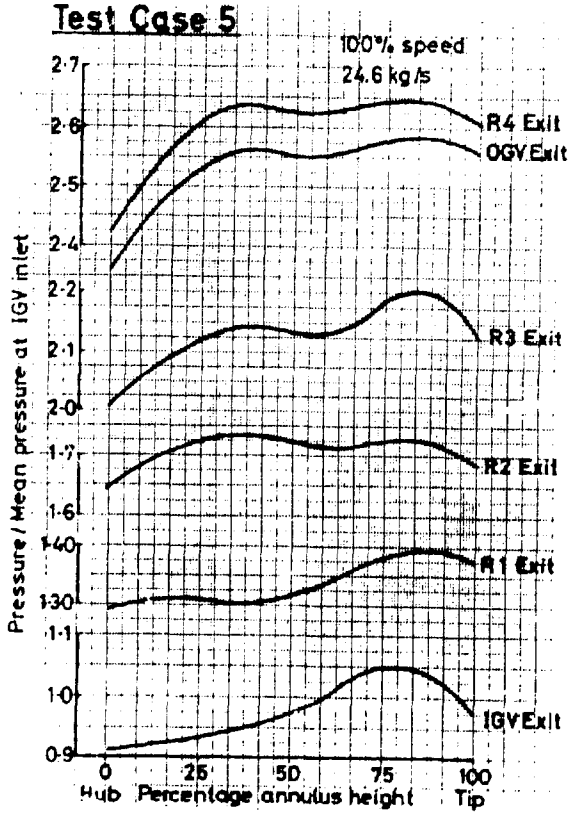

Fig.11 Total pressure ratio at the outlet of guide vanes and rotors versus radius for Test Case 5.

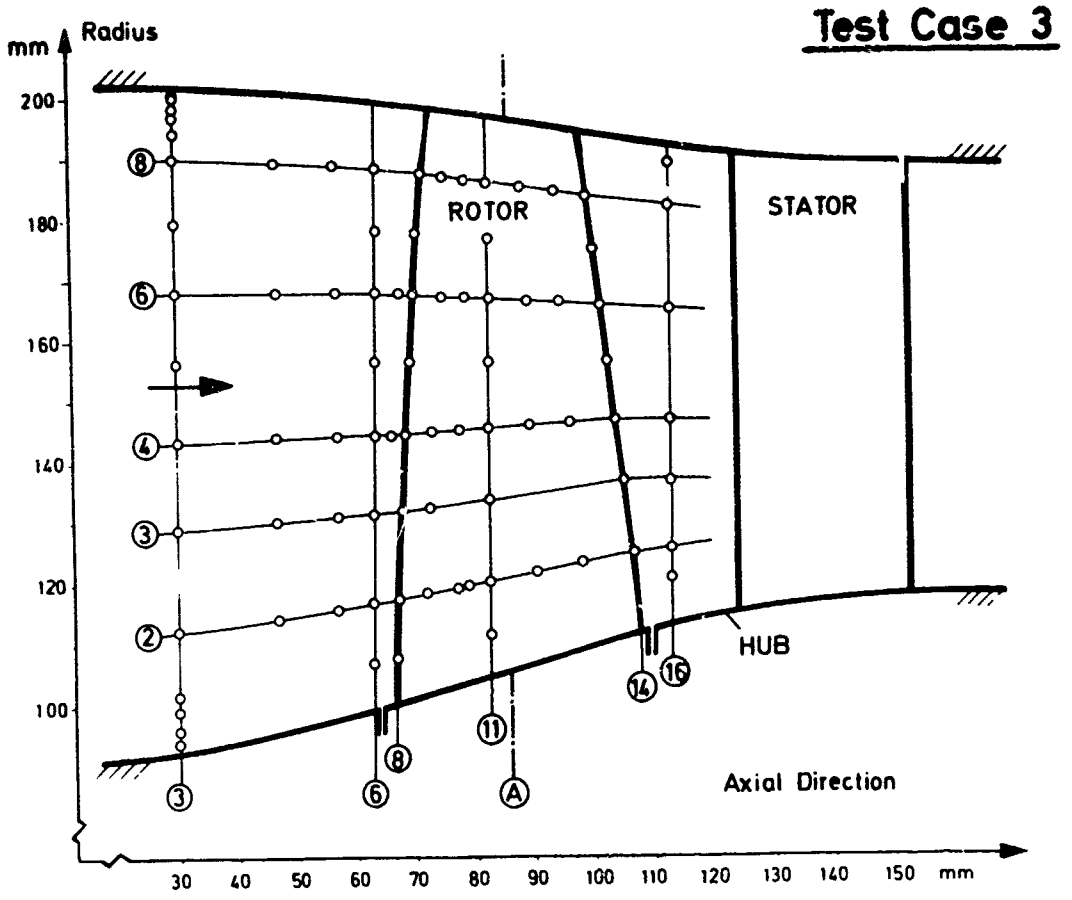

Fig.12 Flowpath with laser velocimeter measuring loci of the 1-stage transonic compressor (Test Case 3).

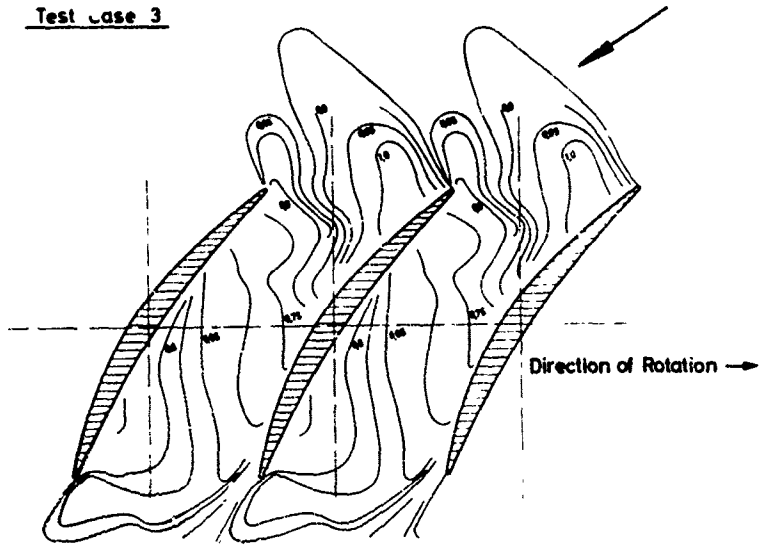

(a) Flow pattern at 18% blade height (stream line 2),

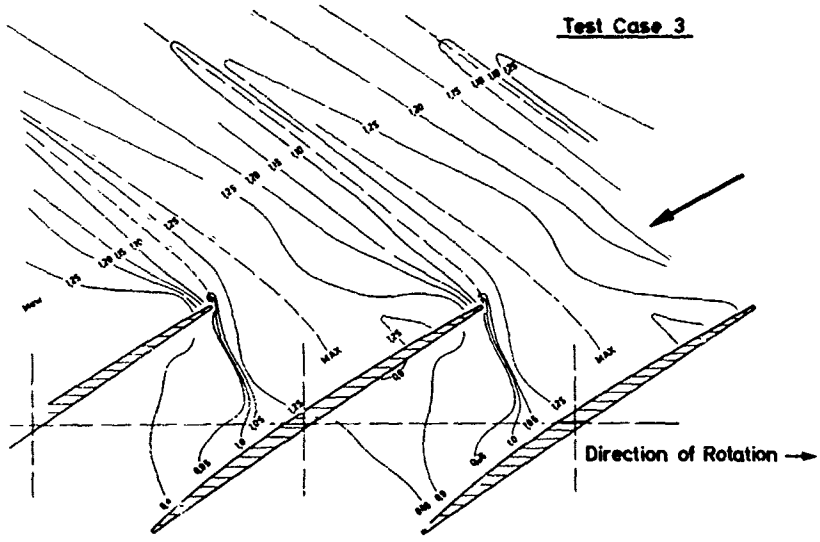

(b) Flow pattern at 68% blade height (stream line 6),

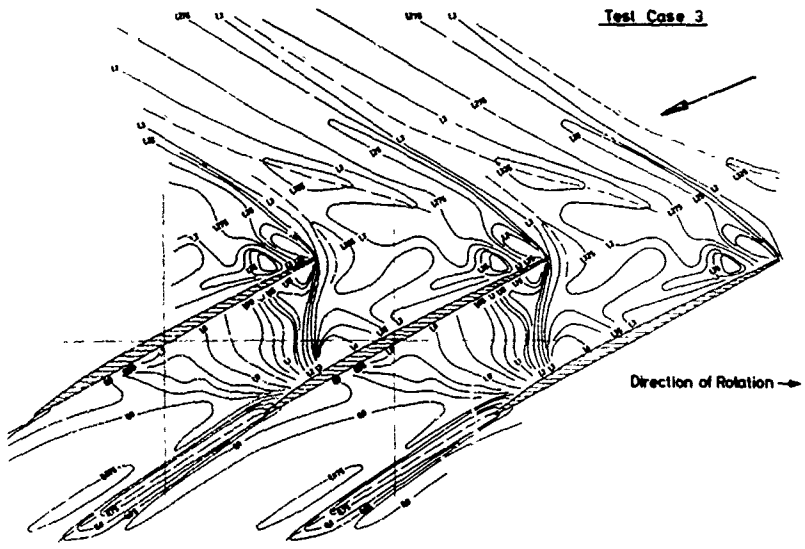

(c) Flow pattern at 89% blade height (stream line 8),

Fig.13 Lines of constant relative Mach number within the rotor blading of Test Case 3 at design speed.

COMPARISON BETWEEN THE CALCULATED AND THE EXPERIMENTAL RESULTS OF THE COMPRESSOR TEST CASES

by

H.B. Weyer

and

R. Dunker

DFVLR-Institut für Luftstrahlantriebe
Linder Höhe, 5 Köln 90, W.Germany

About forty experts originally planned to contribute to this AGARD-Specialists Meeting by carrying out calculations on the five test machines. Concerning the compressor cases eight authors submitted calculated data which finally could be compared to the corresponding experimental results. The names of those few experts are listed below in series of their authors' number:

No.2:	Ch.Hirsch,	University of Brussels, Belgium,
No.3:	F. Farkas,	BBC (Brown, Boveri & Cie), Baden, Switzerland,
No.4:	B. Hüvel, W. Huck	University of Stuttgart, Germany
No.6:	D. Smith,	National Gasturbine Establishment, Pyestock/England,
No.7:	R. Dunker,	DFVLR-Institut für Luftstrahlantriebe, Köln, Germany
No.10:	E. Benvenuti,	Nuovo Pignone, Firenze, Italy,
No.12:	J. Fabri,	O.N.E.R.A., Châtillon-sous-Bagneux, France
No.26:	E. Macchi,	Politecnico di Milano, Italy.

Just to get a quick survey the following table contains some rough informations on the calculation techniques used by the different authors, on the computers available, and on the computing time necessary to perform the data of one compressor operating point. The last four columns present some fundamental features of the loss prediction methods used with the calculation techniques.

Table: General Informations on Calculation Methods

Author	Calculation Method	Computer	Average Comp. Time p.Point	Profile	Loss Correlation Shock	Separat.	Second.
2	Finite Element Method - Through Flow -	CDC 6 5 00	3:70-300 sec 4: 5:70-300 sec	with AVR	yes	no	distri-buted
3	Streamline Curvature Method - Duct Flow -	IBM 370/158	3: 4:max.180 sec 5:	with AVR	yes	yes	distri-buted
4	Streamline Curvature Method - Duct Flow -	UNIVAC 1 108	3: 6 sec 4: 15 sec 5: 37 sec	with AVR	yes	no	distri-buted
6	Streamline Curvature Method - Duct Flow -		3: 4: 5:	yes	yes	no	distri-buted
7	Matrix Method - Through Flow -	TR 440	3:120-300 sec 4:120-300 sec 5:	without AVR	yes	no	uniform
10	Streamline Curvature Method - ? -	IBM 370/400	3: 4:100 sec 5:	with AVR	yes	no	distri-buted
12	Simple Radial Equilibrium						
26	Streamline Curvature Method - Duct Flow -	UNIVAC 1 108	3: 4: 5: 20 sec	without	no	no	uniform

Additional informations on the various flow calculation procedures may be obtained from comments and presentations of the users included at the end of this paper.

Presenting the comparison between the calculated and experimental results of the compressor test examples the authors of this paper will restrict themselves to submit the facts not to try an interpretation which will be imperfect due to the abundance of material and to certain lack of detailed informations. However, the series of the succeeding figures seems to be well appropriate to check the accuracy and reliability of the today's calculation methods. This is especially true because the authors of calculations did not have the experimental results available when carrying out their computations.

Test Case 3 - the single-stage transonic compressor - has been investigated by the authors 2, 4, 6, 7, and 12. Fig.1a to d present the calculated overall performance data compared to the experimental results. The blade element performance for test case 3 at design speed (20 260 rpm) and at a mass flow of 17.3 kg/s is shown in Fig.2 - 6:

- the total pressure ratio at rotor and stator outlet in Fig.2a - e,
- the stage temperature rise and the meridional Machnumber at rotor inlet in Fig.3a - e;
- the meridional Machnumber at rotor and stator outlet in Fig.4a - e;
- the absolute flow angle at rotor and stator outlet in Fig.5a - e;
- the rotor and stator flow losses in Fig.6a - d.

The corresponding data for the maximum efficiency point at design speed (mass flow: 16.8 kg/s) are presented analogously in Fig.7 to 11 (exc. author 2).

Test Case 4 - the 3-stage transonic compressor - has been considered by the authors 3, 4, 7, and 10. As already outlined in paper 10 of this issue the results of the interstage measurements in this compressor are believed being not sufficiently accurate to be included into the comparison; thus, the comparison encloses only the overall performance data which are shown - for the different authors - in Fig.12a to d.

Test Case 5 - the 4-stage compressor - has been treated by the authors 2, 4, and 26. Fig. 13a to c illustrates the results of the theoretical and experimental investigation of this compressor's overall performance. Detailed through-flow calculations were originally required to be done at mass flows of 24.6 and 24.4 kg/s on the 100 % speed line; however, the experimental results of the interstage flow traverses are only available at 24.6 kg/s with a corresponding overall pressure ratio of 2.5. The calculations yielded much higher pressure ratios, such that the comparison between the calculated and the experimental results becomes ineffective, In this case, a true comparison requires the pressure ratio not the mass flow as an input data for the flow calculations.

CONCLUSIONS

Although limited in many aspects the comparison between the compressor experiments and theory allows to make some principal statements. For the calculation of the compressor's overall performance the experts have used one-dimensional techniques as well as duct flow and through flow methods. No characteristic differences encounter from the various methods indicating that a severe effect of a more or less complete physical flow model does not exist. The deviations as far as observed with respect to the experiments are primarily due to the inaccuracy of the flow loss and flow turning predictions, particularly at off-design operating conditions.

The duct-flow and through-flow calculation techniques were mainly utilized to compute in detail the compressor internal flow. Streamline curvature, matrix, and finite element methods thereby served as numerical procedures to resolve the flow equations. Concerning the flow parameters calculated outside of the blade rows no evident superiority was observed for any method even for the through-flow techniques although their physical background seems to be more accomplished taking for instance into account the effects of blade thickness, blade turning, a.s.o.

Discrepancies to the experimental results (test case 3) are believed being caused by an inaccurate loss prediction, by an inexact estimation of the wall boundary-layer blockage, and by 3-dimensional flow effects which are not accounted for in the 2-dimensional calculation techniques.

Inside the blade rows great discrepancies between laser experiments and corresponding through-flow calculations were observed for test case 3 arising to the basic question how to define equivalent mean stream surfaces for calculations, and how to distribute flow losses and turning within the blade channels. This subject is described in more detail by R. Dunker in his succeeding comments.

COMMENTS OF AUTHORS OF CALCULATION

Author: 3; F. Farkas, BBC, Baden

I would like to give you a short comment on our calculation technique for the test case 4.

Here you see again the plotted flow path, which was shown already by Dr. Weyer in the introduction. I want to call your attention to some further detail which were not yet mentioned. Please note the very high specific mass flow of that compressor. It is an engineering work of very high standard. If it were scaled up for 3000 rpm, the corresponding mass flow would be about 1150 kg/s. That is an extremely high figure, about 3 times higher than corresponding values for industrial gas turbine compressors usually are.

All 3 stages are transonic.
The calculation was performed by mean of a stream line curvature type computer system. The correlations for loss and deviation take into account the following parameters: blade element geometry, load, relativ inlet Mach number, axial velocity density ratio, critical throat area, actual throat area and incidence, Reynolds number, surface roughness of the aerofoil, radial clearances, secondary and end wall losses. As an example you see a typical efficiency distribution along the first stage rotor blade height. The efficiency is high in the middle part and has a decreasing character near hub and tip.

Starting the calculation, we experienced same choked areas in the 1st, 2nd and 3rd rotor, and 2nd stator. Due to this choking in the 1st rotor, the original MASS FLOW without choking criteria had to be reduced by about 3 %. For the same reason losses were to adjust as well. The resulted mass flow we got at the end, as you see, is in rather good agreement (1 %) with the experimental value at design speed and pressure ratio.

Concerning the LOSSES, the next thing was to investigate how our correlation system could be applied for the test case given. We had to look if we could find a reference point, where this comppessor would look similar as one can be handled by our program, that means, would have similar minimum throat area and incidence. We succeeded, and the entire calculation was built upon this reference point. The losses and deviations were changed for the off-design calculation always in respect to this reference point. The performance map generated in this manner is again in resonable agreement with the experimental data.

The SURGE LINE calculation for 100 % speed, here the rear stage is supposed to be responsible for surge, was based on the lift coefficient. The point, in which the lift coefficient achives its maximum, was marked as surge or near surge point. At part speeds, where the first highly transonic stage is going to cause stall, we looked for the equivalent diffusion factors and for the change of choke margins. As a result, the stall line prediction turned out to be satisfactory, about 3 % accurate compared with the test results.

Author: 4; B. Hüvel, W. Huck, Uni. Stuttgart

1. CALCULATION METHOD

The two-dimensional calculation method is an axisymmetric "Streamline Curvature Duct-Flow" method (see Ref. 1). The plane, where the computation takes place, is the meridional plane formed by the radius-vector and the axis of the compressor.By dividing the total mass flow in equal parts between the blade-rows, working points or points of the sreamlines are defined. In this points the flow is computable by full filling the r-component of the EULERIAN equation of motion or in other words the radial equilibrium equation. For this the radius of curvature of the meridional section of a streamline must be known. This radius of curvature is determined by a spline-function.

2. LOSS AND FLOW ANGLE CORRELATION

2.1 LOSSES

2.1.1 Subsonic Losses

The cascade loss ζ is defined by the following equation:

$$\zeta = (\zeta_{po} \cdot F_1 \cdot F_2 \cdot F_3 + \zeta_{sec}) \cdot f_{(AVR)}$$

ζ_{po} is calculated by the Lieblein's profile loss correlation (incompressible). The factor F_1 stands for the influence of incidence, F_2 for the influence of compressibility, and F_3 for the Reynolds number influence. As described by WOLF[2], the secondary-loss-coefficient is dependent on the averaged blade loading. With a chosen function this loss coefficient is distributed along the blade-height.

Finally the cascade-loss-coefficient is corrected by a function of the axial velocity ratio ($f_{(AVR)}$).

2.1.2. Transonic losses

The cascade loss ζ is defined by

$$\zeta = (\zeta_{po,\,trans} \cdot F_2 \cdot F_3 + \zeta_{sec} + \zeta_{shock}) \cdot f_{(AVR)}$$

The profile loss $\zeta_{po,trans}$ is determined by SWAN's method [3]. The factor F_2, F_3 and and ζ_{sec} are identical in the subsonic values. The method of LEWIS, MILLER and HARTMANN[4] is used to calculate the shock loss ζ_{shock}.
The correction of the transonic cascade-loss-coefficient by the function of the AVR is identical in the subsonic correction.

2.2 Flow Angles

To determine the deflection $\Delta\beta$ it is necessary to know the nominal angles β^*_1 and β^*_2. For this correlations of CARTER and HOWELL are applied (nominal deviation). The deflection itself is calculated by HOWELL's method with respect to the incidence, the Mach number and the Reynolds number.

3.COMPRESSOR INLET COMPUTATION

In oder to apply the calculation method desribed in section 1 the inlet is divided in 10 to 20 "fictitious" cascades without deflection. The anullus wall boundary layers and flow losses are included in the computation. The flow data behind the last "fictitious" cascade are the inlet data of the first cascade of the compressor.

References

1. NOVAK, R.A. — Streamline Curvature Computation Procedures for Fluid Flow Problems. ASME Journal of Eng. for power, Vol. 89, A, 1967, pp. 478-490

2. WOLF, H. — Untersuchungen von Sekundärströmungen in geraden Verdichtergittern. Maschinenbautechnik 14, 1965, No. 12, pp. 641-645

3. SWAN, W.C. — A practical Method of Predicting Transonis Compressor Performance , Journal of Eng. for Power, Vol. 83, 1961, pp. 322-338

4. LEWIS, G. W., MILLER,G. R., HARTMANN,M.J., — Shock losses in Transonic Compressor Blade Rows, Journal of Eng. for Power, Vol. 83, 1961, pp. 235-242

Author: 6; W. J. Calvert, NGTE,Pyestock

The NGTE predictions were done using a streamline curvature, duct-flow program, with correlations to provide information on the S_1 surfaces. In our experience this method is best suited to well matched points on the compressor characteristics, and so we use a one-dimensional program for predictions of the overall characteristics. Therefore, the correlations do not include corrections for off-design conditions.

The annulus blockage was assumed to be 0.99 at inlet to the first blade row and to decrease by half a per cent with each further blade row. This was allowed for by calculating an effective flow annulus inside the metal annulus, such that the hub displacement thickness was half that at the outer casing. If necessary, further small changes were made to this flow annulus to smooth out regions of high curvature. For the single stage fan test case (test case 3) radial calculating planes were placed at the leading and trailing edges of each blade row, and a further 5 planes were used both upstream and downsream of the blade rows. Five equispaced grid points were taken on each radial line.

The Howell correlation was used to calculate blade deviation with an additional term to allow for axial velocity ratio.

The rotor loss coefficient was found from an NGTE correlation with diffusion factor and percentage blade height, with a shock loss component depending on the inlet Mach number.

The stator loss coefficient was calculated as the sum of factors to allow for profile, secondary and annulus wall losses. The secondary and annulus wall losses were uniformly distributed over the annulus height.

Author: 7; R. Dunker, DFVLR, Cologne

The through-flow calculation technique - based on the matrix method - that has been used at DFVLR to compute the compressor flow is treated in detail by Prof. Marsh and Dr. Davis during this meeting. Thus the following comments are primarily concerned with the comparison between the calculated rotor flow data of test case 3 and the corresponding experimental results of laser velocimetry. Flow data taken outside of the blade rows by conventional probes are included just as an additional information.

In Fig. 14 the compressor flowpath is shown. Indicated are also - by the circular symbols - the radial and axial positions of the optical measurements. At each point up to 15 distinct measuring positions were realized over one blade spacing.

The calculations as well as the measurements were performed at design speed and a mass flow of 16.8 kg/s.

Fig. 15 represents the calculated results and the experiments in plane 3 far upstream of the rotor; the meridional Machnumber Ma_m is plotted against the relative annulus height. The results are in quite good agreement.

It should be clearly emphasized at this point that the data calculated with the through-flow-method represents results, which are only valid on the meridional mean streamsurface S_{2m} and which are not representative in circumferential direction. The experimental data determined by conventional measuring technique are averaged values over a blade pitch considering the rotating system, whereas the optical measurements yield distinct local results in this sense.

Proceeding nearer to the rotor-blade-row, for the experiments as well as for the calculations an influence of the blades on the upstream flow conditions can be observed in addition to the influence of the annulus contraction.
At the same time the differences between the experimental results and those calculated with the through-flow-method become greater. Looking at the quite good agreement of the duct-flow-calculations with the experimental results conventionally measured, near the rotor leading edge, some calculations were performed with the matrix-program ass duct flow-computations. The radial distribution of these results agreed quite well with those measured by probes and calculated by real duct-flow-programs.
The flow-turning -, loss - distribution and the positioning of the calculation planes inside the rotor certainly have a severe influence on the upstream flow conditions in the through-flow-calculation.
For the matrix-method it is a condition sine qua non that the relative Machnumber at the first calculation plane within the rotor must be less unity. Even though this is attended, however a numerical influence of the spreading of the calculation planes remains including the loss distribution. In the following it shall be tried to give some hints, why this influence may occur.

Fig. 16 shows lines of constant relative Machnumber throughout two roter-blade-channels along streamsurface of revolution 2 (s. fig.1). Streamsurface 2 lies at nearly 18% blade height. The lines are constructed with the results of the optical measurements. The relative inflow Machnumber is subsonic. Remarkable is the supersonic bubble on the suction side near the blade leading edge.

In Fig. 17 the relative Machnumber is plotted against the blade pitch for streamsurface 2 in measuring plane 6, which lies upstream of the rotor. The amount of the relative Machnumber determined by conventional measuring technique as well as the calculated one agree rather well with the mean value of the laser-measurements.

In Fig. 18 the relative Machnumber distribution is shown within the rotor at plane 11. Comparing the result of the calculation and the distribution measured with the laser velocimeter an evident discrepancy can be observed.

Fig. 19 demonstrates the relative Machnumber against one blade pitch downstream of the rotor in plane 16. A small difference can be realized between the conventionally measured result and the calculated one. This differenee may result out of a wrong evaluation of the deviation at this blade height. However both values agree tendentiously with the averaged one of the optical measurements.

The following figures represent some experimental and calculated results along streamsurface of revolution 8 for further comparisons. Streamline 8 lies at 89% blade height near the blade tip. Here the upstream relative flow condition is supersonic.

Fig. 20 shows constant relative Machnumber lines throughout two blade-channels. The shock-position can be clearly identified. The oblique shock within the blade-channel impignes on the neighbouring blade at nearly 80% of the blade chord. It is remarkable that the deceleration from supersonic to subsonic velocities gradually takes place over a greater distance of the blade channel.

In Fig. 21 the relative Machnumber is plotted against one blade pitch in plane 6. The variation of the relative Machnumber measured with the laser-velocimeter in circumferential direction is small. The conventionally measured amount agrees quite well with the distribution determined by the optical measurements, whereas the calculated relative Machnumber is a little bit higher.

Proceeding inside the rotor to plane 11 Fig. 22 represents the result of the calculation and the interpretation of the laser-velocimetry. Remarkable is the low relative Machnumber determined by the calculation on the mean streamsurface $S2_m$ compared with the distribution of the experimental results.

Fig. 23 illustrates the relative Machnumber against one blade pitch in plane 16. Again the result of the conventional measurement is in quite good agreement with the optically determined distribution. Striking is the relative small difference between these and the amount of the relative Machnumber calculated by the matrix-program in this point in contrast to the results in plane 11.

Summerizing it is remarkable that a relative good agreement exists upstream and downstream of the rotor-blade-row betweem the calculated data and those measured, whereas within the blade row from hub to tip a significant discrepancy can be observed between the calculated values and the relative Machnumber distributions measured with the laser-velocimeter, in particular in the blade tip region, where subsonic as well as supersonic regions are existing over the blade spacing caused by the shock system.
One has to ask whether or to what extent the calculated flow conditions on the mean streamsurface $S2_m$ can represent the real flow conditions within the rotor. Secondly the question arises, what is the correct mean value or how it can be determined at all, if sub- and supersonic regions exist inside the blade-channel. Another question is, whether it is possible to determine the real three-dimensional flow through turbomachines, inside the blade rows included, by two- or quasi - three dimensional calculation methods.
On the other hand there exists the question, whether through-flow-methods are needed to calculate the performance of compressors, or if duct-flow or even simpler methods give sufficient answers for that purpose with the empirical loss models incorporated.

It has not been the intention of this presentation to give decided explanations, but to present some interesting results and hence resulting questions.

Author: 10; E. Benvenuti, Nuovo Pignone, Firenzl

1. METHOD OF FLOW - ANALYSIS

The calculations were performed using a computer program able to compute all the conditions within an axisymmetric, annular flow-field. The fluid is assumed to be an ideal gas, and a variation of specific heat with temperature is accounted for. It is assumed that there is no transfer of mass, momentum, or energy across streamlines in the flow. Conditions are evaluated at a series of "computing stations" spaced axially in the flow, the locii of a number of sreamlines disposed radially in the flow are sought by the program, and the intersection of the streamlines with the stations forms the finite-difference mesh used in the calculation scheme.
At each computing station, full radial equilibrium is considered, accounting for enthalpy and entropy gradients along the radius, as well as the effect of the streamline curvature and slope.
The streamline locations at the calculation stations are found by means of relaxation procedure; the convergence criterion is based on the comparison between the mass flow obtained by integration of the velocities and fluid densities along a computing station and the input mass flow.

2. CALCULATION OF CASCADE PERFORMANCE

The computer program has several options incorporated for calculating losses and deviations along the streamlines between the leading and the trailing edges of each blade row. Some of these options incorporate proprietory data coming from the Company's experience, and therefore they could not be used for the present demontrative calculations. Therefore, the option incorporating the NASA correlations described in Ref. 1 for calculating profile losses and deviations was used for most of the blade sections specified for the compressor. Some problems were encountered for the supersonic blade portions of the first two rotors, since only the thickness distribution in a small number of points along the chord line was given, but nothing was specified about other parameters, like form of the camber line and supersonic turning on the forward portion of the airfoil. Therefore, shock losses on such sections were not calculated, but losses existing on similar blades tested were introduced (see, for example, Ref. 2,3 and 4). Some extra corrections were introduced to account for end-wall effects (tip clearance and secondary losses) in accordance with the published data used.
Deviations were calculated following the methods described in Ref. 1; however, on the hub sections of the rotor blades and on hub and tip sections of the stator blades empirical corrections of the deviation angles were considered, to account for some secondary effects, again following the experimental results taken from the cited references.

The effect of the axial velocity variation on deviation angles was accounted for using Horlock's formula

$$\delta_{AVR} = 10\ (1 - AVR)$$

3. CALCULATION OF THE PERFORMANCE POINTS

Using the computer program and the data dedcribed above, some performance points were calculated at 83% and 100% of design speed. However, the correlations described above between the present compressor and published experimental data were applied carefully only at 100% speed; for the 83% speed line, the same corrections to the internally computed performance as for 100% were used, since the time required to check the corrections again exceeded that provided for this work. Therefore, the results obtained for the lower speed may be less accurate, expecially for the overall efficiency, which we estimate to be calculated in excess with respect to the experimental values.
The surge points were estimated from the examination of the loading levels on some critical airfoil sections; it seems that surging at 100% speed is originated from stalling of the third stage stator hub section and at 83% speed (probably) by stalling of the second stage stator hub section.
At 100% speed, the calculation for the given 62.1 kg/sec. mass flow was not possible, since the flow resulted excessive; one reason may be that the rotor blade geometry was supplied for the non-rotating conditions, and no blade angle increase produced by the untwisting due to the centrifugal force was considered; therefore, if the value of 62.1.Kg/sec. is experimental, it was produced by blades having, when operating at 100% speed, inlet angles on the supersonic sections different from the values considered in the calculation.
At 83% speed, instead, the calculation was possible with the given value of 48,5 Kg/sec., and this fact was probably due to the minor effect of the centrifugal force on the blade untwist at reduced speed.

4. REPRESENTATION OF THE RESULTS

Overall performance curves are represented on the first sheet. The two points for which detailed data are supplied are indicated. For the description of the data coming from the flow-field calculations, a non-dimensionalized channel height was used, starting from zero at the hub line up to 100% at the outer casing. The quantities (except losses) were given on an inlet and an exit plane, corresponding to the axial coordinates 0 and 406,7 respectively; the two positions corresponding to the indicated measuring planes (Z = -63 and 491,7 respectively) were not used, since there the meridional geometry of the flow path was not specified.

References

1. ROBBINS, W.H., JACKSON, R. J., LIEBLEIN, S., Blade-Element flow in Annular Cascades, Aerodynamic Design of Axial-Flow Compressors, NASA SP-36, Chapt. VII, pp. 227-254
2. SEYLER, D.R., GOSTELOW, J.P., Single Stage Experimental Evaluation of High Mach Number Compressor Rotor Blading, Part 2-Performance of Rotor 1B, NASA CR-54582, 1967
3. URASEK, D.C., MOORE, R.D., OSBORN, W.M., Performance of a Single-Stage Transonic Compressor with a Blade-Tip Solidity of 1.3, NASA TMX-2645, 1972
4. BILWAKESH, K. R., Task II stage Data and Performance Report for Undistorted Inlet Flow Testing, NASA CR-72787, 1971

Auteur: 12; Jean Fabri, O.N.E.R.A., Châtillon-sous-Bagneux

TEST CASE 3

La méthod utilisée, désignée sous le nom "Simulateur Numérique", est une version très simplifiée du programme en cours de développement à l'ONERA. Dans cette version le compresseur est représenté par quatre plans de contrôle situés respectivement à l'entrée de la roue mobile, à la sortie de la roue mobile, à l'entrée du redresseur et à la sortie du redresseur.

Les contours extérieurs et intérieurs du compresseur n'étant que très faiblement évolutifs, on peut se contenter d'écrire dans chacun de ces plans:

- la condition d'équilibre radial simplifié qui assure la compatibilité radiale de pression,
- la condition globale de conservation du débit qui assure la continuité du débit

La géométrie du compresseur est prise en compte sous forme très simple par des lois d'angle d'écoulement à la sortie des roues pour l'angle de sortie de la roue mobile est représenté par un polynôme du second degré utilisant le rayon comme variable dont les coefficients sont déterminés par la connaissance de l'angle géométrique et de l'écart flux profil calculé au moyen de la corrélation NASA SP 36 au moyeu, au rayon moyen et à la périphérie. L'angle de sortie du redresseur est pris égal à zéro. Les angles d'entrée sans pertes sont déduits de la géométrie des aubes.

Les valeurs initiales des nombres de Mach absolu à l'entrée de la roue mobile, relatif à la sortie de cette roue et de nouveau absolu à la sortie du redresseur, sont choisies de façon à priori arbitraire au cours de la première itération à la paroi interne.

A un accroissement r_1 du rayon à l'entrée de la roue mobile on fait correspondre les accroissements de rayon r_2 et r_3 à la sortie de la roue mobile et à la sortie du redresseur tels que le débit masse entrant dans le plan 1 se retrouve dans les deux autres sections. Cela nécessite la connaissance de la variation de densité dans chacune des roues, déduite elle-même de la variation d'enthalpie déduite du théorème d'Euler et de la variation correspondante de pression corrigée pour tenir compte des pertes.

Les pertes de pression d'arrêt sont reliées aux accroissements d'enthalpie respectivement dues à la non adaptation éventuelle de l'écoulement à l'entrée de la grille considérée et du ralentissement du flux dans les canaux interaubes.

Ce même calcul sert à la détermination de la pression statique et le calcul ainsi défini procède d'un rayon au suivant en respectant chaque fois la conversation du débit et la loi d'équilibre radial.

Lorsque tout le débit fixé à l'avance qui entrait dans la roue mobile est ressorti de celle-ci et du redresseur, on obtient les valeurs des rayons du carter externe dans les trois plans de contrôle étudiés. Les valeurs initiales définies plus haut sont modifiées jusqu'à ce que les rayons externes ainsi obtenus soient ceux de la géométrie du compresseur.

Ce calcul peut être programmé sans difficulté avec bouclage automatique sur les trois paramètres précédents. En fait, il se prête très facilement à une exploitation sur ordinateur de bureau ou console de visualisation et le résultat s'obtient très rapidement par dialogue entre l'opérateur et l'ordinateur.

Dans le cas de l'exemple de calcul n° 3 traité par cette méthode, les performances au débit nominal et les répartitions radiales des pressions, températures et nombres de Mach ont été obtenus correctement. En revanche, par un choix d'un coefficient de pertes par non adaptation trop élevé, les performances hors adaptation ont été sousestimées.

Dans le modèle décrit ci-dessus, le décrochage du compresseur correspond au débit pour lequel soit localement à la sortie de la roue mobile, soit globalement à la sortie du redresseur, la pression statique passe par un maximum lorsque le débit décroît.

Dans le premier cas, au maximum de pression statique correspond un remplissage incomplet de la veine pour tout débit inférieur au débit de décrochage ainsi défini, ce qui dans la plupart des cas conduit à des phénomènes instationnaires du type décollement. tournant.

Dans le second cas, le fait que la pression statique décroît lorsque le débit est inférieur au débit critique rend impossible l'établissement d'un régime instable et conduit naturellement à des instabilités longitudinales qui peuvent éventullement dégénérer en instabilités azimutales du type décollement tournant.

Author: 26; E. Macchi , Politecnico di Milano

The present computer program is based on Vavra's (1) technique of solution for axisymmetric and steady flow in axial turbomachines; it solves the complete radial equilibrium equation - accounting for enthalpy and entropy gradients and streamline curvature effects - in a specified number of stations ahead of, between and after the blade rows. An orthogonal curvilinear system of coordinates having the meridional coordinates coincident with the generatrises of the flow stream surfaces is used in the solution. Iterative methods are used both for the numerical solution of radial equilibrium and continuity equation in single stations and for streamlines location and curvatures over the whole machine.

(+) The computer program was developed under a Research Grant by Franco Tosi S.p.A.

PREDICTION OF ANGLES AND LOSSES

a) "reference" conditions

Incidence, deviation and losses produced by the blade rows at "reference" conditions are computed according to NASA rules (2), the only difference being the assumption that the streamline radial position has no influence on them (i.e., in making use of fig. 201-202-203 of Ref. 2, the curves given for 50% of blade height are assumed to be valid for all streamlines).

b) "off-reference" conditions

Off-reference deviations and losses are computed according to the correlations proposed by Creveling and Carmody (3), as a function of incidence angle and inlet relative Mach number. The only modification of original subroutines given in (3) which was considered appropriate is the calculation of flow deviation angle in the negative incidence range.

No axial velocity ratio influence is considered, mostly because the program was developed for calculating low-speed industrial compressors, where axial velocity ratios are always very close to unity. For the same reasons, also shock losses are not accounted for.

SECONDARY LOSSES

The last version of Mellor's theory (4) on casing boundary layer is incorporated in the computer program.
The Mellor's equations are integrated across every blade row; this calculation is carried out every time the continuity equation is solved. The displacement thicknesses are accounted for in locating streamlines, while all other pertinent boundary layer parameters yield the enthalpy and entropy increase caused by secondary losses.
The losses are then mass-averaged, i.e. uniformly distributed in the whole section.
The following values of the four "arbitrary" coefficients in Mellor's theory are assumed, for both hub and tip of rotor and stator blades:

$C_f = 0.003$
$\epsilon = 0$
$K = 0.65$
$H = 1.4$

Flow angle changes due to secondary effects were not considered.

SURGE-LINE DETECTION

Surge conditions are automatically detected by the computer program, when one of the following situations occurs:

1) the radial equilibrium equation does not have meaningful solutions (i.e., it yields very small or even negative values of the meridional velocity at some streamline);
2) the casing boundary layer (almost always at hub) increase in first stages is so large that causes unstable conditions; i. e., the variation of meridional velocity at various stations is so abrupt that convergence cannot be obtained.

In the Author's experience, the two situations occur almost simultaneously, but the second one is more easily detectable.

References

1. VAVRA, M. H., "Aero-Thermodynamics and Flow on Turbomachines" John Wiley & Sons, Inc., New York 1960

2. The Members of the Staff of Lewis Research Center, Cleveland, Ohio "Aerodynamic Design of Axial-flow Compressors" NASA SP-336, 1965

3. CREVELING, H.F., and CARMODY, R.H., "Computer program for Calculating Off Design Performance of Multistage Axial-flow Compressors NASA CR-

4. MELLOR, G.L., "Secondary Flows in Turbomachines", Von Karman Institute for Fluidodynamics Lecture Series, Jan. 1975

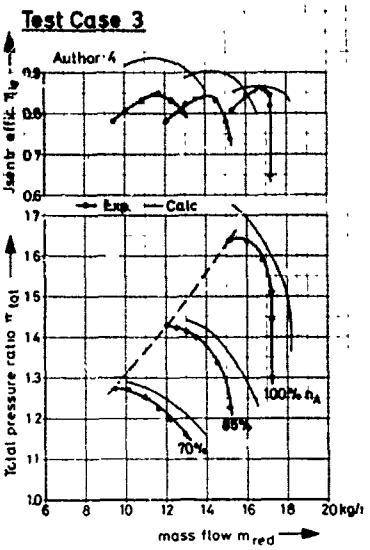

(a) Author 4

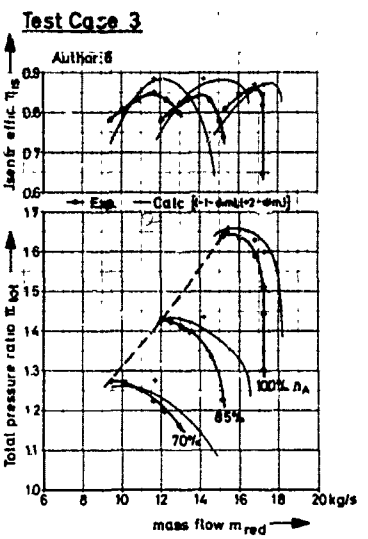

(b) Author 6

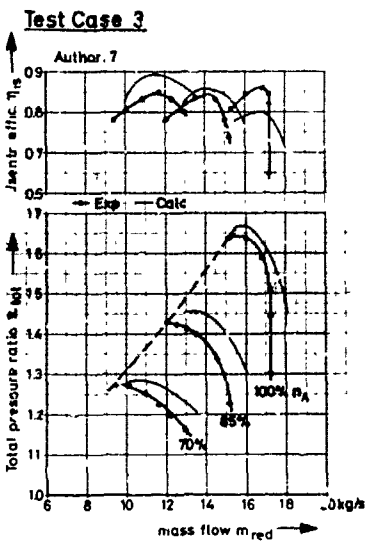

(c) Author 7

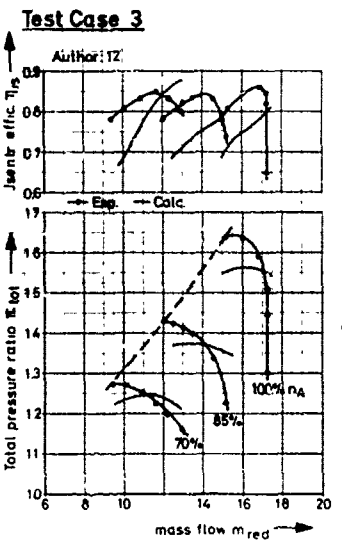

(d) Author 12

Fig.1 Overall performance of the single stage transonic compressor (Test Case 3) compared to performance predictions

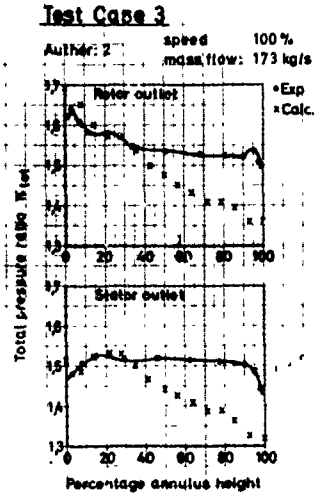

(a) Author 2

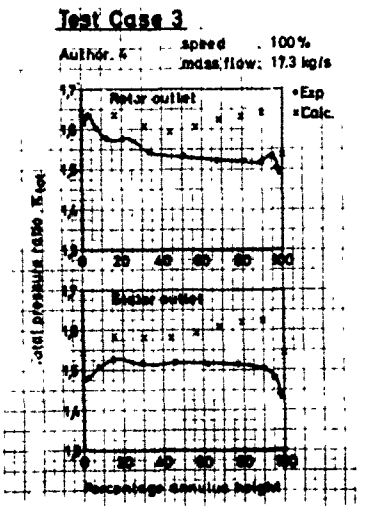

(b) Author 4

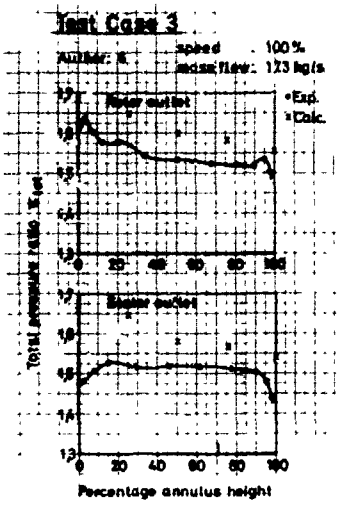

(c) Author 6

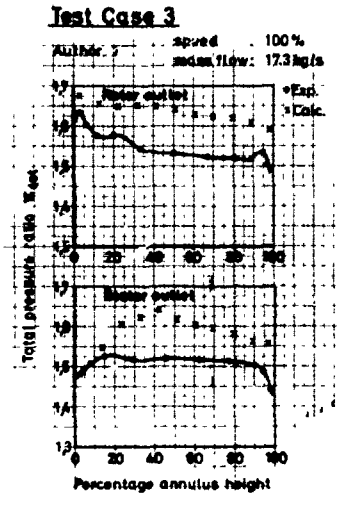

(d) Author 7

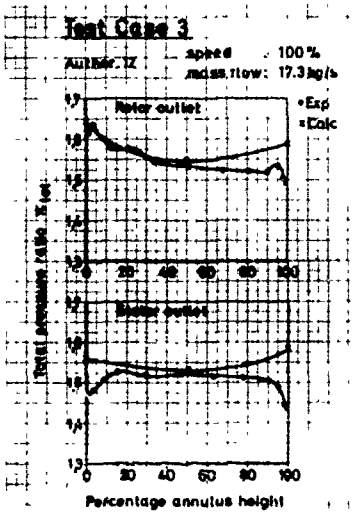

(e) Author 12

Fig.2 Total pressure ratio at rotor and stator outlet-mass flow 17.3 kg/s (exp.-calc.)

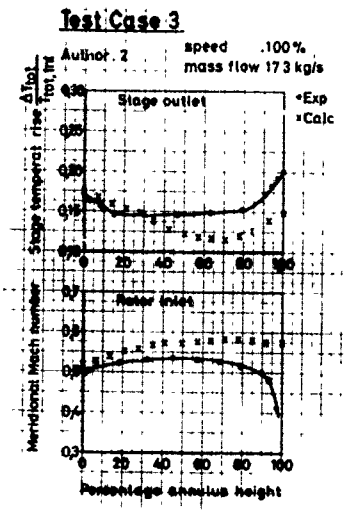

(a) Author 2

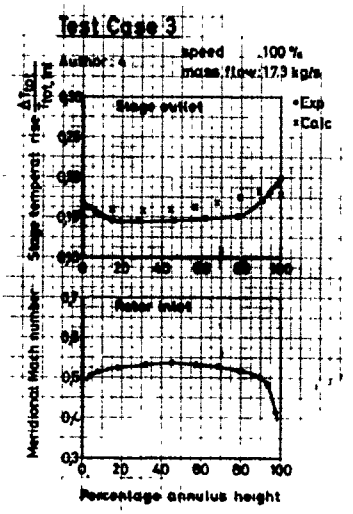

(b) Author 4

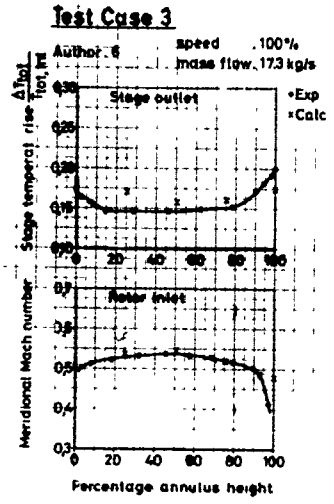

(c) Author 6

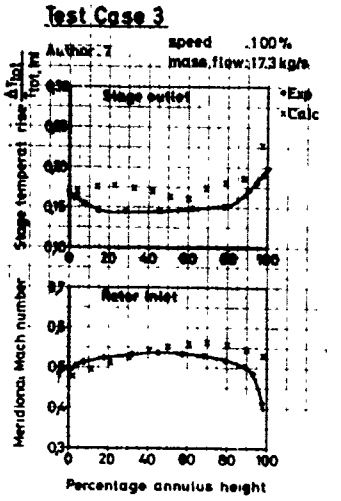

(d) Author 7

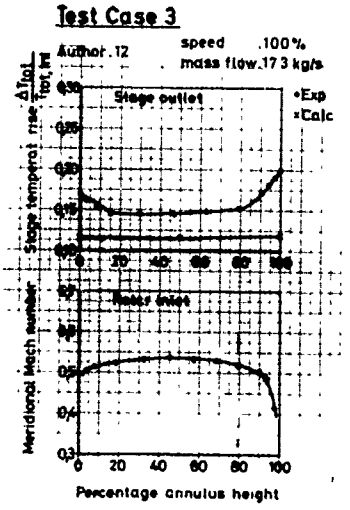

(e) Author 12

Fig.3 Stage temperature rise and meridional Machnumber at rotor inlet – mass flow 17.3 kg/s (exp.-calc.)

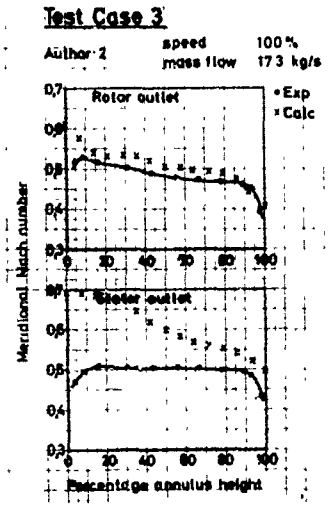

(a) Author 2

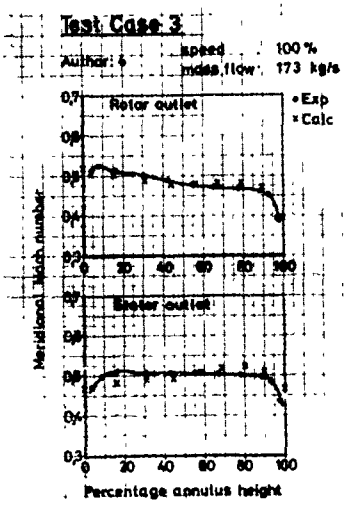

(b) Author 4

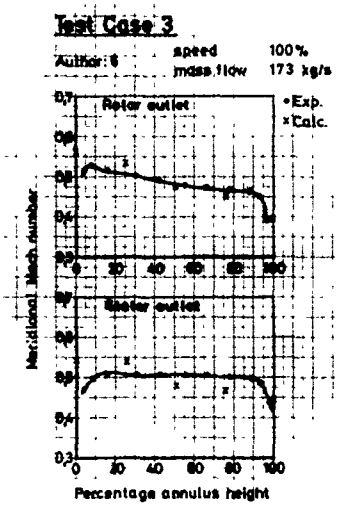

(c) Author 6

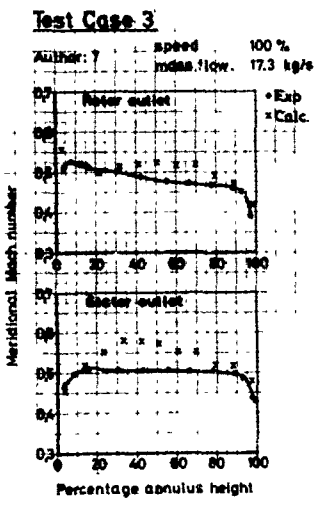

(d) Author 7

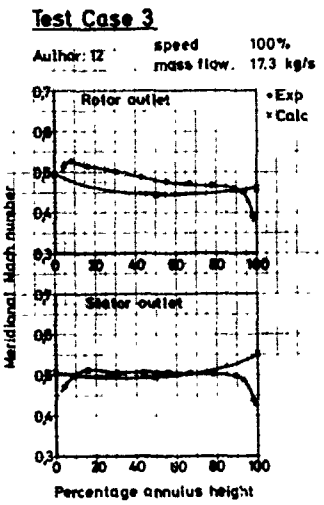

(e) Author 12

Fig.4 Meridional Machnumber at rotor and stator outlet-mass flow 17.3 kg/s (exp.-calc.)

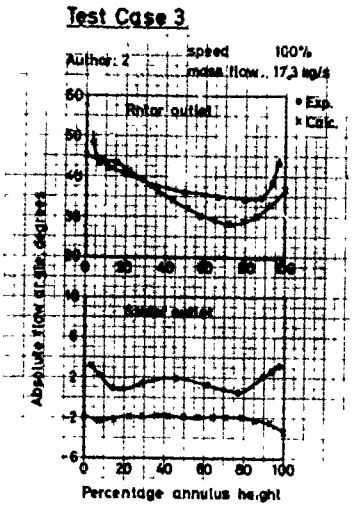

(a) Author 2

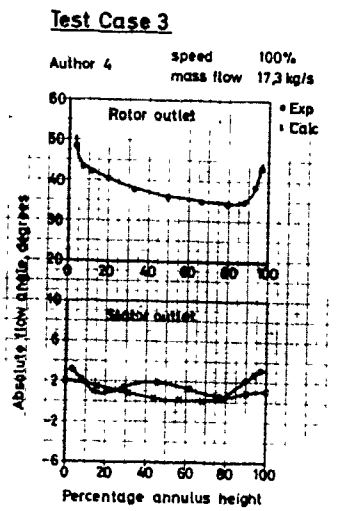

(b) Author 4

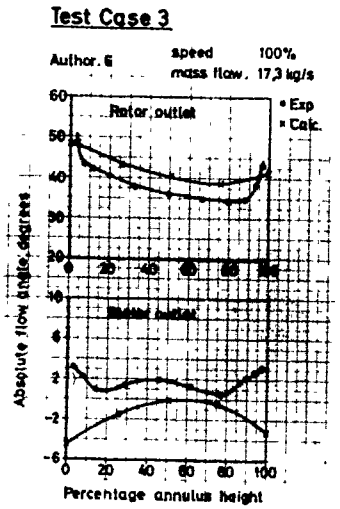

(c) Author 6

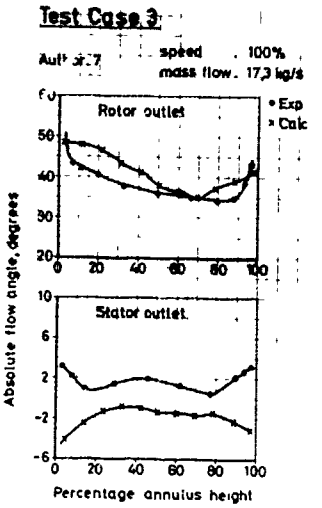

(d) Author 7

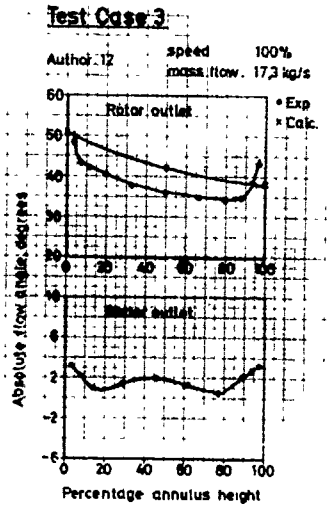

(e) Author 12

Fig.5 Absolute flow angle at rotor and stator outlet-mass flow 17.3 kg/s (exp.-calc.)

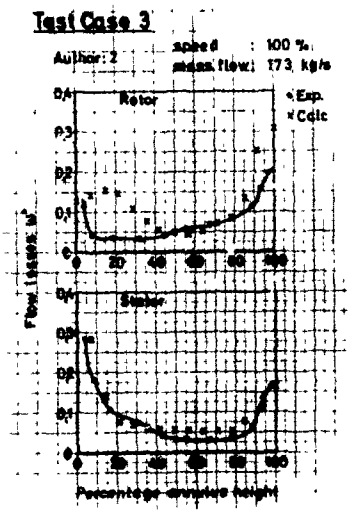

(a) Author 2

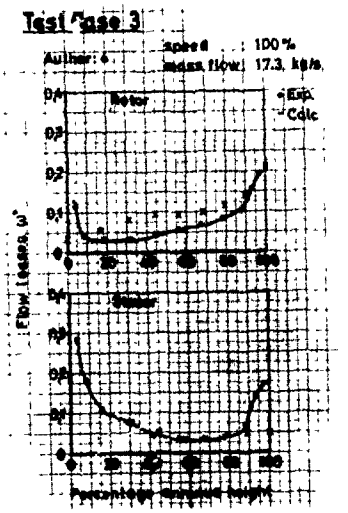

(b) Author 4

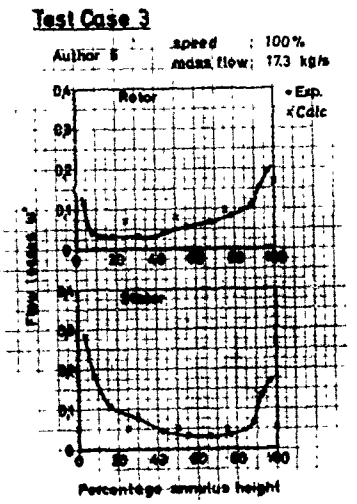

(c) Author 6

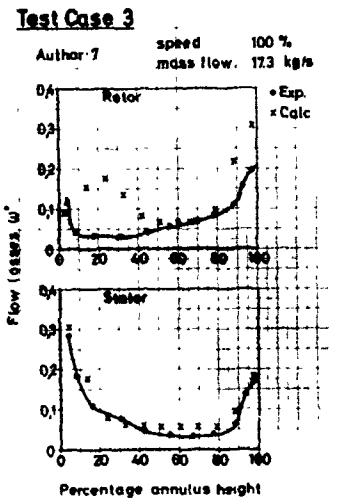

(d) Author 7

Fig.6 Rotor and stator flow losses – mass flow 17.3 kg/s (exp.-calc.)

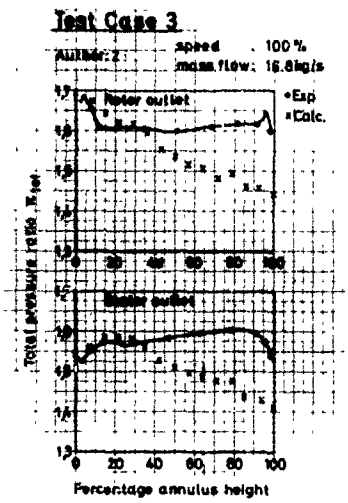

(a) Author 2

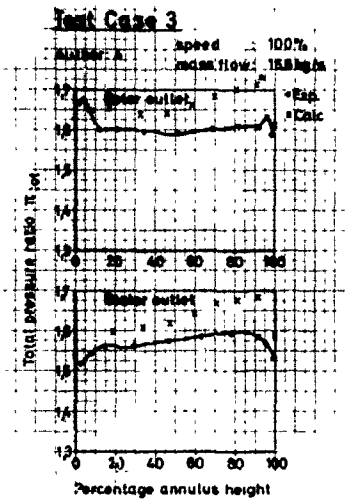

(b) Author 4

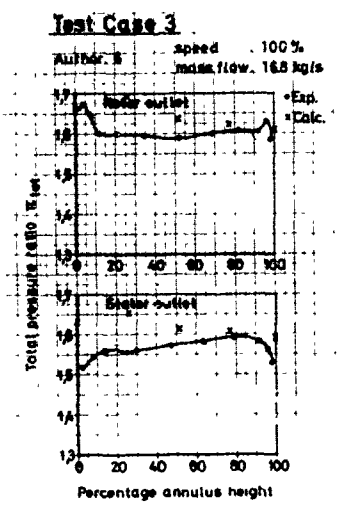

(c) Author 6

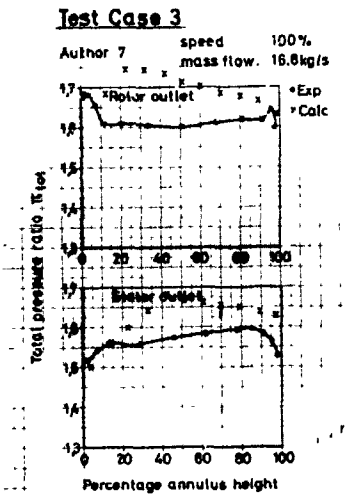

(d) Author 7

Fig.7 Total pressure ratio at rotor and stator outlet-mass flow 16.8 kg/s (exp.-calc.)

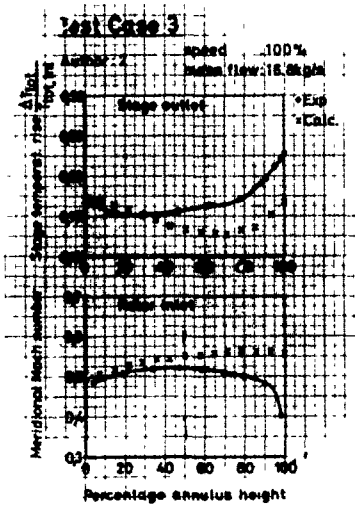

(a) Author 2

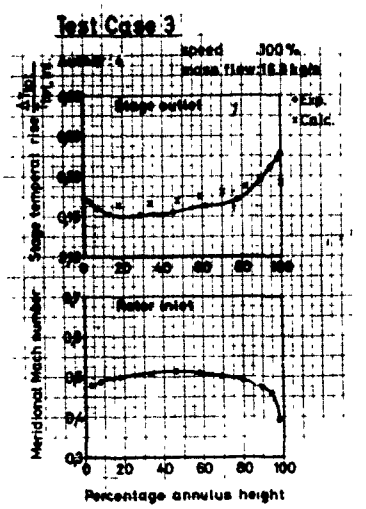

(b) Author 4

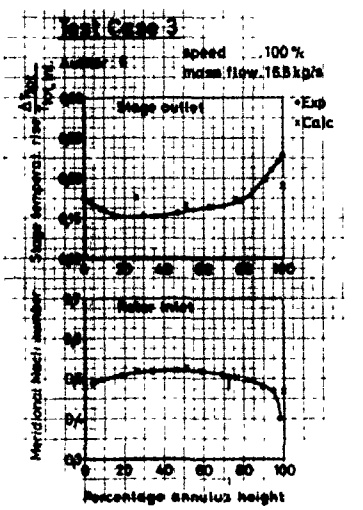

(c) Author 6

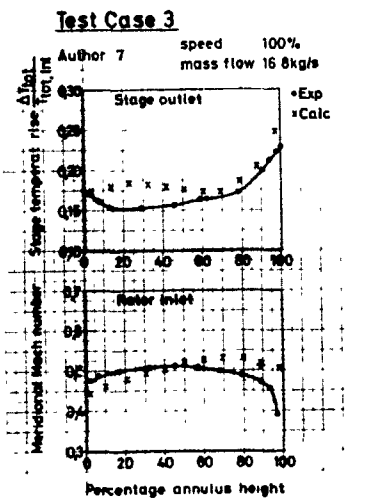

(d) Author 7

Fig.8 Stage temperature rise and meridional Machnumber at rotor inlet – mass flow 16.8 kg/s (exp.-calc.)

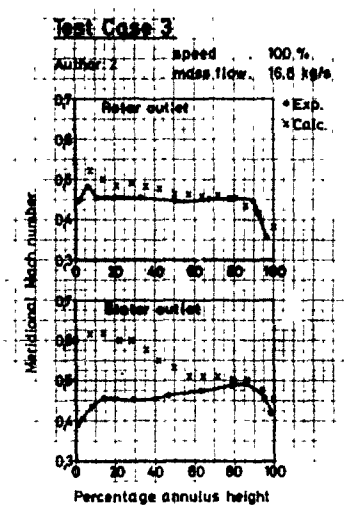

(a) Author 2

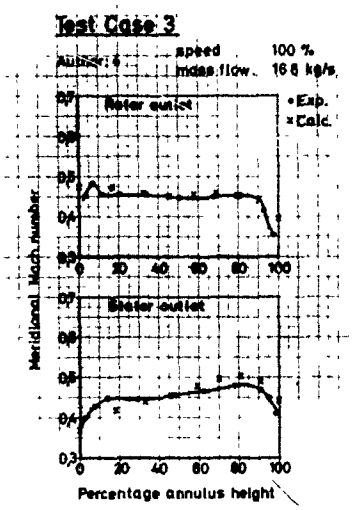

(b) Author 4

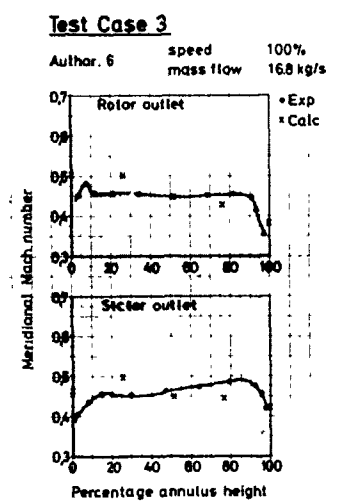

(c) Author 6

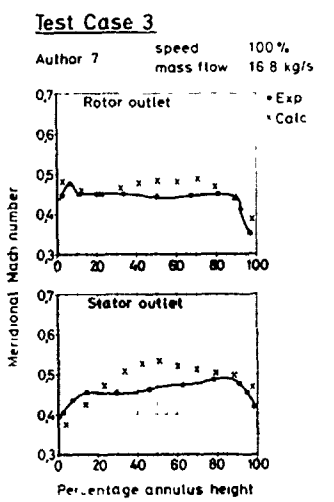

(d) Author 7

Fig.9 Meridional Machnumber at rotor and stator outlet-mass flow 16.8 kg/s (exp.-calc.)

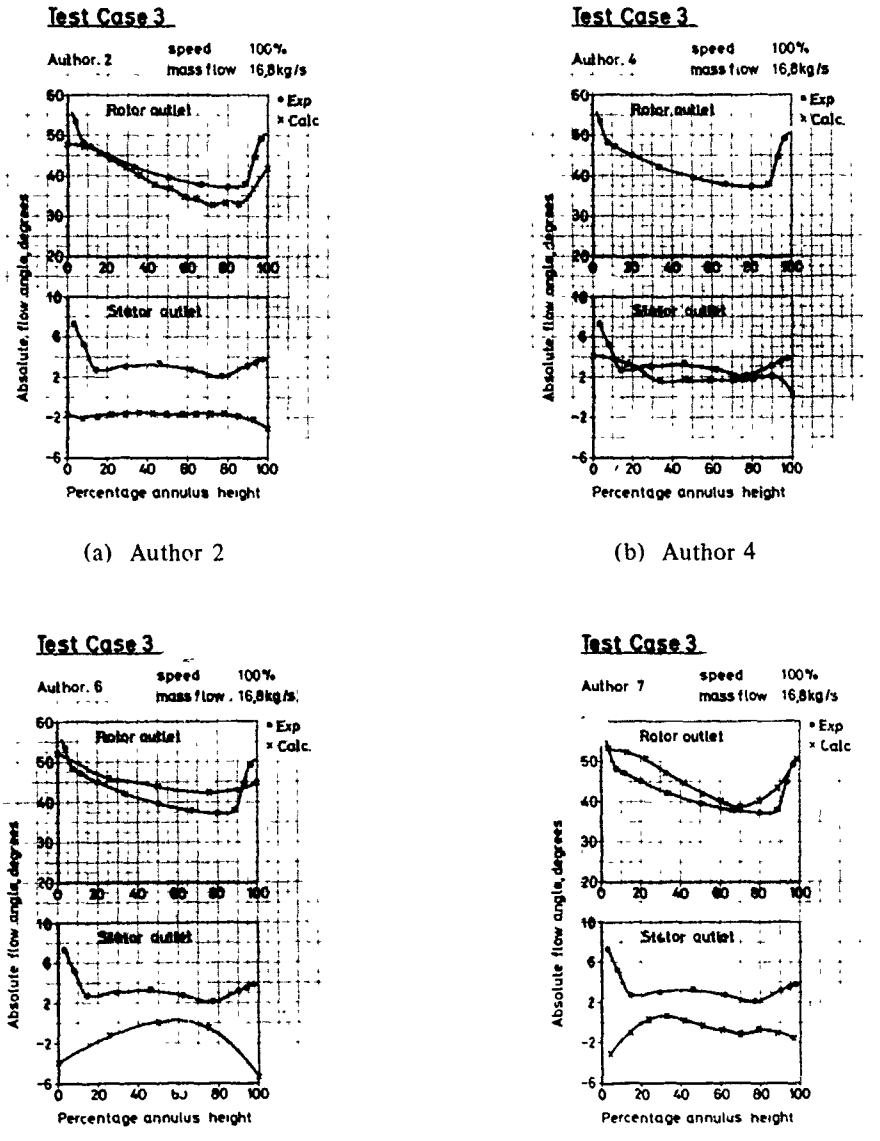

(a) Author 2

(b) Author 4

(c) Author 6

(d) Author 7

Fig.10 Absolute flow angle at rotor and stator outlet-mass flow 16.8 kg/s (exp.-calc.)

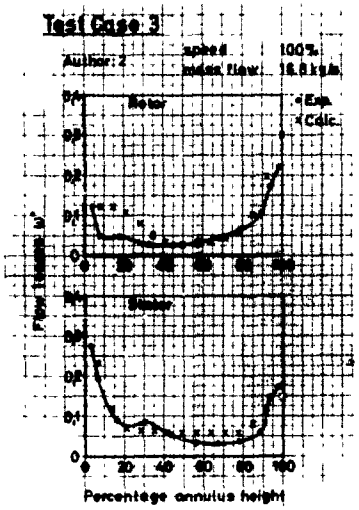

(a) Author 2

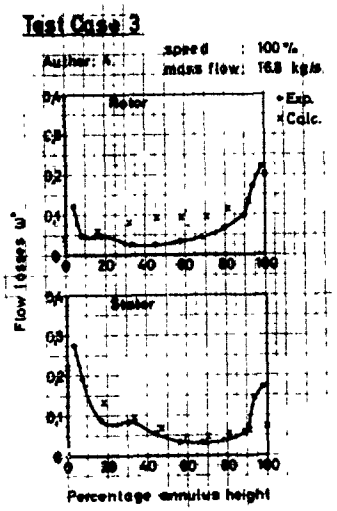

(b) Author 4

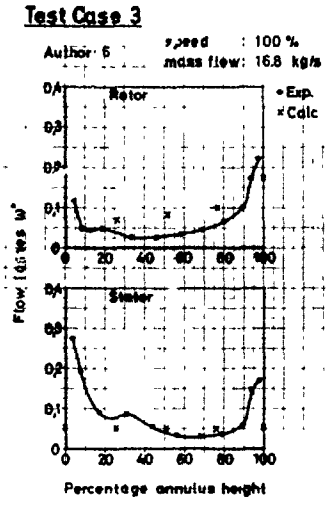

(c) Author 6

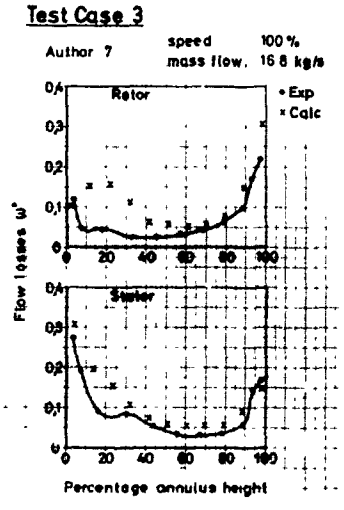

(d) Author 7

Fig.11 Rotor and stator flow losses – mass flow 16.8 kg/s (exp.-calc.)

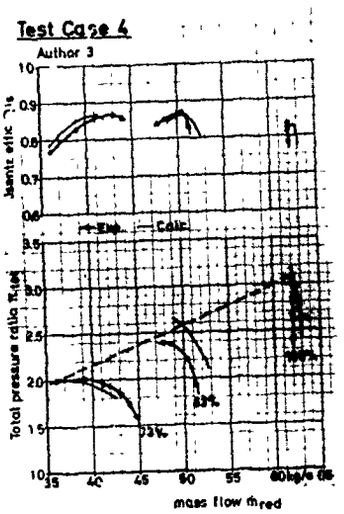

(a) Author 3

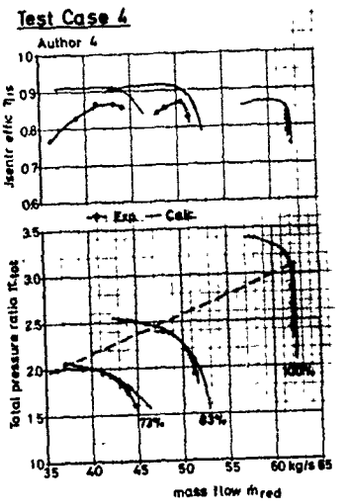

(b) Author 4

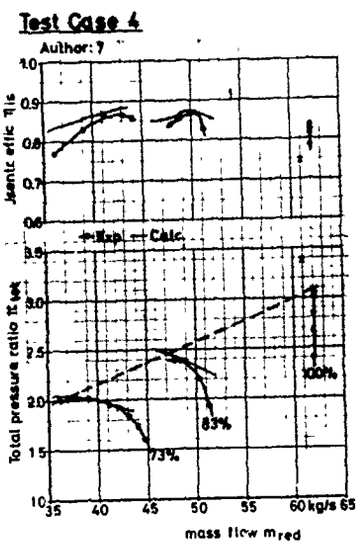

(c) Author 7

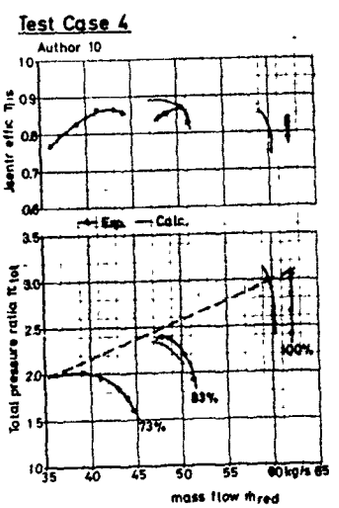

(d) Author 10

Fig.12 Overall performance of the 3-stage transonic compressor (Test Case 4) compared to performance predictions

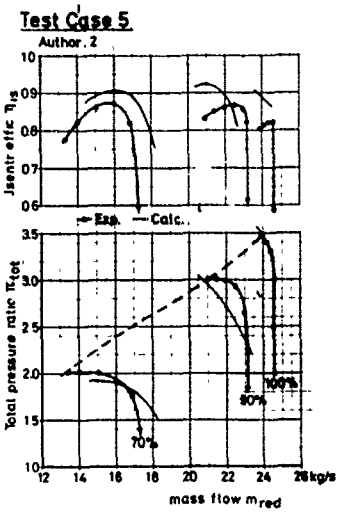

(a) Author 2

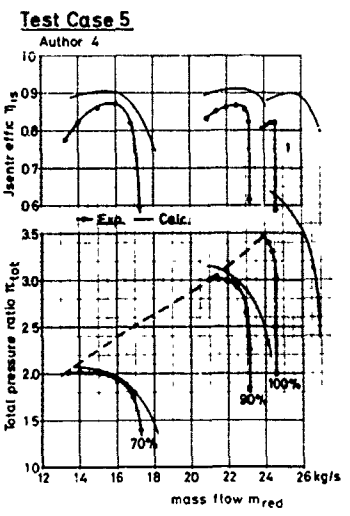

(b) Author 4

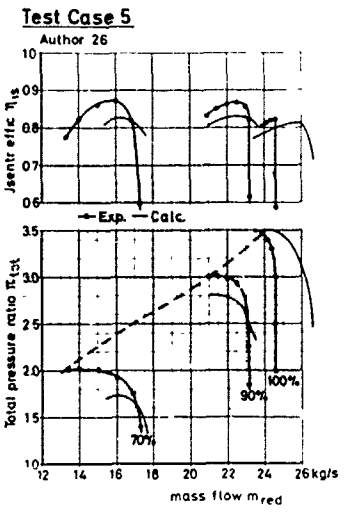

(c) Author 26

Fig.13 Overall performance of the 4 stage transonic compressor (Test Case 5) compared to performance predictions

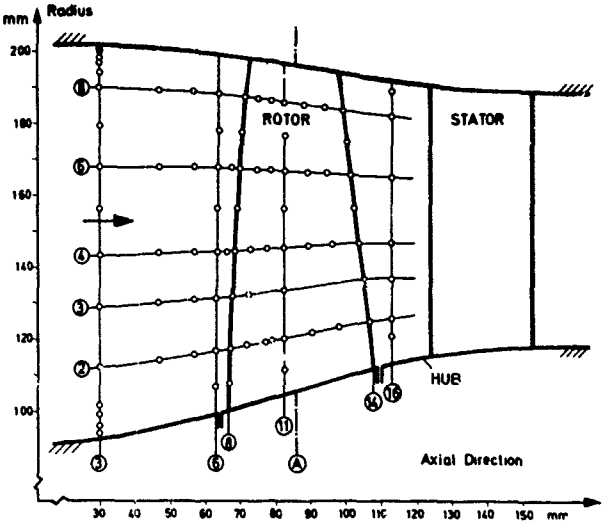

Fig.14 Compressor flowpath with the laser measuring positions – Test Case 3

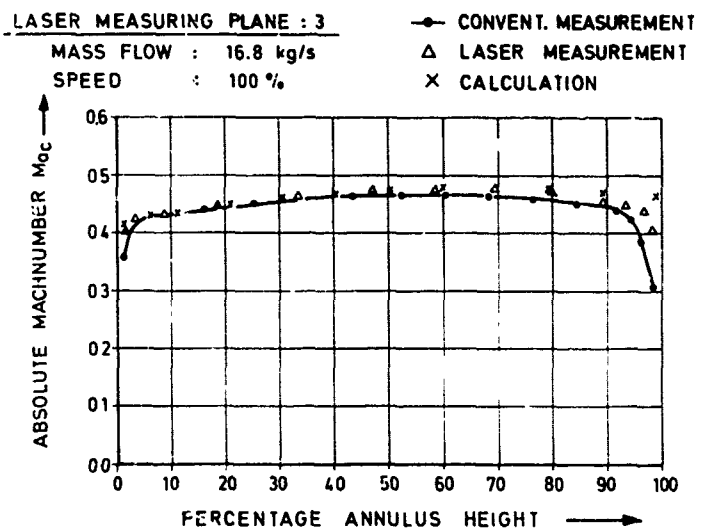

Fig.15 Absolute Mach number distribution against relative annulus height in plane 3 far upstream to the rotor

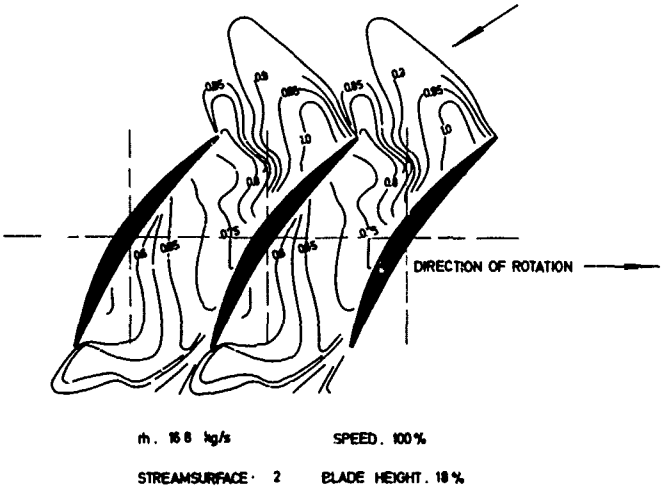

Fig.16 Lines of constant relative Machnumber on streamsurface 2

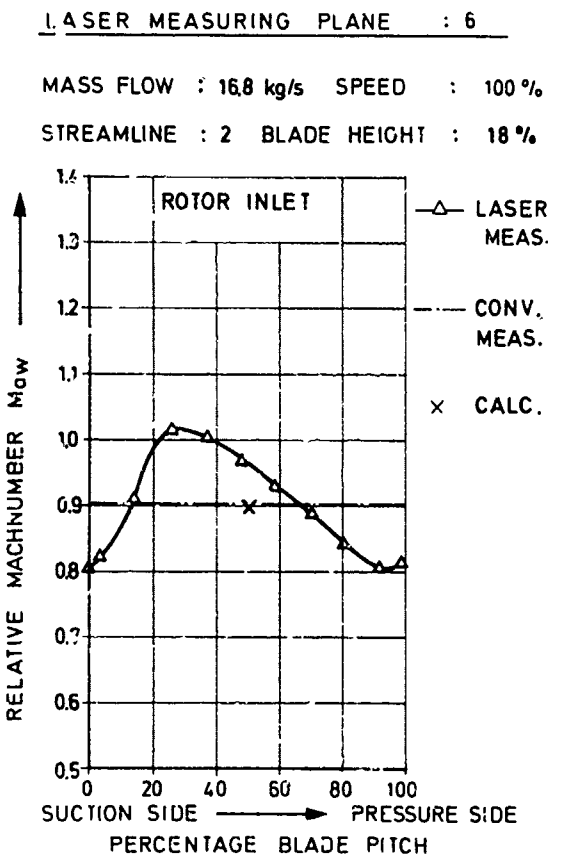

Fig.17 Relative Machnumber plotted against blade pitch in plane 6 for streamsurface 2

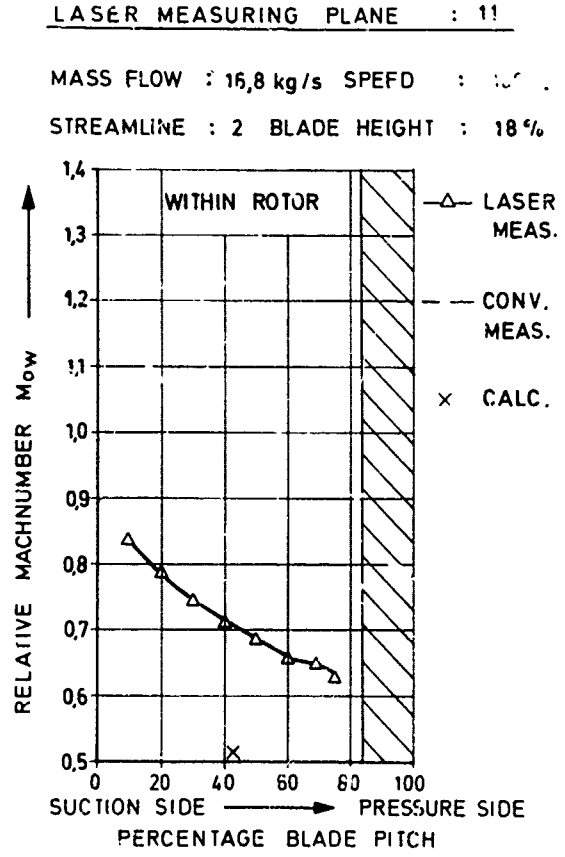

Fig. 18 Relative Machnumber plotted against blade pitch in plane 11 for streamsurface 2

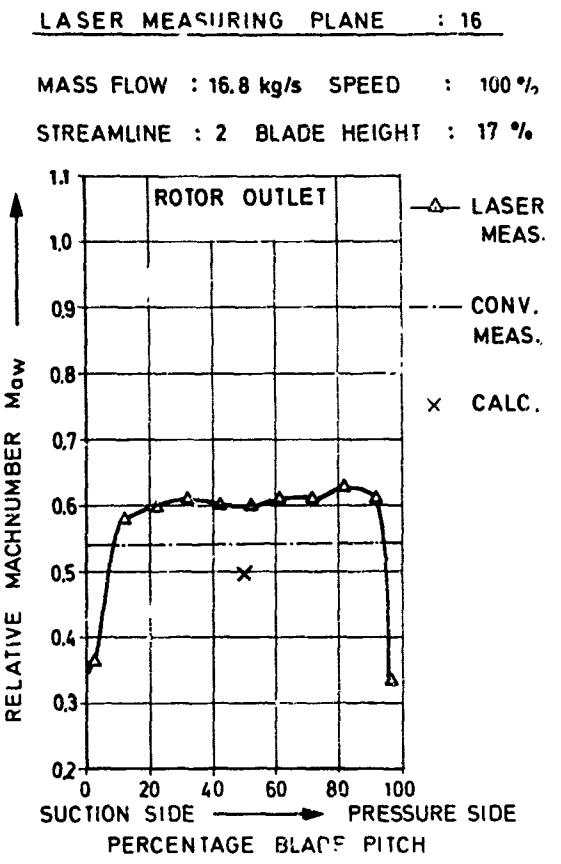

Fig.19 Relative Machnumber plotted against blade pitch in plane 16 for streamsurface 2

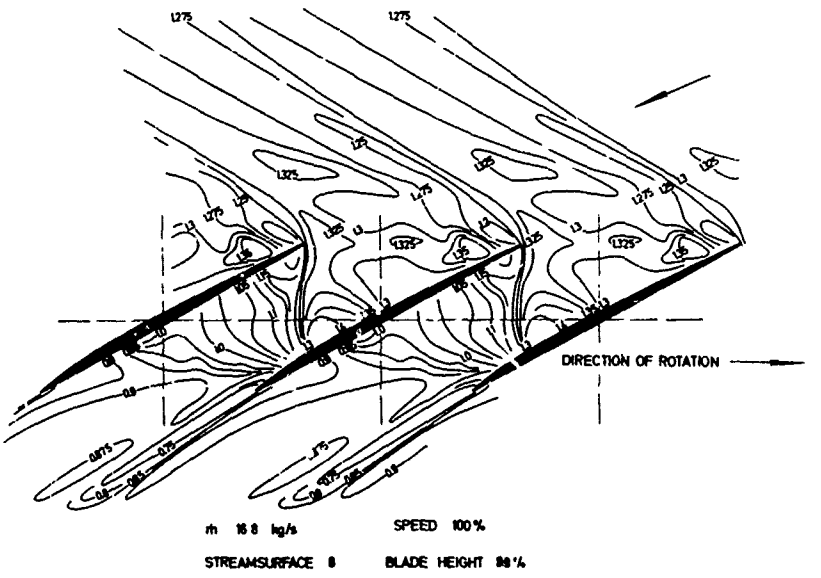

Fig.20 Lines of constant relative Machnumber on streamsurface 8

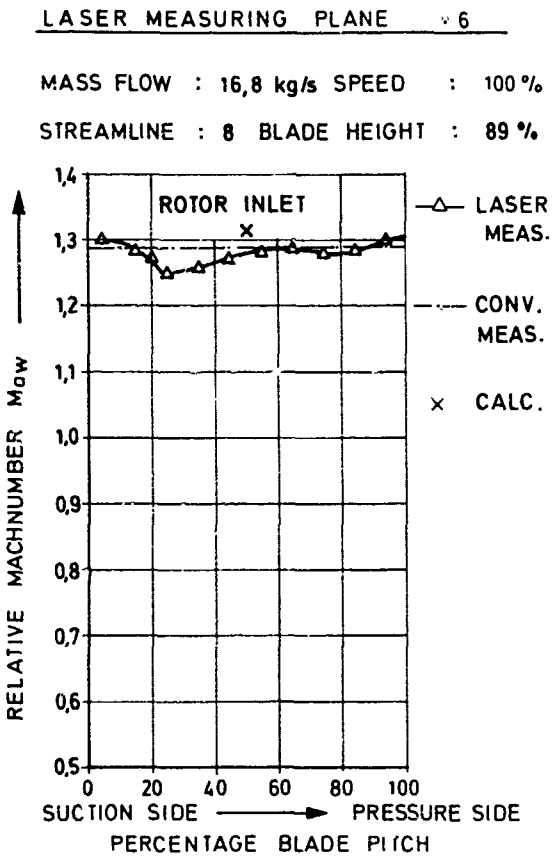

Fig.21 Relative Machnumber plotted against blade pitch in plane 6 for streamsurface 8

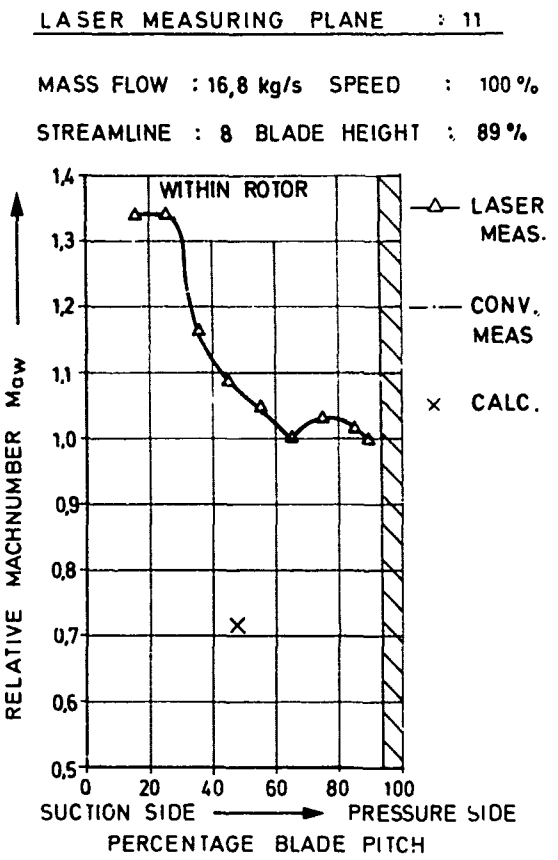

Fig.22 Relative Machnumber plotted against blade pitch in plane 11 for streamsurface 8

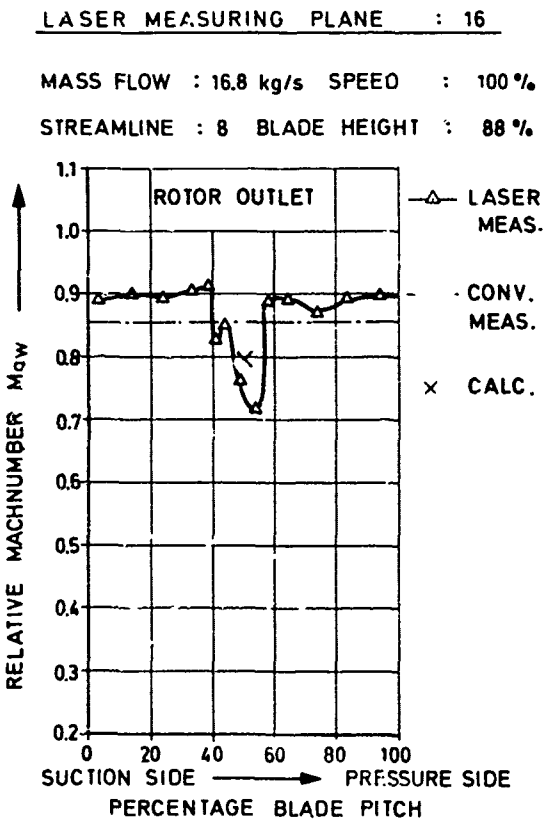

Fig.23 Relative Machnumber plotted against blade pitch in plane 16 for streamsurface 8

TURBINE TEST CASES
PRESENTATION OF DESIGN AND EXPERIMENTAL CHARACTERISTICS

by J. Chauvin and C. Sieverding
Professors
von Karman Institute for Fluid Dynamics
Chaussée de Waterloo 72
1640 Rhode-Saint-Genèse
Belgium

INTRODUCTION

Two tests cases have been made available to the Committee, respectively a two-stage, two-shaft HP-IP turbine, for which complete data, including interstage traverses are available at 100 %, by courtesy of Rolls-Royce (1971), Derby Engine Division, and a three-stage single shaft turbine, for which a full overall performance map is available but no detailed traverse, except at outlet. The latter case is by courtesy of M.T.U. München.

Full geometrical data are presented for the first case. For the second one, publication at large was not possible due to proprietary problems raised by the agencies having sponsored the research on the machine.

The Committee is very thankful to both Rolls-Royce (1971) and M.T.U. for their help, and in particular to Mr. Bryan Barry and Dr.Ing. H.J. Lichtfuss, who spent a considerable time in putting the data in the requested form.

The turbine description and the experimental data are presented in this report.

LIST OF SYMBOLS

M	Mach number
$\dot{m}$	mass flow kg/sec
P_o or P_{tot}	total pressure, bars
p	static pressure
R	radius, mm
$R^* = \frac{R - R_{hub}}{R_{tip} - R_{hub}}$	
Z	axial coordinate, mm
α	absolute angle from axial direction (positive in the direction of camber, for nozzle in direction of rotation for rotor).
ω	blade row relative total pressure loss coefficient $\frac{P_{ci} - P_{oi+1}}{P_{oi} - P_{i+1}}$ (i inlet of blade row, i+1 outlet of blade row)

SUBSCRIPTS

m	in meridional direction
Red	reduced, at ISA sea level conditions
W	relative to rotor
Z	in axial direction
1	upstream of turbine or stage
2	downstream of turbine or stage

I. TEST CASE I (Courtesy of Rolls-Royce 1971 - Derby Engine Division)

1. Geometry and Design Conditions

This is a typical two-stage, two shaft HP-IP turbine for advanced gas turbine engines. The flow path is given in Table 1 and Fig. 1, and the information available on the blading in Table 2 and Figs. 2,3,4. The blades are of the usual type for gas turbine operating at high subsonic/moderate supersonic outlet Mach numbers, i.e. with slightly curved succion side downstream of the throat.
The design conditions are :

Nominal speed (ISA conditions)	:	HP turbine 8250 rpm
		LP turbine 4693 rpm
Reduced nominal mass flow (ISA conditions)	:	4.82 kg/sec.

2. Experimental Data

Tests were carried out at 100% speed with an inlet total pressure of 2.94 bars and an inlet total temperature of 423°K, corresponding to an actual mass flow of 11.50 kg/sec. Overall turbine and stage performances at optimal conditions are given in Table 3 (0,1,2). Efficiencies have been evaluated from brake and total pressure, recalculated from wall static and continuity and from total pressure and temperature traverses, mass averaged between blade rows. The maximum difference between the two evaluations is one point. Traverse data are available before and after each blade row, for total pressure, total temperature, static pressure and absolute angle.

Table 3 - 3 and 4, and Fig. 5 give the total pressure and temperature distribution in function of relative blade height at stage outlets. Table 3 - 5 and Figs. 6,7, 8,9 give the loss coefficient distribution at each blade row outlet, as $\omega = \frac{P_{01}-P_{02}}{P_{01}-P_2}$ = f (reduced radius).

Table 3 - 6 gives inlet and outlet axial and meridional Mach numbers, absolute angle, and outlet relative Mach number for each blade row. In Figs. 10,11,12,13 are plotted the relative outlet Mach numbers and in Figs. 14 and 15 the absolute outlet angles.

The effect of secondary flows is clearly noted in Fig. 5 and is even more evident in the loss distribution of Figs. 6 through 9, which indicate, except for the case of the first nozzle, a quite radical departure for the usually accepted model of a "sound flow" and end wall region. This can be noted also, to a lesser degree, in the angle distribution. The Mach number evaluation is relatively smooth.

Not withstanding the radial evolution of the flow, the overall performance is quite satisfactory.

II. TEST CASE 2 (Courtesy of Motoren- und Turbinen Union, München)

1. Geometry and Design Conditions

This is a three-stage single shaft turbine, typical of gas turbine. It has a flow path diverging more at the root than at the tip (Fig. 6). It uses blading with slightly curved succion downstream of the throat.

Design r.p.m at ISA sea level conditions is 7.718
Reduced nominal mass flow is 7.59 kg/sec.

2. Experimental Data

Test data on overall performance are available for 100, 80, 60 and 20% of nominal r.p.m., and are given in Table 5 and Fig. 16. A pressure ratio of 2.94 with an isentropic efficiency of 0.90 is achieved for the reduced nominal mass flow. Traverse data, taken 80 mm behind the last rotor, are available for nominal conditions. They are given in Table 6 (total pressure ratio, total temperature ratio, axial Mach number, relative Mach number and absolute outlet angle) and plotted in Figs. 17, 18 and 19.

TEST CASE I

Table 1 : FLOW PATH GEOMETRY

Z mm	-101,6	-68,6	-50,8	-25,4	1,8	32,1	39,2	47,3	64,9	73,4
R_{hub} mm	258,3	258,3	258,3	258,3	258,3	265,9	267,0	268,0	217,3	273,2
R_{tip} mm	303,3	303,3	303,3	303,3	302,5	302,9	305,7	308,6	319,3	324,8
Z mm	81,9	144,8	152,4	160,0	177,2	203,2	228,6	254,0	279,4	304,8
R_{hub} mm	275,1	306,0	308,7	311,3	314,7	314,7	314,7	314,7	314,7	314,7
R_{tip} mm	330,4	367,8	372,1	376,3	387,1	389,1	389,1	389,1	389,1	389,1

Table 1.1 : LOCATION OF INSTRUMENTATION (all dimensions in mm)

Z	-68,6	39,2	73,4	152,4	203,2

Table 2 : BLADE GEOMETRIC DATA (on blade sections parallel to axis)(in mm)

Stage No : 1 Blade Row : Nozzle Guide Vanes Number of Blades : 54

Radius	axial location Z leading edge	trailing edge	Solidity L/S	Stagger angle	Blade inlet	outlet angle	Normal to camber max. thickness
272	1,8	30,3	1,46	50,25°	0°	72,96°	8,52
283,5	1,8	30,3	1,40	50,25°	0°	72,81°	8,34
295	1,8	30,3	1,34	50,25°	0°	72,66°	8,16

Stage No : 1 Blade Row : Rotors Number of Blades : 102

273,8	47,3	64,9	1,254	-35,1°	52,62°	-64,27	4,735
291,5	47,3	64,9	1,255	-40,0	46,00	-65,0	4,049
305,0	47,3	64,9	1,261	-43,2	38,45	-65,75	3,695

Stage No : 2 Blade Row : Nozzle Guide Vanes Number of Blades : 36

312,0	81,9	144,8	1,394	34,8°	-22,88°	67,48°	18,52
353,0	81,9	144,8	1,245	36,2°	-21,50°	64,89°	18,45

Stage No : 2 Blade Row : Rotors Number of Blades : 148

308,73	160,02	177,16	1,503	-25,2°	44,2°	-61,8°
339,28	160,02	177,16	1,395	-32°	31,0°	-62,7°
369,95	161,93	175,25	1,171	-44°	15,5°	-63,7°

All angles in axial direction and with respect to compressor axis, positive in camber direction for nozzles, in direction of rotation for rotors.

Table 3

Turbine Test Case I - Experimental Results

Reduced nominal mass flow : 4.82 kg/sec

1. Turbine pressure ratio (mass averaged, total to total)

Overall: 5.8359
HP : 2.8451
LP : 2.0512

2. Turbine efficiency

a) based on "brake" temperature drop and total pressure derived from wall statics and continuity.

Overall: 88.406 %
HP : 85.753 %
LP : 89.628 %

b) based on inter blade row total pressure and total temperature traverse data (mass averaged)

Overall: 89.15 %
HP : 89.76 %
LP : 89.52 %

3. Total pressure ratio

HP	LP	Overall	R^{χ} (%)
2.994	2.118	6.341	2 5
2.973	2.103	6.252	5.0
2.970	2.131	6.329	7.5
2.976	2.125	6.324	10
2.911	2.127	6.190	15
2.717	2.230	6.060	25
2.830	2.180	6.170	50
2.898	1.968	5.703	75
2.929	1.916	5.611	85
2.899	1.912	5.543	90
2.883	1.911	5.511	92.5
2.900	1.892	5.486	95
2.955	1.849	5.463	97.5

Note : mass meaned inlet P_t is assumed.

4. Total temperature ratio

1.162	1.319	1.532	2.5
1.171	1.306	1.529	5.0
1.168	1.313	1.533	7.5
1.163	1 315	1.529	10.0
1.226	1.246	1.528	15
1.305	1.170	1.526	25
1.308	1.194	1.561	50
1.301	1.196	1.556	75
1.287	1.200	1.544	85
1.279	1.198	1.533	90
1.279	1.195	1.528	92.5
1.279	1.193	1.525	95
1.279	1.233	1.577	97.5

5. Flow losses, ω

HP		LP		
Stator[1]	Rotor	Stator	Rotor	R^X (%)
.4531	.3679	.18416	-.0366	2.5
.3072	.3166	.1068	.1561	5.0
.07665	.3904	.0806	.2009	7.5
.07503	.4141	.0846	.1932	10.0
.05243	.2786	.1421	.2489	15
.05196	.1629	.2635	.2408	25
.06029	.0727	.2208	.1394	50
.06082	.1598	.0907	.2169	75
.08362	.1692	-.0062	.2284	85
.07057	.1488	.0041	.3130	90
.0805	.1311	.0113	.2823	92.5
.14822	.1474	.0138	.2434	95
.3140	.2051	.684	.1077	97.5

(1) based on mass meaned inlet P_t.

6. Inter blade row Mach numbers and gas angles

HP Stator inlet

R^*	$M_z=M_m$	α_m
2.5	.1019	0.0
5.0	.1524	0.0
7.5	.1502	0.0
10.	.1468	0.0
15.	.1429	0.0
25.	.1393	0.0
50.	.1446	0.0
75.	.1561	0.0
85.	.1566	0.0
90.	.1545	0.0
92.5	.1529	0.0
95.	.1496	0.0
97.5	.1434	0.0

HP Stator exit

R^* %	M_z	M_m	M_w	α_m
2.5	.2809	.2839	0.87	70.9
5.0	.3074	.3108	1.41	77.31
7.5	.3239	.3277	0.98	70.4
10	.3228	.3269	0.97	70.4
15	.3069	.3113	0.99	71.6
25	.2836	.2886	0.97	72.6
50	.2610	.2681	0.93	73.3
75	.2619	.2723	0.91	72.5
85	.2790	.2916	0.89	70.8
90	.2947	.3089	0.89	69.6
92.5	.3059	.3211	0.88	68.6
95	.3152	.3314	0.86	67.2
97.5	.2885	.3037	0.79	67.4

HP Rotor exit

R^*(%)	M_z	M_m	M_w	α_w
2.5	.1156	.1179	.8310	-59.8
5.0	.1262	.1290	.8654	-60.7
7.5	.1363	.1395	.8752	-59.4
10	.1546	.1586	.8730	-56.5
15	.2472	.2546	.9168	-41.7
25	.4297	.4587	.9645	-18.4
50	.3665	.3912	1.0293	-30.7
75	.3593	.3974	1.0348	-27.9
85	.3378	.3796	1.0483	-30.9
90	.3538	.4011	1.0580	-30.6
92.5	.3594	.4092	1.0806	-30.9
95	.3529	.4037	1.0775	-30.9
97.5	.3396	.3903	1.0453	-28.2

LP Stator exit

R^*(%)	M_z	M_m	M_w	α_m
2.5	.2200	.2330	0.89	74.8
5.0	.2677	.2839	0.914	71.9
7.5	.3112	.3305	0.918	68.9
10	.3410	.3637	0.9085	66.4
15	.3812	.4066	0.896	63.0
25	.3904	.4189	0.892	62.0
50	.3528	.3917	0.816	64.3
75	.3111	.3454	0.777	63.6
85	.2957	.3309	0.774	64.7
90	.3187	.3580	0.77	62.3
92.5	.3521	.3963	0.767	58.9
95	.3496	.3942	0.7545	58.5
97.5	.2340	.2642	0.528	60.0

LP Potor exit

R^*(%)	$M_z=M_m$	M_w	α_m
2.5	.1863	.8471	-62.1
5.0	.2397	.8065	-50.8
7.5	.2881	.8061	-43.4
10	.3331	.8131	-37.8
15	.3924	.8066	-28.7
25	.3959	.8212	-28.8
50	.3346	.8398	-35.3
75	.3747	.8201	-24.3
85	.4158	.8255	-18.9
90	.3966	.8135	-19.0
92.5	.3959	.8352	-21.9
95	.3833	.8456	-24.6
97.5	.3687	.8531	-27.2

Table 4 : FLOW PATH GEOMETRY

Z	0	52,5	72,8	98,7	117,6	145,6	166,6
R_{hub}	171,13	160,91	152,20	142,95	135,66	124,82	116,68
R_{tip}	212,92	212,92	216,92	221,18	224,47	229,45	233,36

Table 4.1 : Location of Instrumentation (all dimensions in mm)

	Inlet	Outlet
Z	-82	245

Table 5 : TEST CASE 2 - OVERALL PERFORMANCE

$\frac{N/\sqrt{T}}{(N/\sqrt{T})_{design}}$	M_{RED}	$\frac{P_{tot\ INL.}}{P_{tot\ OUTL.}}$	η_{is}
[%]	[kg/s]	/	/
100	6.0153	1.2887	0.5786
100	6.4804	1.4025	0.7231
100	6.7884	1.5138	0.7879
100	7.1[illegible]	1.7369	0.8517
100	7.20[illegible]	1.8050	0.8563
100	7.2223	1.8063	0.8615
100	7.4468	1.9361	0.8631
100	7.4754	2.2221	0.8875
100	7.5184	2.2063	0.8815
100	7.5298	2.4459	0.8889
100	7.5435	2.4392	0.8951
100	7.5596	2.7383	0.9034
100	7.5799	2.4369	0.8935
100	7.5811	2.7210	0.8940
100	7.5960	2.8841	0.8913
100	7.6080	2.9657	0.8958
* 100	7.5871	2.8936	0.8975

* Spanwise distribution for that point only.

$$M_{RED} = \frac{M\sqrt{T}_{tot\ INL.}}{P_{tot\ INL.}} \cdot \frac{1.0133}{\sqrt{288.15}} \left[\frac{kg\sqrt{K}}{5bar} \frac{bar}{\sqrt{K}}\right]$$

$$\left(\frac{N}{\sqrt{T}_{tot\ INL.}}\right)_{design} = 315{,}38 \left[\frac{rpm}{\sqrt{K}}\right]$$

$$N_{design} = 10440\ [rpm]$$

80	5.9395	1.3016	0.7734
80	6.2732	1.3660	0.8119
80	6.7257	1.5148	0.8483
80	7.0307	1.6582	0.8776
80	7.5202	2.1451	0.8793
80	7.6193	2.4473	0.8693
80	7.6492	2.7104	0.8784
80	7.6844	2.9159	0.8642
60	5.3593	1.2286	0.8087
60	6.2392	1.3704	0.8526
60	6.8958	1.5528	0.8511
60	7.5029	1.8574	0.8263
60	7.6897	2.1899	0.8107
60	7.7291	2.4804	0.8043
20	5.5491	1.2242	0.5987
20	6.6750	1.4856	0.4822

$$m_{RED} = \frac{m\sqrt{T}_{tot\ INL.}}{P_{tot\ INL.}} \cdot \frac{1.0133}{\sqrt{288.15}} \left[\frac{kg\sqrt{K}}{5bar} \frac{bar}{\sqrt{K}}\right]$$

$$\left(\frac{N}{\sqrt{T}_{tot\ INL.}}\right)_{design} = 315{,}38 \left[\frac{rpm}{\sqrt{K}}\right]$$

$$N_{design} = 10440\ [rpm]$$

Table 6 : TEST CASE 2 - LOCAL OUTLET FLOW PARAMETERS

$\frac{R-R_{HUB}}{R_{TIP}-R_{HUB}}$	$\frac{P_{tot}}{P_{tot\ INL.}}$	$\frac{T_{tot}}{T_{tot\ INL.}}$	M_w |m/s|	M_z |m/s|	α_m
0.0268	0.3623	0.7824	0.5517	0.4691	+1.30
0.0520	0.3609	0.7824	0.5534	0.4999	+2.00
0.0772	0.3599	0.7812	0.5615	0.4638	0.00
0.1191	0.3585	0.7773	0.5761	0.4553	-2.90
0.1611	0.3565	0.7717	0.5322	0.3772	-5.10
0.2450	0.3520	0.7647	0.5920	0. 427	-5 3
0.3708	0.3429	0.7576	0.5952	0.3792	-7.4
0.4966	0.3394	0.7576	0.6109	0.3571	-7.7
0.6225	0.3408	0.7593	0.6389	0.3593	-6.8
0.7483	0.3408	0.7679	0.6560	0.3424	-6.3
0.8322	0.3408	0.7720	0.6777	0.3255	-8.8
0.8742	0.3422	0.7726	0.6851	0.3255	-8.1
0.9161	0.3394	0.7739	0.6854	0.3259	-6.0
0.9497	0.3456	0.7764	0.6675	0.3365	+0.30
0.9832	0.3449	0.7788	0.6530	0.3173	+2.90

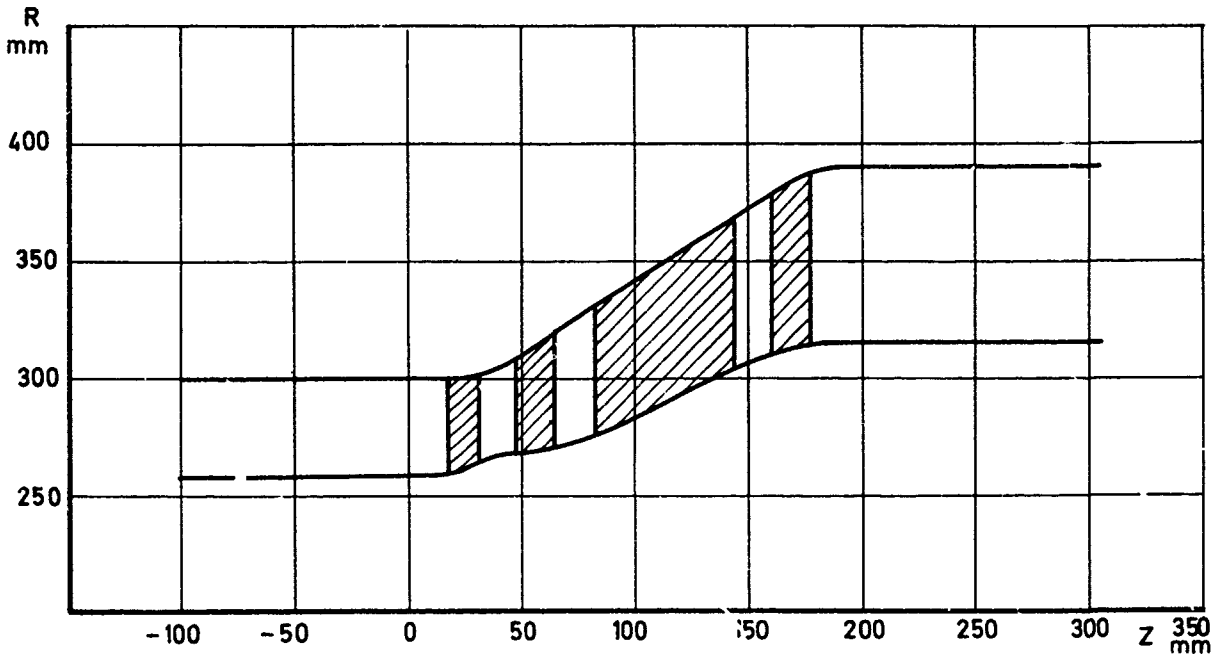

Fig.1 Test Case 1 – flow path

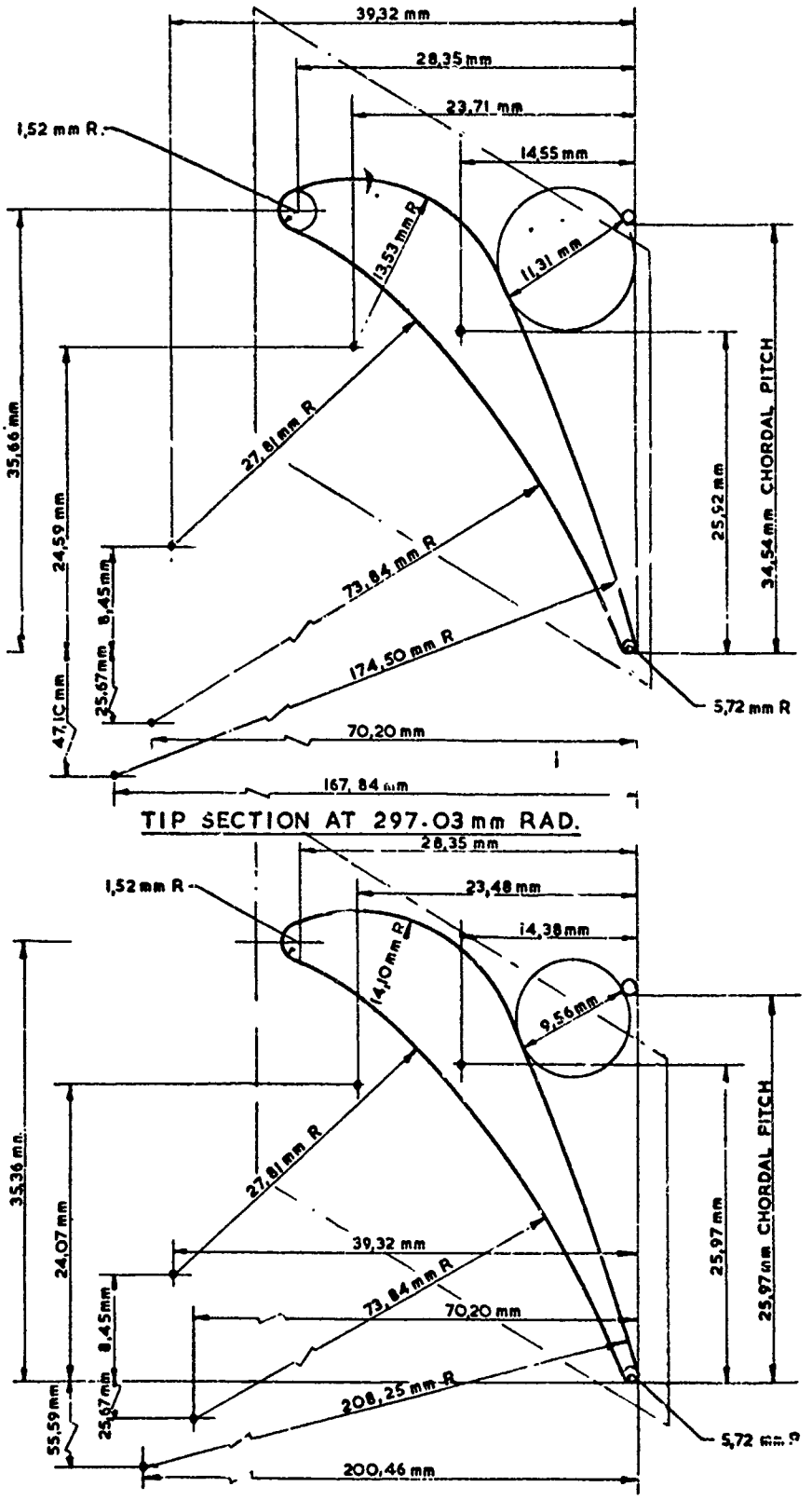

Fig.2 Stage 1 – nozzle guide vane

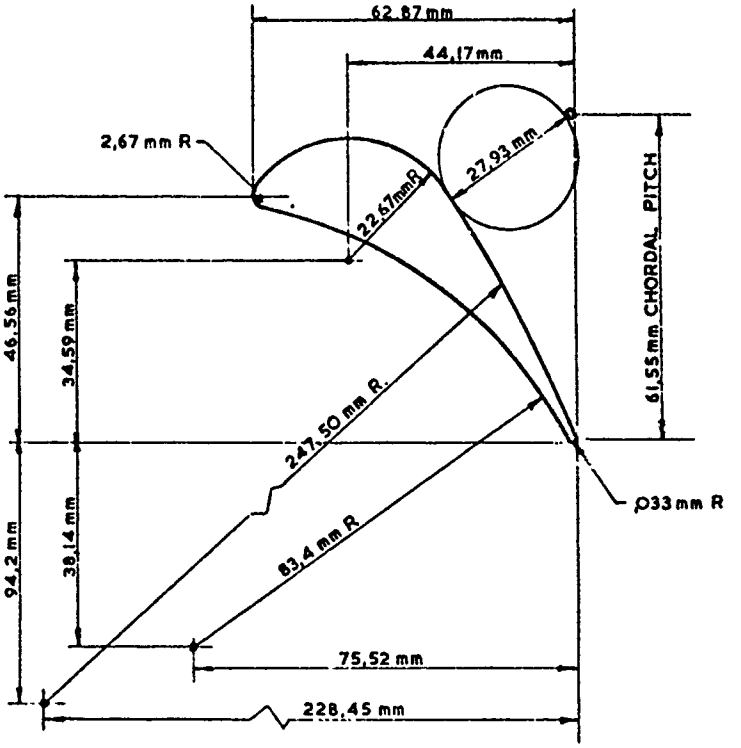

TIP SECTION AT 353·0732mm RAD.

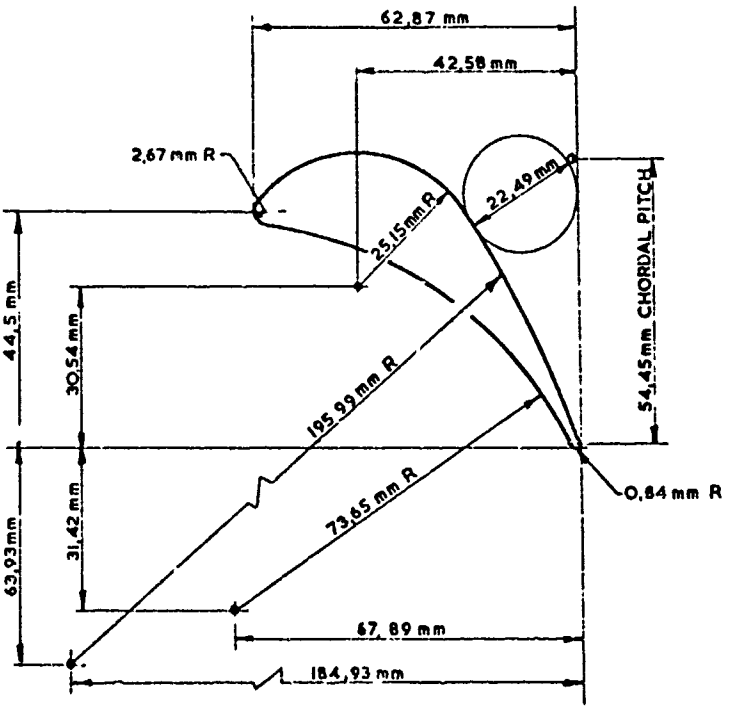

ROOT SECTION AT 312,37 mm RAD.

PROFILE STACKED RADIALLY ON TRAILING EDGE

Fig.3 Stage 2 – nozzle guide vane

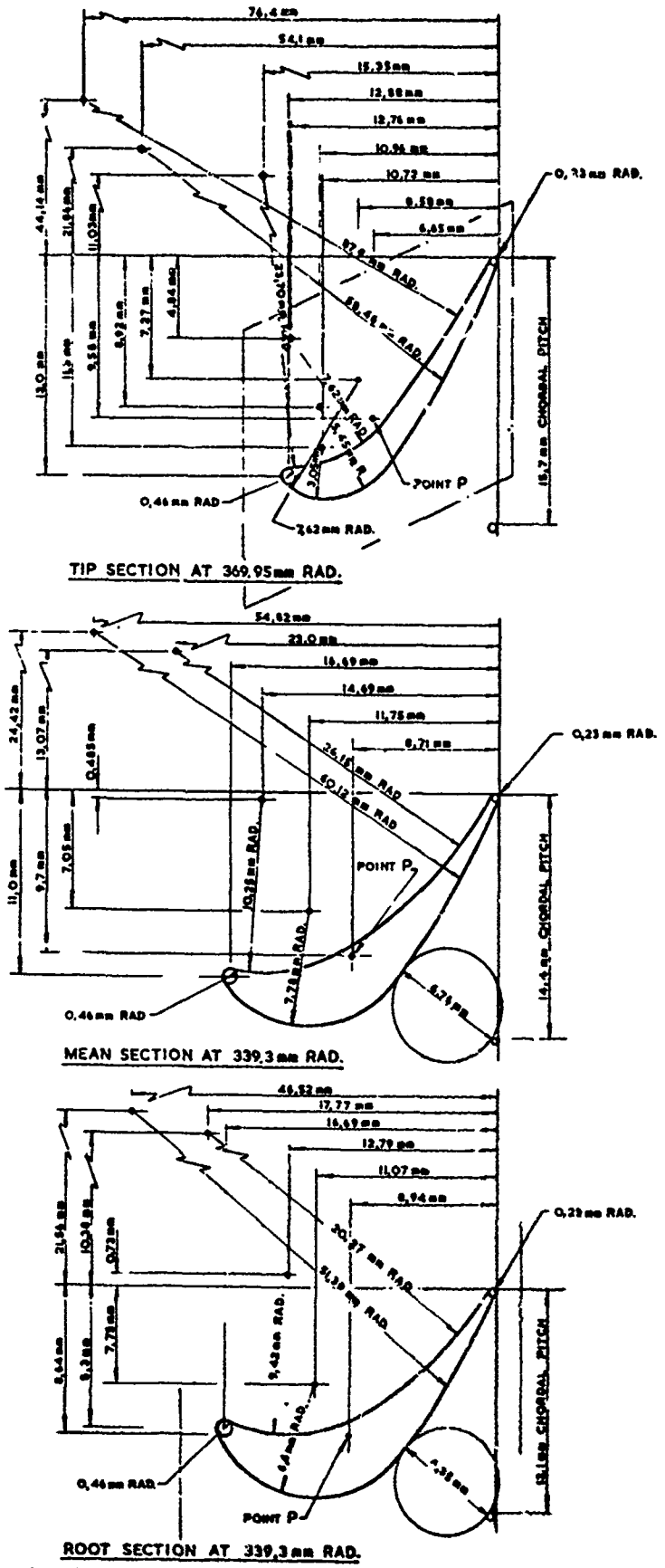

Fig.4 Stage 2 – turbine blade dimensions

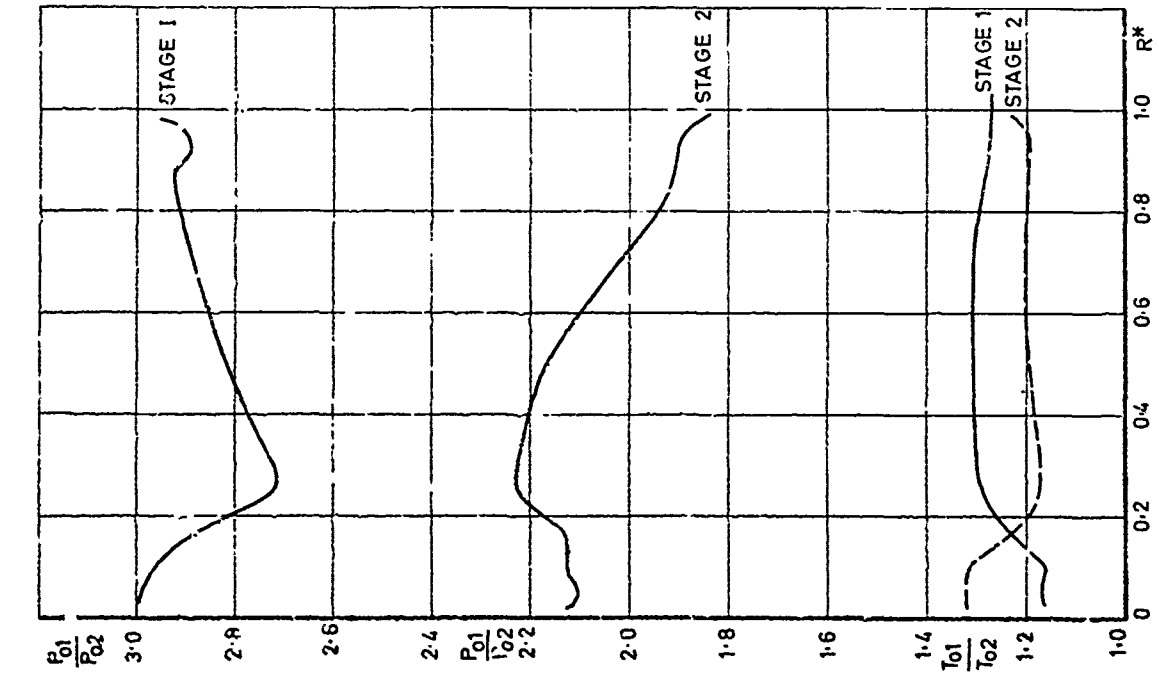

Fig.5 Test Case 1 – local total pressure and temperature ratio

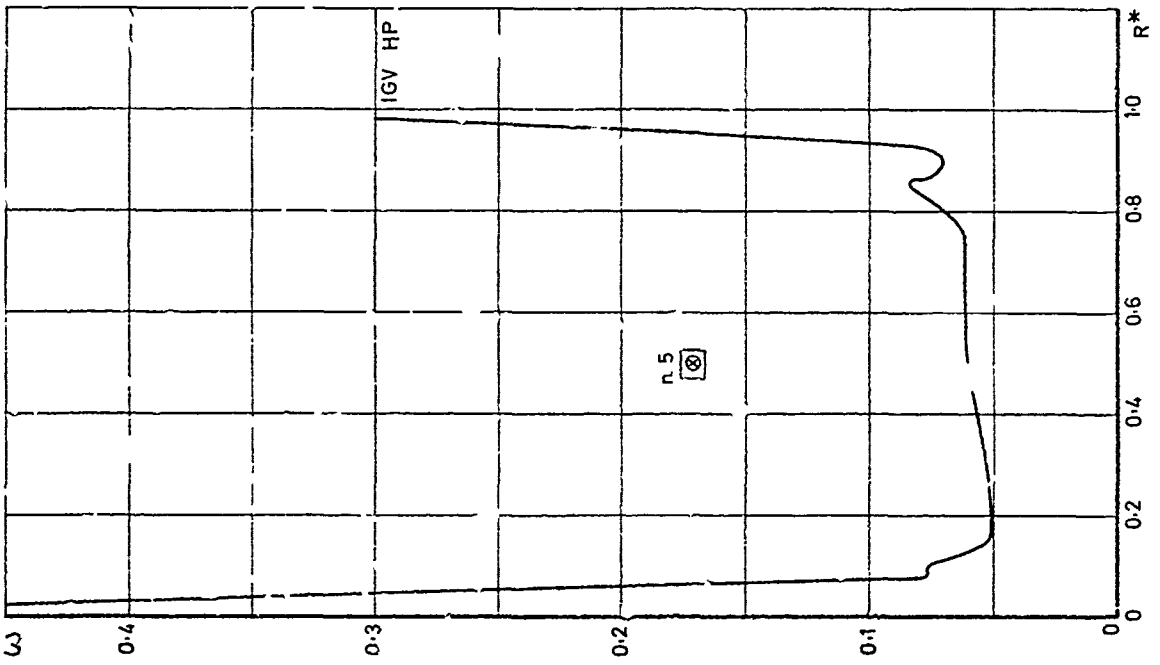

Fig.6 Test Case 1 – loss distribution behind IGV HP

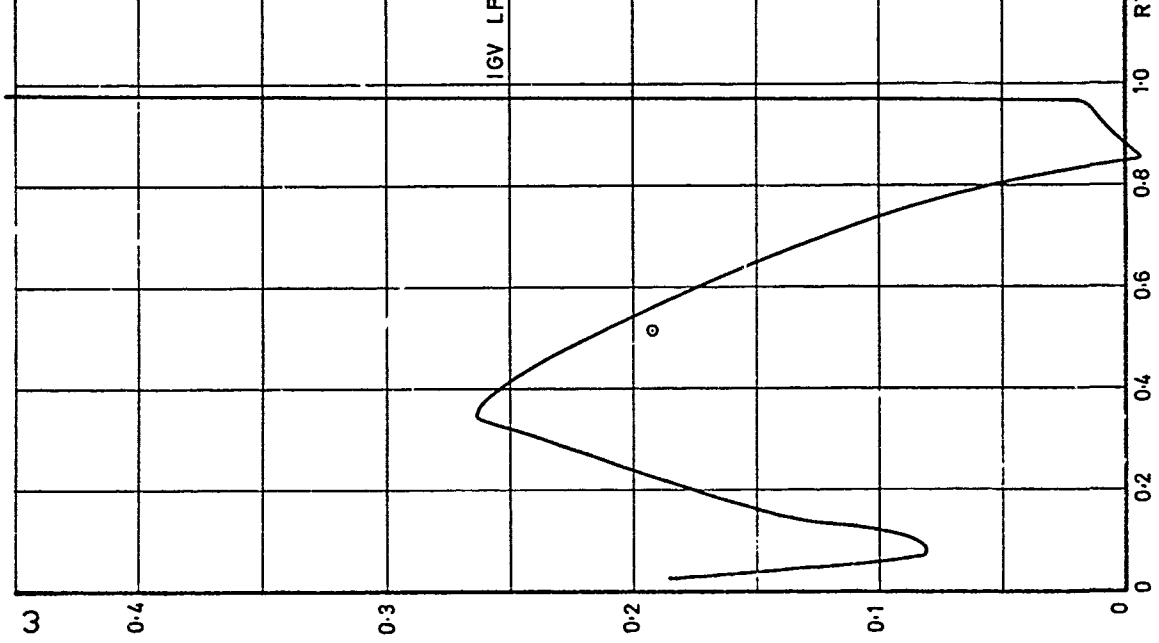

Fig.8 Test Case 1 – loss distribution behind LP nozzle

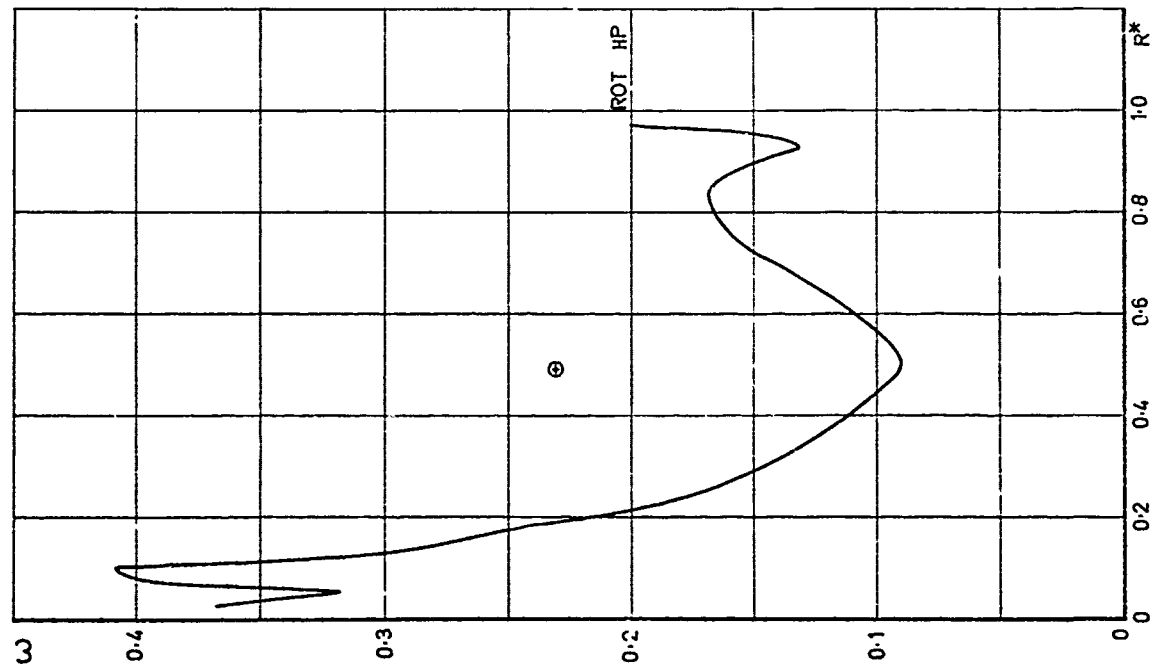

Fig.7 Test Case 1 – loss distribution behind HP rotor

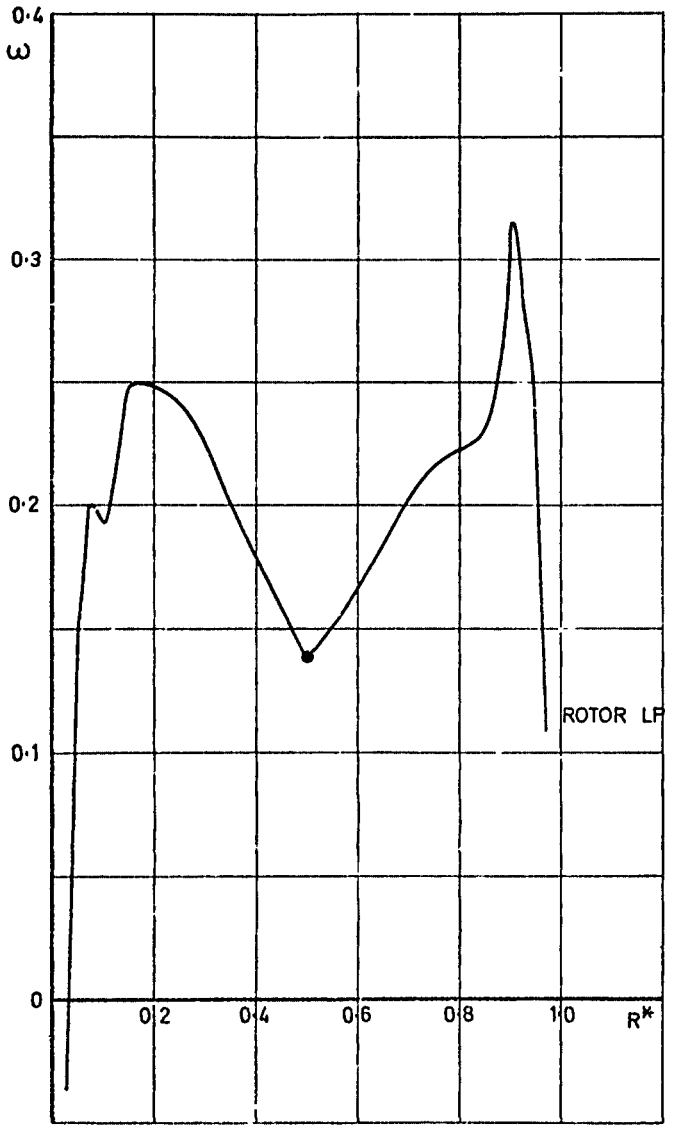

Fig.9 Test Case 1 – loss distribution behind LP rotor

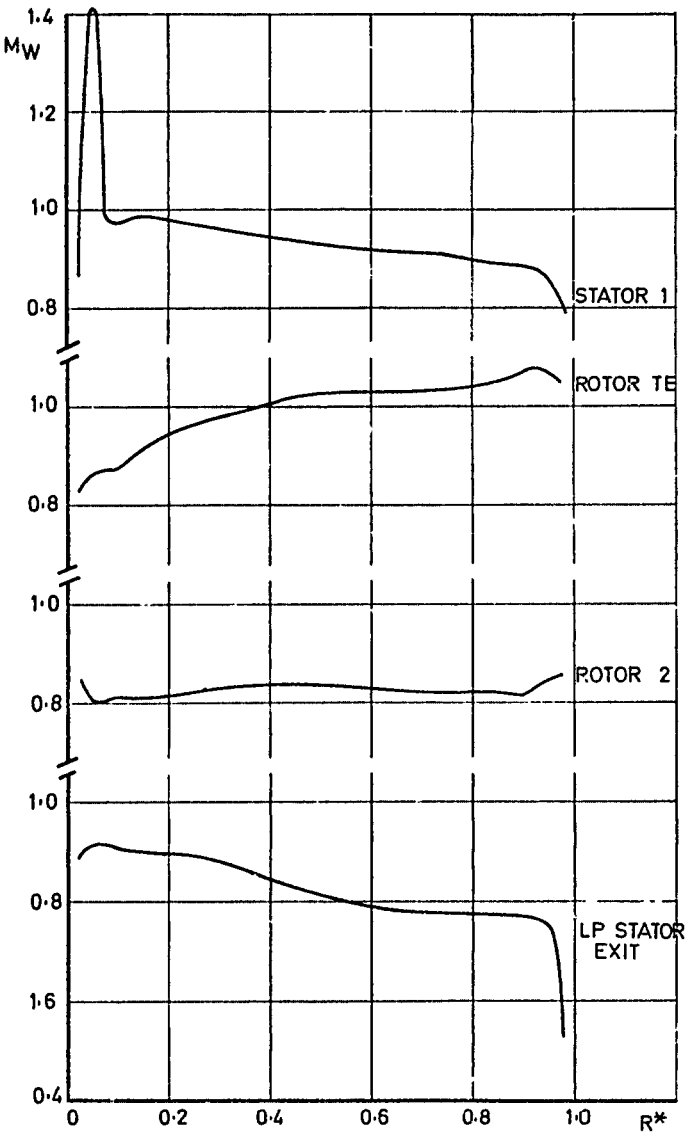

Figs 10–13 Relative Mach number distribution behind nozzle

Fig.10 Test Case 1 – stator

Fig.11 Test Case 1 – rotor T.E.

Fig.12 Test Case 1 – rotor 2

Fig.13 Test Case 1 – LP stator exit

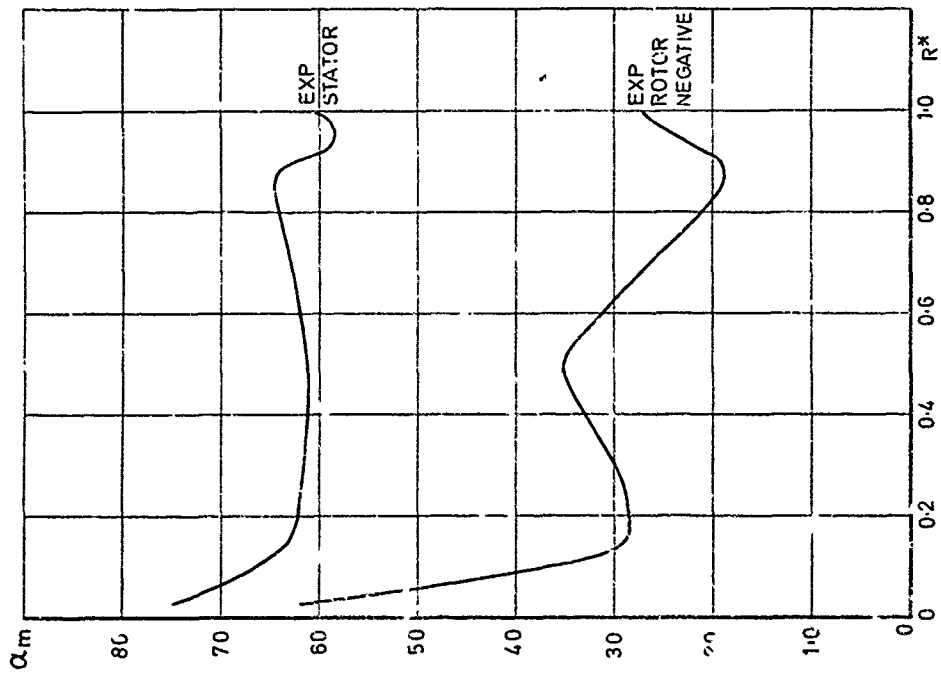

Fig.15 Test Case 1 – stage 2: absolute angle distribution for stage 2

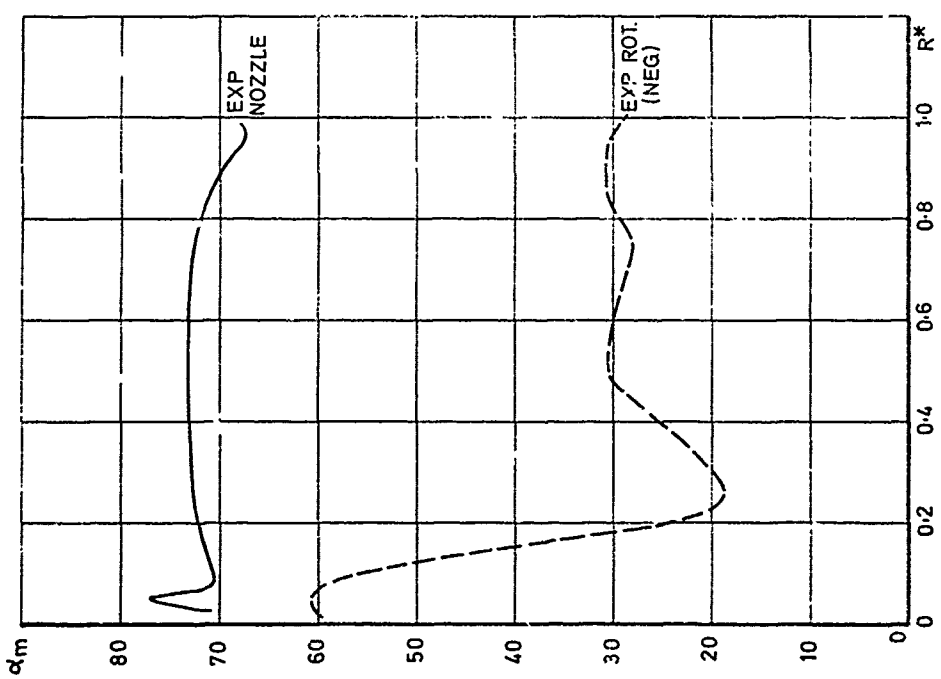

Fig.14 Test Case 1 – stage 1: absolute angle distribution for stage 1

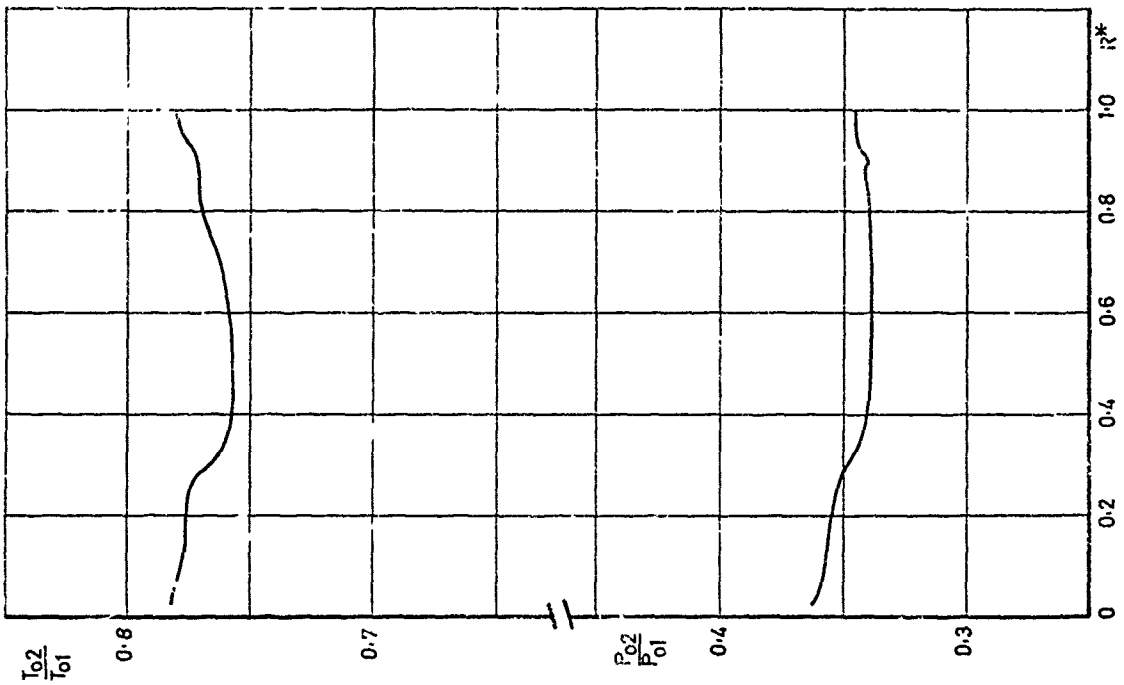

Fig.17 Test Case 2 – local total temperature and pressure

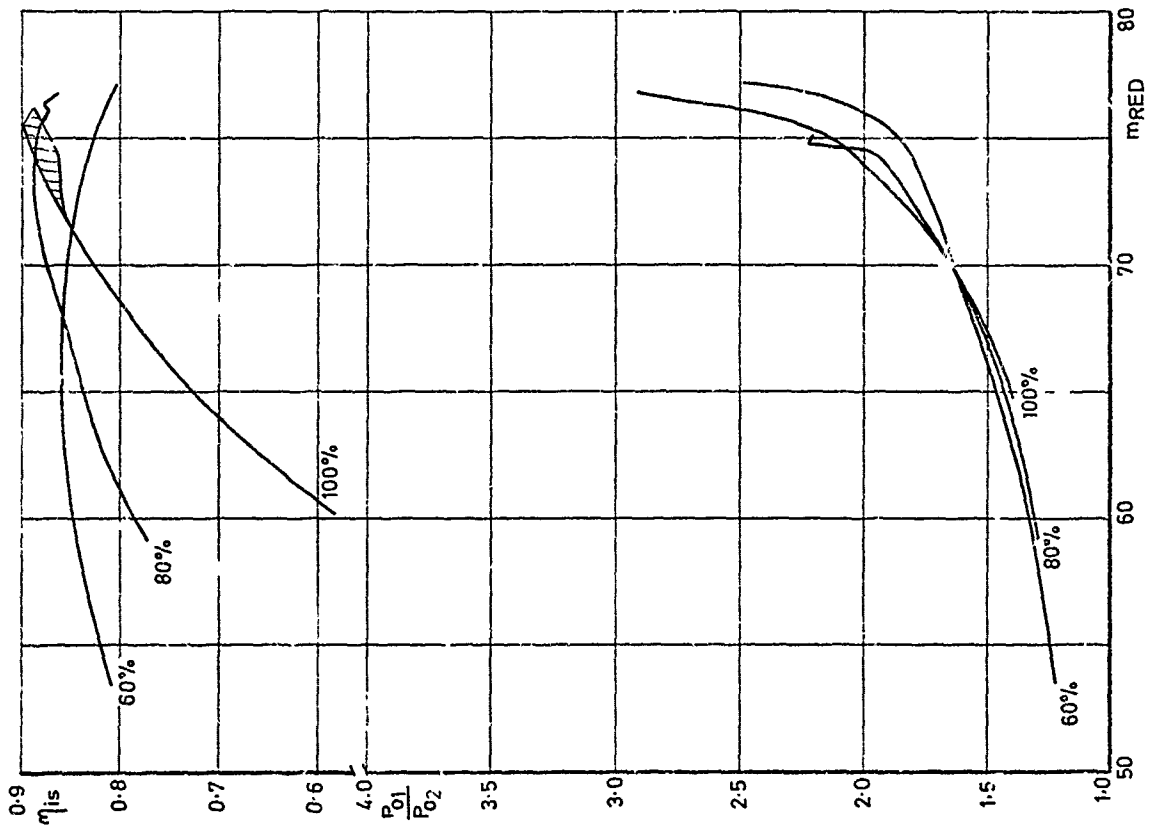

Fig.16 Test Case 2 – overall performance

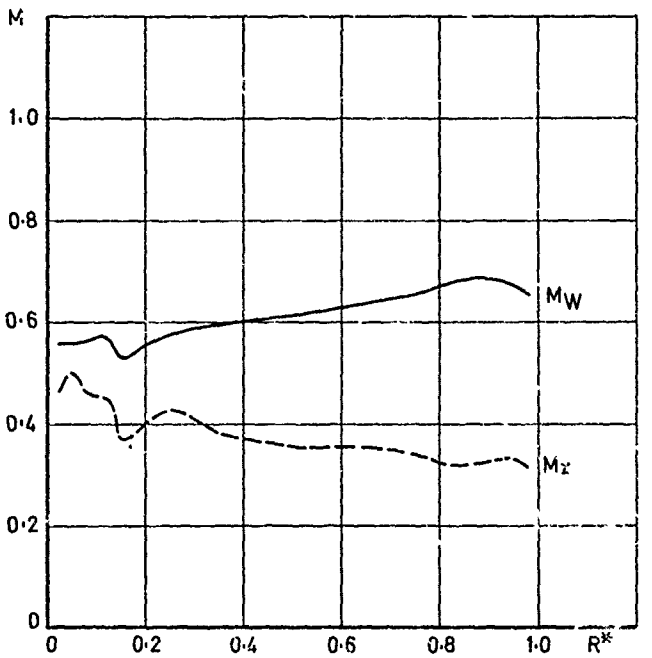

Fig.18 Test Case 2M – local relative and axial Mach numbers distribution at turbine exit

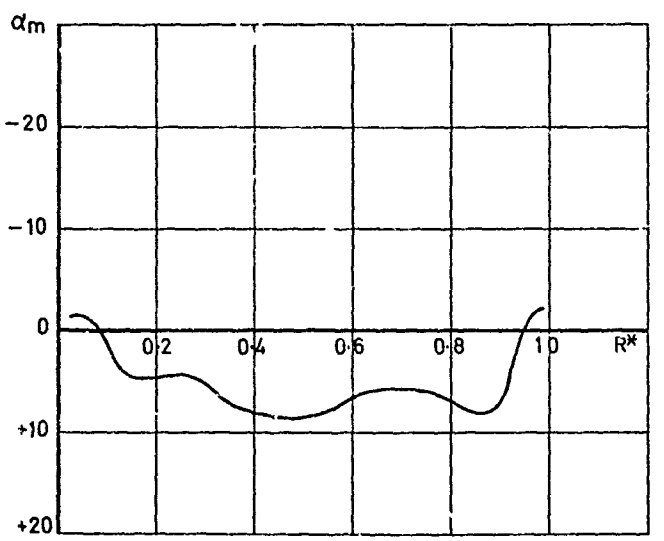

Fig.19 Test Case 2 – local absolute angle distribution

TURBINES

PRESENTATION OF CALCULATED DATA AND COMPARISON WITH EXPERIMENTS

by J. Chauvin
von Karman Institute for Fluid Dynamics
Chaussée de Waterloo 72
1640 Rhode-Saint-Genèse
Belgium

1. INTRODUCTION

For the turbine cases, the geometric data of the two machines were provided, as well as the nominal 2pm and nominal mass flow. The nominal pressure ratio and efficiency had to be found, and for case 2, the full performance map.

Some problem arose because of the way in which data were provided, as the pressure ratio had to be found. Usually, the input data for computer programs are not made for such an approach.

Comparison with the experimental data can also be made somewhat more difficult, because, if the computation provided a wrong pressure ratio, the calculated data pertain in fact to another data point of the performance map.

Computed data were received from two participants for Test Case I, and from four for Test Case II.

The information on the computer programs used is summarized in Table I.

The following sections contain more extensive information on the methods, when available, and a comparison in graphical form, of the calculated and measured data, case by case and author by author.

General comparisons and comments are given in the last section.

LIST OF SYMBOLS

M	Mach number
$\dot{m}$	mass flow kg/sec
P_o or P_{tot}	total pressure, bars
p	static pressure
R	radius, mm
$R^* = \frac{R - R_{hub}}{R_{tip} - R_{hub}}$	
Z	axial coordinate, mm
α	absolute angle from axial direction (positive in the direction of camber, for nozzle in direction of rotation for rotor).
ω	blade row relative total pressure loss coefficient $\frac{P_{oi} - P_{oi+1}}{P_{oi} - P_{i+1}}$ (i inlet of blade row) ($i+1$ outlet of blade row)

SUBSCRIPTS

m	in meridional direction
Red	reduced at ISA sea level conditions
W	relative to rotor
Z	in axial direction
1	upstream of turbine or stage
2	downstream of turbine or stage

LIST OF FIGURES

TABLE I : GENERAL INFORMATION ON COMPUTER PROGRAMS

Author	Calculation Method	Computer	Average Comp. Time per Point	Loss Correlation		Deviation
				Profile	Secondary	
2	Finite element through flow	CDC 6500	II 70 sec	Ainley-Mathieson Without AVR	Distributed	
5	Streamline curvature through flow	CDC 6500	I 45 sec (31 sec CPU)	Traupel Modified Without AVR	Uniform (Traupel)	Mod. Sine Rule
15	Streamline curvature through flow	IBM 370-165	I 20 sec II 20 sec	Without AVR	Linearly Distributed	Subs : Sine Rule Sup : Continuity
18	NASA-CR-710	-	II -	Without AVR		NASA CR-710
28	NASA-CR-710	TR 440	II 8 sec	Without AVR		NASA CR-710

2. RESULTS FOR TEST CASE I

For this case, the performance at the design point only is available, including detailed traverses ahead and downstream of each blade row. There were two participants in the calculation, no. 5 (Dr. Zollinger, Sulzer Brothers) and no. 15 Dr. Denton, C.E.G.B).

A. AUTHOR no. 5

Description of the method

1. Loss model

Basically the loss model of Traupel was used. The total loss is the sum of :

- profile loss

  The profile loss depends on the flow angles. It is corrected for influence of Reynolds number, trailing edge thickness and departure from optimum solidity.

- secondary loss

  This loss depends on the aspect ratio, the blade turning and the ratio of inlet and outlet velocities.

- tip clearance

  It is mainly a function of the tip clearance, the flow annulus area and the flow angles.

Only minor corrections to the published loss model were applied, mainly for the trailing edge loss and for the secondary loss. A uniform loss distribution was assumed throughout.

2. Blade turning

The blade turning is calculated via a momentum balance in a rotating channel by neglecting the contribution of the pressure integral on the control volume to the circumferential momentum. Effects of rotation and variation of stream tube height and radius are included. The calculation scheme is a modification of Traupel's method[2] No correction for over- and underturning due to secondary motion was applied.

3. Computer program

A streamline curvature method was used. The complete radial equilibrium is fulfilled at calculation stations which coincide with the blade leading and trailing edges. Additional stations at the instrumentation planes were introduced. On a CDC 6500 the calculation time for 5 streamlines was 31 CP seconds and 14 10 seconds.

|1| W. Traupel : Thermische Turbomaschinen I
2nd edition, Springer Verlag 1966

|2| W. Traupel : Prediction of flow outlet angle in blade rows with conical stream surfaces
ASME-Paper 73-GT-32

RESULTS OF CALCULATION

For the overall performance, Table 2 compares the calculated and experimental results.

TABLE 2

	$\dot{m}_{red}$	P_{01}/P_{02}	$\Delta P_{01}/P_{02}$%	η	$\Delta\eta$%
Experiment	4.82	5.85		0.8915/0.8841	
Author no.5	4.82	5.92	+1.2 %	0.89	0.6

The agreement is very good.

For the local quantities, the data is given in Figs.1 to 4.

For the total pressure ratio, the trends in function of radius are correct. The performance is underestimated for the first stage and underestimated for the second, with almost perfect compensation.

The total temperature ratio is well predicted, except near the hub.

The angle and Mach number predictions give both the proper trends and average values. The local differences are due to the heavy secondary flow effects appearing in the real flow.

For the losses, a constant value with radius is assumed. It corresponds quite well to the averaged measured value. One has :

TABLE 3

	1st nozzle	1st rotor	2nd nozzle	2nd rotor
ω_{calc} :	17.2	23	19.5	14.5

B. AUTHOR no. 15

Description of the method :

The program is of the streamline curvature type but is not based on any published method. It has been specifically developed to calculate the flow in the low pressure cylinders of large steam turbines where high radial velocity components and large areas of supersonic flow can occur.

The radial equilibrium equation is used to express the gradient of meridional velocity along an arbitrary quasi-orthogonal (QO) in terms of the gradients of enthalpy, entropy and angular momentum and the local values of meridional velocity and streamline curvature. Components of blade force along a quasi-orthogonal are neglected.

The iterative procedure contains 3 loops. An inner loop in which the velocity along a QO is adjusted to satisfy continuity without changing the fluid properties or the RHS of the radial equilibrium equation. A central loop in which the fluid properties and radial equilibrium terms are changed whilst the streamline curvature is held constant. When this second loop has been completed at all QO's a complete radial equilibrium solution is obtained using the current guess of the streamline curvatures. In the outer loop the streamline curvatures are recalculated and the inner loops repeated until overall convergence is obtained.

Quasi-orthogonals can be placed in duct regions, at blade row leading and trailing edges and within blade rows, they can be inclined at any angle to the machine axis so the calculations can be performed for both axial and radial flow machines. The spacing of the QO's determines the streamline curvature relaxation factor and hence the number of main loop iterations. Grid aspect ratios of up to about 15 can be used without excessive computation times.

Streamline slopes and curvatures are obtained by simple parabolic curve fits since it is felt that practical QO spacing (about 3 QO's per blade row) and neglect of non-axisymmetric terms, do not justify more complex curve fits. The calculating grid is formed by the intersection of the streamlines and QO's and so the grid points move as the calculation proceeds.

A subroutine of the program contains an approximate formulation of wet and dry steam properties. This calculates all other required properties when given values of enthalpy and entropy. A perfect gas property subroutine can be substituted when necessary.

The blade outlet (and internal) flow directions are input as data and, in the absence of more complete blade performance data, the outlet angle is taken as $\cos^{-1}$ O/P in subsonic flow. For supersonic outflow the outlet flow direction is obtained by applying the continuity and isentropic flow relations between the throat and trailing edge so the outlet direction changes as the calculation proceeds. With this model choking (i.e. maximum mass flow) occurs when the relative Mach number exceeds unity over the whole of the trailing edge and the mass flow does not change if the outlet Mach number is increased beyond choking.

Blade losses are calculated using correlations for profile loss, secondary loss, wetness loss and tip leakage loss. The secondary loss is distributed linearly between hub and tip. The tip leakage flow is substracted from the blade flow and the two flows are remixed beyond the trailing edge.

The basic program gives solutions at a constant specified mass flow, however, in practice it is far more convenient to obtain solutions at a specified pressure ratio. For low Mach number machines (i.e. subsonic) the mass flow can be adjusted as the calculation proceeds to search for a specified pressure ratio. However, for multistage machines with supersonic flow it becomes very difficult to make this procedure converge. A method has therefore been developed whereby the continuity equation is overridden by a requirement to obtain a specified outlet pressure. The resulting imbalance in mass flow is used to change conditions at the next upstream trailing edge until eventually the inlet mass flow is changed and the continuity equation is satisfied once more.

The program has been extensively tested against experimental data from large (500 MW) steam turbines and from model air turbines. It is generally found to give good agreement with measurements provided that viscous effects are small and that the blade outlet flow directions are accurately specified. In many cases the accuracy with which these angles are known limits the accuracy of the calculation.

Results of the calculation :

For the overall performance, Table 4 gives the comparison :

TABLE 4

	m_{red}	P_{01}/P_{02}	$\Delta P_{01}/P_{02}$%	η	$\Delta\eta$%
Experiment	4.82	5.82		0.8915/0.884	
Author no.15	4.96	5.64	3	0.83	6

Additionally, Author 15 has calculated the performance curve at 100 % r.p.m. It is given in Fig.5.

For the local quantities, the data is given in Figs. 6 to 8. The total pressure and temperature ratio evolutions are not available.

The angle prediction (Figs. 6 and 7) is correct on average and in tendancy, although a little farther than for Author 5. The local secondary flow effects are not predicted, just as for Author 5. The Mach number evolution (Fig.8) is very well predicted with some larger difference for the first nozzle outlet.

The information on loss coefficients is not available.

3. RESULTS FOR TEST CASE II

For this case, a complete performance map is available, but no traverse data, except on absolute Mach number and angle relatively far from the last rotor, for the nominal point.

There were four participants in the calculation :

no. 2 (Professor Ch Hirsch, V.U.B. Belgium)
no.15 (Dr. Denton, C.E.G.B., Great Britain)
no.18 (NASA Lewis Research Center)
no.28 (Drs. Rick and Kurzke, T.H. München, Germany)

A. AUTHOR no. 2

Description of the method :

The general description is given in Paper No.5 of the proceedings of this meeting. The loss correlation is the classical Ainley-Mathieson correlation, with distributed secondary losses.

Results of calculation :

Calculations were made for 60 and 100 % nominal speed. The results are presented in Fig.9. The agreement is quite good for the pressure drop, with, at a given pressure ratio, and error of the order of 3 % in mass flow, for the 100 % speed curve. The maximum error in efficiency is of 2 %n.

The comparison with the traverse data is given in Figs. 10 to 12. The agreement is very good for the temperature ratio, while the calculated pressure drop is too small, but with the proper shape. Mach number profiles (Fig.11) are quite well predicted, except very near the hub and for axial Mach number, near the tip.

The angle distribution (Fig.12) has the correct shape, but is in error by about 5°.

B. AUTHOR No. 15

Description of the method : this has been given under section 2.

Results of calculation :

For the overall performance, calculations were performed for the 100 % speed line only. The data is presented in Fig.13.

Comparing to a given pressure ratio, the error on mass flow is as follows :

P_{02}/P_{01}	2.0	2.5	3.0
$\frac{\dot{m}_{calc}-\dot{m}_{meas}}{\dot{m}_{meas}}$	1.35	+1.85	+2.64

The efficiencies are overestimated by 2.5 % about.

For the traverse data, the calculations were made for P_{02}/P_{01} = 2.63 (vs. 2.89 for the experimental data). Mach numbers agree very well indeed (Fig.14), while the angles (Fig.15) are different by more than 10°.

C. AUTHOR No. 18

Description of the method (see also No. 28) :

Test case 2 was analysed with a computer program which computes the off-design performance of multi-stage axial-flow turbines. The program is applicable to turbines having any number of stages up through eight (8). It allows for a change in mean-section radius between blade rows, and includes provisions for radial variation in loss and flow conditions. The radial variation in loss and flow conditions is calculated at up to six (6) radial positions at the radial center of fixed area sectors. Each sector is a quasi-one-dimensional element and the radial centers are joined utilizing simple radial equilibrium at the stator exit and the rotor exit. Semi-perfect gas properties are assumed with variable specific heat at constant pressure and variable specific heat ratio. Gas properties may be input, and in addition, provision is made to incorporate gas properties as a function of temperature. Geometry may be input as passage distributed area or vector flow angle.

Losses are incorporated by specifying a constant value of kinetic energy loss coefficient and an incidence loss for each blade row. The incidence loss model assumes that some or all of the kinetic energy normal to the flow direction is lost upon entering each blade row.

The overall performance : calculations provided a full performance map (Fig.16). Comparison with the exprimental data is given in Figs.17, 18 and 19 for 100 %, 80 % and 60 % nominal speed, respectively.

The shape of the curves is correct, with a shift towards smaller mass flows, and a somewhat overestimated efficiency. More particularly, for the 100 % curve, one has :

P_{02}/P_{01}	1.5	2.0	2.5	3.0
$\frac{\dot{m}_{calc}-\dot{m}_{meas}}{\dot{m}_{meas}}$	-7.45	-6.7	-4.0	-2.55

The maximum $\Delta\eta = \frac{\eta_{cal}-\eta_{meas}}{\eta_{meas}}$ is 1.5 % (at given pressure ratio).

For the traverse data, the results are given in Figs. 20, 21 and 22.

D. AUTHOR No. 28

Description of the method : This is the same as for author No. 18, except for some aspects of the correlation.

In relation with general digital computer programs for calculating the off-design performance of complex turbo-powerplants a compilation was done for a relative cheap off-design turbine program having a computing time less than 5-10 sec. for one operating point of a multi stage axial turbine. The program includes provisions for radial variation in loss and flow conditions. For test case 2, the radial flow conditions were calculated in 5 sectors. The program method is based on the procedure and computer program presented in NASA-CR-710 by E.E. Flagg. The type of computer was Telefunken TR 440 and the average computer time was about 5 sec. to 10 sec. The estimation of peak efficiency was taken from :
- Warner L.S. : ASME Paper 61-WA-37
- Glassman A.J. : NASA TN-D-6702

The method for computing incidence losses is equal to that presented in :
- Flagg E.E. : NASA-CR-710 (standard option) modified according to Fig.23.

The uncertain magnitude of the incidence losses probably gives greater differences between the calculated and measured performance maps in the efficiency range lower than about 75%.

For the overall performance, full performance maps were calculated and are given in Figs. 24 and 25. The comparison with experimental data is given in Figs. 17 and 18 for 100 % and 80 % nominal speed. Conclusions are the same as for Author No. 18.

For the traverse data, the comparison is made in Figs. 20 to 22.

Additionaly, the calculated loss coefficients for each blade row are given in Fig.26.

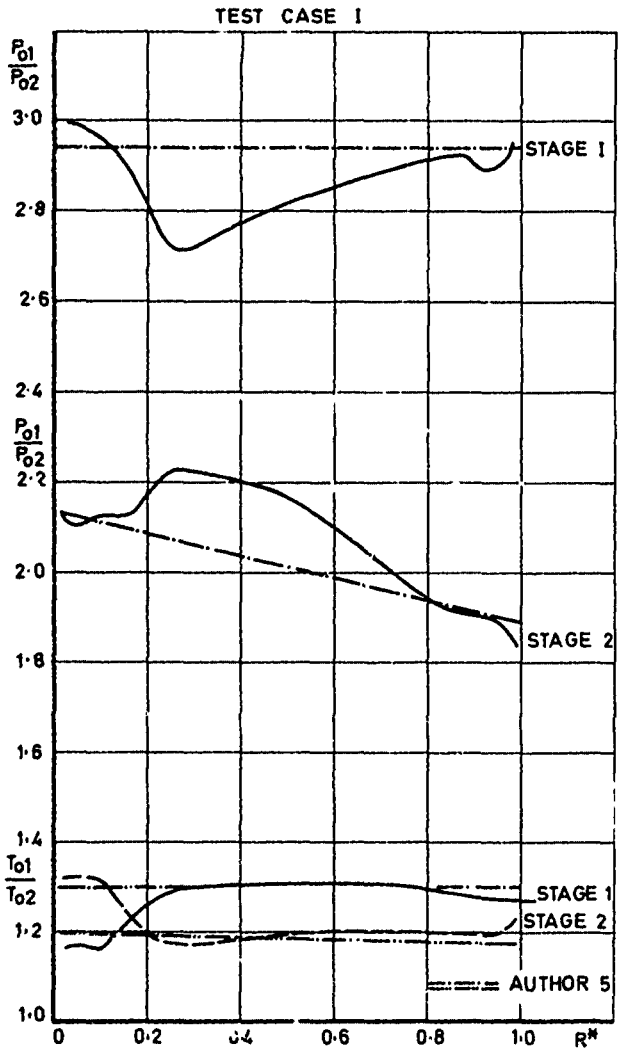

Fig.1 Test Case I, authors 1, 2, 5
Comparison of local total pressure and temperature ratio

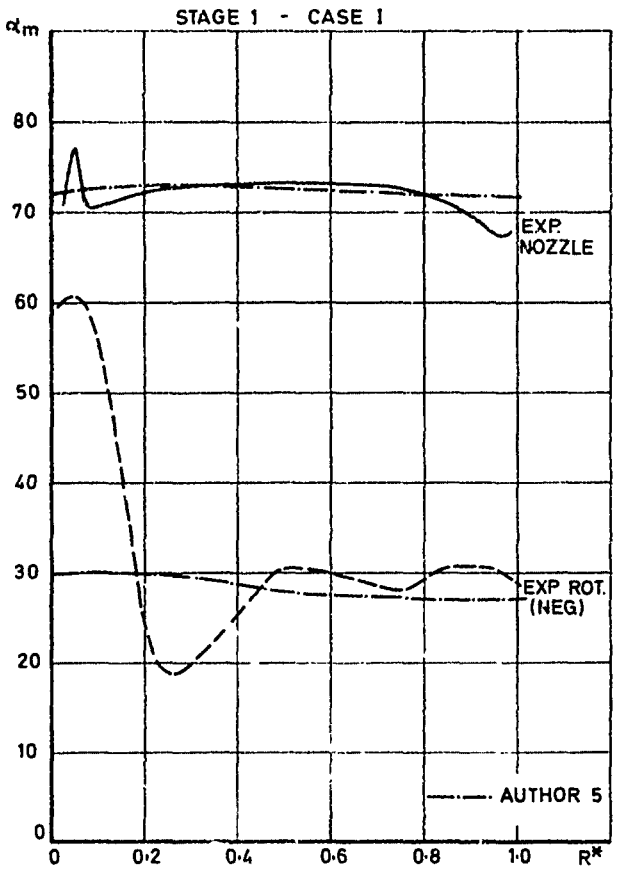

Fig.2 Stage 1, Case I, author 5
Comparison between measured and predicted absolute outlet angles

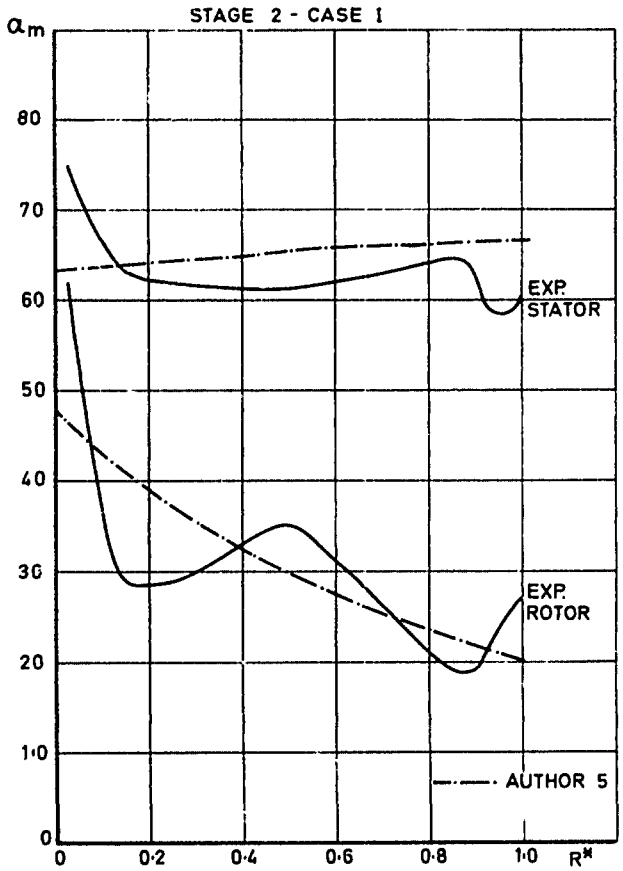

Fig.3 Stage 2, Case I, author 5
Comparison between measured and predicted absolute outlet angles

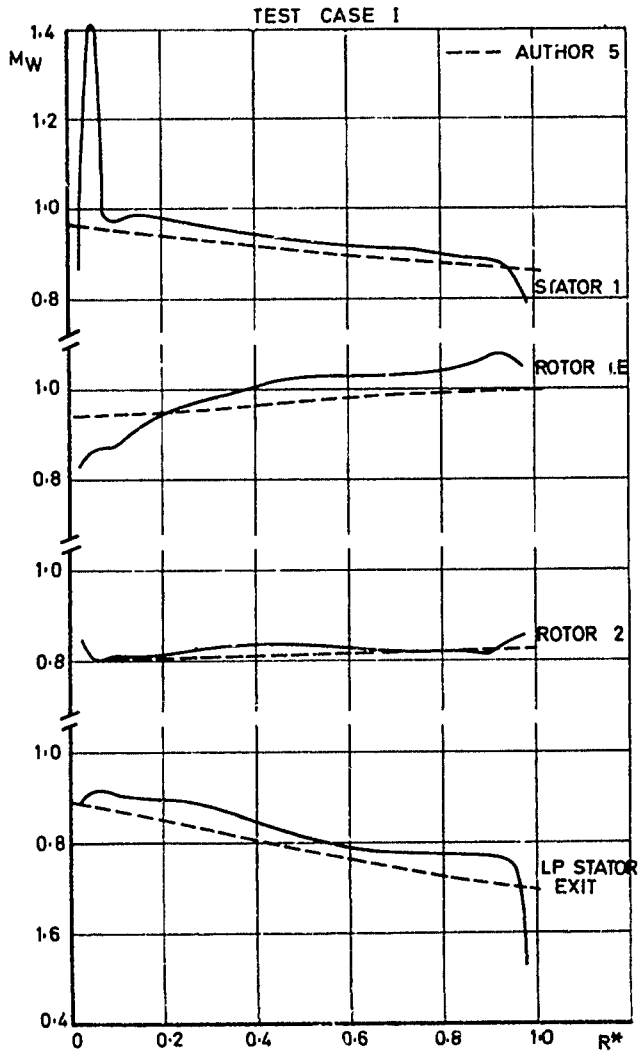

Fig.4 Case I, author 5
Comparison between local calculated and measured relative Mach number

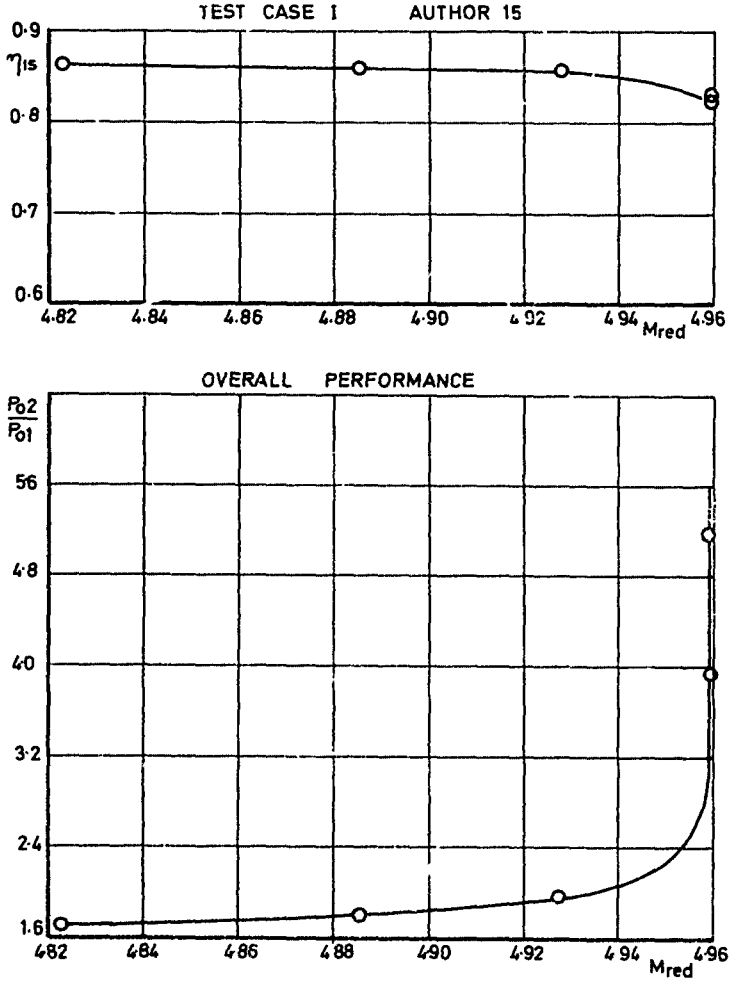

Fig.5 Case I, author 15
Overall performance prediction

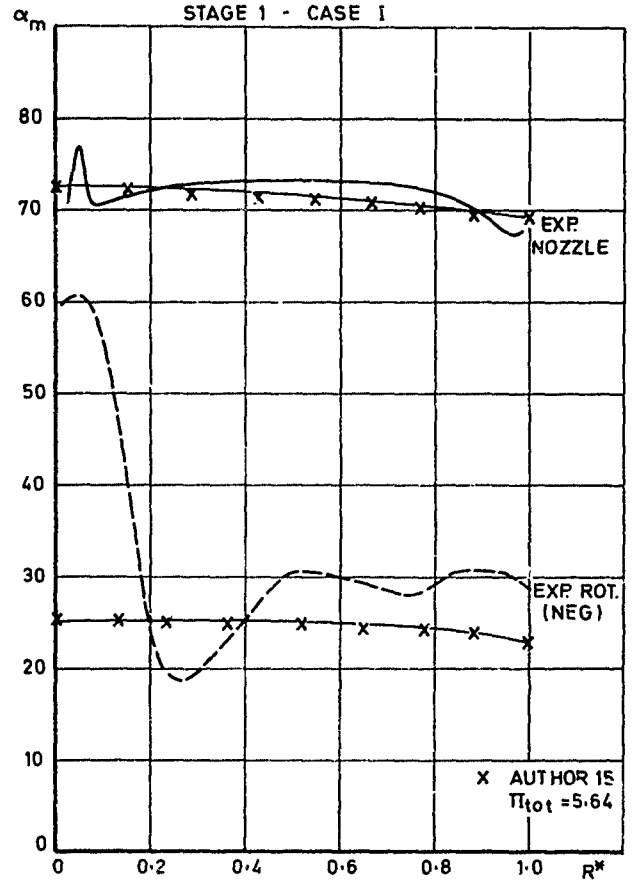

Fig.6 Stage 1, Case I, author 15
Comparison between predicted and measured absolute outlet angle

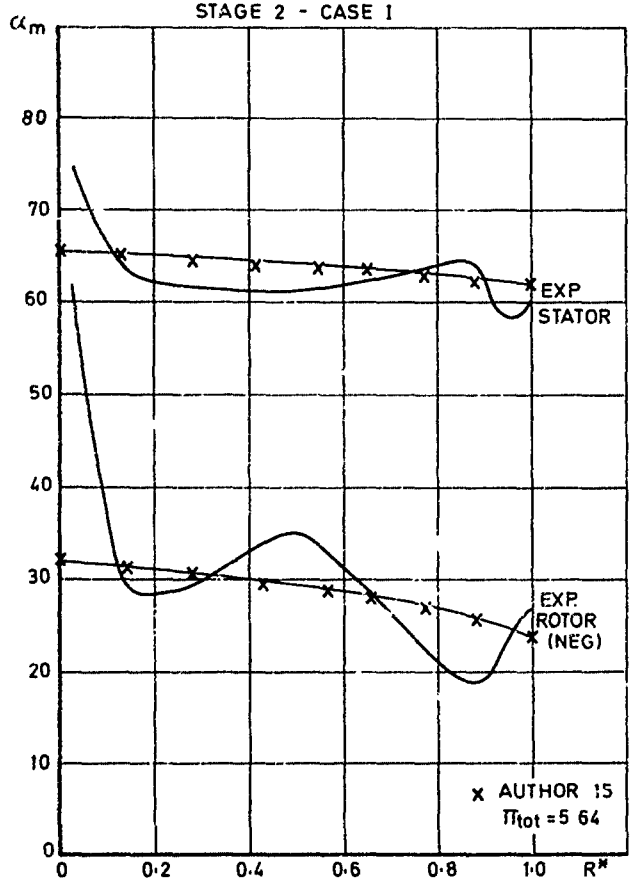

Fig.7 Stage 2, Case I, author 15
Comparison between predicted and measured absolute outlet angle

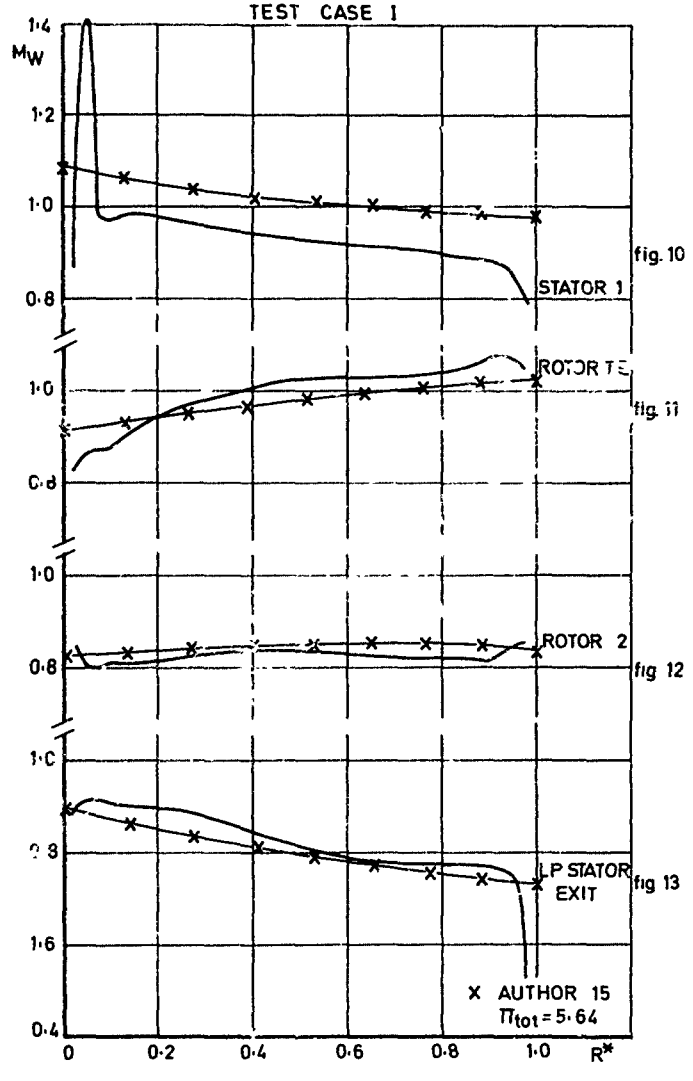

Fig.8 Case I, author 15
Comparison between calculated and measured local relative Mach number

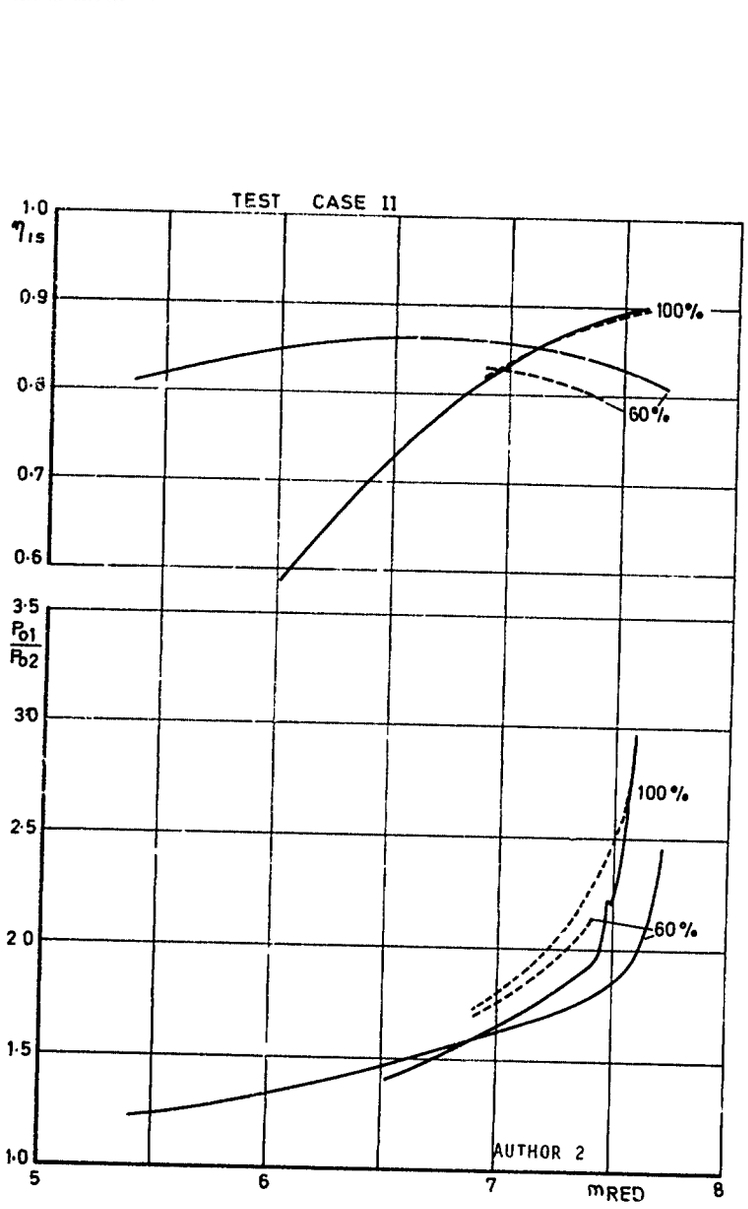

Fig.9 Case II, author 2
Comparison between calculated and measured overall performance

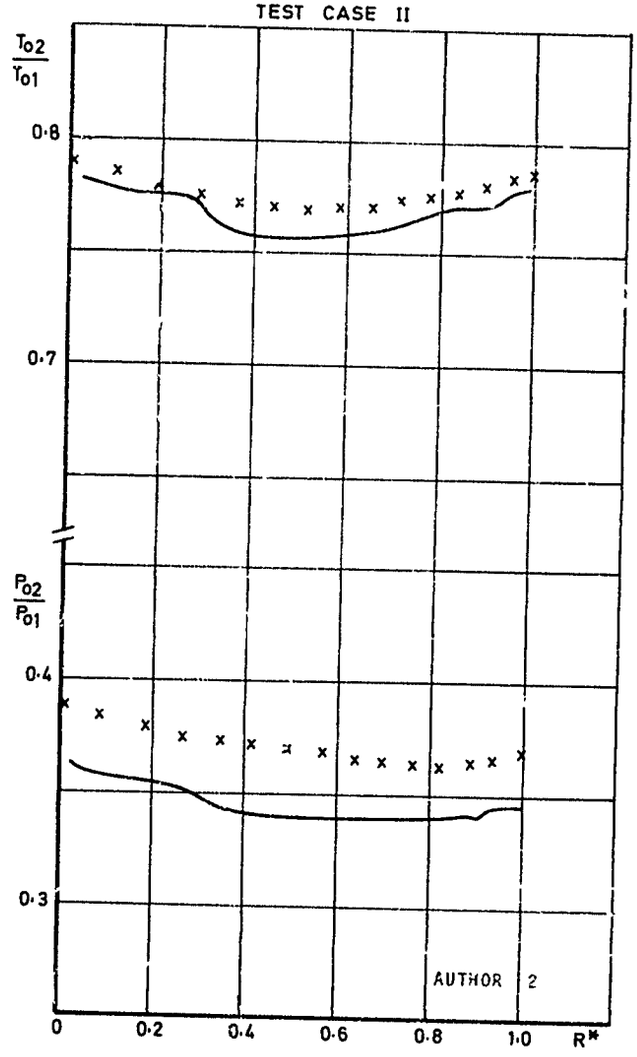

Fig.10 Case II, author 2
Comparison between calculated and measured local total pressure

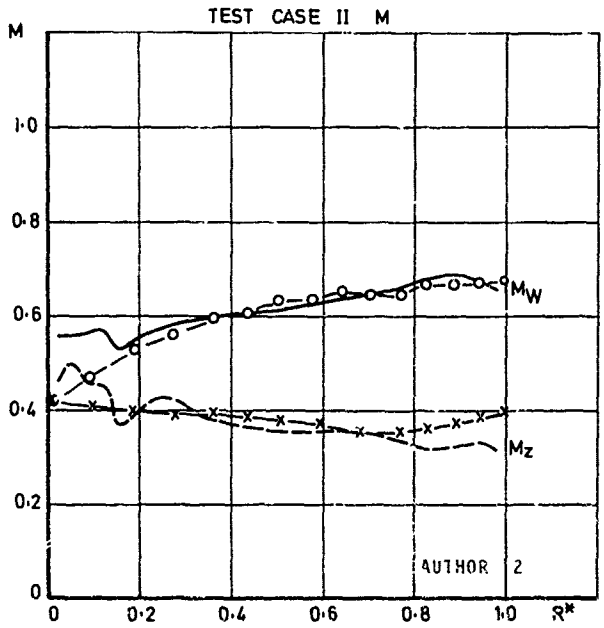

Fig.11 Case IIM, author 2
Comparison between calculated and measured relative and axial Mach number behind turbine

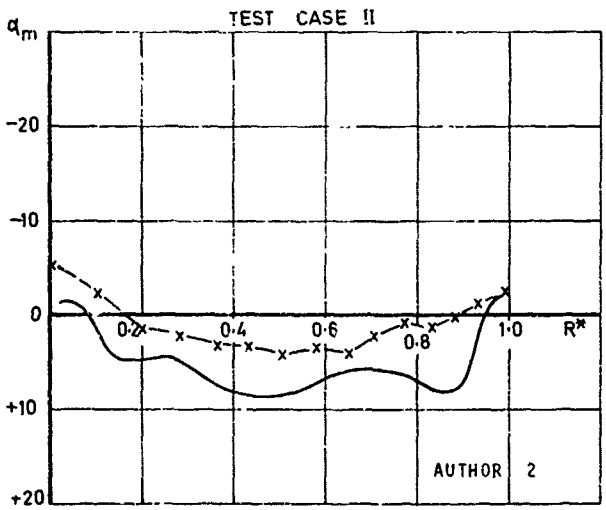

Fig.12 Case II, author 2
Comparison between calculated and measured absolute outlet angle

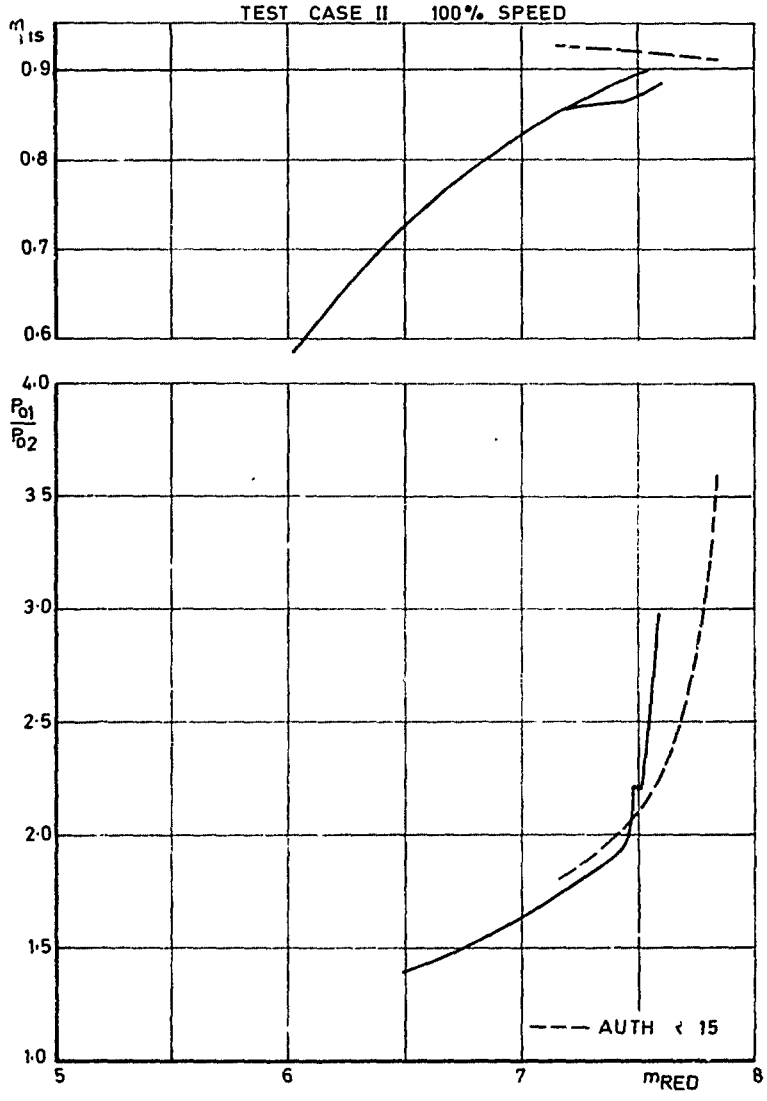

Fig.13 Case II 100% speed, author 15
Comparison between calculated and measured overall performance

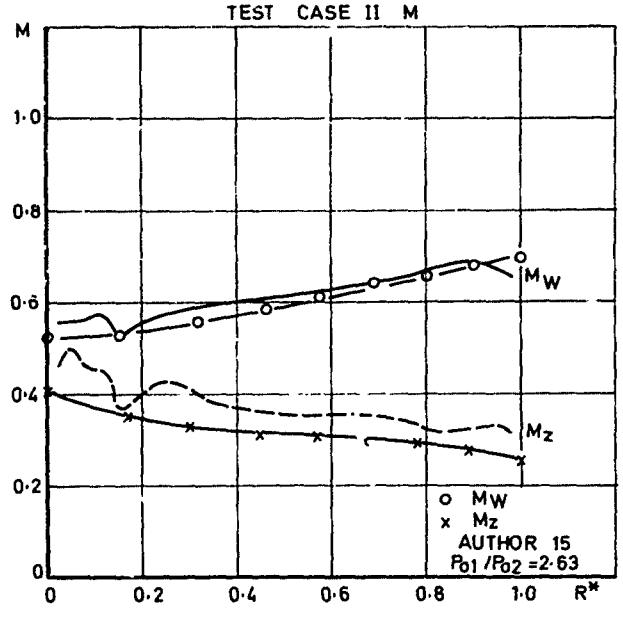

Fig.14 Case IIM, author 15
Comparison between calculated and measured relative and axial Mach number behind turbine

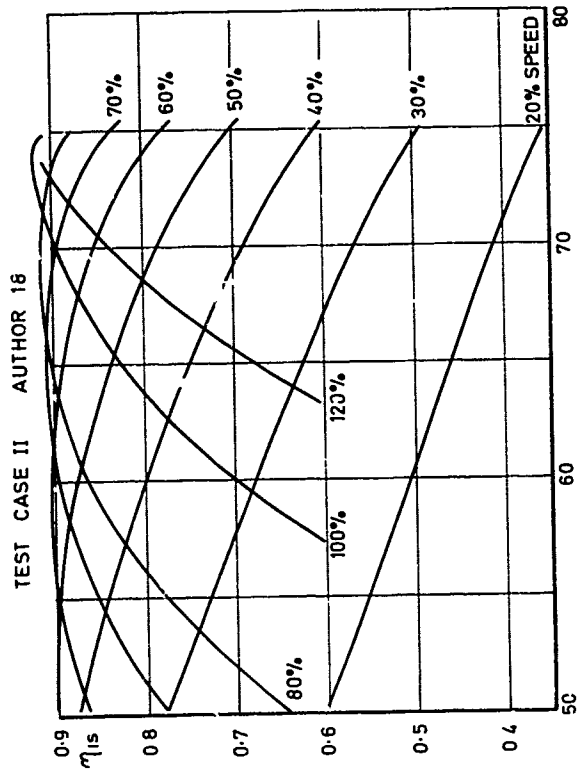

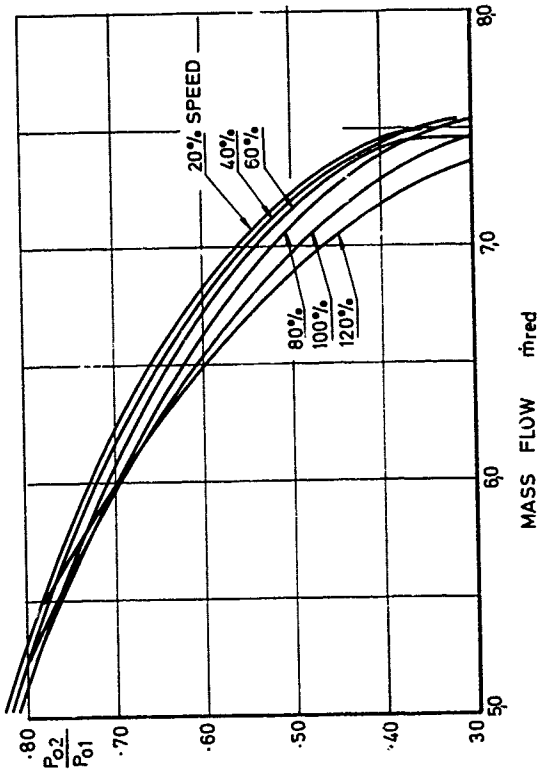

Fig.16 Case II, author 15
Overall predicted performance

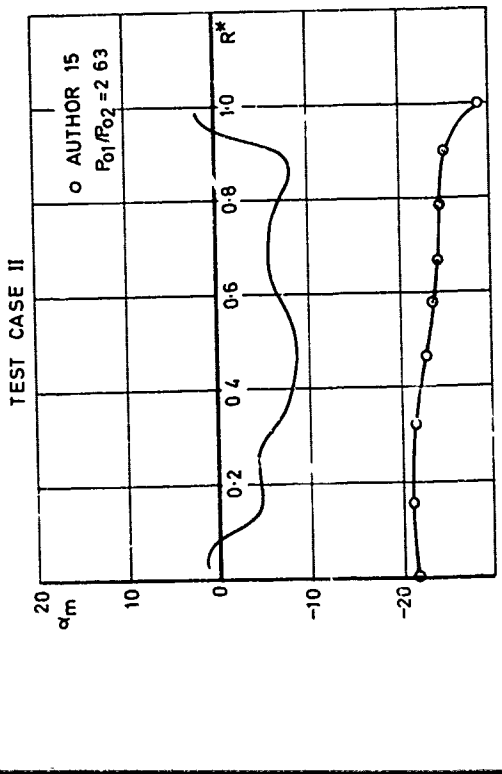

Fig.15 Case II, author 15
Downstream flow angle

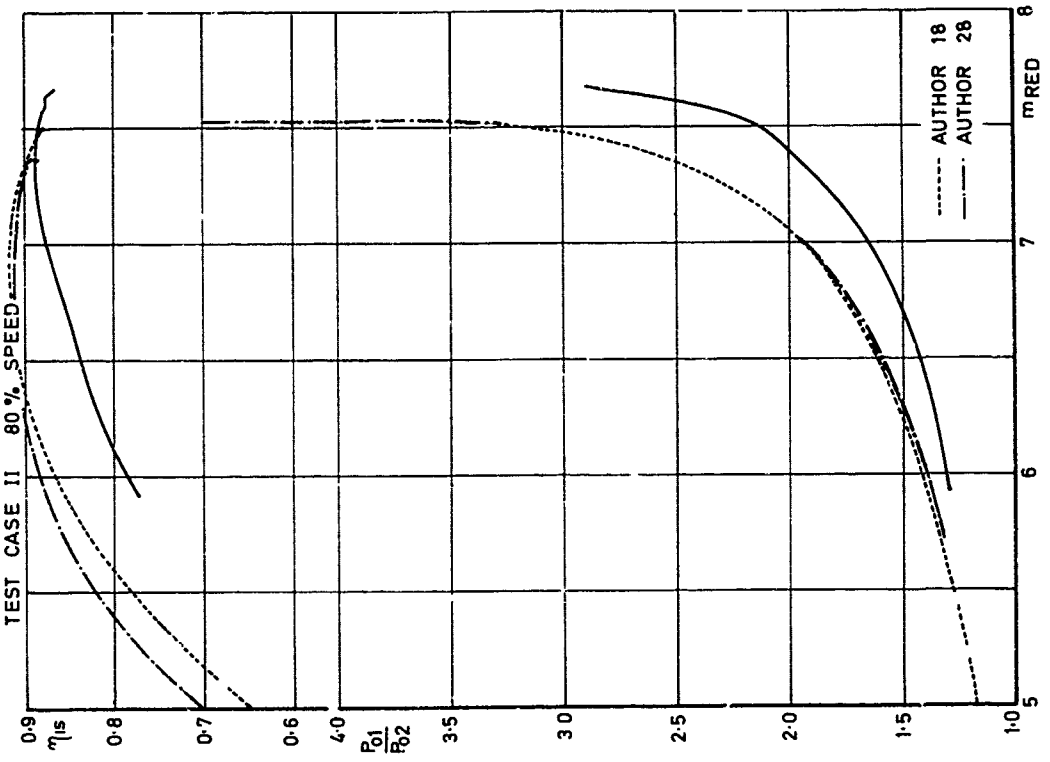

Fig 18 Case II 80% speed, authors 18 and 28
Comparison between measured and calculated overall performance

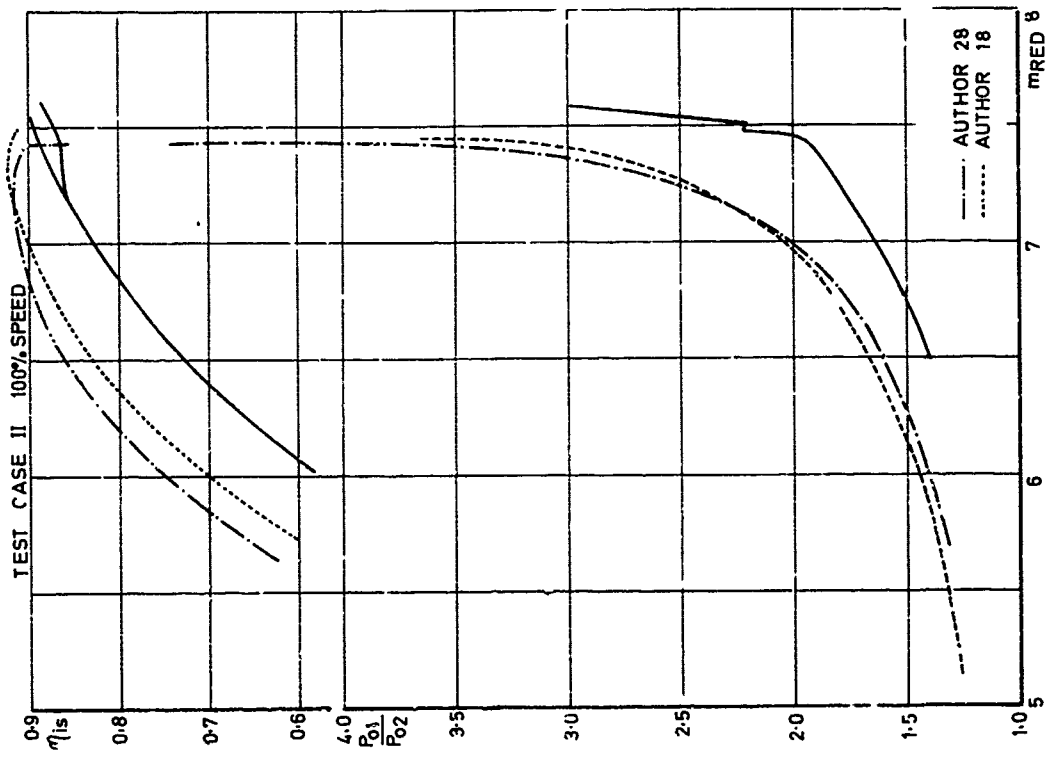

Fig.17 Case II 100% speed, authors 18 and 28
Comparison between measured and calculated overall performance

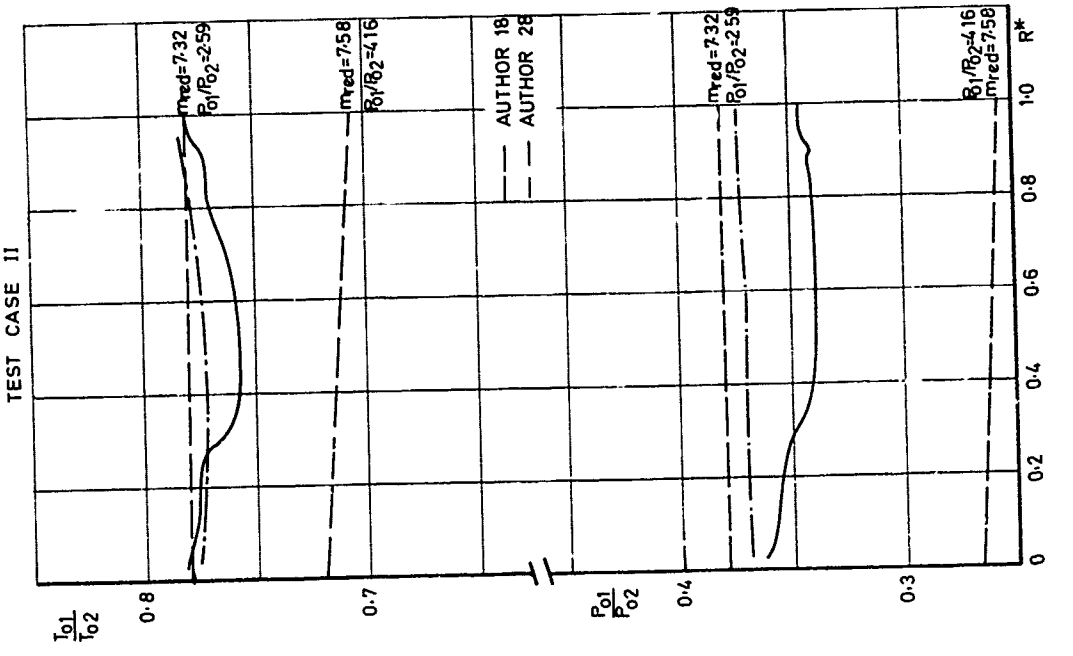

Fig.20 Case II, authors 18 and 28
Comparison between calculated and measured local total pressure and temperature ratio at turbine outlet

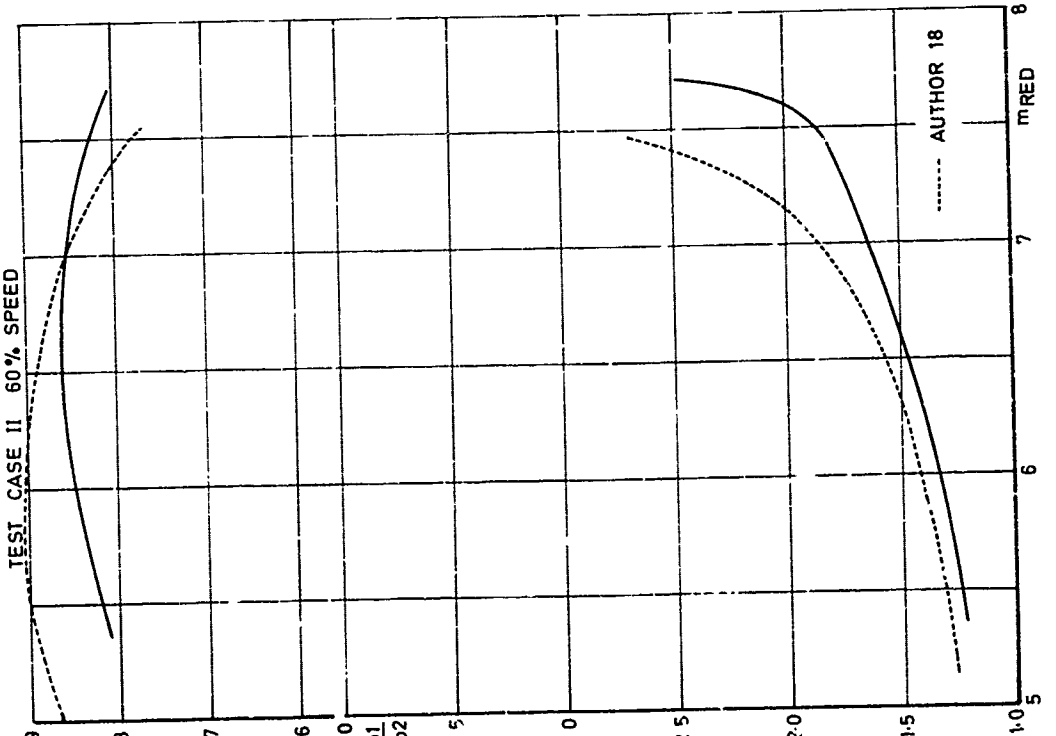

Fig.19 Case II 60% speed, authors 18 and 28
Comparison between measured and calculated overall performance

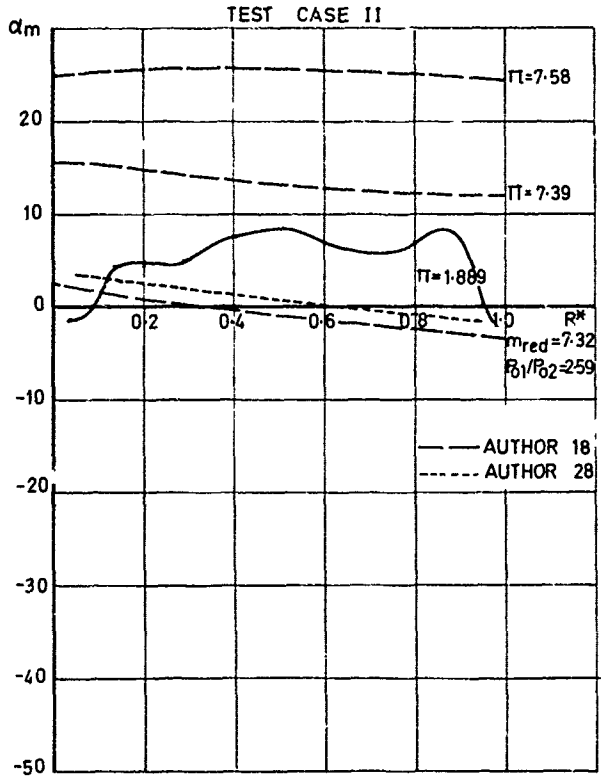

Fig.21 Case II, authors 18 and 28
Absolute angle

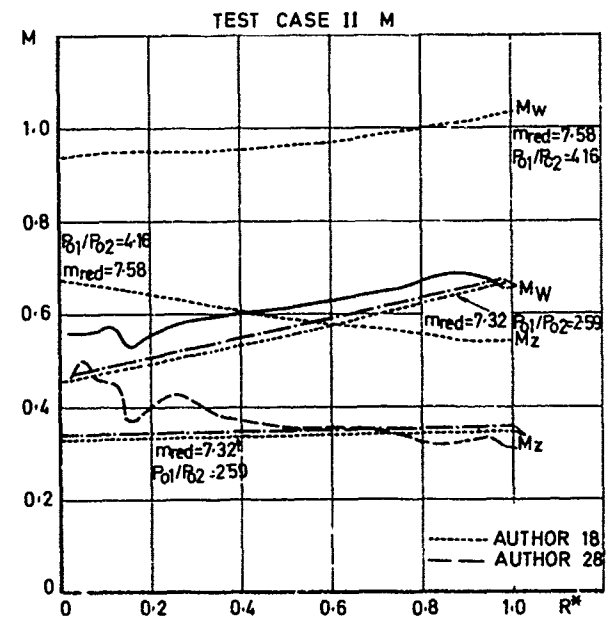

Fig.22 Case IIM, authors 18 and 28
Relative and axial Mach number

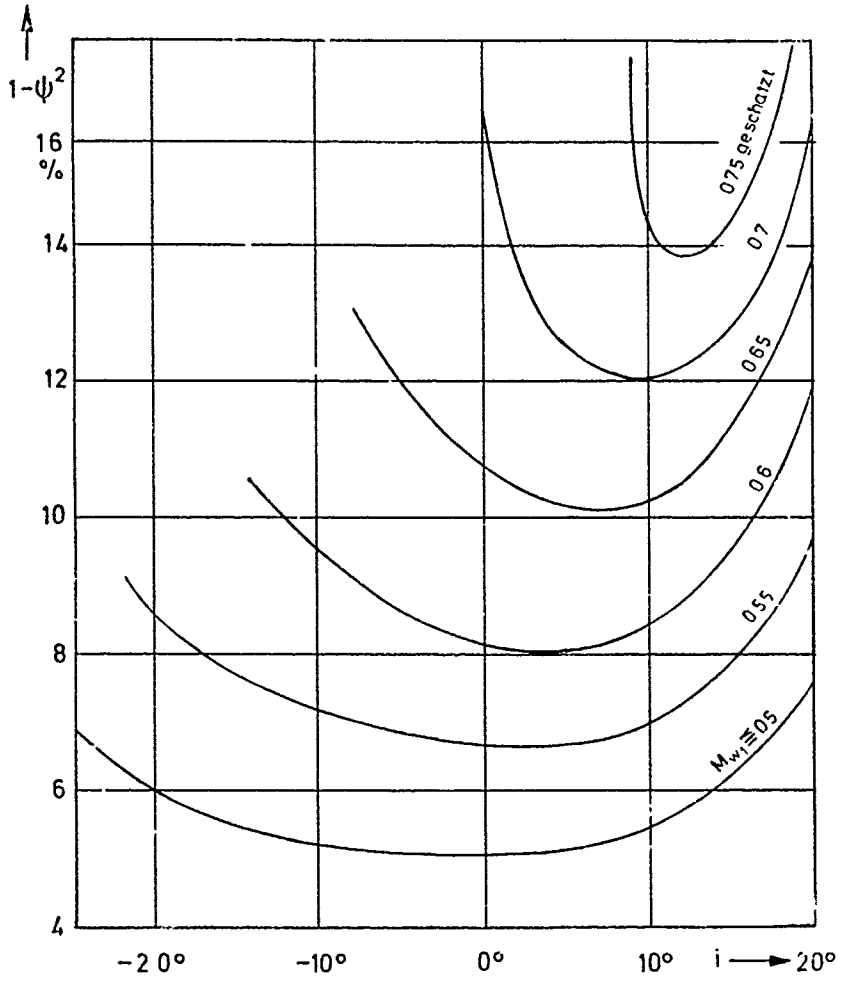

Fig.23 Case II, author 28
Effect of incidence angle ±i and rel. Mach number M_w on velocity coefficient $\Psi = w/w_{is}$

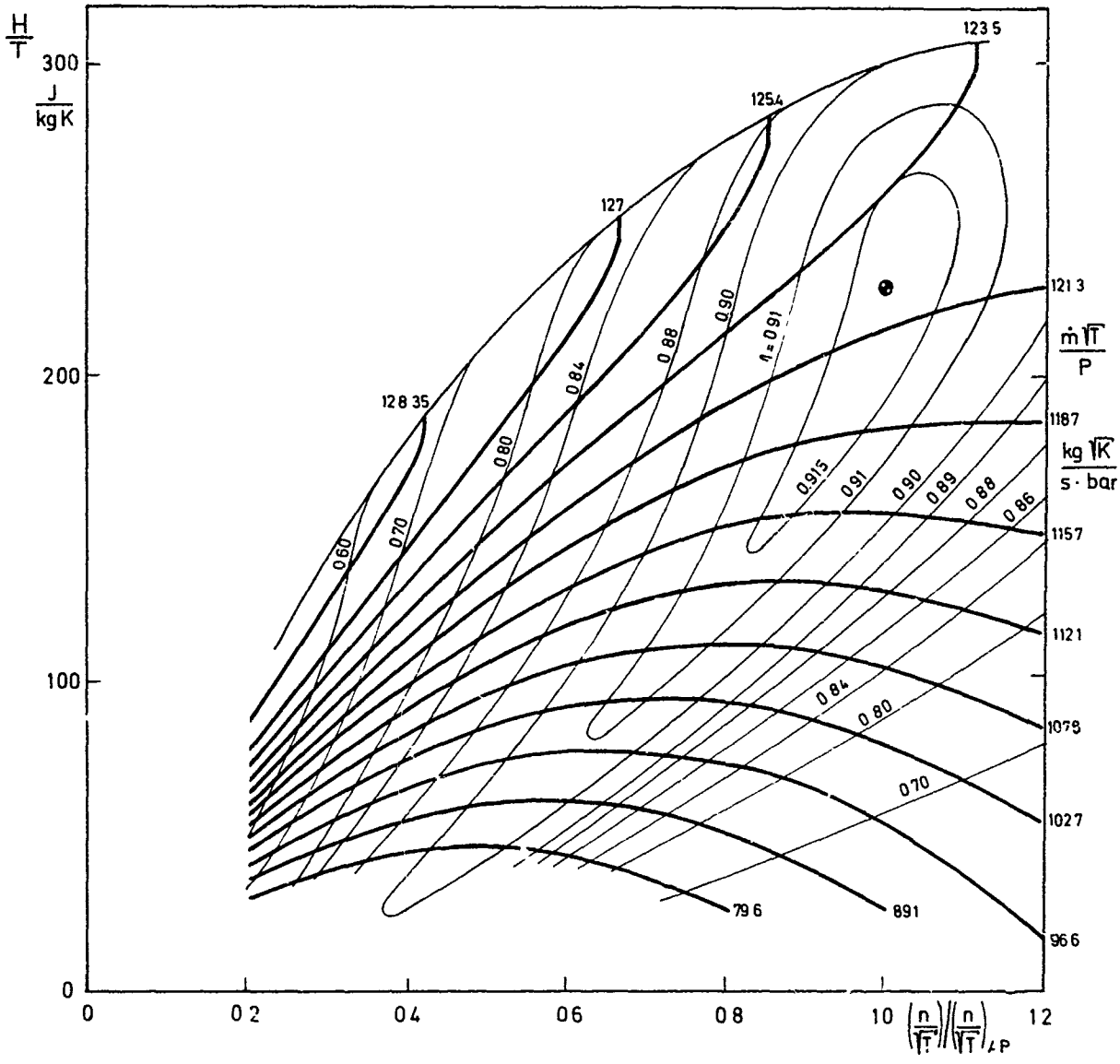

Performance map 3-stage turbine

point ◐ , speed 100 %

pressure ratio $P_{tot,in}$ / P_{out} = 2.94

$P_{tot,in}$ = total pressure stator leading edge stage 1

P_{out} = pressure, rotor trailing edge stage 3

Fig.24 Case II, author 28
Calculated overall performance

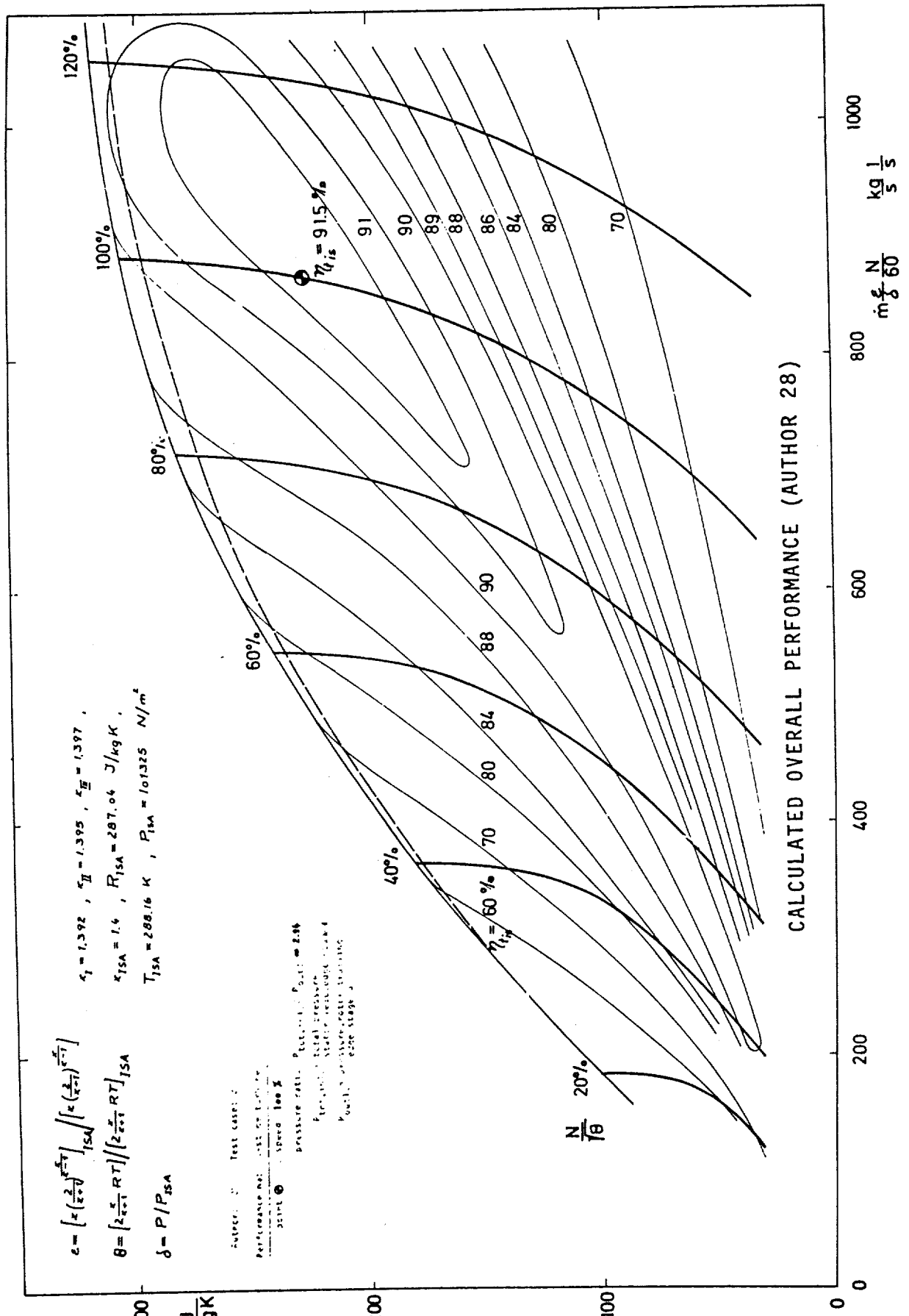

Fig.25 Case II, author 28
Calculated overall performance

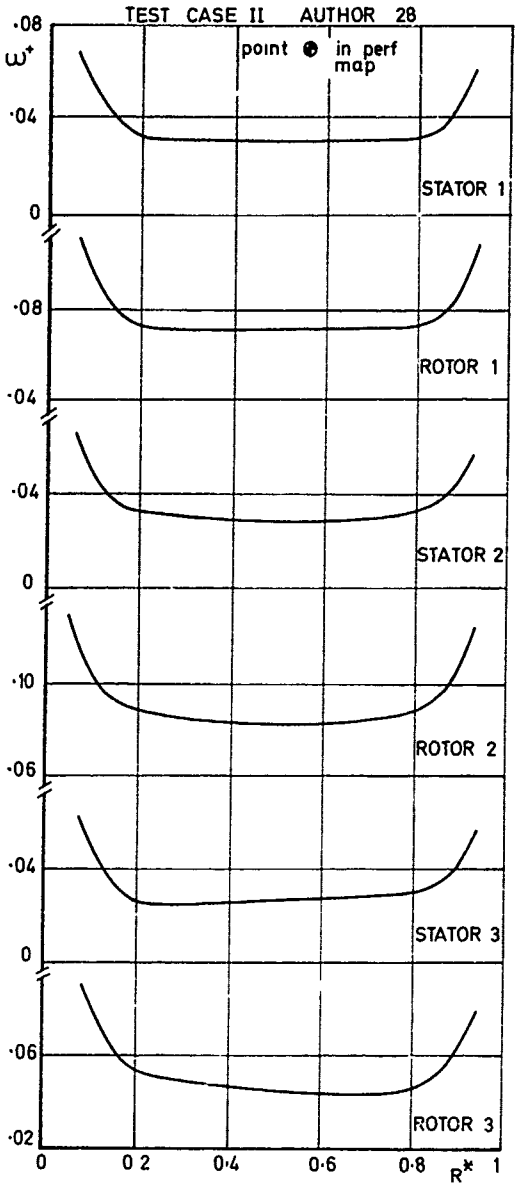

Fig.26 Case II, author 28
Calculated loss distribution between each blade row

ROUND TABLE DISCUSSION

INTRODUCTION

by J. Chauvin, von Karman Institute, Belgium.

Summary of the first impressions of the meeting

Need for test data

It is very difficult to obtain test data, especially on multistage machines, which contain all the information that we want. This is quite normal, in view of the difficulty of carrying detailed measurements in real machines, not specifically designed for obtaining such data.

However, now, new tools have been developed ; i.e., laser velocimeters, which, maybe, still need some calibration, but already show their great usefulness, as seen from the data presented by Dr. Meyer and Mr. Dunker.

One should try to obtain similar data for multistage machines, and maybe, this could be obtained by a cooperative program between research establishments who could share the related cost.

Such detailed information is becoming indispensable because the computer and the associated techniques of calculation are catching up with experimentation. We can now carry out quite sophisticated calculations, like those of Mr. Thompkins. He needs some 25 hours of computing time on a high performance computer. This seems quite a lot, but if you compare the cost with that for the development of a compressor or turbine, it is not that high, if it can save several months in the trial and errors process traditionally involved in designing a successful machine (see Mr. Mc Kain's paper).

I think that we can, or at least will be able in a not too distant future, to treat numerically more realistic physical models. Therefore, we need refined experiments to provide us with the background to define those physical models which will be more complicated and more coherent than those we are using now. The laser velocimeter offers this possibility.

Computing exercise

Coming to the computing exercise, it is clear that it was quite a complicated one, in view of the difficult boundary conditions. Maybe, we should have given some other specifications which would have allowed, on one hand, to evaluate the qualities of the numerical methods used to solve the equations, and on the other hand, what we can predict with the correlations.

We have had approximately a 50% drop out of the people who intended to carry out the calculations. From private conversations before and during this meeting, this fact

is due to the expenses requested in time and/or money.

We have indeed asked for quite complicated analysis calculations, while in most cases, the computer programs are made for design performance evaluation. For some of those programs, it turns out to be very cumbersome and complicated, and therefore costly, to introduce the data for an analysis approach.

It is my experience that, when you develop a computer program, you use it for a limited number of problems ; for instance, design, but you do not make the final effort to bring it to an industrial stage, i.e., render it versatile, especially for the data input.

This effort has to be made. The prime need is now, I think, for off design analysis, and our programs have to be made fully operational for that kind of problems.

Again from private conversations, I could understand that quite a lot of problems were encountered in getting the computation to converge to a solution. It has been known that in some cases, for the streamline curvature approach, one seems to converge on a solution and if you go on calculating, you start converging on an other one (see Frith, ref.1, for instance). This never happens with the finite element approach.

In many cases, you can also obtain non physical solutions, i.e., containing return flow regions, and this can be avoided only if you have a good estimation of the blocage factors (see Frith, ref.1, again).

Computed data

It is, of course, too early to draw definite conclusions. However, we might say that for the turbine cases, we are not too bad off in predicting the overall performance. Slight corrections for mass flow (of the order of a few %) bring the calculated data quite close indeed to the experimental ones. For the detailed flow characteristics, the trends are correct, but nobody, of course, was able to predict the large local changes due to secondary flows as measured for the first test case.
For the compressors, it was pointed out that even the performance map prediction was not too satisfactory, even if the way in which the input for the calculation was given was quite unusual for some people. We most certainly must do something about it.

It is clear that we have to improve on the existing modelling, or maybe, to go to new ones, depending on what we want to achieve. We will have to go back home and think more deeply about those results.

Introduction to the discussion

To start the discussion, I would like to raise some fundamental points which did not appear explicitely during our meeting. The first one is in the form of a question : Is the through flow method a valid model, and a valid tool ? I will give a tentative and personal answer, and no doubt my colleagues here who are more versed in the field than I am will comment on the subject.

The mathematical model is certainly quite sound for its treatment of the "duct" part of the flow. When attempting to describe what happens inside the blade rows, it is partly non physical. For instance, and here again I am inspired by ref.1, once the stream

surfaces going through the blades are defined, the model assumes that the rothalphy is constant on those surfaces. We know that if we have strong secondary flows or centrifugration in the wakes as described earlier by Mr. Cox, there will be mixing between different regions and transfer of energy. In reality, a streamline coming in at the blade tip can come out at the root. This kind of mechanism is certainly not described by the model.

In the recent analysis by Frith (ref.1), prepared for a meeting held at the Australian Aeronautical Laboratory (Melbourne), earlier this year, the author discusses his problem in trying to apply an analysis program to a seven stage Viper compressor. (His method uses the duct flow plus actuator blade approach and is not a full through flow one). He had a lot of difficulties - like us - in predicting the off design performance and could only achieve results when using the experimentally measured blocage factors. Dr. Denton has presented us a similar fact this morning : he would get the right local flow distribution only when using the experimental flow angles.

This is typical of the problem we run into when using either a true through flow or a duct flow plus actuator disk method. With the kind of equations used, one can obtain satisfactory results by using a set of correlations coherent with the particular approach chosen. What I mean is that if it is desired to improve the overall performance prediction, one can work quasi indifferently on any of the correlations influencing any particular term in the equations : correlation for loss, angle, blocage, etc...

The through flow is a simple model and therefore cannot be expected to account for the full complexity of the real phenomena. As a tool, however, the method is excellent. It has its limitations that have to be realised beforehand. It is extremely useful for design and analysis even if approximate. It has the advantage of being quite fast, once a versatile input section is provided. It is fast enough so that it can be run several times a day. This can easily provide a good feeling for the quality of the design in its whole range of operation, at the initial stage.

Now, we can wonder if it is really necessary to make it as complicated as we do, to achieve relatively simple results. When you see what Jean Fabri has achieved in performance prediction with his desk computer, you can ask that question.

Improvements

I think that, however, it can still be pushed to rather high level of sophistication, like Mr. Thiaville and Mr. Cox have shown, to obtain a measure of flow description inside the blading, for instance, for the complicated cases of flows in fans, or large L.P. turbine stages.

We have seen earlier evidence that the assumption of linear variation of the flow characteristics through the blading is not enough to give a realistic answer. A more refined approach has been described in his paper by Mr. Cox.

I am persuaded that we could acquire very useful information by using consistently and systematically the tools already available to calculate the blade to blade flow. There exist fairly reliable and quick methods, even for the transonic/supersonic regions, which can account for streamtube divergence and effect of rotation in wheels when there is a streamline shift. This, at the present, would be valid for non separated flows, of course, but it would bring us a little farther in establishing better correlation for off design conditions.

This approach would also be not valid in the regions near the end walls. This brings me to another point that I would like to raise, namely the problem of secondary flows.

There are, for the moment, two approaches available, especially for the compressor case.

One is the original historical one, i.e., a blocage or a displacement thickness is calculated and the through flow calculation is applied in the supposed inviscid region. The secondary flow losses are introduced, through correlations, in the entropy term. For the moment, however, the other secondary flow effect, i e., the modification of the flow angle, is not accounted for.

Dr. Marsh has shown us (and there are several other methods besides his) that the tool exists, at least to give an order of magnitude of the correction. As for now, these methods are based on a non-viscous vortex stretching approach, and have been applied to non twisted plane cascade. They can be quite easily extended to twisted blading and should provide a mean for improving the correlations on deviation angle. That is one of the things which could be done in the very near future.

The other approach, of the Mellor-Marsh type, tries to calculate a pitch averaged end wall boundary layer, taking into account the pseudo Reynolds stress coming from the non axisymmetric and unsteady nature of the flow. This approach is attractive, in the sense that, potentially, it can provide a blocage which is calculated taking into account the relative blade motion (leading to the well-known asymptotic boundary layer state, in compressors) ; it provides additional losses due to end wall effect (including clearance) and in Mellor's idea, it also provides the equivalent of the "work done factor" introduced a number of years ago in the British Compressor Design System, by assuming that the energy transferred to the end wall region is lost.

Hirsch has recently tried to provide more detailed information from this kind of calculation, by introducing particular pseudo boundary layer stream and cross-wise velocity profiles. He has shown that a great accuracy was not required in the definition of those profiles.

Measurements are being done, at the moment, among others by Mr. Mc Kain, at Allison, by Dr. Papailiou, at Ecole Centrale de Lyon, and by the groups of Professor Hirsch and mine (Professor Breugelmans) at VKI.

If the velocity profiles are right, then a loss and angle distribution can be readily calculated in the end wall region, as long as one can define a boundary layer region. This is not always the case, especially for HP turbines and compressors, where the flow can be fully developed.

I personally think that the two methods will converge to a pseudo 3-D approach taking into better account the physics of the phenomena which could extend the validity of the nice tool that we have with the through flow calculation methods.

Ref.1. D.A. FRITH : Through Flow Method for Axial Flow Turbomachines. An Evaluation of Current Methods. Preprint of ARC Workshop on "Flow Through Turbomachinery" Feb. 1970, Melbourne, Australia.

Mr. Mc KAIN (Detroit Diesel Allison, USA)

The primary emphasis of this meeting has been on the off-design or analysis capabilities of existing through-flow calculations. This is a very difficult problem which is highly dependent upon the viscous characteristics of the airfoils and endwalls. In many instances, especially far from the design point, these viscous effects can overpower the inviscid aerodynamics and, if not handled accurately, any analysis procedure can lead to incorrect results. In relation to this problem, it appears as if not much progress has been made in the past few years. The solution of the inviscid portion of the equations has been accomplished with various techniques such as streamline curvature and matrix methods, and, to the best of my knowledge, the differences are not of great magnitude. The portion of the problem which forces me to go through a number of development cycles to get a final compressor design has not been addressed to completely. Improved viscous models must be incorporated into our calculations. The 3-D approach with viscous terms included is, of course, the way to go. This has not yet been accomplished satisfactorily. Therefore, if we are going to continue to use the same basic techniques in terms of equations and assumptions and do not want or cannot go to the 3-D viscous approach, then the point to attack is the development of better viscous models. Mr. Carter spoke of some of the viscous effects yesterday. I agree with some of his comments but not all. I do believe we have made some gains and do believe we have been able to design better compressors (I have to talk compressors because I am not a turbine man). One of the biggest gains occurred when the computers allowed us to use equilibrium solutions as a part of our every day design work. I believe that helped and what we are trying to accomplish with our research is to develop better methods by which we can reduce the number of development cycles required for any turbomachine component. I would hope but be very surprised if that number of cycles could go to one in the foreseeable future. I feel that with better techniques, especially with regard to the viscous effects and blade-to-blade analyses, designers can make progress towards this goal. Effort must also be expended to better understand such phenomenon as secondary flows, tip clearance leakage and streamline communication. We have observed, for example, that the flow in the last stator of an HP compressor is non-adiabatic on a streamline (i.e., there is a total temperature change along a particular streamline). We have made measurements of total temperature before and after the stator which showed this, especially in low aspect ratio blading. What is the mechanism behind it ? This is one of the questions we need to have answered. To summarize my feelings, I believe more basic research should be conducted on the viscous effects and blade-to-blade analyses with less emphasis placed upon new methods of evaluating the same general equations with the same assumptions.

Mr. J.M. THIAVILLE (SNECMA, France)

If one observes the results of the calculations presented this morning, one could think that the duct flow calculations are better than the through flow ones. I think that, for design, through flow allows to design better turbine and compressor, especially fan-type compressors. In this latter case, we would, using through flow calculations, determine the streamtube thickness distribution inside the blade row, and with that thickness distribution, calculate blade shapes with an inverse blade-to-blade method.

I think that if you do not define and build good profiles, you do not need through flow calculations. On the contrary, using a through flow calculation even not perfect, using streamtube thickness distribution to calculate good profiles, as compared with others, as for instance cascade experiments with contoured side walls, you can really obtain better machines, especially fans.

Indeed, for fans, the secondary flow problem - and I agree with Professor Chauvin to say that it is important in compressor at large - hub-tip ratio is less predominant than in the HP part. For the fan case, we can afford to use secondary flow approximations which would not be acceptable for the HP sections. For those sections, I think that we have to do some progress in the direction of a better evaluation of secondary flows and their effects, i.e., of the viscous part. Another point that I would raise is related to the question of Professor Lewis on my paper for the case of transonic compressor. In that case, in the S-1 surface, you have supersonic, transonic and subsonic zones. The S-1 solutions are essentially different at the different radii. On the S-2 surface (or one could say for the quasi 3-D solution), the calculations would not be too physical.

However, for the design case, we do not need really 3-D solution inside the blade row, and if your through-flow solution is not too far from the real physical phenomena, we can make some progress in our design calculation. The off design performance prediction is another matter. We could see that there is some progress to be made in compressor overall characteristic prediction. I think that we have all losses and deviations scheme which are adapted for our own special cases and if we try to apply them to compressors or turbine built by others, it is very difficult to obtain good data.

Dr. J. DUNHAM (NGTE, United Kingdom)

If I speak bluntly, it is only to provoke disagreement ! First, I would like to repeat that the use of streamline curvature duct flow calculation historically greatly helped in the development of successful compressors, and especially successful fans, for the current generation of aero-engine. I do not think that without these methods of calculation, we should have had such successful record. They have played an important part. But at the same time, they have sometimes given, and still continue to give, misleading information in some cases. In other words, the calculations tell us the wrong thing. Therefore, more work must be done. We cannot be complacent with our existing methods. We certainly do need to improve them in various respects.

The second point I want to make is that, as far as overall performance characteristics are concerned (pressure ratio or efficiency or flow), we do not use, I think, through flow or duct flow calculations of any kind. We use one-dimensional calculations, for both compressors and turbines. If we want to achieve the best overall characteristic prediction on the various graphs shown earlier today, we would not do it by any of the methods we have been discussing this week. I think that we use those methods for detailed analysis and design subsequently.

Thirdly, the only conclusion that I have been able to draw immediately from this afternoon is that we are probably in a better position for turbines than for compressors, probably because the turbine is a less sensitive machine. Certainly we need to improve the situation on compressors rather more than we need to improve the situation on turbines.

The next point I want to make is that, if you do comparisons of this type with compressors or turbines, what you should specify in order to define the operating condition is the pressure ratio, and let the mass flow work itself out. A number of people have made this point and to be honest a number of members of the program committee here made this recommendation a long time ago, but it was not adopted. I hope it is now agreed that next time we specify the pressure ratio.

Coming to the methods, each must contain a calculation framework, loss assumptions, angle assumptions and blockage assumptions. As far as the calculation framework is concerned, this appears satisfactory. If you use Wu's approach, and you are going to go within the blade row, you do have some problems, as we have seen. For instance, axial velocity ratio is a helpful parameter but it does not tell you really all the right things about what is happening within the blade row, because the pressure surface and the suction surface effects are different. We cannot cope with these effects in the framework of the present method. They do not appear to me, at the moment, to cause serious inaccuries.

As far as the methods themselves are concerned, it appears it is a good thing to have a grid with the major axis roughly parallel and normal to the streamlines. Again, it is up to individuals with programs to consider that.

Do we need through-flow calculations or do we need only duct flow calculations ? This is one question which comes up quite regularly. The one reason for supposing that we need through-flow calculations that seems to me very important is that if you have non-radial blading (none of the examples which have been given to this meeting have non-radial blading) then, if you do a duct flow calculation, you cannot get the static pressure gradient across the annulus correctly. You have to go to the through- flow calculation to do that, as far as I am aware, at the moment. I wish that we could develop the duct flow calculation to avoid that problem.

Angles : I believe we should develop the secondary flow approach to them and modify our angles near the ned of the blades. I believe that the selection of outlet angle or deviation is probably the most important single factor which makes our predictions bad if they are bad. It is much more important to get the angle distribution right than the loss distribution.

As far as losses are concerned, we must recognize that a lot of the loss correlations that exist in the world exist in the firms, and we have not seen them this week, either presented or applied. Even so, my impression is that the loss correlations are probably reasonable, but we ought to be able to do something about radial movement of losses, because they do matter in certain circumstances, particularly if you have part span shrouds. I believe it to be entirely unsatisfactory that the standard NASA method should have a loss multiplying factor which is function of radius. Somebody ought to do something about that !

Blockage, again, is a major factor in multistage compressor performance prediction. If you cannot get the blockage right, then the whole of the matching calculation is wrong, and this is very serious for a compressor. I believe some work is still necessary for blockage factor calculation. Again, this is a thing on which firms have various correlations but they are not, at the moment, on the whole, too scientific.

My summary for action is first of all that we keep our current streamline curvature duct flow methods, maybe looking at grids and convergence in particular cases. Secondly, that we have to try to solve the problem of putting non-radial blading forces (body forces pushing the flow inwards or outwards) into the context of the duct flow model. This is a thing we do not know how to do at the moment.

Thirdly, I believe that we need to develop the secondary flow approach along the lines proposed by Marsh to give us outlet angle correction, for tip clearance effects as well as straightforward secondary flow effects.

Then we need to develop methods of predicting the development of annulus wall boundary layer blockage, to include also tip clearance effects. We need also to account for radial movement of losses, and if we are going to try to concentrate losses near the end of blading, we are going also to have to solve the problem of what to do after the first blade row to dissipate this loss somewhat, because you cannot assume these losses accumulate at the ends of the blade row. That is disastrous, we tried it.

As far as 3-D techniques are concerned, I do not see myself the 3-D techniques ever being a design or development tool. I see them as being an excellent research tool which should help us to put our 2-D duct flow calculation into a better light, but not ever as a design tool.

Dr. H. WEYER (DFVLR, Germany)

Concerning design techniques for industrial application, there is a need for very simple design methods, however reliable. I could not imagine that computing times of 10 hours or more are acceptable for industry.

We need through flow calculation in the sense that Dr. Dunham mentionned, but we need them also as an initial step for calculations on S-1 surfaces for blade design. It is my opinion, however, that current through flow calculations do not work in all cases where are steep gradients of the flow parameters over the blade pitch. We have learned this from the comparison between detailed measurement and through flow calculation.

Performing calculation on mean S-2 surfaces is based on the assumption of an axisymmetric flow field. If I think about transonic compressors, there we have in the inlet blade region those shock waves and calculating on mean S-2 surfaces means that we use mean values of all flow parameters mixed from supersonic to subsonic flow regions because we make the average across the shock wave. In those cases of mixed flow (subsonic-supersonic) with steep gradient, I guess we have to leave axisymmetric flow assumption and to define a mean flow averaged on a normal to a mean S-2 surface. There is another aspect of through flow calculation already often discussed during this meeting : the current design techniques all use loss and flow angle correlations. There, a lot of activity is still necessary in the near future to improve those correlations for profile loss, secondary and end wall loss, and, of course, for the flow angles. In the moment, this is of high practical interest, however, in parellel, analytical techniques to calculate blade and wall boundary layers, secondary flows, etc..., must be developed to replace the appropriate empirical correlations.

QUESTIONS

1. Dr. M. MOORE (CEGB, United Kingdom) : Do cascade tests reproduce accurately turbine and compressor blade section performance when the flow is not separated and allowance is made for streamtube diffusion across the blade ?

Mr. Mc KAIN (Detroit Diesel Allison, USA) : The way in which we use cascades now is more on a relative basis. When we are talking cascades now, it is usually the supersonic sections which are of primary interest. Our cascade work is geared for particular applications. We investigate different design philosophies for the same aerodynamic duty on a cascade basis. The best configuration determined from this data is then used for the actual rotor or stator.

Mr. J.M. THIAVILLE (SNECMA, France) : The problem is : are the cascades representative of the real machines ? We do use experiments in plane or annular cascades. The problem of the representativity is that, if you use plane cascades, the flow is not exactly two-dimensional. As you have to use blading systems, even if you are never representative of the real machines, you can compare different profiles and also validate cascade calculations on that sort of experiment, especially for the supersonic cases. If you use annular cascade, the representativity of the periodicity of the flow is insured, you have also three-dimensional effects, like in the real machines, but they are not the same. The problem of representation is different. However, in this case, like in the preceding one, you can compare and validate some through flow calculations for example.

Dr. J. DUNHAM (NGTE, United Kingdom) : In the case of turbines, I do not think that one should do cascade tests to form a data base. One should rely on calculations (I do not think that can be said to apply to the very high Mach number steam turbine case, but to the gas turbine cases). I think we should try to achieve the same thing in compressors. Adequate methods for blade-to-blade calculation in the transonic range are appearing and when we will have them we should use theory as a design tool, and not cascade tests.

Dr. H. WEYER (DFVLR, Germany) : Cascade tests or not, that is a question of philosophy I think. In the compressor field, there are two aspects for the cascade research work. One is to help improving the fundamental understanding of compressor flows, especially in the supersonic regime. On the other side, cascade testing is very useful to us to find out what are losses and deviation angles for profiles corresponding to advanced machines, like the transonic ones. We, at DFVLR, spend a lot of activity to improve the design techniques for transonic compressors, and all the cascade data available to us, from our own wind tunnels as well as from the litterature, helped us to come up with a loss correlation which works quite well. So I think that cascade tests are partly useful. However, the plots of constant Mach number lines (measured by laser velocimeter in the transonic compressor) that I showed to you earlier, illustrate at least for certain cases, quite severe differences with the picture obtained in cascades. Remembering the figure at 89 % of blade span, the most evident difference is that the Mach lines are no longer straight. That is probably due to the outer wall boundary layer and to other heavy 3-D effects. In summary, I still think that cascade work is necessary to understand what happens and to provide useful information on cascade loss and angle, as long as we cannot calculate them.

Mr. Mc KAIN (Detroit Diesel Allison, USA) : It is very difficult to use high Mach number cascade data for general design system correlations as has been done for low speed airfoil sections. The low speed sections were generally of a consistent series such as NACA or "C" series with constant meanline shape and thickness distributions. These types of consistent sections lent themselves better to correlations than do the current high Mach number sections. These new sections are more arbitrary in both meanline shape and thickness distribution and tailored for specific applications. It would be a very large undertaking to form a data base (loss correlation and deviation rules) from these arbitrary sections because there are so many variables which are required to define the section.

Dr. R.L. ELDER (Cranfield Insitute of Technology, United Kingdom) : Would the Panel like to comment on the ability of through flow techniques to handle off design cases of multistage compressors, particularly towards stall. Clearly, if this is to be achieved separation effects have to be incorporated into the various models described. If this is done, would the Panel briefly mention the methods and their success.

Prof. J. CHAUVIN (VKI, Belgium) : As the time left is short, we cannot, unhappily, discuss this interesting question at length. I think that we all agree that separated flows are occuring at off design even before surge. There are steady separation and unsteady ones, like rotating stall. Progress is made in the prediction of rotating stall. Progress is also being made in theoretical blade-to-blade calculations with slightly or more highly separated flows. You can also get by, I suppose (like shown in Mr. Cox's paper), using the simple model, with a proper loss and turning evolution in function of some "carefully selected parameters" (incidence, Mach, AVR, etc...).

QUESTIONS FROM AUDIENCE

Dr. H. MARSH (Durham University, United Kingdom) : I would like to ask a supplementary question to Dr. Moore's queery on the validity of cascade test. The Panel did not refer to the problem of turbulence or unsteadiness that is present in the machine and not in the cascade testing. Is it important ? If you test an isolated airfoil, you get a behaviour which is very different, which varies depending on the turbulence level. It could well be true also with the cascade.

Dr. J. DUNHAM (NGTE, United Kingdom) : I suspect that in the Reynolds number range of interest in the aerogas turbine, the uncertainty in turbine performance (not in heat transfer) associated with different free stream turbulence levels is one of the smaller uncertainties involved. In other words the errors from this turbulence effect in predicting turbine losses are small compared with other things we know even less about.

Dr. R. PARKER (University College Swansea, United Kingdom) : I was going to raise the question of unsteadiness in a slightly different context. I feel that when unsteadiness is mentioned, the general assumption that we mean turbulence is rather an understatement of the problem. Every blade row produces a flow pattern around it which is non uniform even if the flow were totally inviscid, and if we have two blade rows moving relatively to each other in totally inviscid flow we get an interaction between these two rows which excites vibration and generates noise. This is because the pressure gradients, the velocities, etc..., fluctuate in any blade row because of the motion of the adjacent row and its associated potential flow field. Now, we have heard in the discussion that the effect of boundary layer growth, secondary flows, etc..., appear in some complicated ways downstream of the row in which they are generated. This is right in the region of unsteadiness generated by the succeeding row, right in the region where the unsteadiness is very large. We have therefore boundary layers, etc..., growing in unsteady flow situations with the possibility of separation, and the mixing processes take place in the presence of unsteadiness, I think that we have a parameter which has never been seriously looked at The magnitude of this effect in a particular machine is linked to the inter row blade spacing which is relevant parameter in designing a machine. We normally decide the spacing on the basis of vibration, noise generation and how long you like your shaft to be. It has not been mentioned at all in these two days. However, it must have an influence on the mechanism of some of the losses with which we are very concerned, possibly even if you get the turning that you expect out of the blade rows.

It is not a particularly simple parameter, but it would be quite possible to deduce a non dimensional parameter relating blade row spacing to blade pitch and the relative velocity. I say it would not be a very simple parameter. I mention this particularly because when people have talked about blade spacing, they nearly always have talked about the ratio between blade spacing and chord. I would stress that this is a totally inadequate parameter. But we could deduce a relevant parameter. When a design technique which is found to work, say by one particular firm in the context of their particular machines, does not work in relation say to the trial calculation we have been looking at today or in relation to other people's machines, it would be informative to compare the blade row spacings. The practice in one firm may not vary a great deal, they may think they have got a coherent set of data without bothering to look at this parameter, largelly because they do not vary this parameter. It is my feeling that we have a possible explanation for some of our difficulties which is being overlooked.

Mr. H. COX (G.E.C., United Kingdom) : We do include the blade row spacing factor on losses. There is plenty of data published by the Russians on the effect of blade row spacing on turbine stage efficiency from which adequate loss curves can be derived. It is only when you get very close spacing that you tend to get much of a loss increase and generally this spacing is very much closer than is required for stress considerations. So in fact axial spacing becomes virtually an insignificant loss parameter.

Going back to the question of cascade loss analysis versus correlations derived from turbine single stage measurements, I have the following comments.

First of all, in cascade, there must be a turbulence effect, and with modern methods of designing optimized blading profiles, the danger is that we will produce in cascade large regions of laminar flow. In the later stages of a turbine, there could be a level of turbulence such as to trip the laminar boundary layer and result in a significant increase in loss over the cascade value.

What we do not know is the general turbulence level existing within a turbomachine to apply to cascade test. One of the criticisms I would make of people who have reported on turbulence levels is that they have all quoted gross unsteadiness. This gross unsteadiness is made up of two basic components : one is pure random unsteadiness, the other is the type of high frequency harmonic unsteadiness about which effects Professor Parker was speaking. There is some evidence which suggests that the boundary layer will not react to a high frequency unsteadiness, and if this is so, only the random component of the total signal is going to affect the results. What we need is more measurements on turbulence in sufficient detail such that they can be broken down to give the pure random component. We are at present doing this, using a Fourier transform and use an autocorrelator to give the spectrum of the random signal. I suspect that this turbulence level is a lot lower than you think it is.

If you decide that you are not going to use cascade data, but turbine stage data, then you have to determine how to model the turbulence levels that exist in the rear stages of a real turbine. I suggest that the turbulence level and spectrum produced in a single stage is not good enough.

Secondly we know that the performance of a single stage turbine can be modified when a second stage is put behind it. This will lead to considerable difficulties when analysing and subsequently correlating the data and to obtain slightly improved loss correlations from multistage testing will require an awful lot of development cost to achieve it.

The third point that I would like to make is that people on the Panel have said that the thing to look for is the 3-D viscous effects. What makes the Panel think that one will be able to calculate those effects when we cannot calculate 2-D viscous effects? There is no adequate blade to blade solution in 2-D flows which will accurately compute the velocity distribution around a profile and will accurately compute the outlet angle. There is a paper by Serovy in which four different methods of calculating the trailing edge conditions have been compared and they all have shown to give poor deviation correlations.

The problem, undoubtedly, is that you have to take into account the circulation in the wake in the blade to blade calculation. It is known that the correct circulation on an isolated airfoil cannot be obtained until this wake circulation effect is introduced and if it is required for that case, it is certain that we have to put it on for high deflecting blading. What I do not know - and I would like to know if anybody else does - is how to marry the boundary layer on the blade surface with the wake just downstream, where there is a first order discontinuity at the trailing edge in the boundary layer gradients. Essentially, the boundary layers are growing in thickness up to the trailing edge where they separate. From there on, due to increased mixing, the boundary layers tend to decrease in thickness. It is at this separation point, or indeed for the whole base flow region, that we have inadequate theoretical modelling.

This, I think, is the area where people should be working. If you could get that right, you could drop most of the cascade testing and simply compute the information. The first thing to do is to concentrate on a highly accurate 2-D blade to blade method before attempting to solve 3-D effects.

Mr. Mc KAIN (Detroit Diesel Allison, USA) : I do agree that we need a blade to blade solution with associated boundary layer calculations. That, along with the shock structure and streamtube shape, is the problem we are all concerned with. Answering to the criticism you were addressing to the Panel, I am saying that the ultimate is solving the 3-D viscous equation. I also said we cannot do it, yet.

Dr. J. DUNHAM (NGTE, United Kingdom) : I am not too optimistic about 3-D viscous calculations at any time. I think that we are in a position now when we need not worry too much about computer programs, but think more carefully and devise more intelligent flow models which will enable us to do semi-empirical simpler calculations. One of the things that I have in mind and has not been mentioned this week is what I might call the Mikolajczack-Kerrebrock phenomenon, i.e., blade wakes from preceding rows being swept on the suction surface and affecting the boundary layer thickness. Some of these phenomena need physical modelling.

Prof. J. CHAUVIN (von Karman Institute for Fluid Dynamics, Belgium) : We all agree on that. We have the tools. We should start thinking about how to put these tools to better uses, by getting a better grasp of the things we have neglected up to now. As Professor Parker, Dr. Dunham and Mr. Cox pointed out, unsteady flows and the like have to be taken into account.

Mr. M. PIANKO (P.E.P. Chairman) : Au moment de clore cette réunion, je ne veux rien ajouter aux conclusions techniques qui ont été tirées par la table ronde. Je voudrais surtout vous présenter les conclusions que le P.E.P. peut tirer de cette réunion.

La première est qu'il semble qu'elle ait été utile, qu'elle a intéressé tout le monde et qu'elle était appropriée. Le but de cette réunion était d'abord de confronter les outils de travail existants pour aider à la mise au point des turbomachines. Je crois que tout le monde est d'accord pour voir qu'il y a un grand besoin d'outils, mais que l'outil actuel n'est pas parfait, qu'il peut et qu'il doit être amélioré. Le P.E.P. se propose de continuer l'oeuvre commune entreprise ici et la manière dont la continuation sera menée sera vraisemblablement par un groupe de travail dont le rôle sera de régler différents problèmes, d'améliorer certaines méthodes dont on s'est aperçu aujourd'hui qu'elles n'étaient pas parfaites.

Le Président remercie ensuite les organisateurs de la réunion, les auteurs, les participants à la table ronde et les interprètes, ainsi que le Dr. Winterfeld et le DFVLR pour leur accueil.

14-14

REPORT DOCUMENTATION PAGE			
1. Recipient's Reference	2. Originator's Reference AGARD-CP-195	3. Further Reference ISBN 92-835-0179-9	4. Security Classification of Document UNCLASSIFIED
5. Originator	Advisory Group for Aerospace Research and Development North Atlantic Treaty Organization 7 rue Ancelle, 92200 Neuilly sur Seine, France		
6. Title	THROUGH-FLOW CALCULATIONS IN AXIAL TURBOMACHINERY		
7. Presented at	the Propulsion and Energetics Panel Specialists' Meeting held on the 20 and 21 May 1976 at DFVLR, Porz-Wahn, near Cologne, Germany.		
8. Author(s)	Various		9. Date October 1976
10. Author's Address	Various		11. Pages 242
12. Distribution Statement	This document is distributed in accordance with AGARD policies and regulations, which are outlined on the Outside Back Covers of all AGARD publications.		

13. Keywords/Descriptors

Turbomachinery	Computation	Methodology
Axial flow	Axisymmetric flow	
Flow distribution	Rotor blades (turbomachinery)	

14. Abstract

The Conference Proceedings contain the papers presented at the Propulsion and Energetics Panel Specialists' Meeting held on the 20 and 21 May 1976 at DFVLR, Porz-Wahn, near Cologne, Germany.

The purpose of the meeting was to review the current knowledge, methods and techniques available to evaluate the flow pattern at design and off-design conditions in single and multi-stage turbomachines, inside and outside the bladings along the meridional surface, concentrating on the axisymmetric approach.

The meeting comprised two review papers, seven papers on particular methods, two papers describing the various test cases – for both compressors and turbines – which were sent to firms and institutes for calculation by different methods, and two papers discussing the results of calculations with experimental data. There was a Round Table discussion at the end of the meeting which is included herein in its entirety. Conclusions drawn from this meeting are presented in the TECHNICAL EVALUATION REPORT as well as suggestions for future course of actions.

AGARD Conference Proceedings No.195 Advisory Group for Aerospace Research and Development, NATO THROUGH-FLOW CALCULATIONS IN AXIAL TURBOMACHINERY Published October 1976 242 pages The Conference Proceedings contain the papers presented at the Propulsion and Energetics Panel Specialists' Meeting held on the 20 and 21 May 1976 at DFVLR, Porz-Wahn, near Cologne, Germany. The purpose of the meeting was to review the current knowledge, methods and techniques available to evaluate the flow pattern at design and off-design conditions in P.T.O.	AGARD-CP-195 Turbomachinery Axial flow Flow distribution Computation Axisymmetric flow Rotor blades (turbo-machinery) Methodology	AGARD Conference Proceedings No.195 Advisory Group for Aerospace Research and Development, NATO THROUGH-FLOW CALCULATIONS IN AXIAL TURBOMACHINERY Published October 1976 242 pages The Conference Proceedings contain the papers presented at the Propulsion and Energetics Panel Specialists' Meeting held on the 20 and 21 May 1976 at DFVLR, Porz-Wahn, near Cologne, Germany. The purpose of the meeting was to review the current knowledge, methods and techniques available to evaluate the flow pattern at design and off-design conditions in P.T.O.	AGARD-CP-195 Turbomachinery Axial flow Flow distribution Computation Axisymmetric flow Rotor blades (turbo-machinery) Methodology
AGARD Conference Proceedings No.195 Advisory Group for Aerospace Research and Development, NATO THROUGH-FLOW CALCULATIONS IN AXIAL TURBOMACHINERY Published October 1976 242 pages The Conference Proceedings contain the papers presented at the Propulsion and Energetics Panel Specialists' Meeting held on the 20 and 21 May 1976 at DFVLR, Porz-Wahn, near Cologne, Germany. The purpose of the meeting was to review the current knowledge, methods and techniques available to evaluate the flow pattern at design and off-design conditions in P.T.O.	AGARD-CP-195 Turbomachinery Axial flow Flow distribution Computation Axisymmetric flow Rotor blades (turbo-machinery) Methodology	AGARD Conference Proceedings No.195 Advisory Group for Aerospace Research and Development, NATO THROUGH-FLOW CALCULATIONS IN AXIAL TURBOMACHINERY October 1976 242 pages The Conference Proceedings contain the papers presented at the Propulsion and Energetics Panel Specialists' Meeting held on the 20 and 21 May 1976 at DFVLR, Porz-Wahn, near Cologne, Germany. The purpose of the meeting was to review the current knowledge, methods and techniques available to evaluate the flow pattern at design and off-design conditions in P.T.O.	AGARD-CP-195 Turbomachinery Axial flow Flow distribution Computation Axisymmetric flow Rotor blades (turbo-machinery) Methodology

single and multistage turbomachines, inside and outside the bladings along the meridional surfaces, concentrating on the axisymmetric approach.

The meeting comprised two review papers, seven papers on particular methods, two papers describing the various test cases – for both compressors and turbines – which were sent to firms and institutes for calculation by different methods, and two papers discussing the results of calculations with experimental data. There was a Round Table discussion at the end of the meeting which is included herein in its entirety. Conclusions drawn from this meeting are presented in the TECHNICAL EVALUATION REPORT as well as suggestions for future course of actions.

ISBN 92-835-0179-9

single and multistage turbomachines, inside and outside the bladings along the meridional surfaces, concentrating on the axisymmetric approach.

The meeting comprised two review papers, seven papers on particular methods, two papers describing the various test cases – for both compressors and turbines – which were sent to firms and institutes for calculation by different methods, and two papers discussing the results of calculations with experimental data. There was a Round Table discussion at the end of the meeting which is included herein in its entirety. Conclusions drawn from this meeting are presented in the TECHNICAL EVALUATION REPORT as well as suggestions for future course of actions.

ISBN 92-938-0179 9

single and multistage turbomachines, inside and outside the bladings along the meridional surfaces, concentrating on the axisymmetric approach.

The meeting comprised two review papers, seven papers on particular methods, two papers describing the various test cases – for both compressors and turbines – which were sent to firms and institutes for calculation by different methods, and two papers discussing the results of calculations with experimental data. There was a Round Table discussion at the end of the meeting which is included herein in its entirety. Conclusions drawn from this meeting are presented in the TECHNICAL EVALUATION REPORT as well as suggestions for future course of actions.

ISBN 92-835-0179-9

single and multistage turbomachines, inside and outside the bladings along the meridional surfaces, concentrating on the axisymmetric approach.

The meeting comprised two review papers, seven papers on particular methods, two papers describing the various test cases – for both compressors and turbines – which were sent to firms and institutes for calculation by different methods, and two papers discussing the results of calculations with experimental data. There was a Round Table discussion at the end of the meeting which is included herein in its entirety. Conclusions drawn from this meeting are presented in the TECHNICAL EVALUATION REPORT as well as suggestions for future course of actions.

ISBN 92-835-0179-9

AGARD

NATO OTAN

7 RUE ANCELLE · 92200 NEUILLY-SUR-SEINE

FRANCE

Telephone 745.08.10 · Telex 610176

DISTRIBUTION OF UNCLASSIFIED AGARD PUBLICATIONS

AGARD does NOT hold stocks of AGARD publications at the above address for general distribution. Initial distribution of AGARD publications is made to AGARD Member Nations through the following National Distribution Centres. Further copies are sometimes available from these Centres, but if not may be purchased in Microfiche or Photocopy form from the Purchase Agencies listed below.

NATIONAL DISTRIBUTION CENTRES

BELGIUM
Coordonnateur AGARD – VSL
Etat-Major de la Force Aérienne
Caserne Prince Baudouin
Place Dailly, 1030 Bruxelles

CANADA
Defence Scientific Information Service
Department of National Defence
Ottawa, Ontario K1A OZ2

DENMARK
Danish Defence Research Board
Østerbrogades Kaserne
Copenhagen Ø

FRANCE
O.N.E.R.A. (Direction)
29 Avenue de la Division Leclerc
92 Châtillon sous Bagneux

GERMANY
Zentralstelle fur Luft- und Raumfahrt-
dokumentation und -information
D-8 Munchen 86
Postfach 860880

GREECE
Hellenic Armed Forces Command
D Branch, Athens

ICELAND
Director of Aviation
c/o Flugrad
Reykjavik

ITALY
Aeronautica Militare
Ufficio del Delegato Nazionale all'AGARD
3, Piazzale Adenauer
Roma/EUR

LUXEMBOURG
See Belgium

NETHERLANDS
Netherlands Delegation to AGARD
National Aerospace Laboratory, NLR
P.O. Box 126
Delft

NORWAY
Norwegian Defence Research Establishment
Main Library
P O Box 25
N-2007 Kjeller

PORTUGAL
Direccao do Servico de Material
da Forca Aerea
Rua de Escola Politecnica 42
Lisboa
Attn: AGARD National Delegate

TURKEY
Department of Research and Development (ARGE)
Ministry of National Defence, Ankara

UNITED KINGDOM
Defence Research Information Centre
Station Square House
St. Mary Cray
Orpington, Kent BR5 3RE

UNITED STATES
National Aeronautics and Space Administration (NASA),
Langley Field, Virginia 23365
Attn: Report Distribution and Storage Unit

THE UNITED STATES NATIONAL DISTRIBUTION CENTRE (NASA) DOES NOT HOLD STOCKS OF AGARD PUBLICATIONS. AND APPLICATIONS FOR COPIES SHOULD BE MADE DIRECT TO THE NATIONAL TECHNICAL INFORMATION SERVICE (NTIS) AT THE ADDRESS BELOW.

PURCHASE AGENCIES

Microfiche or Photocopy

National Technical
Information Service (NTIS)
5285 Port Royal Road
Springfield
Virginia 22151, USA

Microfiche

Space Documentation Service
European Space Agency
114, Avenue Charles de Gaulle
92200 Neuilly sur Seine, France

Microfiche

Technology Reports
Centre (DTI)
Station Square House
St. Mary Cray
Orpington, Kent BR5 3RF
England

Requests for microfiche or photocopies of AGARD documents should include the AGARD serial number, title, author or editor, and publication date. Requests to NTIS should include the NASA accession report number. Full bibliographical references and abstracts of AGARD publications are given in the following journals:

Scientific and Technical Aerospace Reports (STAR),
published by NASA Scientific and Technical
Information Facility
Post Office Box 8757
Baltimore/Washington International Airport
Maryland 21240, USA

Government Reports Announcements (GRA),
published by the National Technical
Information Services, Springfield
Virginia 22151, USA

Printed by Technical Editing and Reproduction Ltd
Harford House, 7–9 Charlotte St, London W1P 1HD